



Durham E-Theses

Studies of the role of Tin(II) in the rhodium(I) chloride catalysed hydrocarbonylation of alkenes

Brown, Andrew Paul

How to cite:

Brown, Andrew Paul (1994) *Studies of the role of Tin(II) in the rhodium(I) chloride catalysed hydrocarbonylation of alkenes*, Durham theses, Durham University. Available at Durham E-Theses Online: <http://etheses.dur.ac.uk/5532/>

Use policy

The full-text may be used and/or reproduced, and given to third parties in any format or medium, without prior permission or charge, for personal research or study, educational, or not-for-profit purposes provided that:

- a full bibliographic reference is made to the original source
- a [link](#) is made to the metadata record in Durham E-Theses
- the full-text is not changed in any way

The full-text must not be sold in any format or medium without the formal permission of the copyright holders.

Please consult the [full Durham E-Theses policy](#) for further details.

The copyright of this thesis rests with the author.
No quotation from it should be published without
his prior written consent and information derived
from it should be acknowledged.

STUDIES OF THE ROLE OF TIN(II) IN THE RHODIUM(II)
CHLORIDE CATALYSED HYDROCARBONYLATION OF
ALKENES

ANDREW PAUL BROWN

Submitted for the Degree of
DOCTOR OF PHILOSOPHY

University of Durham
Department of Chemistry

1994



22 NOV 1994

To my Mum and Dad

The material contained in this thesis has not been submitted for examination for any other degree or part thereof, at the University of Durham, or any other institution. The material contained herein is the sole work of the author except where formally acknowledged by reference.

The copyright of this thesis rests with the author. No quotation from it should be published without his prior consent, and information derived from it should be acknowledged.

Acknowledgements

I would like to thank Dr M. Kilner for his advice and supervision. Many thanks also to the following people; Dr K. Dillon, Dr G. Morris (BP Chemicals), Dr N. Greener (BP Chemicals), Prof. J. Howard and Jason Cole (Crystal structure determinations), and Mr D. Hunter.

I would also like to express my thanks and best wishes to my family and friends, who have supported me throughout the past few years, and with whom I have shared many enjoyable times in Durham. You know who you are.

Finally, I am indebted to the SERC and BP Chemicals for funding.

Abstract

Batch catalytic and high pressure infra-red studies of catalytic systems have provided detailed information about the homogeneous rhodium-chloride catalysed hydrocarbonylation of ethene to form propanoic acid in $\text{CH}_3\text{COOH}/\text{c.HCl}$ at 180°C and 60 bar pressure. $[\text{Rh}(\text{CO})_2\text{Cl}_2]^-$ was shown to be an active catalyst for this process. Tin(II) chloride as a co-catalyst was shown to have an effect on the rate of propanoic acid production for a rhodium-chloride catalytic process, but a clear promotional effect was only observed for systems employing a Sn:Rh molar ratio of 2:1. Sn:Rh molar ratios higher than 2:1 lead to a decrease in the selectivity for propanoic acid, while those lower than 2:1 result in catalytic activity consistent with $[\text{Rh}(\text{CO})_2\text{Cl}_2]^-$ being an active species.

The reactions of rhodium(I) carbonyl chlorides with tin(II) chlorides were carried out at atmospheric pressure to investigate the reaction chemistry between species present in the catalytic process. $[\text{Rh}(\text{CO})_2\text{Cl}_2]^-$ and $\text{Rh}_2(\text{CO})_4\text{Cl}_2$ react with SnCl_2 and SnCl_3^- in both THF and CH_2Cl_2 to form Rh(I)-CO- SnCl_3 complexes. Infra-red and ^{119}Sn NMR data identified the 5-coordinate complex $[\text{Rh}(\text{CO})_2(\text{SnCl}_3)_3]^{2-}$ as the favoured species formed in solution. Its crystal structure is reported. However, it appears to be related by a series of facile reactions, involving dissociation of SnCl_3^- and CO groups, to several other 4 and 5-coordinate Rh(I)-CO- SnCl_3 complexes. $[\text{Rh}(\text{CO})(\text{SnCl}_3)_4]^{3-}$, $[\text{Rh}(\text{CO})(\text{SnCl}_3)_2\text{Cl}]^{2-}$, and $[\text{Rh}(\text{CO})_2(\text{SnCl}_3)\text{X}]^-$ ($\text{X} = \text{Cl}^-$ or SnCl_3^-) have been isolated from solution, often as mixtures along with $[\text{Rh}(\text{CO})_2(\text{SnCl}_3)_3]^{2-}$. Spectroscopic and X-ray crystallographic data indicated that SnCl_3^- is a significant π -acceptor ligand, thus explaining its ability to form 5-coordinate 18-electron rhodium(I) complexes. The effect of tin(II) chloride on the rhodium-chloride catalytic reaction is attributed to changes in π -acceptor and trans effect properties when SnCl_3^- replaces chloride ligand(s).

High pressure infra-red studies are consistent with both $[\text{Rh}(\text{CO})_2\text{Cl}_2]^-$ and a Rh(I)-CO- SnCl_3 complex being catalytically active in a rhodium-tin-chloride system, and the carbonyl absorptions observed are consistent with $[\text{Rh}(\text{CO})(\text{SnCl}_3)_4]^{3-}$, $[\text{Rh}(\text{CO})_2(\text{SnCl}_3)_3]^{2-}$ and $[\text{Rh}(\text{CO})(\text{SnCl}_3)_2\text{Cl}]^{2-}$ as catalytic precursors. The general predominance of $[\text{Rh}(\text{CO})_2(\text{SnCl}_3)_3]^{2-}$ in solution at atmospheric pressure and room temperature, suggests that it may be the favoured catalytic precursor, undergoing conversion to a catalytically active 16-electron Rh(I)- SnCl_3 complex such as $[\text{Rh}(\text{CO})_2(\text{SnCl}_3)\text{X}]^-$ ($\text{X} = \text{Cl}^-$ or SnCl_3^-) via dissociation of SnCl_3^- .

Notes on abbreviations and terminology

The following is a list of chemical symbols and formulae which are reported in an abbreviated form throughout this thesis:

COD	-	1,5-cyclooctadiene
NBD	-	Norbornadiene
[Bz(Et) ₃ N] ⁺	-	[(C ₆ H ₅)CH ₂ (C ₂ H ₅) ₃ N] ⁺
Bz(Et) ₃ NCl	-	[(C ₆ H ₅)CH ₂ (C ₂ H ₅) ₃ N]Cl
[PPN] ⁺	-	[{(C ₆ H ₅) ₃ P=} ₂ N] ⁺
PPNCl	-	[{(C ₆ H ₅) ₃ P=} ₂ N]Cl
THF	-	Tetrahydrofuran
Ph	-	C ₆ H ₅
EtOH	-	C ₂ H ₅ OH
Me	-	CH ₃
Et	-	C ₂ H ₅
FT-IR	-	Fourier Transform Infra-Red Spectroscopy
NMR	-	Nuclear Magnetic Resonance Spectroscopy
GC	-	Gas Chromatography
GCMS	-	Gas Chromatograph Mass Spectroscopy

Infra-Red

The following are abbreviations used to describe the intensity of infra-red absorptions:

vw - very weak w - weak mw - medium weak m - medium
ms - medium strong s - strong sh - shoulder

NMR

The following abbreviations are used to state the multiplicity of NMR signals:

s - singlet d - doublet t - triplet q - quartet

CONTENTS

	Page
Notes on abbreviations and terminology	i
Chapter 1 Introduction and Literature Review Transition Metal-Tin Chemistry	1
1.1 Introduction	2
1.2 Industrial processes	4
1.2.1 Acetic acid production	4
1.2.2 Acetic anhydride	6
1.2.3 Hydrocarbonylation	7
1.3 Transition metal-tin complexes	10
1.3.1 Introduction	10
1.3.2 Synthetic routes to transition metal-tin complexes	11
1.3.3 The trans effect and the trans influence	11
1.3.4 Formation of transition metal-tin complexes by insertion	13
1.3.4.1 Insertion into a metal-carbon bond	13
1.3.4.2 Insertion into a metal-metal bond	13
1.3.4.3 Insertion into a metal-chloride bond	15
1.4 Transition metal-trichlorostannate complexes	17
1.4.1 Rhodium and iridium trichlorostannate complexes	17
1.4.2 Palladium and platinum trichlorostannate complexes	19
1.4.3 Bonding in transition metal-trichlorostannate complexes	21
1.5 The catalytic activity of transition metal-trichlorostannate complexes	24
1.5.1 Hydrogenation and isomerisation of olefins	24
1.5.2 Reductions under Water Gas Shift conditions	26
1.5.3 Polymerisation	26
1.5.4 Hydroformylation of olefins	27
1.5.5 The rhodium-tin catalysed hydrocarbonylation of ethene to form propanoic acid	30
1.5.6 Other transition metal/tin carbonylation reactions to form acids and esters	34
1.5.7 Coupling Reactions	36
1.5.8 Other reactions	36
1.6 References	37

Chapter 2	The Reaction Chemistry of Rhodium(I) Carbonyl Chlorides with Tin(II) Chlorides	42
2.1	Introduction	43
2.2	Fourier Transform Infra-Red studies of the reaction chemistry occurring between rhodium(I) carbonyl chlorides and tin(II) chlorides	45
2.2.1	Reactions of $[\text{Rh}(\text{CO})_2\text{Cl}_2]^-$ with SnCl_2	46
2.2.2	Reaction of $[\text{Rh}(\text{CO})_2\text{Cl}_2]^-$ with SnCl_2 at low temperature	52
2.2.3	Reaction of $[\text{Rh}(\text{CO})_2\text{Cl}_2]^-$ with SnCl_3^-	54
2.2.4	Reaction of $\text{Rh}_2(\text{CO})_4\text{Cl}_2$ with SnCl_2	55
2.2.5	Reaction of $\text{Rh}_2(\text{CO})_4\text{Cl}_2$ with $\text{Bz}(\text{Et})_3\text{NCl}$ and SnCl_2	57
2.2.6	Reaction of $\text{Rh}_2(\text{CO})_4\text{Cl}_2$ with $\text{Bz}(\text{Et})_3\text{NSnCl}_3$	62
2.2.7	Reaction of $\text{Rh}_2(\text{CO})_4\text{Cl}_2$ with SnCl_2 and $\text{HCl}_{(\text{g})}$	66
2.3	^{119}Sn NMR studies of rhodium(I) carbonyl chloride/tin chloride reaction solutions	69
2.3.1	Introduction	69
2.3.2	^{119}Sn NMR studies of the stability of SnCl_3^- in solution	70
2.3.3	^{119}Sn NMR studies of the reactions of rhodium(I) carbonyl chlorides and tin(II) chlorides	72
2.3.4	Discussion of the ^{119}Sn NMR data	72
2.4	Discussion of results	75
2.5	Conclusions	81
2.6	References	82
Chapter 3	Synthesis, Characterisation and Properties of Rhodium(I) Trichlorostannate Complexes	84
3.1	Introduction	85
3.2	Experimental	85
3.2.1	Preparation of $[\text{Bz}(\text{Et})_3\text{N}]_3[\text{Rh}(\text{CO})(\text{SnCl}_3)_4]$	85
3.2.2	Attempted preparation of $[\text{Bz}(\text{Et})_3\text{N}]_2[\text{Rh}(\text{CO})(\text{SnCl}_3)_2\text{Cl}]$	90
3.2.3	Preparation of $[\text{PPN}]_2[\text{Rh}(\text{COD})(\text{SnCl}_3)_3]$	92
3.2.4	Preparation of $\text{Rh}(\text{COD})_2(\text{SnCl}_3)$	95
3.2.5	Preparation of $[\text{PPN}]_2[\text{Rh}(\text{CO})_2(\text{SnCl}_3)_3]$	95
3.2.6	Reaction of $[\text{Bz}(\text{Et})_3\text{N}][\text{Rh}(\text{CO})_2\text{Cl}_2]$ and SnCl_2 in THF	107
3.2.7	Reaction of $[\text{Bz}(\text{Et})_3\text{N}][\text{Rh}(\text{CO})_2\text{Cl}_2]$ with $\text{Bz}(\text{Et})_3\text{NSnCl}_3$ and 37% $\text{HCl}_{(\text{aq})}$ in acetic acid	110

3.2.8	Reaction of $\text{Rh}_2(\text{CO})_4\text{Cl}_2$ and $\text{Bz}(\text{Et})_3\text{NSnCl}_3$ in acetic acid	110
3.3	Discussion	111
3.3.1	Crystal structure information	111
3.3.2	Rationalisation of the formation of complexes isolated from solution	114
3.4	Conclusions	121
3.5	References	123
Chapter 4	The Hydrocarbonylation of Ethene using Rhodium(I)-Tin(II) Catalytic Systems	124
4.1	Introduction	125
4.2	Experimental procedures, summary of data obtained, and calculation of rate data, propanoic acid production and selectivity for propanoic acid	127
4.2.1	Experimental procedures	127
4.2.2	Calculation of selectivity and amount of propanoic acid production	135
4.2.3	Calculation of rates of reaction	136
4.3	'Blank' reactions	137
4.4	Rhodium(III) chloride trihydrate as a catalytic precursor in the absence of tin	138
4.5	Addition of tin(II) chloride to the rhodium-chloride catalytic system	140
4.6	Addition of benzyltriethylammonium chloride to rhodium-chloride and rhodium-tin-chloride catalytic systems	141
4.7	Catalytic activity of model rhodium(I) carbonyl chloride complexes	142
4.8	Addition of benzyltriethylammonium trichlorostannate to a rhodium-chloride catalytic system	145
4.9	Effect of ethene on reactivity	154
4.10	Isotopic exchange experiments	157
4.11	Catalyst injection techniques	162
4.12	Hydrocarbonylation using model rhodium-tin complexes	166
4.13	Promotional effect of tin(IV) species	170
4.14	Dichloromethane as a co-solvent	171
4.15	Tin(II) bromide as a promoter	172
4.16	Conclusions	173
4.17	References	176

Chapter 5	High Pressure Infra-Red Studies of Rhodium-Tin-Chloride Catalytic Systems	177
5.1	Introduction	178
5.2	RhCl ₃ /SnCl ₂ /Bz(Et) ₃ NCl as catalytic precursors under a pressure of CO	179
5.3	RhCl ₃ /SnCl ₂ /Bz(Et) ₃ NCl as catalytic precursors under a pressure of CO and C ₂ H ₄	184
5.4	Studies of systems containing model rhodium(I) carbonyl chloride complexes	184
5.5	Studies with acetic acid as a single solvent	188
5.6	Conclusions	191
5.7	Summary of reagents and reaction conditions	192
5.8	References	193
Chapter 6	Studies of the role of triphenylphosphine and zinc(II) chloride as co-catalysts in the rhodium catalysed hydrocarbonylation of ethene and the hydrocarbonylation of alkenes other than ethene	194
6.1	Introduction	195
6.2	Synthesis	196
6.2.1	Preparation of Rh(CO)Cl(PPh ₃) ₂	196
6.2.2	Preparation of Rh(C ₈ H ₁₂)(PPh ₃)Cl	196
6.2.3	Preparation of [Bz(Et) ₃ N][Rh(C ₈ H ₁₂)(SnCl ₃) ₂ (PPh ₃)]	196
6.2.4	Preparation of [PPN][Rh(C ₈ H ₁₂)(SnCl ₃) ₂ (PPh ₃)]	197
6.2.5	Preparation of Rh(C ₈ H ₁₂)(SnCl ₃)(PPh ₃) ₂	198
6.3	The Rhodium Catalysed Hydrocarbonylation of Ethene Promoted by Triphenylphosphine and Triphenylphosphine/Trichlorostannate Mixed Ligand Complexes	199
6.4	The Rhodium Catalysed Hydrocarbonylation of Ethene Promoted by Zinc(II) Chloride	203
6.4.1	Catalytic studies	203
6.4.2	The reaction chemistry of rhodium(I) carbonyl chlorides and zinc(II) chlorides	204
6.5	Hydrocarbonylation of other alkenes	206
6.6	Conclusions	207
6.7	References	209

Chapter 7	The Reaction Chemistry of Several Rhodium(I) Trichlorostannate Complexes	211
7.1	Introduction	212
7.2	Experimental	213
7.2.1	^{31}P NMR studies of the reactions of Rh-COD- PPh_3 - SnCl_3 complexes with CO	213
7.2.1.1	Reaction of $\text{Rh}(\text{COD})(\text{SnCl}_3)(\text{PPh}_3)_2$ with CO	213
7.2.1.2	Reaction of $[\text{Bz}(\text{Et})_3\text{N}][\text{Rh}(\text{COD})(\text{SnCl}_3)_2(\text{PPh}_3)]$ with CO	213
7.2.2	FT-IR studies of the reactions of Rh-COD- PPh_3 - SnCl_3 complexes with CO	214
7.2.3	^{31}P NMR studies of the reactions of Rh-CO- SnCl_3 complexes with PPh_3	215
7.2.3.1	Reaction of the product of $[\text{Rh}(\text{CO})_2\text{Cl}_2]^- + \text{SnCl}_2$ with PPh_3	215
7.2.3.2	Reaction of $[\text{PPN}]_2[\text{Rh}(\text{CO})_2(\text{SnCl}_3)_3]$ with PPh_3	215
7.2.3.3	Reaction of PPh_3 with the solid product obtained from $\text{Rh}_2(\text{CO})_4\text{Cl}_2 + \text{SnCl}_2 + \text{Bz}(\text{Et})_3\text{NCl}$ in ethanol	216
7.2.4	FT-IR studies of the reactions of Rh-CO- SnCl_3 complexes with PPh_3	217
7.2.5	The reaction chemistry of Rh-CO- SnCl_3 complexes with chloride ions	220
7.2.5.1	Reaction of $[\text{Bz}(\text{Et})_3\text{N}][\text{Rh}(\text{CO})_2\text{Cl}_2]$ with SnCl_2 in THF followed by addition of $\text{Bz}(\text{Et})_3\text{NCl}$	220
7.2.5.2	Reaction of Rh(I)-CO- SnCl_3 complexes with chloride ions	221
7.2.6	Carbonylation of the product from $[\text{Bz}(\text{Et})_3\text{N}][\text{Rh}(\text{CO})_2\text{Cl}_2] + \text{SnCl}_2$ in THF	221
7.2.7	The reaction chemistry of miscellaneous rhodium complexes followed by ^{31}P NMR spectroscopy	221
7.2.7.1	Reaction of $\text{Rh}(\text{CO})\text{Cl}(\text{PPh}_3)_2$ with SnCl_2	222
7.2.7.2	Reaction of $\text{Rh}(\text{COD})\text{Cl}(\text{PPh}_3)$ with SnCl_2	222
7.2.7.3	Reaction of $\text{Rh}(\text{COD})_2(\text{SnCl}_3)$ with PPh_3	222
7.2.8	The reaction chemistry of miscellaneous rhodium complexes followed by FT-IR spectroscopy	223
7.2.8.1	Reaction of $\text{Rh}(\text{CO})\text{Cl}(\text{PPh}_3)_2$ with SnCl_2	223

7.2.8.2 Reaction of Rh(COD) ₂ (SnCl ₃) with CO and PPh ₃	223
7.3 Discussion	224
7.3.1 The formation of Rh-SnCl ₃ -CO-PPh ₃ complexes	224
7.3.2 The reaction of Cl ⁻ with Rh-CO-SnCl ₃ complexes	235
7.4 Conclusions	236
7.5 References	237
Chapter 8 Conclusions	238
Appendices	243
Appendix 1 Preliminary Synthesis	244
Appendix 2 High Pressure Autoclaves	247
Appendix 3 Instrumental Parameters	250
Appendix 4 Scientific meetings and colloquia attended	253

Chapter 1

Introduction and Literature Review

Transition Metal - Tin Chemistry



1.1 Introduction

The aim of this thesis is to probe the fundamental chemistry occurring in the rhodium-tin-chloride homogeneously catalysed hydrocarbonylation of ethene to form propanoic acid. In doing so it is intended to investigate the nature of the active catalytic species, to rationalise the observed activity, and ultimately to improve the performance of the catalytic process using model systems.

B.P. Chemicals is the major company in the United Kingdom involved in carbonylation chemistry, and manufactures acetic acid and acetic anhydride at Hull using homogeneous rhodium catalysts. Propanoic acid is a by-product of the acetic acid process and there is a growing world market for it. Consequently, there is a desire to find new and efficient processes to produce it on an industrial scale.

It has been found recently that rhodium will catalyse the hydrocarbonylation of ethene to form propanoic acid in a chloride system, rather than the usual iodide system, although at much lower rates of reaction. Reactivity is only found to occur, however, when tin(II) chloride or other metal chlorides e.g. ZnCl_2 , NiCl_2 , etc. are present⁽¹⁾. This process utilises rhodium complexes as homogeneous catalysts at typically 180°C and 80 atm pressure of carbon monoxide and ethene pressure.



The high catalytic activity and selectivity found when tin(II) chloride is used as a promoter is the reason for the studies undertaken in this thesis, since the nature of the active catalyst remained unidentified and the role of tin(II) chloride was speculative. It is known, however, that the optimum rhodium:tin molar ratio is 1:2, and that high tin content will lower the selectivity of the reaction. It is also known that under the conditions employed for the catalytic reaction, $\text{RhCl}_3 \cdot 3\text{H}_2\text{O}$, the usual rhodium catalytic precursor, will react to form the rhodium(I) complex $[\text{Rh}(\text{CO})_2\text{Cl}_2]^-$, and that tin(II) chloride will react with chloride ions present in the system as 37% $\text{HCl}_{(\text{aq})}$ to form SnCl_3^- . As a result the catalytic species is thought to be formed by a possible reaction of species of this kind.

The ability of tin(II) chloride to form M-SnCl_3 complexes with transition metals is well documented, and many of these complexes play a key role in many homogeneously catalysed organic transformations. The role of tin(II) chloride as a

co-catalyst has been attributed to the nature of its bonding with transition metals. A full discussion of this chemistry is outlined later in this chapter.

The work described in this thesis was divided into several parts, with the common aim of exploring the chemistry involved in the catalytic process.

1. FT-IR and ^{119}Sn NMR spectroscopic studies of the reaction chemistry of rhodium(I) carbonyl chlorides and tin(II) chlorides were carried out, with the aim of investigating the type of chemistry which may be occurring under more forcing conditions in the catalytic process, and to provide information on the bonding and properties of the trichlorostannate ion in such systems.
2. FT-IR spectroscopic studies of rhodium-chloride and rhodium-tin-chloride systems at high temperature and pressure, to investigate the chemistry occurring under catalytic conditions.
3. Synthesis and isolation of Rh-SnCl_3 complexes which have been observed by spectroscopic methods under ambient and high temperature and pressure conditions. The solid state structural properties and reaction chemistry of several complexes were investigated, paying particular attention to the bonding of the trichlorostannate ligand and its possible effect on the catalytic process. The use of these model Rh-SnCl_3 complexes to develop the catalytic process is also discussed.
4. Batch catalytic studies were carried out with the aim of investigating and improving the rhodium-chloride and rhodium-tin-chloride catalytic processes.
5. The effect of other co-catalysts e.g. PPh_3 , ZnCl_2 on the rhodium-chloride catalytic process was also investigated.

1.2 Industrial Processes

It has been estimated that approximately 70% of all chemicals produced by the chemical industry will involve the use of a catalyst somewhere along the production process⁽²⁾. Most industrial processes, however, have involved the use of heterogeneous rather than homogeneous catalysts to produce, in the main, petroleum based products. The relatively low use of homogeneous catalysts has been mainly due to problems of their stability at higher temperatures and the difficulties of catalyst separation and regeneration⁽²⁾. This is surprising, considering the advantages offered by homogeneous catalysts, which are gradually causing an increasing interest in their activity. It is possible to tailor homogeneous catalysts to provide a specific coordination site for a particular reacting group, thus giving them a higher selectivity than heterogeneous catalysts. Homogeneous catalysts also show a higher catalytic activity, with all metal atoms theoretically being available for reactivity, in contrast to heterogeneous systems where reactivity is restricted to particular active sites. Another advantage of homogeneous catalysts is the greater control of temperature on the catalyst site⁽²⁾, and in general the much lower temperature required for catalytic activity. For certain processes it has been deemed that the advantages of these catalysts outweigh the economic problems associated with catalyst recovery. There are relatively few industrial processes in operation which employ homogeneous catalysts. Several warrant consideration at this point, however, since the catalytic systems involved and organic species formed have an influence on the work described in this thesis.

1.2.1 Acetic acid production

Acetic acid has been produced in large quantities for more than 100 years⁽³⁾ and is a major industrial chemical used in the manufacture of vinyl acetate, cellulose acetate, pharmaceutical products, dyes and pesticides. The various changes in production technology throughout this period reflect the changes in available raw materials and also the increasing impact of homogeneous catalysis in modern industrial chemistry.

Early synthetic methods involved the 'distillation' of various forms of wood or the fermentation of grains. Indeed, fermentation processes are still retained for vinegar production⁽⁴⁾. The first major industrial process for production of acetic acid was based on the hydrolysis of acetylene to acetaldehyde catalysed by the mercury(II) ion. This process was used until the late 1950's⁽⁴⁾ at which time two processes were developed which have since monopolised the world acetic acid market. Celanese and British Petroleum developed short-chain paraffin oxidation using manganese or

cobalt catalysts, while Wacker Chemie introduced the palladium-copper catalysed oxidative hydration of ethene to acetaldehyde.

1965 saw the introduction of the B.A.S.F high pressure process for the carbonylation of methanol to acetic acid using a cobalt-iodide promoted catalyst^(5,6), and in 1968 Paulik and Roth of the Monsanto company introduced the low pressure carbonylation of methanol utilising a rhodium or iridium iodide promoted catalyst⁽⁷⁾. This was more efficient than the cobalt process and in 1973 a patent was filed relating to it⁽⁸⁾. The cobalt process required conditions of 230°C and 500-700 atm and only had a selectivity for acetic acid of 90% whereas the rhodium process operated at 180°C and 30-40 atm and had a selectivity for acetic acid of greater than 99%. The process can utilise almost any form of rhodium. The rhodium species identified in solution during the catalytic process is the diiododicarbonyl rhodium(I) anion $[\text{Rh}(\text{CO})_2\text{I}_2]^-$ ^(9,10). The iodide promoter can also be employed in several different forms, thus methyl iodide, iodine or even alkali metal salts can be used. Forster⁽¹¹⁾ found that when a solution containing $[\text{Rh}(\text{CO})_2\text{I}_2]^-$ was reacted with excess methyl iodide the 5-coordinate acyl complex $[\text{Rh}(\text{CH}_3\text{CO})(\text{CO})\text{I}_3]^-$, isolated as a dimer, is formed, and can be reacted to give the 6-coordinate acyl complex $[\text{Rh}(\text{CH}_3\text{CO})(\text{CO})_2\text{I}_3]^-$ upon introduction of carbon monoxide. This species decomposes at room temperature to give the starting rhodium(I) complex $[\text{Rh}(\text{CO})_2\text{I}_2]^-$ and acetyl iodide. Kinetic studies have shown that the rate determining step for the reaction is the oxidative addition of methyl iodide to the rhodium complex $[\text{Rh}(\text{CO})_2\text{I}_2]^-$ with the rate equation

$$\text{Rate} = k[\text{Rh}]^1[\text{I}]^1[\text{MeOH}]^0[\text{CO}]^0$$

applying, thus showing that the reactants carbon monoxide and methanol have no influence on the rate of reaction. The catalytic cycle proposed for the Monsanto process, based on the known reaction chemistry, is shown in Figure 1.1.

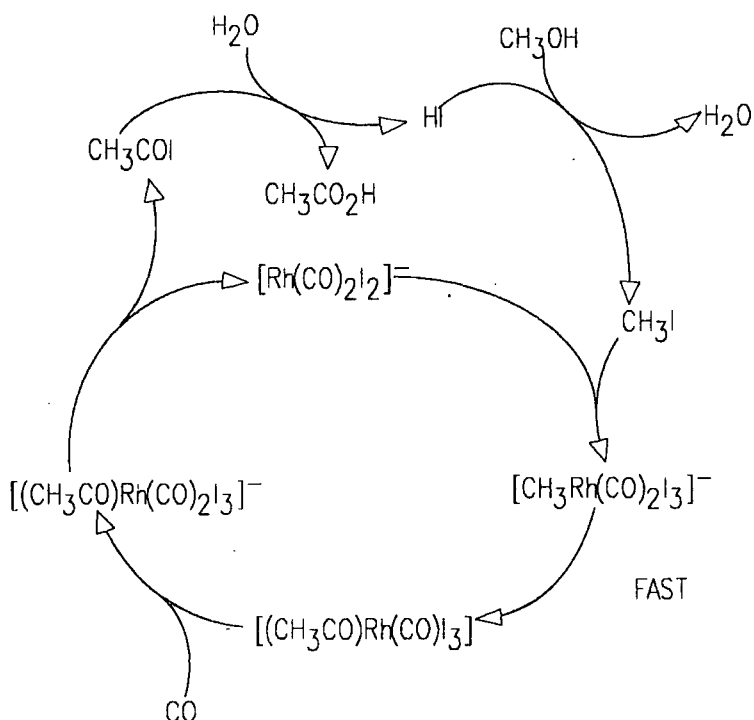


Figure 1.1 Catalytic Cycle for the Monsanto Process

1.2.2 Acetic anhydride

Since 1983 Tennessee Eastman have operated a commercial process for the conversion of acetic acid to acetic anhydride. The process typically employs a rhodium catalytic system promoted by lithium iodide and methyl iodide to carbonylate methyl acetate to acetic anhydride, and is carried out in acetic acid as solvent⁽¹²⁾. The process has produced selectivities for acetic anhydride of greater than 95%. Kinetic studies have shown that the dependence of the rate on rhodium and methyl iodide concentrations is a function of the lithium iodide concentration. At high lithium concentrations the rate shows first order dependence on both rhodium and methyl iodide concentrations, and is consistent with a rate limiting step involving the oxidative addition of methyl iodide to the active rhodium(I) species $[\text{Rh}(\text{CO})_2\text{I}_2]^-$, which has been observed by infra-red spectroscopy. At low lithium concentrations the rate approaches zero order dependence on rhodium and methyl iodide concentrations, with the rate limiting step believed to involve consumption of acetyl iodide by methyl acetate or lithium acetate. A proposed mechanism for the process is shown in Figure 1.2.

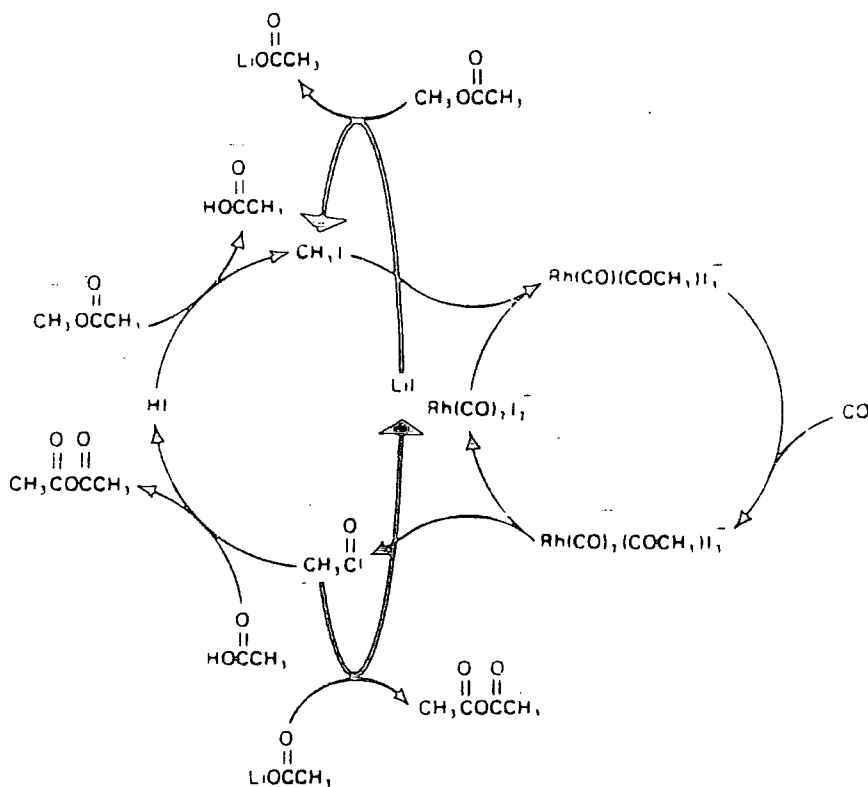
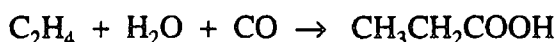


Figure 1.2 Proposed mechanism for the rhodium/iodide catalysed carbonylation of methyl acetate

1.2.3 - Hydrocarbonylation

This thesis concerns the hydrocarbonylation of ethene to form propanoic acid:

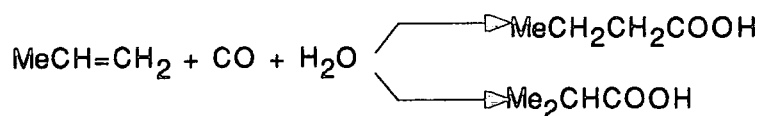


Throughout this thesis it will be referred to as hydrocarbonylation. Alternative names include hydrocarboxylation, hydroxycarbonylation, and carboalkoxylation.

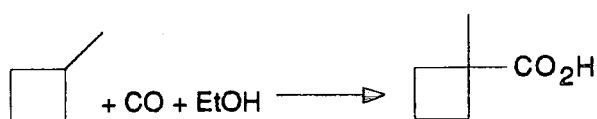
Thus, at this juncture, other hydrocarbonylation processes, in particular those used to form propanoic acid and other organic acids deserve consideration. The nickel catalysed hydrocarbonylation of ethene to form propanoic acid has been operated as an industrial process by B.A.S.F. The nickel species is nickel propanoate which is converted to nickel tetracarbonyl under the reaction conditions of typically 270-320°C and 200-240atm⁽⁴⁾. The problems associated with this process are due to the high pressures involved, catalyst instability, and low selectivity and reactivity,

with a mixture of polyketones and polycarboxylic acids obtained if the reaction is carried out in the presence of tetracyanonickelate^(13,14,15).

Nickel catalysts can also be employed for the hydrocarbonylation of other alkenes, for example propene



and also strained alkenes which can be more readily carbonylated, such as methylene cyclobutene⁽¹⁶⁾.



The problems associated with the nickel catalysed carbonylation process were overcome to a large extent by the use of rhodium and iridium-iodide promoted catalytic processes, involving the hydrocarbonylation of primary alkenes which were patented by Monsanto^(17,18,19,20). This process utilises more reactive and more stable catalyst compositions, thus enabling the use of lower temperatures (140-180°C) and lower pressures (400-700psi), which led to a much more efficient and highly selective process, which could be operated in both liquid and vapour phases. Like the methanol to acetic acid process many forms of rhodium, iridium and iodide may be used. The iridium-iodide system had a preferred molar ratio of these components of 1:3 to 1:300 with preferred rhodium-iodide ratios being very similar. The preferred solvents used were linear carboxylic acids containing between 2 and 20 carbon atoms, with C₃ to C₁₁ carboxylic acids produced by hydrocarbonylation of the appropriate olefins. Selectivities for these acids were generally in the range of 75-90% with an 85% selectivity for propanoic acid. The suggested reaction mechanism for the rhodium-iodide promoted process is shown in Figure 1.3.

Oxidative addition of hydrogen iodide followed by coordination of an ethene ligand is followed by hydride cis-migration, and then addition of carbon monoxide to the vacant site. Alkyl cis-migration to CO then occurs, and the catalytic cycle is completed by reductive elimination of the acid iodide which is hydrolysed to produce the desired product, and regeneration of HI. Work carried out by Forster⁽²¹⁾ showed that at 125°C and 35bar pressure ethyl iodide gave an 80 times greater rate of reaction than when HI was employed as initiator, and that addition of HI to the ethyl

iodide promoted system decreased the rate. It was proved, however, that ethene hydrocarbonylation did proceed predominantly by a 'HI addition' mechanism, although it was also shown that high concentrations of HI inhibited the rate by poisoning the catalyst to give the rhodium(III) species $[\text{Rh}(\text{CO})_2\text{I}_4]^{2-}$.

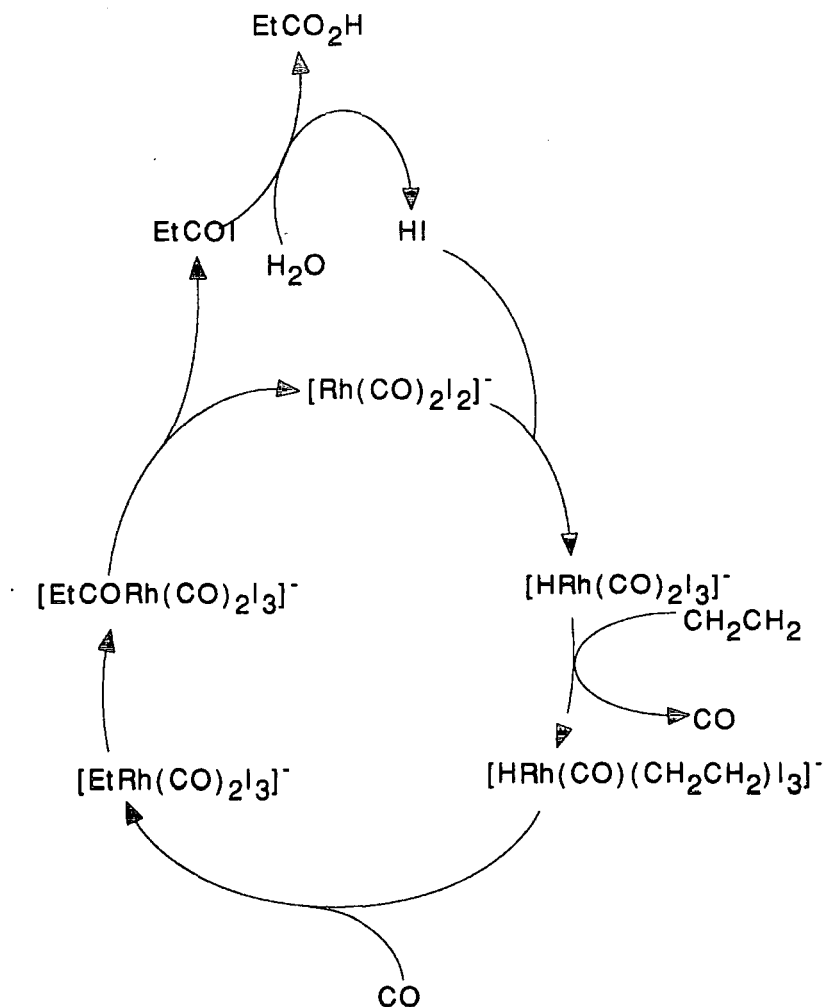
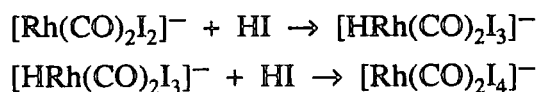
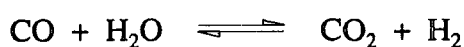


Figure 1.3 Catalytic cycle for the Rhodium-Iodide Catalysed Hydrocarbonylation of Ethene

Improvements in the propanoic acid process were later outlined in patents filed by Paulik et al⁽¹⁹⁾ and Craddock et al⁽²⁰⁾ of the Monsanto company, which detailed the iridium-bromide and rhodium-bromide promoted hydrocarbonylation of ethene. The

optimum ratio of iridium:bromide was found to be in the range of 1:3 to 1:300 with the preferred range being from 1:3.1 to 1:150. The catalytic precursors used were iridium trichloride and ethyl bromide with acetic acid as solvent. Water was also present. Hydrocarbonylation was found to occur at 195°C and 400psi total pressure with a selectivity for propanoic acid of greater than 99%. The rhodium-bromide promoted system had an optimum rhodium:bromide ratio in the range of 1:40 to 1:350 with the preferred range being from 1:80 to 1:250. Rhodium trichloride and $\text{HBr}_{(\text{aq})}$ /bromoethane were used as catalytic precursors with acetic acid present as solvent. Hydrocarbonylation occurred at 175°C and 400psi total pressure with a selectivity for propanoic acid of greater than 99% being achieved. The Water Gas Shift reaction



was not a feature of the bromide promoted systems, reflected by the absence of aldehyde moieties as by-products. This is in contrast to the rhodium-iodide promoted system where the selectivity can be lowered due to the formation of products instigated by the production of hydrogen via the Water Gas Shift reaction, which is catalysed by a rhodium-carbonyl-iodide promoted system⁽²²⁾, via initial formation of $[\text{Rh}(\text{CO})_2\text{I}_2]^-$.

1.3 Transition Metal - Tin Complexes

1.3.1 Introduction

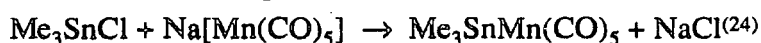
In recent years there has been an increased interest in transition metal-tin chemistry and many experimental probes have been used to study the properties of these complexes. Considerable spectroscopic information has been obtained, providing not only structural information, but also information on transition metal-tin bonding and the nature of various species in solution, which can often involve multistage equilibria⁽²³⁾. There has been an increasing use of these species, particularly platinum-tin complexes, in the homogeneous catalysis of organic transformations such as hydroformylation, hydrocarbonylation, olefin hydrogenation and isomerisation. It has been possible to explain some of this chemistry by considering the nature of the structure and bonding of transition metal-tin complexes. Recent work⁽¹⁾ has found that a rhodium chloride system in the presence of excess chloride ions will catalyse the hydrocarbonylation of ethene to form propanoic acid, but only if tin(II) chloride is included as a co-catalyst. The development and rationalisation of this chemistry is described in this thesis. At this point, therefore, a review of

transition metal-tin chemistry, the nature of the bonding in these complexes, and their ability to catalyse organic transformations is considered appropriate. Particular emphasis will be placed on the reason why tin(II) chloride will promote certain organic transformations and also the known chemistry of rhodium halides and rhodium carbonyl halides with tin(II) chloride, which is of direct relevance to this thesis.

1.3.2 Synthetic Routes to Transition Metal - Tin Complexes

Many synthetic routes to transition metal-tin complexes have been utilised and examples of these are shown below:

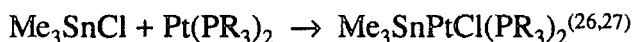
1. Salt elimination (Nucleophilic attack)



2. Elimination of small molecules



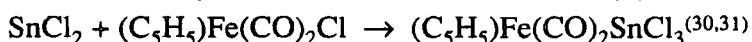
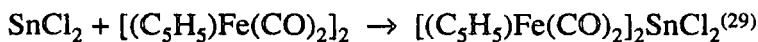
3. Oxidative addition



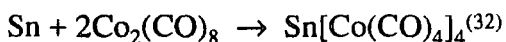
4. Oxidative elimination



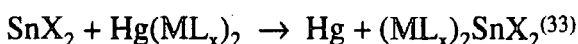
5. Insertion of Tin (II)



6. Activated tin addition



7. Transmetalation



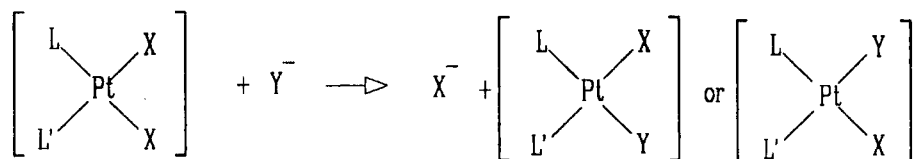
Oxidative addition reactions have been used to synthesise complexes for all transition metal groups and are only limited by the availability of low-valent metal complexes. Tin nucleophiles usually operate with early to middle transition metals. Transition metal anionic species provide a route to transition metal-tin complexes via nucleophilic attack on tin.

1.3.3 The Trans Effect and the Trans Influence

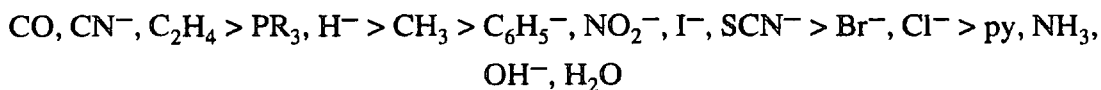
Much of the discussion in this chapter and throughout this thesis refers to the ability of the trichlorostannate ligand to promote many catalytic transformations due to its ability to behave as a trans influencing ligand or ability to cause a trans effect. At

this juncture, therefore, a discussion of the two and a distinction between them is of relevance.

It has long been known that ligand exchange reactions in square complexes show a preference for the site trans to one ligand rather than the other. Consider a reaction of the type:



Two isomeric products are possible. From results on this and other related reactions, a series of ligands has been arranged in order of their tendency to facilitate substitution in a position trans to themselves. This is known as the trans effect. The approximate ordering of ligands is

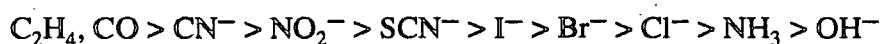


This order spans a factor of 10^6 in rate and holds for square planar platinum complexes. The trans effect is a kinetic effect, depending on activation energies, with the stability of the ground state and the activated complex being relevant factors. It is in principle possible for the activation energy to be affected by changes in one or the other of these energies or by changes in both.

The influence of one ligand on the strength of the bond of the ligand trans to it is called the trans influence. It is a ground state property and can be evaluated from bond lengths or M-C stretching frequencies. Trans influence is attributed to the fact that two trans ligands will both depend on the participation of one metal orbital, and the more one ligand preempts this orbital, the weaker the bond to the other will be. The general order of trans influencing ligands is



This is similar to the trans effect sequence, except for the positions of CN^- and CO , due to these having the ability to cause a trans effect by participating in π -bonding in the transition state. A general trend for the π -bonding ability of some ligands is



Discussions in this chapter indicate that SnCl_3^- is a strong π -acceptor, and has the ability to labilise CO and lengthen the M-CO bond. Thus, it will occupy a position high in the trans influencing series and is therefore likely to have a significant trans effect if the similar trend is applicable.

1.3.4 Formation of Transition Metal - Tin Complexes by Insertion

Tin(II) compounds have the ability to insert into metal-metal, metal-halogen, metal-hydride and metal-carbon bonds. Of particular interest to this thesis is the insertion of tin(II) halides into a transition metal-halide bond to form transition metal-trichlorostannate complexes. Sections 1.3.3.1-1.3.3.3 contain a general review of the formation of transition metal-tin complexes by such insertion reactions.

1.3.4.1 Insertion in to a Metal - Carbon Bond

Reports of insertions of tin(II) chloride into transition metal-carbon bonds have been confined to iron complexes. SnCl_2 inserts⁽³⁴⁾ into the iron-carbon σ bond of $\text{MeFe}(\text{CO})_2(\text{C}_5\text{H}_5)$ in methanol or THF to give $\text{MeCl}_2\text{SnFe}(\text{CO})_2(\text{C}_5\text{H}_5)$, but with $\text{EtFe}(\text{CO})_2(\text{C}_5\text{H}_5)$, a mixture of the insertion product, $\text{Cl}_3\text{SnFe}(\text{CO})_2(\text{C}_5\text{H}_5)$ and $\text{Cl}_2\text{Sn}[\text{Fe}(\text{CO})_2(\text{C}_5\text{H}_5)]_2$ is formed. Insertion of SnCl_2 was not observed for molybdenum and manganese complexes $\text{MeMo}(\text{CO})_3(\text{C}_5\text{H}_5)$ or $\text{MeMn}(\text{CO})_5$.

1.3.4.2 Insertion in to a Metal - Metal Bond

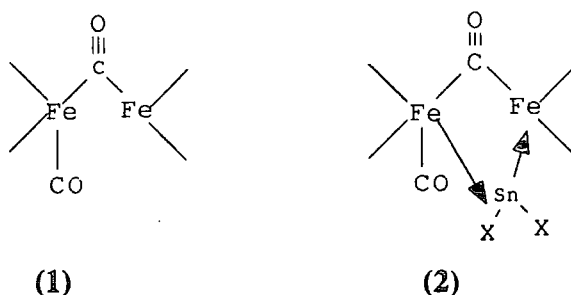
Insertion of tin(II) chloride into metal-metal bonds is much more common than into metal-carbon bonds:

Chromium, Molybdenum, and Tungsten

Tin (II) chloride will insert^(29,35,36,37) into the Mo-Mo bond of $[(\text{C}_5\text{H}_5)\text{Mo}(\text{CO})_3]_2$ to give the insertion product $[(\text{C}_5\text{H}_5)\text{Mo}(\text{CO})_3]_2\text{SnCl}_2$. Likewise, insertion can also occur with the analogous tungsten and chromium complexes⁽³⁷⁾, with the extent of reaction depending on the degree of exposure to light.

Iron, Ruthenium, and Osmium

Bonati and Wilkinson⁽²⁹⁾ showed that tin(II) chloride inserts into the Fe-Fe bond of $[(C_5H_5)(CO)_2Fe]_2$ forming $[(C_5H_5)(CO)_2Fe]_2SnCl_2$. Barrett and Sun⁽³⁸⁾ studied the kinetics of this reaction and indicated that they are consistent with a two stage mechanism involving the formation of a carbonyl bridged intermediate (1) followed by nucleophilic attack of $SnCl_2$ on this intermediate (2).



Barrett and Jacobs⁽³⁹⁾ studied the insertion of $SnCl_2$ into the metal-metal bonded complex $(C_5H_5)_2Fe_2(CO)_3P(OC_6H_5)_3$ indicating that this proceeds via an intermediate in which the Fe-Fe bond breaks, but the carbonyl bridges remain. There is also an example of insertion of $SnCl_2$ into the Os-Os bond of $Os_3(CO)_{11}(\mu-CH_2)$ to form the planar cluster $Os_3SnCl_2(CO)_{11}(\mu-CH_2)$ which contains a pentacoordinate tin atom⁽⁴⁰⁾.

Rhodium

An interesting example of insertion into a Rh-Rh bond involves the insertion of $SnCl_2$ into the rhodium metallocycle $Rh_2(CO)_2Cl_2[\mu-(Ph_2P)_2py]_2$ to form $Rh_2Sn_2(CO)_2Cl_6[(Ph_2P)_2py]_2$ ⁽⁴¹⁾. One tin is present as a trichlorostannate group while the other resides within the cavity of the metallocycle and is coordinated to two nitrogen atoms, two rhodium atoms and one chloride as shown in Figure 1.4. The structural aspects are indicative of a high trans influence caused by the Rh- $SnCl_3$ bond.

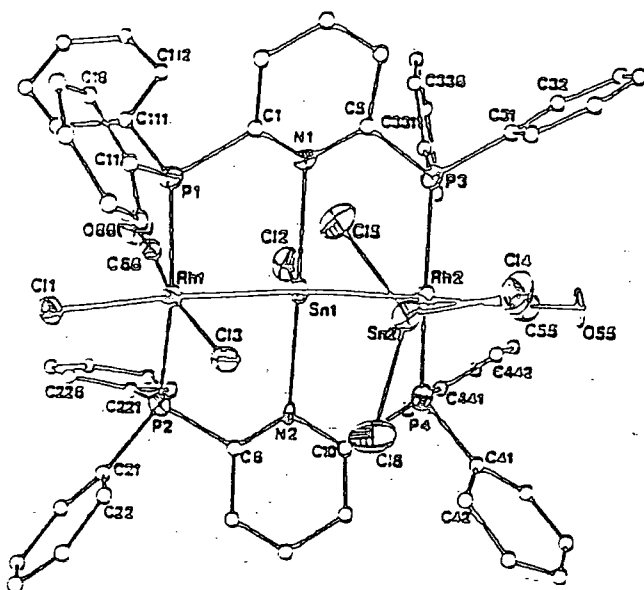


Figure 1.4 A perspective view of $\text{Rh}_2\text{Sn}_2(\text{CO})_2\text{Cl}_6[\mu\text{-(Ph}_2\text{P)}_2\text{py}]_2$

Crystals of $\text{mer-}[\{\text{Rh}(\text{CNC}_8\text{H}_9)_3(\text{SnCl}_3)(\mu\text{-SnCl}_2)\}_2]^{(42)}$ have been isolated from the reaction of $[\text{Rh}(\text{CNC}_8\text{H}_9)_3\text{Cl}]$ with SnCl_2 . The two edge sharing octahedral rhodium centres are linked by two bridging SnCl_2 groups. The reaction of SnCl_2 with $[\text{Rh}(\text{PMe}_3)_3\text{Cl}]^{(43)}$ yielded the diamagnetic complex $[\text{Cl}_2\text{Sn}[\text{Rh}(\text{PMe}_3)_3\text{Cl}]_2]$ with the tin group bridging the two rhodium atoms.

Nickel, Palladium, and Platinum

There are several examples of the insertion of SnCl_2 into the metal-metal bond of nickel, and platinum complexes. Patmore and Graham⁽⁴⁴⁾ have reported that SnCl_2 will insert into $[(\text{C}_5\text{H}_5)(\text{CO})\text{Ni}]_2$ to yield $[(\text{C}_5\text{H}_5)(\text{CO})\text{Ni}]_2\text{SnCl}_2$, while SnCl_2 will also insert into the Pt-Pt bond of $[(\eta\text{-Bu})_4\text{N}]_2[\text{Pt}_2\text{Cl}_4(\text{CO})_2]^{(45)}$.

1.3.4.3 Insertion into Metal-Chloride Bonds

The insertion of tin(II) chloride into a transition metal-chloride bond is of relevance to this thesis and will be discussed with respect to the known formation of rhodium-trichlorostannate complexes described in Chapters 2 and 3. The insertion of SnCl_2 into a transition metal-halogen bond is a well known reaction which has been used extensively to prepare M-SnCl_3 complexes of various transition metals. Many trichlorostannate complexes of ruthenium, rhodium, iridium and platinum have been formulated⁽⁴⁶⁾, including $[\text{RuCl}_2(\text{SnCl}_3)_2]^{2-}$, $[\text{Rh}_2\text{Cl}_2(\text{SnCl}_3)_4]^{4-}$, $[\text{Ir}_2\text{Cl}_6(\text{SnCl}_3)_4]^{4-}$,

and *cis* and *trans*-[PtCl₂(SnCl₃)₂]²⁻. The chemistry which takes place to form species such as these is discussed in more detail in Section 1.4 which relates specifically to rhodium, iridium and platinum trichlorostannate complexes.

There are, however, examples of the insertion of SnCl₂ into other transition metal-halide bonds. SnCl₂ will insert into the cobalt-halide bond to yield the trihalostannate complexes⁽⁴⁷⁾. More unusual, however, is the formation of trichlorostannate complexes of the earlier transition metals. For example, the rhenium and manganese complexes of *fac*-[M(CO)₃(S₂(PR₃)Cl)] (M=Mn or Re; R=cyclohexyl or isopropyl) will react with SnCl₂ in THF to give the trichlorostannate complexes *fac*-[M(CO)₃(S₂(PR₃)(SnCl₃)]⁽⁴⁸⁾. Insertion into the metal-chloride bond of vanadium and niobium complexes can also occur. Carbon monoxide has been shown to promote the insertion of SnCl₂ into the V-Cl bond of [V(cp)₂Cl]⁽⁴⁹⁾, and a trichlorostannate complex can be obtained by insertion of SnCl₂ into the Nb-Cl bond of (C₅H₅)₂Nb(CO)Cl⁽⁵⁰⁾. A molybdenum trichlorostannate complex has also been formed, by insertion of SnCl₂ into the Mo-Cl bond of (C₇H₇)Mo(CO)₂Cl, yielding (C₇H₇)Mo(CO)₂(SnCl₃). Mixed trihalostannate complexes have been similarly prepared⁽⁵¹⁾.

The mechanism of transition metal-tin bond formation by insertion of tin(II) halides into transition metal-halide bonds has been the subject of much deliberation, with information not easily obtained. Although it has not been proven, there is evidence for the mechanism shown in Figure 1.5 ^(52,53), which proceeds via an intramolecular rearrangement.

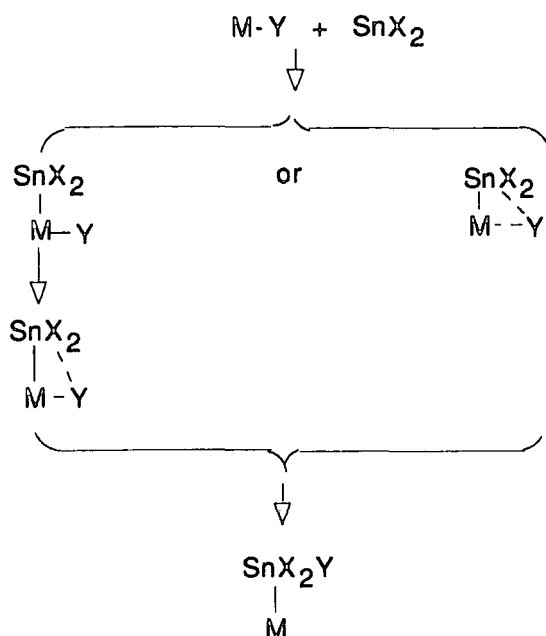


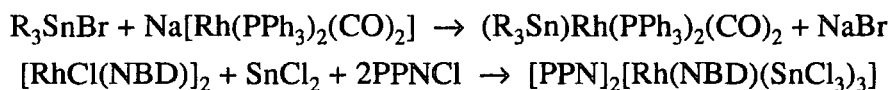
Figure 1.5 Mechanism of Insertion of a Tin(II) Halide into a Metal-Halide Bond

1.4 Transition Metal - Trichlorostannate Complexes

Transition metal-trichlorostannate complexes have been used extensively as catalysts for organic transformations (Section 1.5). Much work has also been carried out to investigate the formation, synthesis, bonding and properties of these complexes, and is described in this section. This review covers the trichlorostannate complexes of the transition metals rhodium, iridium, platinum and palladium, whose chemistry is relevant to catalytic work which is reported in this thesis and to other related catalytic processes.

1.4.1 Rhodium and Iridium Trichlorostannate Complexes

Rhodium-tin complexes can exist in the rhodium(I) and rhodium(III) oxidation states and the tin may also be in two oxidation states, tin(II) and tin(IV). Reaction can occur for both organotin compounds⁽⁵⁴⁾, tin(II) halides⁽⁵⁵⁾ and mixed systems, e.g.



Rhodium(III) chloride reacts with tin(II) chloride in acidic solution to produce the rhodium(I) complex $[\text{Rh}_2\text{Cl}_2(\text{SnCl}_3)_4]^{4-}$, which was precipitated using tetraalkylammonium salts as shown by Young et al⁽⁵⁶⁾. Neutral complexes of

rhodium(I) and iridium(I) have also been prepared by Young et al⁽⁵⁶⁾, with an SnCl_3^- group bound to the metal along with diolefin ligands, for example $(\text{C}_7\text{H}_8)_2\text{RhSnCl}_3$.

A series of rhodium(I) carbonyl trichlorostannate complexes have been prepared^(56,57). $[\text{Rh}(\text{CO})\text{Cl}(\text{SnCl}_3)_2]^{2-}$ was synthesised by reaction of $\text{Rh}_2(\text{CO})_4\text{Cl}_2$ and SnCl_2 in ethanol by Young et al⁽⁵⁶⁾, while in 1971 Kingston and Scollary synthesised complexes of the general type $[\text{Rh}(\text{CO})(\text{SnX}_3)\text{X}_2]^{2-}$ ($\text{X}=\text{Cl}, \text{I}$), $[\text{Rh}(\text{CO})(\text{SnX}_3)_2\text{X}]^{2-}$ ($\text{X}=\text{Cl}, \text{Br}$), and $[\text{Rh}(\text{CO})(\text{SnX}_3)_3]^{2-}$ ($\text{X}=\text{Cl}, \text{Br}$), by reacting halogenocarbonyl rhodium(I) solutions containing for example $[\text{Rh}(\text{CO})_2\text{Cl}_2]^-$ with the respective tin(II) halide⁽⁵⁷⁾. Addition of a 1 molar equivalent of SnCl_2 to a solution of $[\text{Rh}(\text{CO})_2\text{Cl}_2]^-$ yielded salts of $[\text{Rh}(\text{CO})(\text{SnCl}_3)\text{Cl}_2]^{2-}$ upon precipitation. Increasing the amount of SnCl_2 by 2-fold formed $[\text{Rh}(\text{CO})(\text{SnCl}_3)_2\text{Cl}]^{2-}$, whilst 3 molar equivalents of SnCl_2 gave the tri-trichlorostannate rhodium(I) species $[\text{Rh}(\text{CO})(\text{SnCl}_3)_3]^{2-}$, with formation of the trichlorostannate ligands presumably due to insertion of SnCl_2 into the Rh-Cl bond, and by displacement of CO by SnCl_3^- nucleophilic attack. The order of stability towards decomposition was found to be,



Addition of triphenylphosphine replaces all the tin groups from $[\text{Rh}(\text{CO})(\text{SnCl}_3)_3]^{2-}$ yielding $\text{Rh}(\text{CO})(\text{PPh}_3)_2\text{Cl}$. Kingston and Scollary were surprised to find that in the chloro and bromo series, the carbonyl infra-red stretching frequencies of the rhodium-trihalostannate species formed did not vary upon successive replacement of X by SnX_3^- . Successive replacement of Cl^- by a stronger π -acceptor group such as SnCl_3^- would normally be expected to be accompanied by a shift of the carbonyl infra-red bands to a higher frequency.

More recently, rhodium-trichlorostannate complexes have been subjected to extensive NMR studies. ^{119}Sn NMR studies of solutions of RhCl_3 with various molar equivalents of SnCl_2 in aqueous hydrochloric acid⁽⁵⁸⁾ indicated that a redox process operates between rhodium(III) and tin(II) species to form a rhodium(I) complex with five trichlorostannate ligands, $\text{Rh}(\text{SnCl}_3)_5^{4-}$:



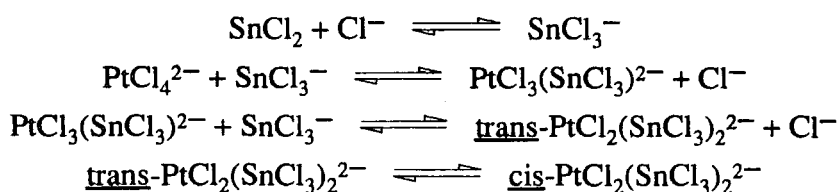
Rhodium(I) and iridium(I) complexes of diolefins $[\text{M}(\text{SnCl}_3)_3(\text{diolefin})]^{2-}$, $[\text{M}(\text{SnCl}_3)_2(\text{diolefin})(\text{PR}_3)]^-$ and $[\text{M}(\text{SnCl}_3)(\text{diolefin})(\text{PR}_3)_2]$ have been prepared

with the diolefin being NBD or COD and their NMR parameters studied^(55,59,60). This data is discussed in more detail with reference to the relevant studies reported throughout this thesis. ¹¹⁹Sn, ¹³C and ³¹P NMR studies were indicative of SnCl₃⁻ behaving as a moderate σ-donor and having an unusually high trans influence. NMR studies in this area have also been carried out by Garralda et al^(61,62,63). Studies of the reaction chemistry of [Rh(SnCl₃)₂(diolefin)(PR₃)]⁻ indicated that reaction with CO yielded [Rh(SnCl₃)₂(CO)₂(PR₃)]⁻ if the diolefin is COD, whereas if the diolefin is NBD then SnCl₃⁻ displacement is effected to give Rh(SnCl₃)(CO)(NBD)(PR₃).

Synthetic and spectroscopic studies of hydrido and carbonylhydrido complexes of iridium containing the trichlorostannate ligand⁽⁶⁴⁾, for example, IrHCIXL₃, IrH₂XL₃, IrH₂XL₃ and IrHCIX(CO)L₂, where X=SnCl₃⁻ or Cl⁻ and L=PPh₃, indicated that the SnCl₃⁻ ligand is a weak σ-donor and a strong π-acceptor, exhibiting a large trans effect. Extensive ¹¹⁹Sn, ³¹P and ¹H NMR studies have also been carried out on iridium trichlorostannate complexes of this nature, and iridium trichlorostannate mixed ligand systems by Pregosin et al^(65,66).

1.4.2 Palladium and Platinum Trichlorostannate Complexes

Early work on the chemistry of tin(II) chloride with platinum and palladium salts focused on the intense colours formed. Later work concentrated on the assignment of structures to these species. The interaction of platinum metal salts with tin(II) chloride^(56,67) led to the formation of cis and trans-[PtCl₂(SnCl₃)₂]²⁻ with the d_π-d_π bonding between platinum and tin, thought to be the reason why the cis isomer is more stable than the trans. The trans isomer was found to be kinetically favoured with the cis form thermodynamically preferred. A series of equilibria are thought to exist in solution:



Several 5-coordinate platinum complexes were also isolated⁽⁶⁸⁾ including [Pt(SnCl₃)₅]³⁻ and [HPt(SnCl₃)₄]³⁻. These 5-coordinate Pt(II) complexes were stabilised by the π-acceptor properties of the trichlorostannate ligand which withdraws electron density from the central platinum atom thus preventing reduction to platinum(0).

It was shown using the criteria of Chatt⁽⁶⁹⁾, through a series of studies of the Pt-H infra-red stretching frequencies for a series of Pt(II) hydrides, that SnCl_3^- is a strongly trans activating ligand⁽⁷⁰⁾. The SnCl_3^- ligand is also a weak σ -donor and a strong π -acceptor⁽⁷¹⁾, with vacant 5d orbitals of the correct size and symmetry to form π -bonds with the filled 5d orbitals of platinum. Thus, it has the ability to stabilise 5-coordinate d^8 transition metal species whilst also favouring a trigonal bipyramidal arrangement of ligands.

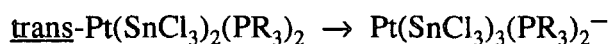
The formation of Pt-SnCl₃ complexes by insertion of SnCl₂ in to the Pt-Cl bond is well documented^(23,67,72-76), and NMR studies have been carried out on the reactions of SnCl₂ with platinum(II) complexes containing mixed ligand systems^(75,77,78,79). Reaction of SnCl₂ with cis-PtCl₂(PR₃)₂⁽⁷⁵⁾ proceeds via insertion into the Pt-Cl bond, followed by isomerisation to the trans species:



Addition of a second mole of SnCl₂ leads to further insertion,

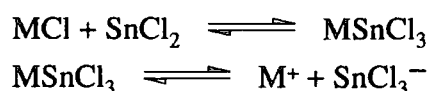


whilst addition of a third mole of SnCl₂ gives rise to a 5-coordinate complex⁽⁷⁷⁾:



It has become clear⁽⁷⁹⁾ that SnCl_3^- promotes 5-coordination in the chemistry of Pt(II) and that its role in catalysis (Section 1.5) with Pt(II) species can be due to its ability to stabilise 5-coordination and also to its ability to labilise other ligands. Pt-SnCl₃ complexes promote the activation of molecular hydrogen such that hydride complexes are formed, thus making them beneficial hydrogenation and hydroformylation catalysts (Section 1.5).

Although solid state structures are known for a number of platinum and palladium complexes the identification of the M-SnCl₃ unit in solution is complicated by the equilibria:



In the presence of excess SnCl_2 poly SnCl_3^- complexes can be formed⁽⁷⁵⁾.

Insertion of SnCl_2 into a palladium-chloride bond also occurs. For example, the addition of SnCl_2 to $\text{Pd}_2(\text{dppm})_2\text{Cl}_2$ ($\text{dppm}=\text{Ph}_2\text{PCH}_2\text{PPh}_2$) to produce $\text{Pd}_2(\text{dppm})_2(\text{SnCl}_3)\text{Cl}$ ⁽⁸⁰⁾ indicates that SnCl_2 will insert into a Pd-Cl bond in preference to a Pd-Pd bond in this stereochemically confined complex.

1.4.3 Bonding in Transition Metal - Trichlorostannate Complexes

Transition metal-trichlorostannate complexes have the ability to catalyse many organic transformations (Section 1.5). The formation of trichlorostannate-transition metal bonds, or the introduction of tin(II) chloride into many of these systems has a promotional effect on the chemistry taking place. Tin(II) chloride also has a promotional effect on the homogeneous rhodium catalysed hydrocarbonylation of ethene, the subject of this thesis⁽¹⁾, clearly implying a synergy between rhodium and tin, and suggesting that the nature of the transition metal-trichlorostannate bond has an effect on the chemistry and transformations taking place at the transition metal centre. Two excellent reviews concerning the nature and structural aspects of this bond have been published^(23,81).

The bonding in molecular tin(II) compounds is explained by considering the use of only two of the valence shell electrons for bonding. This means that in its II+ oxidation state the outer electronic configuration of the element must contain a completely filled s orbital and empty p and d orbitals that could be used in compound formation. The bonding can be described from either a covalent or an electrostatic viewpoint, although it will be an intermediate of both with the best argument depending on the electronegativity between the tin and the bound atom. Based on its outer electronic configuration it is possible to predict four possible ways for tin to form bonds in the II+ oxidation state:

1. By loss of two 5p electrons to form Sn^{2+} .
2. By use of the two 5p electrons for covalent bond formation.
3. By complex formation with the empty 5p and 5d orbitals being included in the hybridisation.
4. By overlap of a directed lone pair orbital on the tin atom with an empty orbital on the acceptor species.

If tin(II) molecules and complex ions contain sterically active lone pairs, they can act as σ -donor species. The ability of a lone pair orbital to act as a donor generally decreases as the atomic mass of the atom increases, and thus the σ -donor strength of the 5s orbital on tin should be small. It is possible, however, for the orbital to act as a donor towards a very powerful acceptor, especially if the empty d orbitals or other orbitals on the tin can also act as π -acceptors to increase the strength of the resulting bond.

The bonding in tin-transition metal species contains both σ and π components. The π -bonding can extend to any of the substituent groups on tin. Coordination via the tin lone pair to a transition metal removes electron density from the tin atom, lowering the energy of its empty orbitals and thus enhancing tin's potential π -backbonding capability with the transition metal and/or the lone pairs of tin's substituent groups. Detailed studies of the behaviour of the trichlorostannate ion as a ligand have shown that it is a weak σ -donor^(24,70,71,82) but that it exhibits a large trans effect^(70,71) because of its ability to form strong d_{π} - d_{π} bonds, especially in the case of platinum group metals. Graham et al^(24,82) analysed carbonyl force constants and concluded that the SnCl_3^- group was a poor σ -donor but an excellent π -acceptor. Parshall^(70,71) studied ^{119}F NMR shielding parameters of fluorophenyl platinum complexes as a sensitive criterion for the σ -donor and π -acceptor properties of a ligand trans to the phenyl group. The results obtained with the trichlorostannate group in the trans position characterised it as a weak σ -donor and a strong π -acceptor. The π -acceptor properties of SnCl_3^- were found to be comparable to those of the two moderate π -acceptor ligands NCS^- and CN^- ⁽⁷⁰⁾. The ability of the SnCl_3^- ligand to shift the Pt-H infra-red stretching frequency and the hydrogen NMR line in trans- $[(\text{C}_2\text{H}_5)_3\text{P}]_2\text{PtHSnCl}_3$ compounds also shows that it is strongly trans activating⁽⁷⁰⁾. The d-orbitals of SnCl_3^- are of the correct size and symmetry to form π -bonds with the filled d orbitals on the platinum metals.

The strength of transition metal-tin bonds and an explanation of why SnCl_3^- has such a strong π -acceptor ability can be rationalised by a consideration of metal-tin bond lengths as shown in Table 1.1.

For $\text{R}_3\text{SnMn}(\text{CO})_3$ complexes there is no change in the tin-manganese bond length when R is changed from phenyl to methyl, since the σ -donor and π -acceptor properties of Me_3Sn^- and Ph_3Sn^- are similar. In contrast, when R is chlorine the tin-manganese bond is significantly shorter than when R is Ph or Me, due to the enhanced π -bonding of SnCl_3^- . This enhanced transition metal-tin π -bonding results

from the removal of electron density from the tin by the electronegative chlorines and the subsequent donation of electron density from the manganese d orbitals to the tin.

Compound	Bond Length/Å	Reference
$(\text{CO})_5\text{MnSnPh}_3$	2.674 (4)	83, 84
$(\text{CO})_5\text{MnSnMe}_3$	2.674 (3)	85, 86
$(\text{CO})_5\text{MnSnCl}_3$	2.590 (5)	87

Table 1.1 Selected Manganese-Tin bond lengths

Tin has also been shown to compete for π -electron density with other ligands coordinated to a transition metal. An example occurs in the case of $[\text{Ru}(\text{CO})_3(\text{SnMe}_3)]_2(\mu\text{-SnMe}_2)_2$ where the Ru-Sn bond trans to the SnMe_3 group is longer than that trans to CO^(88,89). When two tin groups are trans to one another they will compete for electron density from the same metal d orbital, but when CO, which is a weaker π -acceptor ligand, is trans to a tin group, then the π -electron density is preferentially donated to tin, thus shortening the metal-tin bond.

The strong π -acceptor properties of the SnCl_3^- group^(70,71) can be used to explain the trigonal bipyramidal coordination of the platinum(II) species $\text{Pt}(\text{SnCl}_3)_5^{3-}$. Five SnCl_3^- groups can be placed in the environment of the platinum metal atom without an excessive build-up of electrons around the platinum atom, thus stabilising Pt(II) in its 5-coordinate state.

The strong trans influence of the SnCl_3^- ion has been confirmed by a study of the hydrido and carbonyl hydrido complexes of iridium containing SnCl_3^- ⁽⁶⁴⁾. The high metal carbonyl infra-red stretching frequency in trichlorostannato-monocarbonyl bis(1,2-bisdiphenylphosphino-ethane) rhodium(I) also indicates the strong π -acceptor properties of the SnCl_3^- ion⁽⁹⁰⁾. It should be pointed out that there is also significant π -bonding between the tin and the chloride atoms in SnCl_3^- ⁽²³⁾.

1.5 The Catalytic Activity of Transition - Metal Trichlorostannate Complexes

Tin compounds and transition metal-trichlorostannate complexes have been shown to be important co-catalysts and catalysts respectively for many organic transformations, in many cases with tin compounds acting as very efficient promoters. The effectiveness of tin ligands, in particular trichlorostannate ligands in aiding catalytic transformations is generally regarded as being due to their strong labilising effect on the trans ligand and also due to the inherent lability of M-SnCl₃ complexes. Thus, trichlorostannate ligands promote migratory insertions or provide vacant coordination sites on the transition metal by dissociation^(70,71).

There are many examples of organic transformations which can be effected by transition metal-trichlorostannate complexes, in particular those of platinum, palladium, rhodium, iridium and ruthenium. These processes are discussed in the following sections with particular reference to the role of the trichlorostannate ligand and the comparisons and similarities with the rhodium-tin catalysed hydrocarbonylation of ethene, discussed later in this thesis.

1.5.1 Hydrogenation and Isomerisation of Olefins

Early interest in the use of tin(II) halides as co-catalysts was sparked by the discovery that solutions of chloroplatinic acid and tin(II) chloride qualitatively reduced ethene and acetylene at room temperature and atmospheric pressure of hydrogen^(91,92). The reaction is first order with respect to platinum with tin:platinum ratios of at least 5:1 required for maximum rates. A hydride species [PtH(SnCl₃)₄]³⁻ has been detected⁽⁶⁸⁾ under the conditions of catalysis, while the action of ethene alone forms Zeise's salt K[PtCl₃.C₂H₄].H₂O⁽⁹²⁾, with rapid exchange between free and co-ordinated ethene observed in solution. The high trans effect of the SnCl₃⁻ ligand is thought to be responsible for the chemistry taking place, with the ability of the platinum-tin(II) chloride species in solution to cleave the hydrogen molecule and to coordinate a hydrogen atom, along with the olefin, probably taking place at the metal centre via an alkyl intermediate. SnCl₂ also prevents, due to its high π -acceptor ability, the reduction of platinum(II) to platinum metal, and thus prolongs the catalyst life and retention of catalytic activity.

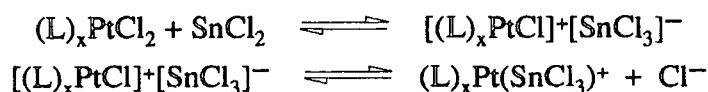
Bond and Hellier⁽⁹³⁾ have shown that in methanol H₂PtCl₆:5SnCl₂ catalyses the isomerisation of 1-pentene to 2-pentene under hydrogen to form trans:cis forms in a

ratio of 85:15. Very little hydrogenation occurs in this system, although 1-hexene can be hydrogenated but with competition from isomerisation⁽⁹⁴⁾.

Jardine and McQuillin⁽⁹⁵⁾ found that $(PPh_3)_2PtHCl$ along with $SnCl_2$ is an effective catalyst for the reduction of norbornadiene, although a similar iridium system was not found to be catalytically active. Bailar et al^(96,97,98) also studied platinum-tin hydrogenation catalysts extensively, examining the effects of solvent, halide, phosphine, temperature and hydrogen pressure on catalytic activity. They found that for polyenes double bond migration to form conjugated dienes, thought originally to precede hydrogenation⁽⁹⁹⁾, is not required. The isomerisation of 1,5-cyclooctadiene⁽⁹⁶⁾ was effected by $[PtCl_2(PPh_3)_2]$ but only in the presence of $SnCl_2 \cdot 2H_2O$, with isomerisation occurring by stepwise migration of the double bonds, via an hydridoplatinum olefin complex as an intermediate. It was suggested that tin(II) chloride activates the catalyst by being coordinated to it through the $SnCl_3^-$ ligand. The π -acceptor properties of the ligand are thought to make the platinum atom susceptible to attack by nucleophiles such as the hydride ion or olefin double bond by removing electron density from the metal centre, and also by stabilising the intermediates formed, thus preventing reduction of the platinum(II) atom.

Studies have also shown that rhodium chloride and platinum chloride systems will effect the isomerisation of butene in the presence of $SnCl_2$ and hydrogen as co-catalysts, via formation of a metal hydride⁽¹⁰⁰⁾. Rhodium and iridium compounds⁽¹⁰¹⁾, $MCl_3 \cdot 3H_2O$ with $SnCl_2$ have also been used to catalyse hydrogen transfer from 2-propanol to cyclohexanones.

Recent studies⁽¹⁰²⁾ have also shown that complexes of the type $LL'PtCl_2$ (L and L' are triarylphosphines) are, in the presence of $SnCl_2$, efficient catalysts for the reduction of styrene. Unlike most cases where high (>10:1) tin:platinum ratios are required for good catalysis, these complexes have maximum efficiency at ratios of 2:1. The two phosphine ligands show opposite dependencies on the electronic properties of the para substituents of the aryl group, suggesting that the ligands have different functions in the catalytic cycle. It has been proposed that $SnCl_3^-$ labilises the weaker base towards substitution, thus providing a vacant coordination site⁽¹⁰³⁾. In support of this, ligand scrambling occurs readily in the reaction of $(R_3P)_2PtCl_2$ with $SnCl_2$ to produce several species⁽¹⁰⁴⁾. Thus, the following equilibria are probably important:



Studies of this transformation have also been carried out for $[PtCl_2(L)(PR_3)]/SnCl_2 \cdot 2H_2O$ systems where $L=SR_2$, $p-XC_6H_4NH_2$; $R=aryl$ ⁽¹⁰⁵⁾.

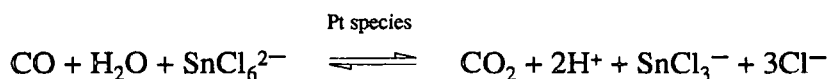
1.5.2 Reductions Under Water Gas Shift Conditions

An active catalytic system for the Water Gas Shift Reaction

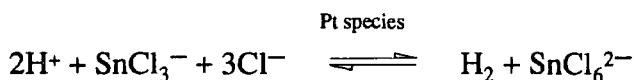


is K_2PtCl_4 and $SnCl_4$ in a mixture of acetic and hydrochloric acid⁽¹⁰⁶⁾. A proposed mechanism for this reaction is shown in Figure 1.6.

Several species have been identified including $[PtCl(CO)(SnCl_3)_2]^-$, $[PtCl_2(CO)(SnCl_3)]^-$ and $[SnCl_6]^{2-}$. The mechanism shows that the formation of CO_2 is catalysed by a tin(IV) species:



while formation of hydrogen is catalysed by a tin(II) species:



Ethene can be reduced to ethane under these conditions with no added hydrogen. Propene is also hydrogenated, though hydrogen formation lowers the yield⁽¹⁰⁷⁾.

1.5.3 Polymerisation

Examples of polymerisation processes affected by transition metal-trichlorostannate complexes are rare, although there are notable exceptions. A catalyst prepared from anhydrous $SnCl_2$ and $RuCl_3 \cdot 3H_2O$ in nitromethane catalyses the trimerisation of 2-methylpropene to hexamethylcyclohexane⁽¹⁰⁸⁾.

Also, the rhodium-trichlorostannate complex $[Rh(SnCl_3)_2Cl_4]^{3-}$, when supported on AV-17-8 anion exchange resin, is a highly active, stable and selective catalyst for the dimerisation of ethene to cis and trans-2-butene⁽¹⁰⁹⁾.

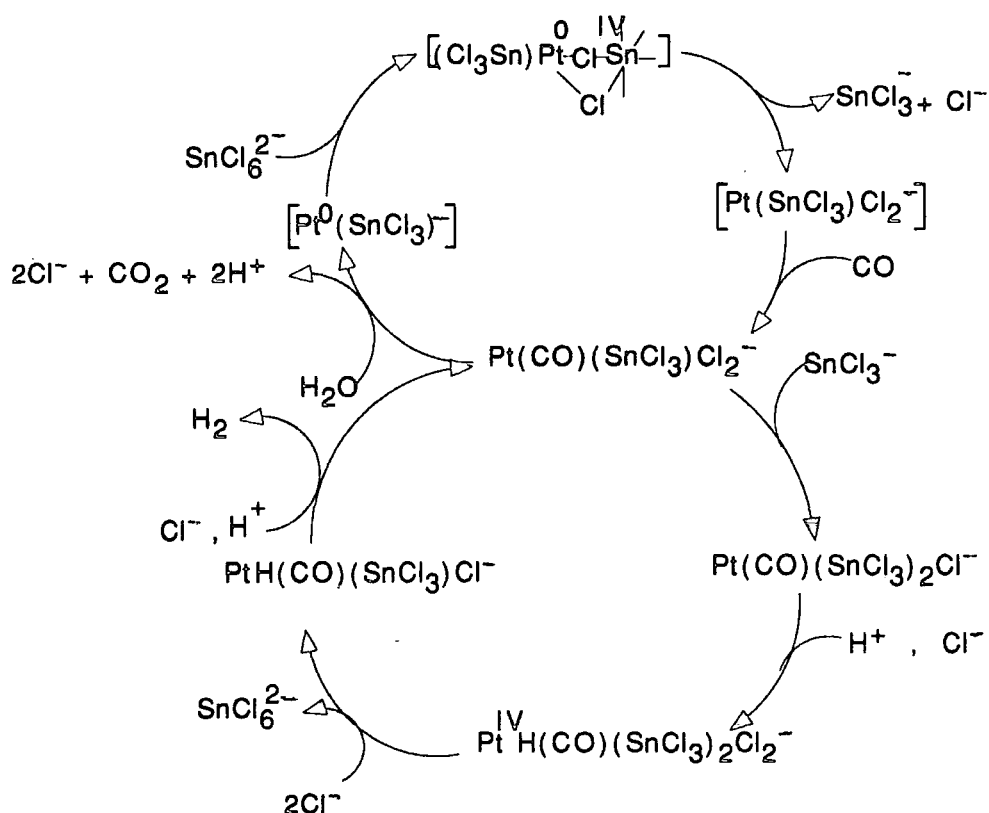


Figure 1.6 Mechanism for the platinum-tin catalysed water gas shift reaction

1.5.4 Hydroformylation of olefins

Hydroformylation generally refers to the reactions of olefins with carbon monoxide and hydrogen. Many transition metals catalyse the hydroformylation of olefins with a sizeable proportion utilising the trichlorostannate ligand or tin(II) chloride as a catalyst.

Clark and co-workers^(72,73,105,110) extensively studied the hydroformylation mechanism for platinum-tin systems and identified several catalytically active species. Using ³¹P, ¹⁹⁵Pt and ¹¹⁹Sn NMR spectroscopy, they have shown that PtPh(SnCl₃)L₂ (L=PPh₃, PPh₂Me) complexes react with CO to yield [Pt(CO)PhL₂]⁺[SnCl₃]⁻, which then goes on to form Pt(COPh)(SnCl₃)L₂ via a migratory insertion reaction, as shown in Figure 1.7.

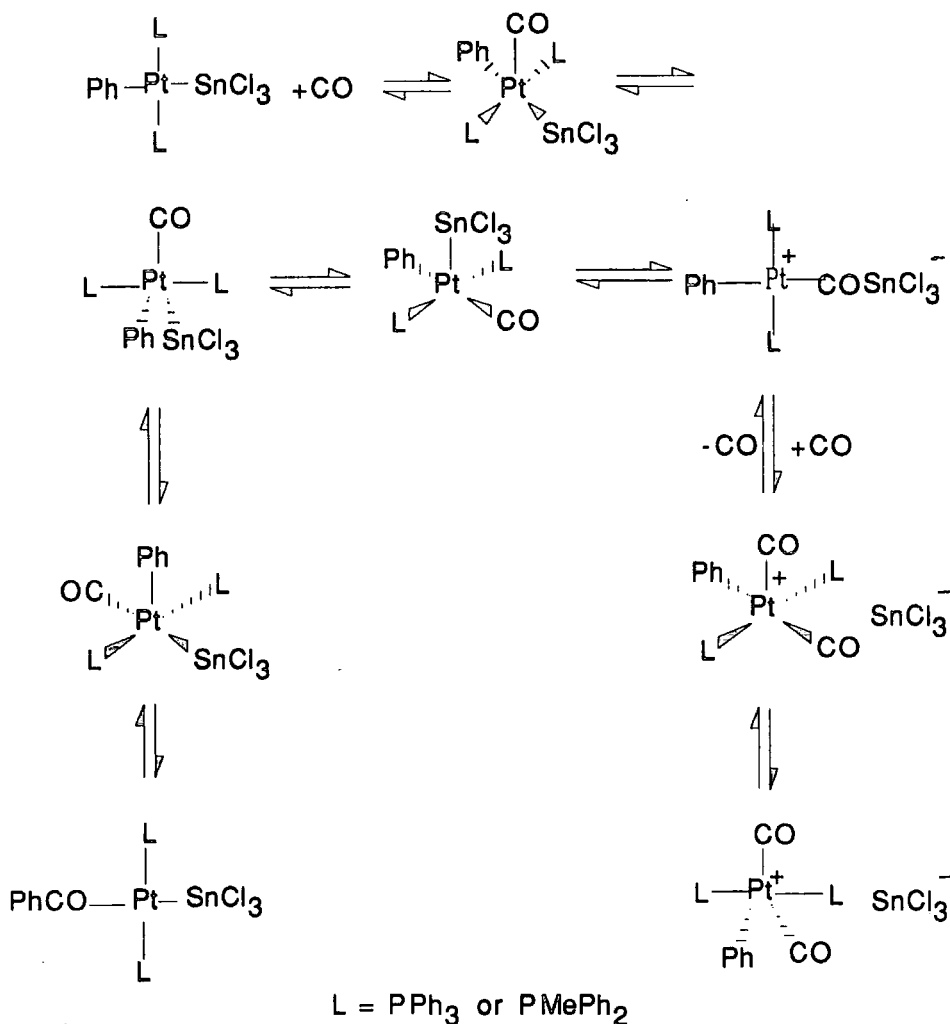


Figure 1.7 The reaction of $\text{PtPh}(\text{SnCl}_3)\text{L}_2$ complexes with CO

The ability of tin(II) chloride to promote the reactions taking place at the metal centre was attributed to the trans influence and trans effect of the SnCl_3^- ligand and its ability to stabilise 5-coordinate species.

Reaction of $\text{Pt}(\text{CO})(\text{PR}_3)\text{Cl}_2$ with $\text{SnCl}_2 \cdot 2\text{H}_2\text{O}$ ^(72,73,105) yielded several species, as shown in Figure 1.8, via insertion reactions into the Pt-Cl bonds and also via displacement reactions. The species shown in Figure 1.8 are themselves hydroformylation catalysts, catalyst precursors⁽¹¹¹⁾, or reaction intermediates⁽¹¹²⁾.

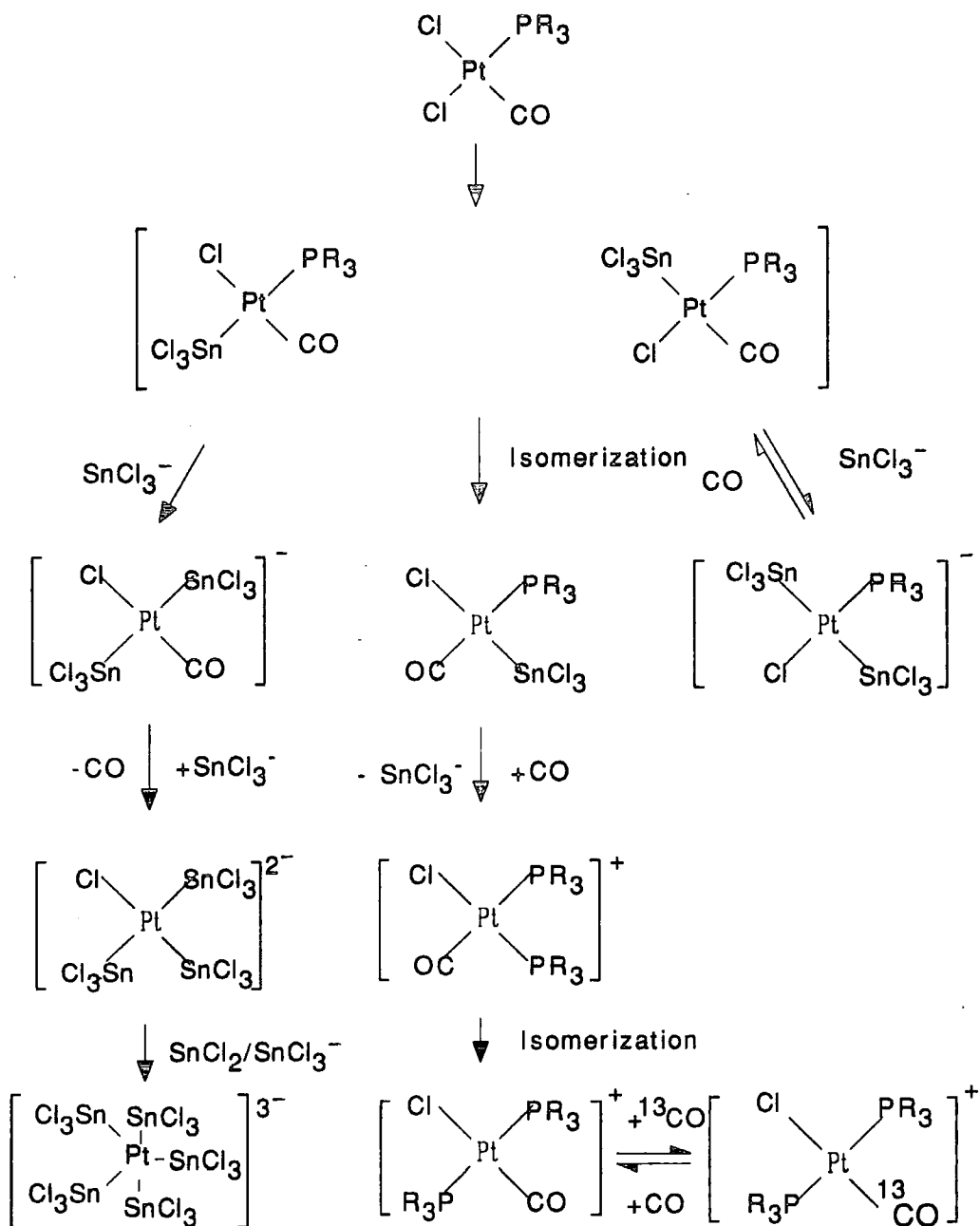


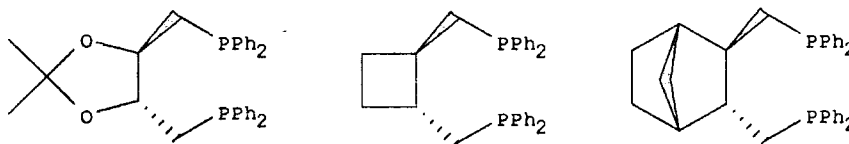
Figure 1.8 The reaction of $\text{Pt}(\text{CO})(\text{PR}_3)\text{Cl}_2$ with $\text{SnCl}_2 \cdot 2\text{H}_2\text{O}$

The work of Clark indicated the complex role of the trichlorostannate ligand, with factors such as solvent type and coordinated ligand affecting reactivity. The work also demonstrated that species in solution under catalytic conditions can differ from those at room temperature and pressure.

Asymmetric hydroformylation employing transition metal catalysts has also been carried out. Optical yields have been modest, being typically 35-50%. The asymmetric hydroformylation of straight chain butenes⁽¹¹³⁾ using a [(-)-DIOP]

PtCl₂-SnCl₂ system showed that asymmetric induction took place after formation of an intermediate metal alkyl complex. The [(-)-DBP-DIOP]PtCl₂/SnCl₂ system had optical yields of 70% although reaction rates were slow⁽¹¹⁴⁾.

Kawabata et al^(115,116,117) have shown that diphosphine derivatives of bis (diphenylphosphino)butane (DPPB) can be part of an efficient catalyst system along with PtCl₂(PhCN)₂/SnCl₂.2H₂O in the hydroformylation of 1-pentene. These systems were found to compare favourably with the important industrial hydroformylation catalyst HRh(CO)(PPh₃)₃. In accordance with the results using monophosphines, steric effects are thought to be more important than electronic effects. It is thought that the rigid skeletons of species such as



increase the instability of the chelate ring and promote the dissociation of one of the phosphines, probably the one trans to the SnCl₃⁻ ligand, thus providing a vacant coordination site.

Hydroformylation of butenoic acid esters⁽¹¹⁸⁾ using cis-Pt(PPh₃)₂Cl₂/SnCl₂ catalysts gave a 95.9% yield of five-carbon ester aldehydes in a linear:branched ratio of 3.93:1. Propene has been hydroformylated using a Pt(acac)₂/SnCl₂.2H₂O/PPh₃ system as catalyst, resulting in a 95% yield of a mixture of 96% linear/4% branched butanals⁽¹¹⁹⁾.

1.5.5 The rhodium-tin-chloride catalysed hydrocarbonylation of ethene to form propanoic acid

Hydrocarbonylation refers to the reaction of olefins with CO and water to form carboxylic acids. Esters are produced by the carbonylation of an olefin in the presence of an alcohol, rather than water.

Several industrial processes employing transition metal catalysts to hydrocarbonylate alkenes have been reported in Section 1.2.3. Recent studies⁽¹⁾, which form the basis for the work described in this thesis, have shown that rhodium(III) chloride

trihydrate is an active catalytic precursor for the hydrocarbonylation of ethene to form propanoic acid, but only when tin(II) chloride is present as a co-catalyst. A summary of the important data obtained from these studies is shown in Table 1.2.

A comparison of Reactions 1 and 2 in Table 1.2 shows that addition of an alkyl ammonium salt, benzyltriethylammonium chloride, to the rhodium-tin-chloride catalytic system, led to an approximate six-fold enhancement in the rate of propanoic acid production. A comparison of Reactions 3, 4 and 5 shows that optimum rates and selectivities for propanoic acid were achieved for the rhodium-tin-chloride systems when a 1:2 molar ratio of rhodium:tin was employed, as in Reactions 2 and 4. Lower tin content led to a decrease in rate and higher tin content lowers both the rate and selectivity. A comparison of Reactions 6, 7 and 8 shows that the optimum temperature for propanoic acid production is 180°C, with the majority of by-product formation occurring at temperatures lower than this. It is interesting to note that in Reactions 2 and 4, both of which were carried out in the same reaction vessel and which are apparently identical systems, the rate of gas uptake and selectivity observed for Reaction 4 are significantly lower than those observed for Reaction 2, but the rate of propanoic acid production is strangely higher for Reaction 4 than for Reaction 2. Although activity was not found to occur for a rhodium-chloride system in the absence of tin(II) chloride, no data has been made available to verify this.

The major organic by-products obtained from the rhodium-tin-chloride catalytic systems were chloroethane, ethyl acetate and ethyl propanoate, and the butyl moieties, butyl acetate, butyl propanoate and 2-chlorobutane. Studies indicated that these products were primarily formed by initial reaction at the catalytically active rhodium centre, but that tin(II) chloride had the ability to generate ethyl moieties such as chloroethane via formation of $C_2H_5SnCl_3$ in solution.

Table 1.2 A summary of the important features of the rhodium-tin-chloride catalysed hydrocarbonylation of ethene taken from the data obtained by a previous worker⁽¹⁾

Moles of propanoic acid produced	Rate bar.hr ⁻¹	Rate of propanoic acid production mol.Kg ⁻¹ .hr ⁻¹	% Selectivity for propanoic acid	Rh:Sn :Bz(Et) ₃ NCl Molar Ratio	Temperature °C
1. Components:		RhCl ₃ .3H ₂ O, SnCl ₂ .2H ₂ O, 37%HCl _(aq) , CH ₃ COOH, CO, C ₂ H ₄			
0.101	21.0	0.89	80.1	1:2:0	180
2. Components:		RhCl ₃ .3H ₂ O, SnCl ₂ .2H ₂ O, Bz(Et) ₃ NCl, 37%HCl _(aq) , CH ₃ COOH, CO, C ₂ H ₄			
0.121	137	5.4	88.6	1:2:3	180
3. Components:		Same as Reaction 2			
0.115	63.0	2.97	91.4	1:1:3	180
4. Components:		Same as Reaction 2*			
0.116	88.0	5.72	79.6	1:2:3	180
5. Components:		Same as Reaction 2			
0.016	160	1.69	50.7	1:4:3	180
6. Components:		RhCl ₃ .3H ₂ O, SnCl ₂ .2H ₂ O, Bu ₄ NCl, 37%HCl _(aq) , CH ₃ COOH, CO, C ₂ H ₄			
0.088	220	8.97	44.2	1:2:2	180
7. Components:		Same as Reaction 6			
6 x 10 ⁻⁴	240	0.097	0.5	1:3:2	150
8. Components:		Same as Reaction 6			
5.6 x 10 ⁻³	102	0.17	10.1	1:3:2	120

For Reactions 1-8 CO pressure = 40 bar, C₂H₄ pressure = 40 bar

* Reactions 2 and 4 are essentially the same, carried out with similar quantities of reagents and in the same reaction vessel.

Studies also showed that no catalytic activity occurred in the absence of HCl from the systems⁽¹⁾. A decrease in the HCl concentration accompanied by an increase in the amount of water in the system led to a decrease in the rate of propanoic acid production (see Table 1.3 below). A completely anhydrous system gave an extremely fast though poorly-selective reaction (see Reaction 3, Table 1.3 below):

Table 1.3 The effect of HCl concentration on the rate of propanoic acid production and the selectivity for propanoic acid (data taken from ref.1)

	Moles of propanoic acid produced	Rate/ bar.hr ⁻¹	Rate of propanoic acid production/ Mol.Kg ⁻¹ .hr ⁻¹	% Selectivity for propanoic acid
1. Components: 2.4ml.2M.HCl _(aq)	0.047	66.2	0.97	88.1
2. Components: 2.4ml.2M.HCl _(aq) + 7.6ml H ₂ O	0.013	15.0	0.27	†
3. Components: HCl _(g)	0.053	236	5.55	46.5

Standard components for each reaction were RhCl₃.3H₂O, SnCl₂.2H₂O, Bz(Et)₃NCl, CH₃COOH - 34ml, CO - 40bar, C₂H₄ - 40bar. Reaction 3 also contained (CH₃CO)₂O to maintain anhydrous conditions. † The percentage selectivity was not reported.

The results in Table 1.3 indicate that an amount of water is detrimental to the yield of acid, but is beneficial to achieve a highly selective production of propanoic acid. Increasing the amount of water above a certain volume, i.e. lowering the HCl_(aq) concentration, lowers the selectivity for propanoic acid, and leads to an increase in the formation of other organic products. The large quantities of water were interpreted as destabilising the complexes involved in the catalytic reaction, thus leading to by-product formation.

Tin(IV) complexes such as $[\text{Bz}(\text{Et})_3\text{N}]_2\text{SnCl}_6$ were also found to catalyse the hydrocarbonylation of ethene to form propanoic acid.

The data obtained under the optimum conditions clearly suggested a synergy between rhodium and tin. The data was found to be consistent with the formation of species such as $[\text{Rh}(\text{CO})_2(\text{SnCl}_3)_2]^-$ and $[\text{Rh}(\text{CO})_2(\text{SnCl}_3)_3]^{2-}$ as potential catalysts or catalytic precursors. The reaction was then thought to proceed via initial oxidative addition of species such as HCl , HSnCl_3 , $\text{C}_2\text{H}_5\text{Cl}$ or $\text{C}_2\text{H}_5\text{SnCl}_3$. However, the exact nature of the active catalyst was unclear, and the role of the tin was deemed speculative.

1.5.6 Other transition metal/tin carbonylation reactions to form acids and esters

Esters are produced by the carbonylation of an olefin in the presence of an alcohol, whereas water is used in the hydrocarbonylation of olefins to form acids.

Knifton et al⁽¹²⁰⁻¹²³⁾ investigated the reactions of α -olefins to form carboxylic acids and esters using platinum and palladium phosphine, arsine and stibine complexes with SnCl_2 as a co-catalyst. For the platinum systems^(120,122) phosphine complexes generally proved to be better catalysts than arsine and stibine analogues, although $\text{Ph}_3\text{As-Pt}$ complexes were very good catalysts in certain cases. Co-catalyst activity decreased in the order



Up to 98 mol % selectivity for linear esters can be achieved with SnCl_2 as co-catalyst with hydrogenation and isomerisation acting as competing reactions. Complexes such as $\text{HPt}(\text{PPh}_3)_2\text{CO}(\text{SnCl}_3)$ and $(\text{PPh}_3)_2\text{PtCl}(\text{SnCl}_3)$ have been isolated from solutions under carbonylation conditions. The addition of SnCl_2 to solutions of the complex $(\text{Ph}_3\text{As})_2\text{PtCl}_2$ in non or moderately polar solvents generates an active and very regiospecific carbonylation catalyst which is highly sensitive to co-ordinated ligand structure and the structure of the olefin.

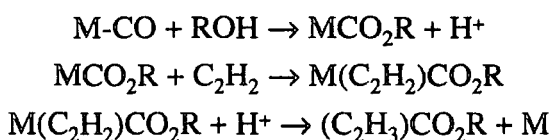
Amongst stabilised Pt(II)- SnCl_3 catalysts, the highest yields have been obtained with ligands of low basicity and high π -acceptor strength such as AsPh_3 , AsClPh_2 , and $\text{P}(\text{OPh})_3$ and the co-catalysts with a high π -acceptor strength i.e. SnCl_3^- . These ligands lower the electron density of the platinum favouring platinum hydride

formation⁽¹²⁴⁾ and attack by nucleophiles such as CO and the olefin⁽⁹⁶⁾. $\text{PtH}(\text{SnCl}_3)(\text{CO})(\text{PPh}_3)_2$ has also been found to be catalytically active for the hydroformylation of 1-pentene to hexanal showing 95% selectivity⁽¹²⁵⁾.

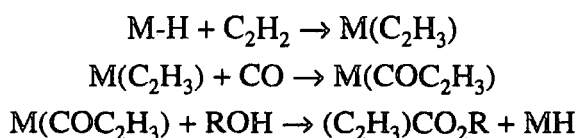
Studies of palladium systems^(121,123) indicated that the catalyst activity was related to the steric and electronic nature of the phosphine ligands, although simple correlations proved difficult to formulate⁽¹²¹⁾. Again SnCl_2 , as co-catalyst, gave the best selectivity. GeCl_2 was equally efficient whereas PbCl_2 and SnI_2 proved to be worse than no catalyst at all. In general both linear and branched carbonylation products are obtained, depending on the nature of the Pt or Pd catalyst used.

The selectivity of linear:branched esters obtained by using $\text{Pt}(\text{PPh}_3)_2\text{Cl}_2/\text{SnCl}_2$ as a carbonylation catalyst system has been enhanced to approximately 150:1 by using a polymer support⁽²³⁾ although a long catalyst life could not be achieved. Knifton improved this reaction. Carbonylation of acetylenes allowed formation of unsaturated esters in >65% yield with 81% linear selectivity. High CO pressures of 136atm were necessary for fast rates, whereas a lower temperature(295K) and pressure(1atm) increased selectivity at the expense of only slightly lowering the percentage conversion⁽¹²⁶⁾. A proposed mechanism is shown below⁽¹²⁷⁾.

Scheme 1



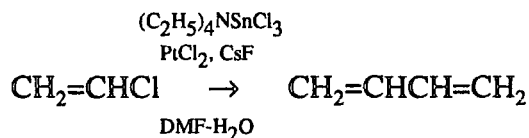
Scheme 2



Kehoe and Schell⁽¹²⁸⁾ have used mixture of chloroplatinic acid and tin(II) chloride to hydrocarbonylate terminal olefins to acids in water and to carbonylate them to esters in alcohols. Forcing conditions of 363K and 3000psi CO were required although high conversions of up to 98% were obtained. Yields of up to 90% could be reached depending on the olefin employed. Linearity of the products was generally around 85% with the alkenes used including 1-hexene, 1-dodecene and 1,7-octadiene.

1.5.7 Coupling Reactions

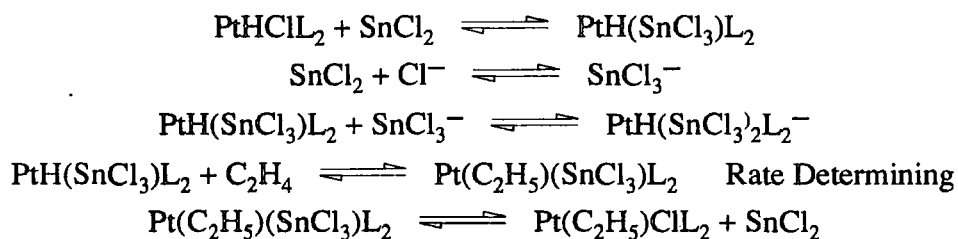
Reductive coupling of vinyl chloride to butadiene is effected at 25°C by tin (II) in solutions containing catalytic amounts of PtCl_2 ⁽¹²⁹⁾. The reaction is co-catalysed by caesium fluoride:



Under the best conditions conversion to butadiene is nearly quantitative but falls rapidly with Sn:Pt ratios greater than 5:1.

1.5.8 Other Reactions

The addition of SnCl_2 to solutions of PtCl_4^{2-} and ethene increases the rate of formation of Zeise's salt, $\text{K}[(\text{C}_2\text{H}_4)\text{PtCl}_3]\cdot\text{H}_2\text{O}$ ⁽¹³⁰⁾. This has been attributed to the high trans effect of SnCl_3^- . Tin(II) will also catalyse the insertion of ethene into the platinum hydride bond of HPtL_2Cl ($\text{L}=\text{P}(\text{C}_2\text{H}_5)_3$)⁽¹³¹⁾. Kinetic studies are in accordance with the following mechanism:



A homogeneous catalyst mixture of $\text{RhCl}_3\cdot 3\text{H}_2\text{O}/\text{SnCl}_2\cdot 2\text{H}_2\text{O}$ and LiCl is well known to dehydrogenate propan-2-ol yielding acetone and dihydrogen^(132,133) with ^{119}Sn and ^1H NMR studies showing that the complexes $[\text{RhCl}_n(\text{SnCl}_3)_{6-n}]^{3-}$ ($n=1$ to 5) and $[\text{RhH}(\text{SnCl}_3)_5]^{3-}$ exist in solution, with the hydride ligand stabilised only by the SnCl_3^- ligands⁽¹³⁴⁾.

1.6 References

1. N.J. Winter, Ph.D. Thesis, University of Durham, 1991.
2. R.S. Dickson, 'Homogeneous Catalysis with Compounds of Rhodium and Iridium'. D. Reidel Publishing Company.
3. D. Forster, *Adv. Organometal. Chem.*, 1979, 17.
4. R.P.A. Sneedon, *Comprehensive Organometallic Chemistry*, Ed. G.W. Wilkinson, F.G.A. Stone, E.W. Abel, Pergamon Press, First Edition, 1982, 8, 19.
5. N. Kutepow, *Chem. Ing. Tech.*, 1965, 37, 385.
6. H. Hohenschutz, *Hydrocarbon Processes*, 1966, 45(11), 141.
7. F.E. Paulik, J.F. Roth, *Chem. Commun.*, 1968, 1578.
8. F.E. Paulik, U.S. Patent 3 769 329, 1973, *Chem. Abstr.*, 1970, 72, 44817n.
9. B.R. James, G.L. Rempel, *Chem. Commun.*, 1967, 158.
10. D. Forster, *Inorg. Chem.*, 1969, 8, 2556.
11. D. Forster, *J. Am. Chem. Soc.*, 1976, 98, 846.
12. S.W. Polichnowski, *J. Chem. Ed.*, 1986, 63, 207.
13. B.A.S.F., Br. Patent 714659, 1954, *Chem. Abstr.*, 1956, 50, 6500.
14. W. Reppe, A. Magin, U.S. Patent 2 577 208, 1951, *Chem. Abstr.*, 48, 11306e.
15. T.M. Shryne, H.V. Holler, (Shell Oil Co.), U.S. Patent 3 984 388, 1976.
16. P. Diversi, R. Rossi, *Synthesis*, 1971, 758.
17. G.B. Patent 1 253 758 (London), 1971, *Chem. Abstr.*, 1970, 72, 110, 811j.
18. U.S. Patent 3 579 551, 1971, *Chem. Abstr.*, 1970, 72, 110811j.
19. U.S. Patent 3 989 748, 1976, *Chem. Abstr.*, 1970, 72, 110811j.
20. U.S. Patent 3 989 747, 1976, *Chem. Abstr.*, 1970, 72, 110811j.
21. D. Forster, *Catal. Rev. Sci. Eng.*, 1981, 23, 89.
22. E.C. Bohr, D.E. Hendriksen, R. Eisenberg, *J. Am. Chem. Soc.*, 1980, 102, 1020.
23. M.S. Holt, W.L. Wilson, J.H. Nelson, *Chem. Rev.*, 1989, 89, 11.
24. W. Jetz, P.B. Simons, J.A.J. Thompson, W.A.G. Graham, *Inorg. Chem.*, 1966, 5, 2217.
25. J.R. Mass, W.A.G. Graham, *J. Organometal. Chem.*, 1969, 18, P24.
26. M.C. Baird, *J. Inorg. Nucl. Chem.*, 1967, 29, 367.
27. H.C. Clark, K. Itoh, *Inorg. Chem.*, 1971, 10, 1707.
28. M. Elder, D. Hall, *Inorg. Chem.*, 1969, 8, 1268.
29. F. Bonati, G. Wilkinson, *J. Chem. Soc. (A)*, 1964, 179.
30. A.R. Manning, *Chem. Commun.*, 1966, 906.

31. P. Mazerolles, J. Dubac, M. Lesbre, *J. Organometal. Chem.*, 1968, 12, 143.
32. G. Schmid, G. Etzrodt, *J. Organometal. Chem.*, 1977, 131, 477.
33. E.N. Gladyshev, V.I. Ermolaev, N.S. Vyazankin, Y.A. Sorobin, *Zh. Obshch. Khim.*, 1968, 38, 662.
34. B.J. Cole, J.D. Cotton, D. McWilliam, *J. Organometal. Chem.*, 1974, 64, 223.
35. J.K. Ruff, *Inorg. Chem.*, 1967, 6, 2080.
36. C.M. Giandomenico, J.C. Devan, S.J. Lippard, *J. Am. Chem. Soc.*, 1981, 103, 1407.
37. P. Hackett, A.R. Manning, *J. Chem. Soc. Dalton.*, 1972, 50, 977.
38. P.F. Barrett, K.K.W. Sun, *Can. J. Chem.*, 1970, 48, 3300.
39. P.F. Barrett, W.J. Jacobs, *Can. J. Chem.*, 1972, 50, 972.
40. N. Viswanathan, E.D. Morrison, G.L. Geoffrey, S.J. Geil, A.C. Rheingold, *Inorg. Chem.*, 1986, 25, 3100.
41. A.L. Balch, H. Hope, F.E. Wood, *J. Am. Chem. Soc.*, 1985, 107, 6936.
42. S.G. Bott, J.C. Machell, D.M.P. Mingos, M.J. Watson, *J. Chem. Soc. Dalton. Trans.*, 1991, 859.
43. D.M.T. Chan, T.B. Marder, *Angew. Chem. Int. Ed. Engl.*, 1988, 27, 442.
44. D.J. Patmore, W.A.G. Graham, *Inorg. Chem.*, 1966, 5, 1405.
45. R.J. Goodfellow, I.R. Herbert, *Inorg. Chim. Acta.*, 1982, 65, L161.
46. J.F. Young, *Adv. Inorg. Chem. Radiochem.*, 1968, 11, 92.
47. J. Fortune, A.R. Manning, *Inorg. Chem.*, 1980, 19, 2590.
48. B. Alvarez, D. Miguel, J.A.P-Martinez, V. Riera, S.G-Grandu, *J. Organometal. Chem.*, 1992, 427, C33.
49. G. Fachinetti, S. Del Nero, C. Floriani, *J. Chem. Soc. Dalton. Trans.*, 1976, 203.
50. Y.V. Skrinki, O.G. Volkov, A.A. Pasynskii, A.S. Antsyshkina, L.M. Dikareva, V.N. Ostrikova, M.A. Porai-Koshits, L.S. Davydova, S.G. Sakharov, *J. Organometal. Chem.*, 1984, 263, 345.
51. H.E. Sosse, G. Hoch, M.L. Ziegler, *Z. Anorg. Allg. Chem.*, 1974, 405, 95.
52. B. O'Dwyer, A.R. Manning, *Inorg. Chim. Acta.*, 1980, 38, 103.
53. T. Kruck, E. Ehlert, W. Moltz, M.Z. Schless, *Z. Anorg. Allg. Chem.*, 1975, 414, 277.
54. P.G. Harrison, 'The Chemistry of Tin', 1989, Published Blackie & Sons (Glasgow).

55. M. Kretschmer, P.S. Pregosin, H. Rügger, *J. Organometal. Chem.*, 1983, 241, 87.
56. J.F. Young, R.D. Gillard, G. Wilkinson, *J. Chem. Soc.*, 1964, 5176.
57. J.V. Kingston, G.R. Scollary, *J. Chem.Soc. (A)*., 1971, 3399.
58. H. Moriyama, T. Aoki, S. Shinoda, Y. Saito, *J. Chem. Soc. Dalton.*, 1981, 639.
59. M. Kretschmer, P.S. Pregosin, M. Garralda, *J. Organometal. Chem.*, 1983, 244, 63.
60. R. Uson, L.A. Oro, M.T. Pinillos, A. Arruebo, K.A.O. Starzewski, P.S. Pregosin, *J. Organometal. Chem.*, 1980, 192, 227.
61. M. Garralda, V. Garcia, M. Kretschmer, P.S. Pregosin, H. Rügger, *Helv. Chim. Acta.*, 1981, 54, L5.
62. V. Garcia, M.A. Garralda, E. Zugosti, *J. Organometal. Chem.*, 1987, 332, 249.
63. M.A. Garralda, E. Pinilla, M.A. Monge, *J. Organometal. Chem.*, 1992, 427, 193.
64. R.C. Taylor, J.F. Young, G. Wilkinson, *Inorg. Chem.*, 1966, 5, 20.
65. M. Kretschmer, P.S. Pregosin, *Inorg. Chim. Acta.*, 1982, 61, 247.
66. H. Moriyama, P.S. Pregosin, Y. Saito, T. Yamakawa, *J. Chem. Soc. Dalton. Trans.*, 1984, 2329.
67. A.G. Davies, G. Wilkinson, J.F. Young, *J. Am. Chem. Soc.*, 1963, 83, 1692.
68. R.D. Cramer, R.V. Lindsey Jr., C.W. Prewitt, U.G. Stolberg, *J. Am. Chem. Soc.*, 1965, 87, 658.
69. J. Chatt, A. Duncanson, B.L. Shaw, *Chem. Ind. (London)*, 1958, 859.
70. R.V. Lindsey Jr., G.W. Parshall, U.G. Stolberg, *J. Am. Chem. Soc.*, 1965, 87, 658.
71. G.W. Parshall, *J. Am. Chem. Soc.*, 1966, 88, 704.
72. G.K. Anderson, H.C. Clark, J.A. Davies, *Inorg. Chem.*, 1983, 22, 434.
73. G.K. Anderson, H.C. Clark, J.A. Davies, *Inorg. Chem.*, 1983, 22, 427.
74. A.S. Mayer, G.H. Ayres, *J. Am. Chem. Soc.*, 1955, 77, 2671.
75. P.S. Pregosin, S.N. Sze, *Helv. Chim. Acta.*, 1978, 61, 1848.
76. T.A.K. Al-Allaff, C. Ealom, P.B. Hitchcock, M.F. Lappert, A. Pidcock, *J. Chem. Soc. Chem. Commun.*, 1985, 548.
77. K.H.A.O. Starzewski, P.S. Pregosin, H. Rügger, *Helv. Chim. Acta.*, 1982, 65, 785.
78. A.B. Goel, S. Goel, *Inorg. Chim. Acta.*, 1984, 82, 41.
79. A. Albinati, P.S. Pregosin, H. Rügger, *Inorg. Chem.*, 1984, 23, 3223.

80. M.M. Olmstead, L.S. Benner, H. Hope, A.L. Balch, *Inorg. Chim. Acta.*, **1979**, 32, 193.
81. J.D. Donaldson, 'Progress in Inorganic Chemistry', Vol. 8., p287.
82. W.A.G. Graham, *Inorg. Chem.*, **1968**, 7, 315.
83. B.Y.K. Ho, J.J. Zuckerman, *J. Organometal. Chem.*, **1973**, 49, 1.
84. J.A. Zubieta, J.J. Zuckerman, S.J. Volzy, 'Progress in Inorganic Chemistry', Interscience: New York, **1978**, p251.
85. P.B. Hitchcock, M.F. Lappert, A.T. Sunday, A. Thorn, A.J. Carthy, N.J. Naylor, *J. Organometal. Chem.*, **1986**, 315, 27.
86. P. Jutzi, B. Hampel, W. Stroppel, C. Kruger, K. Angermund, P. Hoffman, *Chem. Ber.*, **1985**, 118, 2789.
87. M.I. Bruce, 'Comprehensive Organometallic Chemistry', 9, 1209.
88. A. Bonny, *Coord. Chem. Rev.*, **1978**, 28, 229.
89. J.D. Cotton, S.R.A. Knox, F.G.A. Stone, *Chem. Commun.*, **1967**, 965.
90. M. Freni, V. Valenti, D. Guisto, *J. Inorg. Nucl. Chem.*, **1965**, 27, 2635.
91. J.F. Young, *Adv. Inorg. Radiochem.*, **1968**, 11, 91.
92. R.D. Cramer, E.L. Jenner, R.V. Lindsey Jr., U.G. Stolberg, *J. Am. Chem. Soc.*, **1963**, 85, 1691.
93. G.C. Bond, M. Hellier, *J. Catal.*, **1967**, 7, 217.
94. L.P. Vant Hof, B.G. Linsen, *J. Catal.*, **1967**, 7, 295.
95. I. Jardine, F.J. McQuillin, *Tetrahedron Lett*, **1966**, 40, 4871.
96. H.A. Tayim, J.C. Bailar Jr., *J. Am. Chem. Soc.*, **1967**, 89, 3420.
97. J.C. Bailar Jr., H. Itatani, *J. Am. Chem. Soc.*, **1967**, 89, 1592.
98. J.C. Bailar Jr., H. Itatani, *Inorg. Chem.*, **1965**, 4, 1618.
99. H.A. Tayim, J.C. Bailar Jr., *J. Am. Chem. Soc.*, **1968**, 90, 6051.
100. R. Cramer, R.V. Lindsey Jr., *J. Am. Chem. Soc.*, **1966**, 88, 3534.
101. J. Kaspar, R. Spogliarich, M. Graziani, *J. Organometal. Chem.*, **1982**, 231, 71.
102. H. Motschi, P.S. Pregosin, L.M. Venanzi, *Helv. Chim. Acta.*, **1979**, 62, 667.
103. H.C. Clark, C. Billard, C.S. Wong, *J. Organometal. Chem.*, **1980**, 190, C105.
104. M.S. Holt, J.J. MacDougall, F. Mathey, J.H. Nelson, *Inorg. Chem.*, **1984**, 23, 449.
105. G.K. Anderson, C. Billard, H.C. Clark, J.A. Davies, C.S. Wong, *Inorg. Chem.*, **1983**, 22, 439.
106. C. Cheng, R. Eisenberg, *J. Am. Chem. Soc.*, **1968**, 100, 2968.
107. C. Cheng, L. Kuritzkes, R. Eisenberg, *J. Organometal. Chem.*, **1980**, 190, C21.
108. J. E. Hamlin, P.M. Maitlis, *J. Mol. Catal.*, **1981**, 11, 129.

109. P.G. Antonov, N.V. Borunova, V.I. Anufriev, V.M. Ignatov, *Izv. Vyssh. Uchebn. Zaved. Khim. Khim. Technal.*, 1979, 22, 952.
110. G.K. Anderson, H.C. Clark, J.A. Davies, *Organometallics*, 1982, 1, 64.
111. G. Cavinato, L. Toniolo, *J. Organometal. Chem.*, 1983, 241, 275.
112. A. Scrivanti, G. Cavinato, L. Toniolo, C. Botteghi, *J. Organometal. Chem.*, 1985, 286, 115.
113. G. Consiglio, P. Pino, *Helv. Chim. Acta.*, 1976, 59, 642.
114. G. Consiglio, P. Pino, L.I. Flowers, C.U. Pittman Jr., *J. Chem. Soc. Chem. Commun.*, 1983, 612.
115. Y. Kawabata, T. Suzuki, I. Ogata, *Bull. Chem. Soc. Jpn.*, 1978, 361.
116. Y. Kawabata, T. Hayashi, I. Ogata, *J. Chem. Soc. Chem. Commun.*, 1979, 462.
117. T. Hayashi, Y. Kawabata, T. Isoyama, I. Ogata, *Bull. Chem. Soc. Jpn.*, 1981, 54, 3438.
118. G. Moretti, C. Botteghi, L. Toniolo, *J. Mol. Catal.*, 1987, 39, 177.
119. C.Y. Hsu, *Eur. Pat. Appl. EP 81921*.
120. J.F. Knifton, *J. Org. Chem.*, 1976, 41, 2885.
121. J.F. Knifton, *J. Org. Chem.*, 1976, 41, 793.
122. I. Schwager, J.F. Knifton, *J. Catal.*, 1976, 45, 256.
123. J.F. Knifton, *J. Am. Oil. Chem. Soc.*, 1978, 55, 496.
124. H.A. Tayim, J.C. Bailar Jr., *J. Am. Chem. Soc.*, 1967, 89, 4330.
125. C.Y. Hsu, M. Orchin, *J. Am. Chem. Soc.*, 1975, 97, 3553.
126. J.F. Knifton, *J. Mol. Catal.*, 1977, 2, 293.
127. T.F. Murray, J.R. Norton, *J. Am. Chem. Soc.*, 1979, 101, 4107.
128. L.J. Kehoe, R.J. Schell, *J. Org. Chem.*, 1970, 35, 2846.
129. F.N. Jones, *J. Org. Chem.*, 1967, 32, 1667.
130. R. Cramer, *Inorg. Chem.*, 1965, 4, 445.
131. H.C. Clark, C. Jablonski, J. Halpern, A. Mantovani, J.A. Weil, *Inorg. Chem.*, 1974, 13, 1541.
132. H.B. Charman, *J. Chem. Soc.*, 1970, B584.
133. H. Moriyama, T. Aoki, S. Shinoda, Y. Saito, *J. Chem. Soc. Perkin. Trans (II)*, 1982, 369.
134. T. Yamakawa, S. Shinoda, Y. Saito, H. Moriyama, P.S. Pregosin, *Mag. Res. Chem.*, 1985, 23 202.

Chapter 2

The Reaction Chemistry of Rhodium(I) Carbonyl Chlorides with Tin(II) Chlorides

2.1 Introduction

Homogeneous catalytic work has been carried out to investigate the rhodium(I) catalysed hydrocarbonylation of ethene promoted by tin(II) chloride⁽¹⁾. During the heating process of the reaction, rhodium(III) chloride trihydrate reacts with carbon monoxide⁽²⁾ to produce dichlorotetracarbonyldirrhodium(I) which reacts quickly with the excess chloride ions present in the catalytic system to form the dichlorodicarbonylrhodium(I) anionic species, $[\text{Rh}(\text{CO})_2\text{Cl}_2]^-$ ^(3,4). In the tin(II) promoted reaction⁽¹⁾ further reaction occurs with SnCl_2 and/or SnCl_3^- to form complexes implicated in the catalysis. Under the reaction conditions used, tin(II) chloride, in the presence of chloride ions, will be in equilibrium with the trichlorostannate species SnCl_3^- ,



with the equilibrium being highly in favour of the trichlorostannate species as indicated by ^{119}Sn NMR studies discussed in Section 2.3 of this chapter.

Catalytic work has shown that the optimum rhodium to tin molar ratio for the hydrocarbonylation process is 1:2, with a large cation, typically benzyltriethylammonium chloride, also giving a significant six-fold increase in the rate of reaction when in combination with tin(II) chloride.⁽¹⁾

The chemistry achieved during the catalytic process has prompted an investigation of the reaction chemistry of the rhodium(I) carbonyl chlorides, dichlorotetracarbonyldirrhodium(I) and the benzyltriethylammonium salt of dichlorodicarbonylrhodium(I) with tin(II) chlorides, which is reported in this chapter. The reactions were carried out at atmospheric pressure with the intention of probing the fundamental chemistry occurring between the species, and of relating this to chemistry which occurs during the catalytic process.

The reactions were primarily followed by the use of Fourier Transform Infra-Red spectroscopy to monitor changes in the stretching frequencies of the carbonyl absorptions as the reactions progressed. The solution samples were contained within a liquid cell having CaF_2 windows. Each spectrum was recorded using 16 scans and a resolution of 2cm^{-1} . Several reactions were also monitored using ^{119}Sn NMR spectroscopy. Table 2.1 summarises the known infra-red data in various solvents for the rhodium(I) carbonyl chloride starting materials used throughout this work, and

also the infra-red data for various known rhodium(I) carbonyl trichlorostannate complexes, reported in later chapters.

Table 2.1 Carbonyl infra-red stretching frequencies of various rhodium(I) carbonyl chloride and rhodium(I) carbonyl trichlorostannate complexes.

Complex	Solvent	$\nu(\text{CO})/\text{cm}^{-1}$
$\diamond[\text{Rh}(\text{CO})_2\text{Cl}_2]^-$ $\square[\text{Rh}(\text{CO})_2\text{Cl}_2]^-$	THF CH_2Cl_2 CH_3COOH Nujol Nujol ⁽⁴⁾	1984 _s 2062 _s 1994 _s 2071 _s 2001 _s 2076 _s 1991 _s 2081 _s 1982 2060
$\text{Rh}_2(\text{CO})_4\text{Cl}_2$	THF* CH_2Cl_2 CH_3COOH Nujol Hexane ⁽²⁾	2034 _s 2090 _s 2107 _w 2035 _s 2092 _s 2108 _w 2037 _s 2093 _s 2034 _s 2088 _s 2104 _w 2035 _s 2089 _s 2105 _m
$\diamond[\text{Rh}(\text{CO})(\text{SnCl}_3)_2\text{Cl}]^{2-}$ (Chapter 3, Sec. 3.2.2) $^+[\text{Rh}(\text{CO})(\text{SnCl}_3)_2\text{Cl}]^{2-}$ $^+[\text{Rh}(\text{CO})(\text{SnCl}_3)_2\text{Cl}]^{2-}$	Nujol Nujol KBr	2013 _s 2000 ⁽⁵⁾ 2005 ⁽⁶⁾
$\diamond[\text{Rh}(\text{CO})(\text{SnCl}_3)_4]^{3-}$ (Chapter 3, Sec. 3.2.1)	Nujol	2012 _s
$\diamond[\text{Rh}(\text{CO})_2(\text{SnCl}_3)_3]^{2-}$ (Chapter 3, Sec. 3.2.5) $\diamond[\text{Rh}(\text{CO})_2(\text{SnCl}_3)_3]^{2-}$	THF CH_2Cl_2 KBr	2011 _s 2072 _{vw} 2018 _s 2069 _{vw} 2010 2060 ⁽⁷⁾

\diamond $[\text{Bz}(\text{Et})_3\text{N}]^+$ \diamond $[\text{PPN}]^+$ $+$ $[\text{Me}_4\text{N}]^+$ \square $[\text{Ph}_4\text{As}]^+$

* The absorptions at 2034, 2090 and 2107 cm^{-1} are only seen when $\text{Rh}_2(\text{CO})_4\text{Cl}_2$ is in a higher molar quantity than THF. Addition of $\text{Rh}_2(\text{CO})_4\text{Cl}_2$ to a molar excess of THF leads to immediate cleavage of the Rh-Cl-Rh bridges by the solvent molecule to give $\text{Rh}(\text{CO})_2\text{Cl}(\text{THF})$ ⁽⁸⁾ which has strong carbonyl absorptions at 2004 and 2080 cm^{-1} . As a result all of the reactions described in this chapter with $\text{Rh}_2(\text{CO})_4\text{Cl}_2$ dissolved in THF, can be envisaged as reactions of $\text{Rh}(\text{CO})_2\text{Cl}(\text{THF})$.

Dichlorotetracarbonyldirrhodium(I) and benzyltriethylammonium dichlorodicarbonyl rhodium(I) were prepared by methods similar to those used by Wilkinson et al⁽²⁾, and Cleare et al⁽⁴⁾ respectively, and are described in Appendix 1, where the preparation of benzyltriethylammonium trichlorostannate from $\text{Bz}(\text{Et})_3\text{NCl}$ and SnCl_2 is also reported. $[\text{Bz}(\text{Et})_3\text{N}]_2[\text{Rh}(\text{CO})_2(\text{SnCl}_3)_3]$ was prepared by bubbling CO through

solutions of $[\text{Bz}(\text{Et})_3\text{N}]_2[\text{Rh}(\text{COD})(\text{SnCl}_3)_3]$ to remove the 1,5-cyclooctadiene ligand. This, along with the syntheses of $[\text{Bz}(\text{Et})_3\text{N}]_2[\text{Rh}(\text{CO})(\text{SnCl}_3)_2\text{Cl}]$ and $[\text{Bz}(\text{Et})_3\text{N}]_3[\text{Rh}(\text{CO})(\text{SnCl}_3)_4]$ is described in detail in Chapter 3.

The reactions reported in this chapter were carried out in glassware which was evacuated and then flushed with nitrogen prior to the addition of reactants. A counter current of nitrogen was maintained through the systems at all times while the reactions were proceeding. Samples were withdrawn from the reaction mixtures at intervals using a syringe, and injected into the infra-red solution cell.

2.2 Fourier Transform Infra-Red Studies of the Reaction Chemistry Occurring Between Rhodium(I) Carbonyl Chlorides and Tin(II) Chlorides

The reactions were mostly carried out in THF since it aided the solubility of both the rhodium and tin starting materials at ambient temperatures. Reactions in dichloromethane and acetic acid were affected by the relative insolubility of SnCl_2 , and have thus been used less extensively. All solvents were dried and degassed prior to use.

The carbonyl stretching frequency of free carbon monoxide at ca. 2140cm^{-1} is shifted to a lower frequency on bonding to a transition metal. This can be explained in terms of molecular orbital theory⁽⁹⁾. A σ -bond is formed by donation of σ -electrons of CO to an empty orbital of the metal. This tends to raise $\nu(\text{CO})$ since the σ orbital is slightly anti-bonding. A π -bond is also formed by back donation of the $d\pi$ electrons of the metal to empty anti-bonding orbitals, the $2p\pi^*$ orbitals of CO. This tends to lower $\nu(\text{CO})$. The two bonding components are synergic, the net result in the case of bonding to a metal such as rhodium in a low oxidation state being a drift of electrons from rhodium to CO. Thus, the overall effect is to lower the carbonyl stretching frequency, e.g. $\text{Rh}(\text{CO})(\text{PPh}_3)_2\text{Cl}$, $\nu(\text{CO})$ 1977cm^{-1} in nujol.⁽¹⁰⁾

The formation of a Rh-SnCl_3 bond in place of a Rh-Cl bond is expected to shift $\nu(\text{CO})$ to a higher frequency, since the strong π -acceptor ability of the SnCl_3^- group⁽¹¹⁻¹⁴⁾ compared with Cl^- is likely to cause a decrease in the Rh-CO π -backbonding.

2.2.1 Reactions of $[\text{Rh}(\text{CO})_2\text{Cl}_2]^-$ with SnCl_2

These reactions were carried out in various solvents, and employed different molar ratios of rhodium to tin.

Reactions in THF

Table 2.2 summarises the reagents, conditions and infra-red data for the reactions of $[\text{Rh}(\text{CO})_2\text{Cl}_2]^-$ with various molar equivalents of SnCl_2 in THF at 20°C , and clearly shows that, as the amount of SnCl_2 in the system is increased, there is an increase in the intensity of a new absorption at 2011cm^{-1} , assigned to Product A. This is accompanied by a decrease in the amount of $[\text{Bz}(\text{Et})_3\text{N}][\text{Rh}(\text{CO})_2\text{Cl}_2]$ present, until at a Rh:Sn molar ratio of 1:3, all of the $[\text{Bz}(\text{Et})_3\text{N}][\text{Rh}(\text{CO})_2\text{Cl}_2]$ has completely reacted, and only a single strong symmetrical absorption at 2013cm^{-1} and a very weak absorption at 2072cm^{-1} , also assigned to Product A, remain. Unfortunately, the very weak $\nu(\text{CO})$ stretching frequency at 2072cm^{-1} , assigned to Product A, was not observed at Sn:Rh molar ratios lower than 3:1. The weak intensity of this absorption, and the presence of other complexes e.g. $[\text{Rh}(\text{CO})_2\text{Cl}_2]^-$ and $\text{Rh}(\text{CO})_2\text{Cl}(\text{THF})$, having absorptions in the same region at these molar ratios, all contribute to its lack of detection at Sn:Rh molar ratios less than 3:1. These arguments may also be used to explain the inability to detect this weak absorption for other similar reactions in both THF and CH_2Cl_2 reported throughout this chapter, although the possibility that this absorption is not present at Sn:Rh molar ratios less than 3:1 cannot be ruled out. Nevertheless, since their frequencies compare so closely the absorptions at 2011 and 2013cm^{-1} are assigned to the same species, Product A. The absorptions observed at 2013_s and $2072_{\text{vw}}\text{cm}^{-1}$ when the Rh:Sn molar ratio is 1:3 are shown in Figure 2.1. Figure 2.2 clearly illustrates the changes in the intensities of the carbonyl absorptions as the Rh:Sn molar ratio is changed from 1:1 to 1:3, and the appearance of the new absorption at 2011cm^{-1} .

Several rhodium(I) carbonyl trichlorostannate complexes have carbonyl absorptions in the region $2010\text{-}2013\text{cm}^{-1}$ (see Table 2.1), and therefore although the new absorptions at $2011/2013_s$ and $2072_{\text{vw}}\text{cm}^{-1}$ appear to be consistent with the formation of a Rh(I)-CO-SnCl₃ complex, they cannot be categorically assigned to one particular species purely on the basis of infra-red data, particularly since the very weak high frequency absorption is only observed in certain reactions. However, the data is possibly consistent with the formation of a rhodium(I) complex containing two carbonyl groups and several SnCl₃⁻ groups, and since all of the starting material is consumed when a Rh:Sn stoichiometry of 1:3 is used, the product complex may be of the type $[\text{Rh}(\text{CO})_2(\text{SnCl}_3)_3]^{2-}$. Indeed, the infra-red data for Product A when

using a Sn:Rh molar ratio of 3:1 ($\nu(\text{CO})$ 2013_s, 2072_{vw} cm⁻¹) compares very closely with that observed for [Bz(Et)₃N]₂[Rh(CO)₂(SnCl₃)₃] in THF ($\nu(\text{CO})$ 2011_s, 2072_{vw} cm⁻¹, see Table 2.1 and Chapter 3, Section 3.2.5), which is prepared from the reaction of [Bz(Et)₃N]₂[Rh(COD)(SnCl₃)₃] with CO by a method similar to that of Pregosin et al⁽⁷⁾.

Addition of higher molar equivalents of Sn:Rh to the system, (i.e. Reactions 2.2.1.E and 2.2.1.F) where the Rh:Sn molar ratio is 1:4 and 1:6 respectively), produced no change in the frequency position or the intensity of the absorption at 2011/13 cm⁻¹. The sequence of reactions indicate that the reaction is complete when a Rh:Sn molar ratio of 1:4 is reached, although the very weak absorption at 2072 cm⁻¹ was not observed for a Rh:Sn molar ratio of 1:6. Reactions 2.2.1.A-2.2.1.C showed a decrease in the intensity of the new absorption at 2011/2013 cm⁻¹ on storing over a 2 day period, coupled with a small increase in the intensity of the absorptions corresponding to [Bz(Et)₃N][Rh(CO)₂Cl₂], indicating loss of tin from the product complex.

Figure 2.1 Carbonyl absorptions observed for the 1:3 reaction of [Rh(CO)₂Cl₂]⁻ with SnCl₂ in THF at 20°C

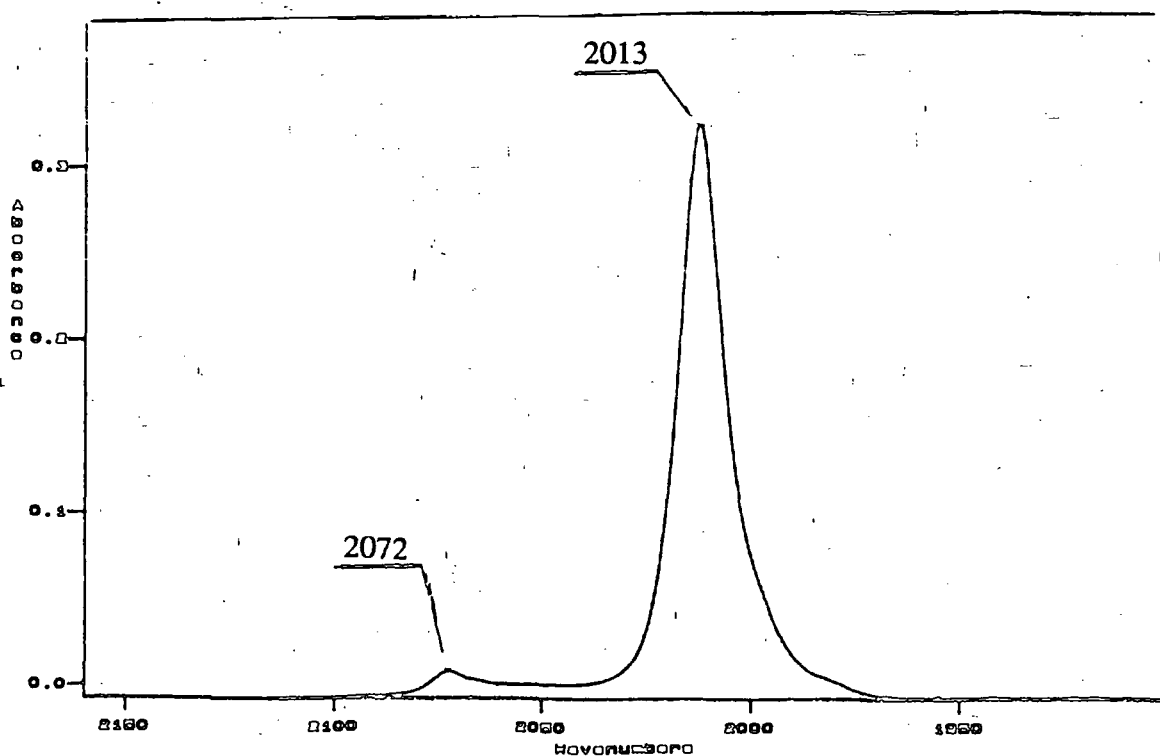


Table 2.2 Reagents, conditions and infra-red data for the reactions of $[\text{Rh}(\text{CO})_2\text{Cl}_2]^-$ with SnCl_2 in THF at 20°C

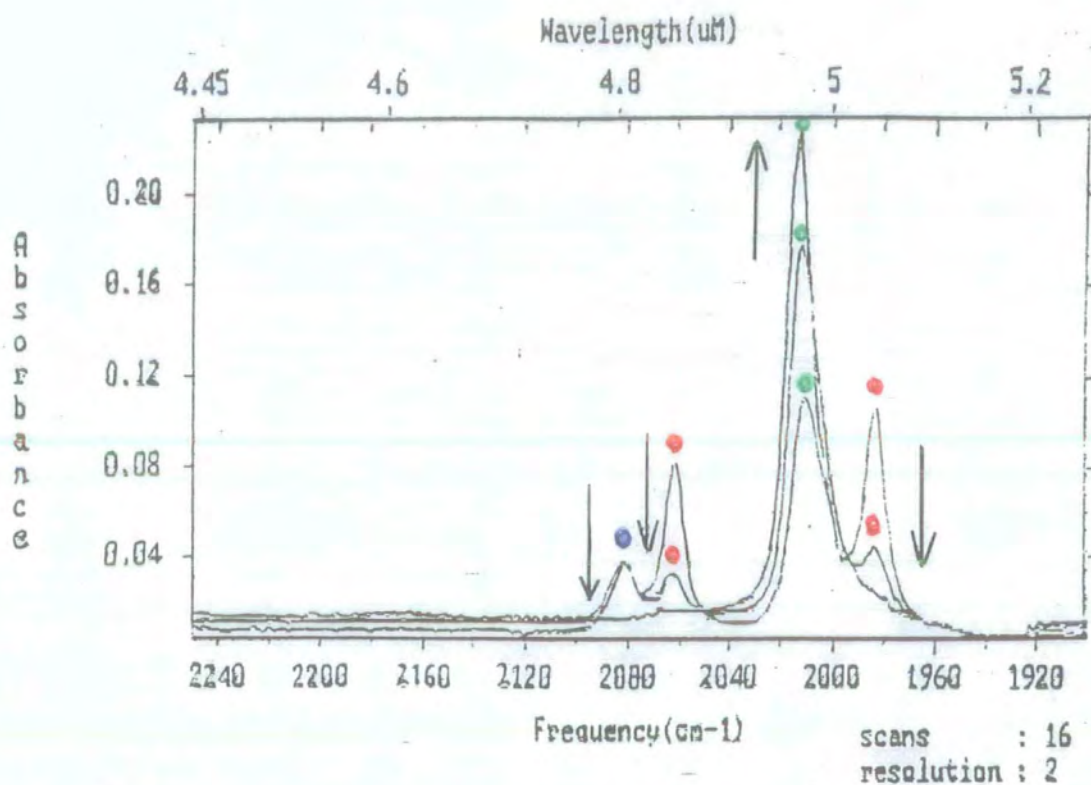
Reaction Code	Reactants	Rh:Sn Molar Ratio	Solvent	Reaction Time	Colour Changes	$\nu(\text{CO})/\text{cm}^{-1}$ Observed	Assignment
2.2.1.A	* $[\text{Rh}(\text{CO})_2\text{Cl}_2]^-$ SnCl_2	2 : 1 ^a	THF ^{a1}	Instantaneous	Yellow→Pale orange	1984 _s 2062 _s 2004 _{sh} 2080 _{vw} 2011 _w	$[\text{Rh}(\text{CO})_2\text{Cl}_2]^-$ $\text{Rh}(\text{CO})_2\text{Cl}(\text{THF})$ Product A
2.2.1.B	* $[\text{Rh}(\text{CO})_2\text{Cl}_2]^-$ SnCl_2	1 : 1 ^b	THF ^{b1}	Instantaneous	Yellow→Orange	1984 _{ms} 2062 _{ms} 2004 _{sh} 2081 _{ws} 2011 _{ms}	$[\text{Rh}(\text{CO})_2\text{Cl}_2]^-$ $\text{Rh}(\text{CO})_2\text{Cl}(\text{THF})$ Product A
2.2.1.C	* $[\text{Rh}(\text{CO})_2\text{Cl}_2]^-$ SnCl_2	1 : 2 ^c	THF ^{c1}	Instantaneous	Yellow→Orange	1984 _w 2061 _w 2004 _{sh} 2081 _w 2011 _s	$[\text{Rh}(\text{CO})_2\text{Cl}_2]^-$ $\text{Rh}(\text{CO})_2\text{Cl}(\text{THF})$ Product A
2.2.1.D	* $[\text{Rh}(\text{CO})_2\text{Cl}_2]^-$ SnCl_2	1 : 3 ^d	THF ^{d1}	Instantaneous	Yellow→Deep orange	2013 _s 2072 _{vw}	Product A
2.2.1.E	* $[\text{Rh}(\text{CO})_2\text{Cl}_2]^-$ SnCl_2	1 : 4 ^e	THF ^{e1}	Instantaneous	Yellow→Deep orange	2013 _s 2972 _{vw}	Product A
2.2.1.F	* $[\text{Rh}(\text{CO})_2\text{Cl}_2]^-$ SnCl_2	1 : 6 ^f	THF ^{f1}	Instantaneous	Yellow→Deep orange	2013 _s	Product A

* Cation = $[\text{Bz}(\text{Et})_3\text{N}]^+$

a-32.1mg(0.076mmol):6.5mg(0.034mmol),a1-5ml b-19.8mg(0.047mmol):9.7mg(0.051mmol),b1-5ml c-19.8mg(0.047mmol):18.8mg(0.099mmol),c1-5ml

d-19.8mg(0.047mmol):30.1mg(0.159mmol),d1-5ml e-19.8mg(0.047mmol):40.3mg(0.21mmol),e1-5ml f-19.8mg(0.047mmol):58.7(0.310mmol),f1-5ml

Figure 2.2 Changes in the intensity of the carbonyl absorptions observed upon addition of increasing amounts of SnCl_2 to $[\text{Rh}(\text{CO})_2\text{Cl}_2]^-$ in THF at 20°C .



Assignment

- $[\text{Rh}(\text{CO})_2\text{Cl}_2]^-$
- $\text{Rh}(\text{CO})_2\text{Cl}(\text{THF})$
- Product A

Table 2.3 Reagents, conditions and infra-red data obtained for the reactions of $[\text{Rh}(\text{CO})_2\text{Cl}_2]^-$ with SnCl_2 in CH_2Cl_2 at 20°C

Reaction Code	Reactants	Rh:Sn Molar Ratio	Solvent	Colour Changes	Reaction Time	$\nu(\text{CO})/\text{cm}^{-1}$ Observed	Assignment
2.2.1.G	$*[\text{Rh}(\text{CO})_2\text{Cl}_2]^-$ SnCl_2	1 : 1 ^g	$\text{CH}_2\text{Cl}_2^{\text{g1}}$	Yellow→Orange	2 hours	1994 _s 2072 _s 2036 _w 2092 _w 2018 _m	$[\text{Rh}(\text{CO})_2\text{Cl}_2]^-$ $\text{Rh}_2(\text{CO})_4\text{Cl}_2$ Product B
2.2.1.H	$*[\text{Rh}(\text{CO})_2\text{Cl}_2]^-$ SnCl_2	1 : 3 ^h	$\text{CH}_2\text{Cl}_2^{\text{h1}}$	Yellow→Pale orange	1 min	1994 _s 2071 _s 2036 _w 2092 _w 2012 _w	$[\text{Rh}(\text{CO})_2\text{Cl}_2]^-$ $\text{Rh}_2(\text{CO})_4\text{Cl}_2$ Product B
				Yellow→Orange	8 min	1995 _w 2072 _w 2035 _s 2092 _s 2108 _w 2018 _s	$[\text{Rh}(\text{CO})_2\text{Cl}_2]^-$ $\text{Rh}_2(\text{CO})_4\text{Cl}_2$ Product B
				Yellow→Red	16 min	2035 _s 2092 _s 2107 _w 2018 _s	$\text{Rh}_2(\text{CO})_4\text{Cl}_2$ Product B
				Yellow→Deep red	30 min	2035 _m 2091 _m 2107 _w 2018 _s	$\text{Rh}_2(\text{CO})_4\text{Cl}_2$ Product B
				Deep red	120 min	2035 _{sh} 2091 _m 2018 _s	$\text{Rh}_2(\text{CO})_4\text{Cl}_2$ Product B

* Cation = $[\text{Bz}(\text{Et})_3\text{N}]^+$ g-52.1mg(0.123mmol):24.9mg(0.132mmol),g1-3ml h-37.4mg(0.089mmol):51.5mg(0.272mmol),h1-10ml

Reactions in CH_2Cl_2

Reactions carried out in dichloromethane, summarised in Table 2.3, were much slower than in THF, mainly due to the insolubility of SnCl_2 which slowly dissolved as the reaction progressed, thus allowing the changes in the intensities of the carbonyl absorptions to be measured as a function of time.

The absorption observed at 2018cm^{-1} in CH_2Cl_2 in Reactions 2.2.1.G and 2.2.1.H (Table 2.3), and assigned to Product B, is consistent with the presence of a rhodium(I) carbonyl complex. The other ligands are probably SnCl_3^- groups, and since a only small amount of starting material remains when a Rh:Sn stoichiometry of 1:3 is used, the product complex may contain either 3 or 4 SnCl_3^- ligands, and is probably the same species which gave an absorption at $2011/13\text{cm}^{-1}$ in THF in Reactions 2.2.1.A-E. This difference in the position of the carbonyl absorptions is likely to be due to solvent effects and is not uncommon, e.g. see Table 2.1, $\nu(\text{CO})$ for $[\text{Rh}(\text{CO})_2\text{Cl}_2]^-$: $1984, 2062\text{cm}^{-1}$ in THF, $1994, 2071\text{cm}^{-1}$ in CH_2Cl_2 . Thus, Product A and Product B appear to be the same.

The data show that an increase in the amount of tin(II) chloride added to the system leads to an increase in the intensity of the absorption at 2018cm^{-1} coupled with a decrease in the intensity of the absorptions due to $[\text{Rh}(\text{CO})_2\text{Cl}_2]^-$. Interestingly, absorptions due to $\text{Rh}_2(\text{CO})_4\text{Cl}_2$ were also observed. Reaction 2.2.1.H, employing a Rh:Sn molar ratio of 1:3, stopped after a 2 hour period, but did not go to completion with $[\text{Rh}(\text{CO})_2\text{Cl}_2]^-$ still present in solution. On standing, this solution became darkly coloured due to decomposition.

Reaction in acetic acid

Reaction of $[\text{Bz}(\text{Et})_3\text{N}][\text{Rh}(\text{CO})_2\text{Cl}_2]$ and SnCl_2 was also studied in acetic acid because this was the solvent used for the rhodium catalysis of the hydrocarbonylation of ethene. No reaction was observed at ambient temperature, however, probably due to the insolubility of tin(II) chloride under these conditions. The yellow colour of $[\text{Rh}(\text{CO})_2\text{Cl}_2]^-$ and its accompanying carbonyl absorptions at 2001 and 2076cm^{-1} were retained throughout the reaction, with no other carbonyl absorptions observed. Attempts to achieve reaction by heating the solution gave a black colouration due to decomposition.

2.2.2 Reaction of $[\text{Rh}(\text{CO})_2\text{Cl}_2]^-$ with SnCl_2 at Low Temperature

Reaction in THF

The reaction of $[\text{Bz}(\text{Et})_3\text{N}][\text{Rh}(\text{CO})_2\text{Cl}_2]$ with SnCl_2 in THF at room temperature was too rapid to follow using the standard FT-IR spectroscopic procedure. Consequently, the reaction was carried out at low temperature in an attempt to identify reaction intermediates. The reaction was initially attempted using a methanol bath cooled to -40°C , but at this temperature, however, the reaction was still found to proceed too quickly for any intermediates to be observed. Consequently, the reaction was carried out at -78°C by first dissolving $[\text{Bz}(\text{Et})_3\text{N}][\text{Rh}(\text{CO})_2\text{Cl}_2]$ in THF and cooling the solution in solid CO_2 . A CaF_2 liquid cell was also cooled in solid CO_2 . Solid SnCl_2 was then added to the solution, and the reaction monitored by following the changes in the carbonyl absorptions. By using a cooled CaF_2 liquid cell it was possible to ensure very little warming of the solution, and as a consequence, no significant further reaction occurred while the spectra were recorded. Table 2.4 summarises the data obtained for the reaction.

Table 2.4 Summary of infra-red data obtained for the reaction of $[\text{Bz}(\text{Et})_3\text{N}][\text{Rh}(\text{CO})_2\text{Cl}_2]^a$ with SnCl_2^b in a 1:1 molar ratio, carried out in THF^c at low temperature

Reaction Code	Reaction Time	New absorptions observed [†] $\nu(\text{CO})/\text{cm}^{-1}$
2.2.2.A	2 min	2010 _{vw}
	12 min	2010 _w
	25 min	2010 _m
	53 min	2011 _m
	200 min	2011 _m

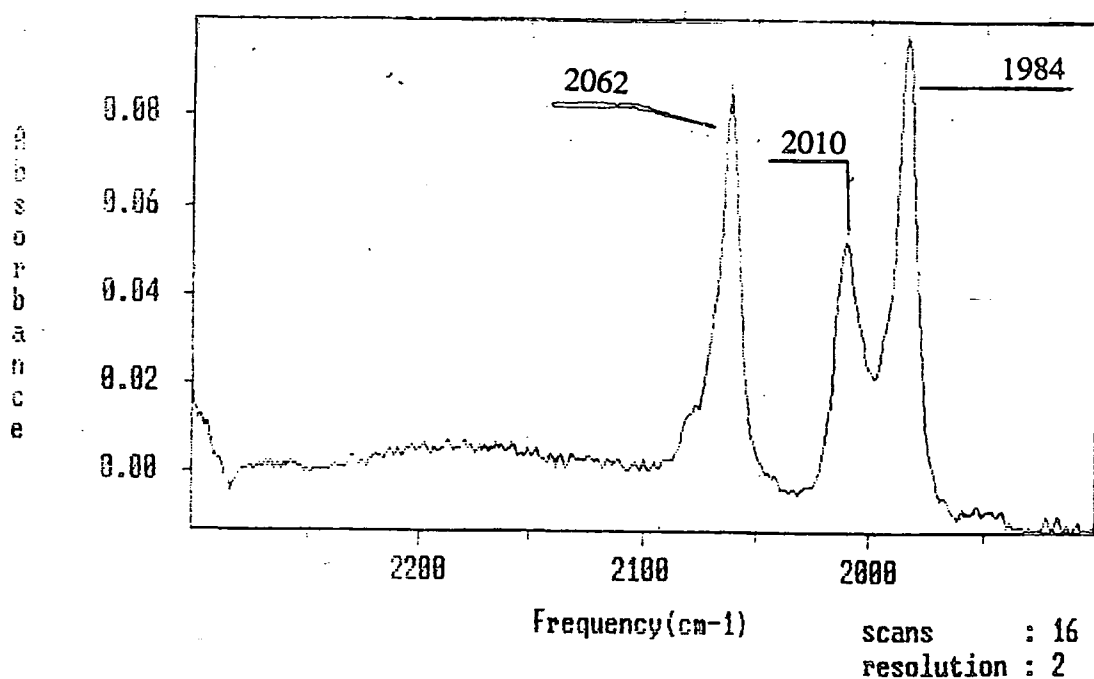
a - 21.0mg (0.05mmol) b - 12.0mg(0.063mmol) c - 6ml

[†] Absorptions at 1984 and 2062cm^{-1} , due to $[\text{Rh}(\text{CO})_2\text{Cl}_2]^-$, remained strong throughout the reaction. Unassigned weak shoulders were also observed at 1989 , 2008 , 2066 and 2077cm^{-1} from a period of 25 minutes onwards.

There was a colour change from yellow to pale orange as the reaction progressed over a period of 200 minutes. This was accompanied by a gradual increase in intensity of the absorption at 2011cm^{-1} as observed in previous reactions (see Table 2.2) which is assigned to the same rhodium(I) carbonyl trichlorostannate complex, Product A. A small decrease in the amount of the starting material $[\text{Bz}(\text{Et})_3\text{N}][\text{Rh}(\text{CO})_2\text{Cl}_2]$ was detected. Several unassigned weak shoulders were also observed at 1989, 2008, 2066 and 2077cm^{-1} , those at 2008 and 2077cm^{-1} probably being due to $\text{Rh}(\text{CO})_2\text{Cl}(\text{THF})$, $\{\nu(\text{CO}) - 2004, 2080\text{cm}^{-1}$ in THF}. Figure 2.3 shows the carbonyl absorptions observed after 53 minutes. The absorption at 2011cm^{-1} due to the product was lost after 1 day leaving only absorptions due to $[\text{Rh}(\text{CO})_2\text{Cl}_2]^-$. This is consistent with loss of tin from the complex, the reasons for which are unclear, but which is common to solutions of other tin complexes on ageing e.g. Reactions 2.2.1.A-C.

No reaction intermediates were identified, the reaction proceeding similar to that at room temperature, but at a much slower rate.

Figure 2.3 Infra-red spectrum of the reaction of $[\text{Rh}(\text{CO})_2\text{Cl}_2]^-$ with SnCl_2 in THF at -78°C after 53 minutes



2.2.3 Reaction of $[\text{Rh}(\text{CO})_2\text{Cl}_2]^-$ with SnCl_3^-

In the catalytic reactions investigated previously⁽¹⁾, and in Chapter 4, SnCl_2 is added to a solution containing a molar excess of concentrated hydrochloric acid, and thus will form SnCl_3^- . It is therefore relevant to investigate the reaction of SnCl_3^- with $[\text{Rh}(\text{CO})_2\text{Cl}_2]^-$, which is also formed in the catalytic process as indicated by infra-red studies of the carbonylation of $\text{RhCl}_3 \cdot 3\text{H}_2\text{O}$ in the presence of additional chloride ions (see Chapter 5).

Reactions in THF and acetic acid

Due to the insolubility of $[\text{Bz}(\text{Et})_3\text{N}][\text{SnCl}_3]$, reactions of $[\text{Bz}(\text{Et})_3\text{N}][\text{Rh}(\text{CO})_2\text{Cl}_2]$ with $[\text{Bz}(\text{Et})_3\text{N}][\text{SnCl}_3]$ in acetic acid or THF as solvents proved unsuccessful even when the reaction mixtures were heated.

Reaction in CH_2Cl_2

CH_2Cl_2 was a more suitable solvent than THF and acetic acid due to the solubility of both reactants. Table 2.5 summarises the infra-red data obtained for the reaction of $[\text{Bz}(\text{Et})_3\text{N}][\text{Rh}(\text{CO})_2\text{Cl}_2]$ with $[\text{Bz}(\text{Et})_3\text{N}][\text{SnCl}_3]$ in CH_2Cl_2 .

Table 2.5 Summary of infra-red data for the reaction of $[\text{Bz}(\text{Et})_3\text{N}][\text{Rh}(\text{CO})_2\text{Cl}_2]^a$ with $[\text{Bz}(\text{Et})_3\text{N}][\text{SnCl}_3]^b$ in a Rh:Sn molar ratio of 1:2, carried out in CH_2Cl_2^c at 20°C

Reaction Code	Colour Changes	Reaction Time	$\nu(\text{CO})/\text{cm}^{-1}$ Observed	Assignment
2.2.3.A	Yellow→Red	Instantaneous	1994 _w , 2072 _w 2036 _w , 2092 _w 2018 _s	$[\text{Rh}(\text{CO})_2\text{Cl}_2]^-$ $\text{Rh}_2(\text{CO})_4\text{Cl}_2$ Product B

a - 50mg (0.12mmol)

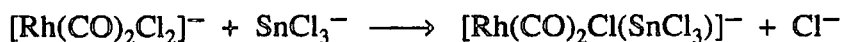
b - 99mg (0.237mmol)

c - 10ml

Based on the frequency of the $\nu(\text{CO})$ absorption, the reaction product is identical to that of Reactions 2.2.1.G and 2.2.1.H between $[\text{Rh}(\text{CO})_2\text{Cl}_2]^-$ and SnCl_2 carried out in CH_2Cl_2 at room temperature (see Table 2.3), both infra-red spectra showing the same strong absorption at 2018 cm^{-1} . The fact that the product absorptions are identical indicates that the reactions are related by the equilibrium:



with both insertion of SnCl₂ into a Rh-Cl bond, and substitution of SnCl₃⁻ for Cl⁻ being possible modes of formation of Rh-SnCl₃ bonds:



Interestingly, scavenging of chloride ions, causing the formation of Rh₂(CO)₄Cl₂ from [Rh(CO)₂Cl₂]⁻, also occurs, as observed previously.

2.2.4 Reaction of Rh₂(CO)₄Cl₂ with SnCl₂

Reaction in THF

Infra-red data obtained for the reaction of Rh₂(CO)₄Cl₂ with SnCl₂ in THF is shown in Table 2.6.

Table 2.6 Summary of infra-red data for the reaction of Rh₂(CO)₄Cl₂^a with SnCl₂^b in a 1:2 molar ratio, carried out in THF^c at 20°C

Reaction Code	Colour Changes	Reaction Time	$\nu(\text{CO})/\text{cm}^{-1}$ Observed
2.2.4.A	Yellow	1 day	(2004-2009) _s (2081-2086) _s
	↓ Black	7 days	No change

a - 25.1mg (0.065mmol) b - 26.6mg (0.140mmol) c - 5ml

Reaction in THF, effectively of Rh(CO)₂Cl(THF) ($\nu(\text{CO})/\text{cm}^{-1}$ - 2004_s, 2080_s) and SnCl₂, was accompanied by small fluctuations in the positions of the maxima for the carbonyl absorptions, indicating interaction of the rhodium complex with SnCl₂ possibly by a reversible insertion of SnCl₂ into the Rh-Cl bond, or displacement of THF by SnCl₂.THF. However, spectral changes were small.

Reaction in CH₂Cl₂ and acetic acid

No reaction was observed in dichloromethane with only carbonyl absorptions for Rh₂(CO)₄Cl₂ observed ($\nu(\text{CO})/\text{cm}^{-1}$ - 2035_s, 2092_s, 2108_w). A pale yellow colouration was retained throughout. Likewise, no reaction was observed in acetic acid, with only the carbonyl absorptions for Rh₂(CO)₄Cl₂ observed yet again

$\nu(\text{CO})/\text{cm}^{-1}$ - 2037_s, 2093_s). After 7 days, however, there was a colour change from orange to brown, with only a single weak carbonyl band at 2079 cm^{-1} remaining, its position suggesting the formation of a monocarbonyl rhodium(III) complex.

Reaction of $\text{Rh}_2(\text{CO})_4\text{Cl}_2$ and SnCl_2 in Ethanol

This reaction, originally carried out by Young et al⁽⁵⁾, for which the final stage was addition of $(\text{CH}_3)_4\text{NCl}$ to precipitate $[(\text{CH}_3)_4\text{N}]_2[\text{Rh}(\text{CO})(\text{SnCl}_3)_2\text{Cl}]$, was not reported in detail. Infra-red data collected for the same reaction is summarised in Table 2.7.

Table 2.7 Summary of infra-red data for the reaction of $\text{Rh}_2(\text{CO})_4\text{Cl}_2^{\text{a}}$ with SnCl_2^{b} in ethanol^c at 25°C

Reaction Code	Rh : Sn Molar Ratio	Reaction Time	$\nu(\text{CO})/\text{cm}^{-1}$ Observed	Assignment
2.2.4.B	1 : 2	3 minutes	2010 _{sh} 2085 _m 2014 _s 2075 _{sh}	Rh(CO) ₂ Cl(EtOH) Product A Product A?
		7 minutes	2010 _{sh} 2085 _w 2017 _s 2075 _{vw}	Rh(CO) ₂ Cl(EtOH) Product A Product A?

a - 26.4mg (0.068mmol) b - 51.4mg (0.271mmol) c - 5ml

Initial addition of $\text{Rh}_2(\text{CO})_4\text{Cl}_2$ to ethanol resulted in absorptions at 2010_s and 2085_s cm^{-1} due to formation of $\text{Rh}(\text{CO})_2\text{Cl}(\text{EtOH})$ via cleavage of the Rh-Cl-Rh bridge in $\text{Rh}_2(\text{CO})_4\text{Cl}_2$. Addition of SnCl_2 produced a steady decrease in the intensity of these absorptions coupled with the appearance of absorptions at 2017_s and 2075_{vw} cm^{-1} . It is interesting that this reaction occurs in ethanol but not in THF, acetic acid or dichloromethane. Addition of $\text{Bz}(\text{Et})_3\text{NCl}$ to this solution precipitates $[\text{Bz}(\text{Et})_3\text{N}]_2[\text{Rh}(\text{CO})(\text{SnCl}_3)_2\text{Cl}]$ $\{\nu(\text{CO}) - 2013\text{cm}^{-1}$ in nujol} as outlined in Chapter 3, Section 3.2.2. The main product $\{\nu(\text{CO}) - 2017\text{cm}^{-1}\}$ produced in solution after 7 minutes is possibly the same anionic complex as Product A and Product B referred to earlier, and although the nature of the very weak absorption $\{\nu(\text{CO}) - 2075\text{cm}^{-1}\}$ is not altogether clear, it may be due to the same complex as the absorption at 2017 cm^{-1} . This would suggest formation of a rhodium(I) dicarbonyl trichlorostannate complex in solution.

2.2.5 Reaction of $\text{Rh}_2(\text{CO})_4\text{Cl}_2$ with a mixture of $\text{Bz}(\text{Et})_3\text{NCl}$ and SnCl_2

There is a high probability that $\text{Rh}_2(\text{CO})_4\text{Cl}_2$, SnCl_2 and $\text{Bz}(\text{Et})_3\text{NCl}$ will be present together in solution at some time in the rhodium-tin-chloride catalytic system. Therefore, the reactions of these compounds together were studied and are reported as follows.

Table 2.8 Summary of infra-red data for the reactions of $\text{Rh}_2(\text{CO})_4\text{Cl}_2$ with SnCl_2 and $\text{Bz}(\text{Et})_3\text{NCl}$ in THF at 20°C

Reaction Code	Reagents	Rh : Sn : $\text{Bz}(\text{Et})_3\text{NCl}$ Molar Ratio	Reaction Time	$\nu(\text{CO})/\text{cm}^{-1}$ Observed	Assignment
2.2.5.A	$\text{Rh}_2(\text{CO})_4\text{Cl}_2$, SnCl_2 , $\text{Bz}(\text{Et})_3\text{NCl}$	1 : 1 : 1 ^a	2 min	1989 _w 2067 _w 2004 _{sh} 2080 _w 1994 _m 2070 _m 2010 _s	$[\text{Rh}(\text{CO})_2\text{Cl}_2]^-$ $\text{Rh}(\text{CO})_2\text{Cl}(\text{THF})$ Product C Product A
			10 min	1989 _{vw} 2067 _{vw} 2077 _{vw} 1994 _s 2070 _{ms} 2010 _s	$[\text{Rh}(\text{CO})_2\text{Cl}_2]^-$ $\text{Rh}(\text{CO})_2\text{Cl}(\text{THF})$ Product C Product A
			180 min	1989 _{sh} 2067 _{sh} 2077 _{sh} 1994 _s 2070 _s 2010 _m	$[\text{Rh}(\text{CO})_2\text{Cl}_2]^-$ $\text{Rh}(\text{CO})_2\text{Cl}(\text{THF})$ Product C Product A
			2 days	1984 _s 2062 _{ms} 2004 _m 2081 _m	$[\text{Rh}(\text{CO})_2\text{Cl}_2]^-$ $\text{Rh}(\text{CO})_2\text{Cl}(\text{THF})$
2.2.5.B	$\text{Rh}_2(\text{CO})_4\text{Cl}_2$, SnCl_2 , $\text{Bz}(\text{Et})_3\text{NCl}$	1 : 2 : 1 ^b	Instantaneous	1984 _w 2062 _w 2004 _{sh} 2081 _m 2011 _s	$[\text{Rh}(\text{CO})_2\text{Cl}_2]^-$ $\text{Rh}(\text{CO})_2\text{Cl}(\text{THF})$ Product A

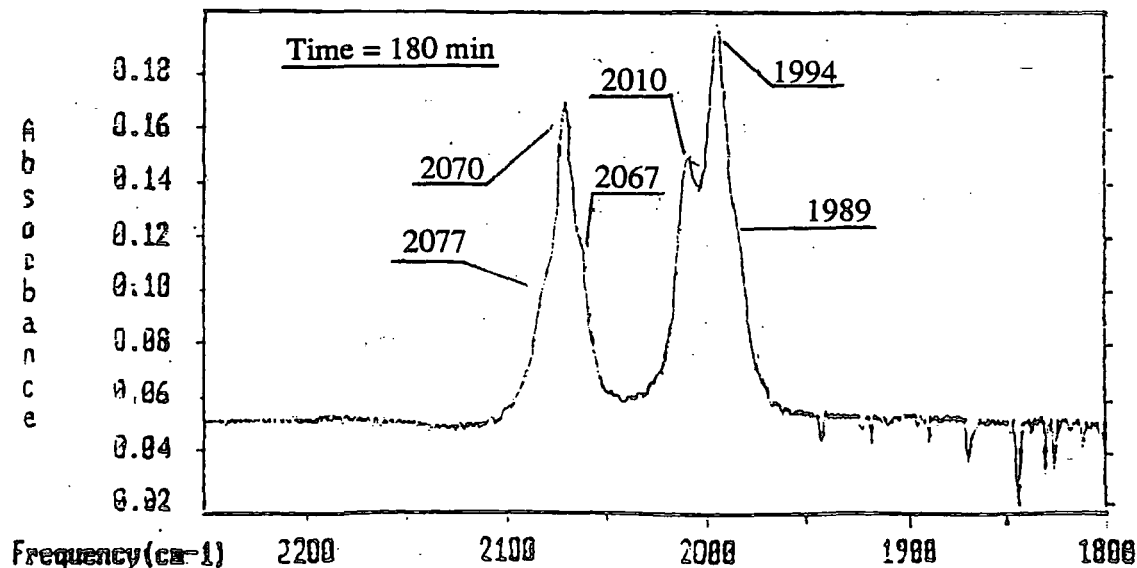
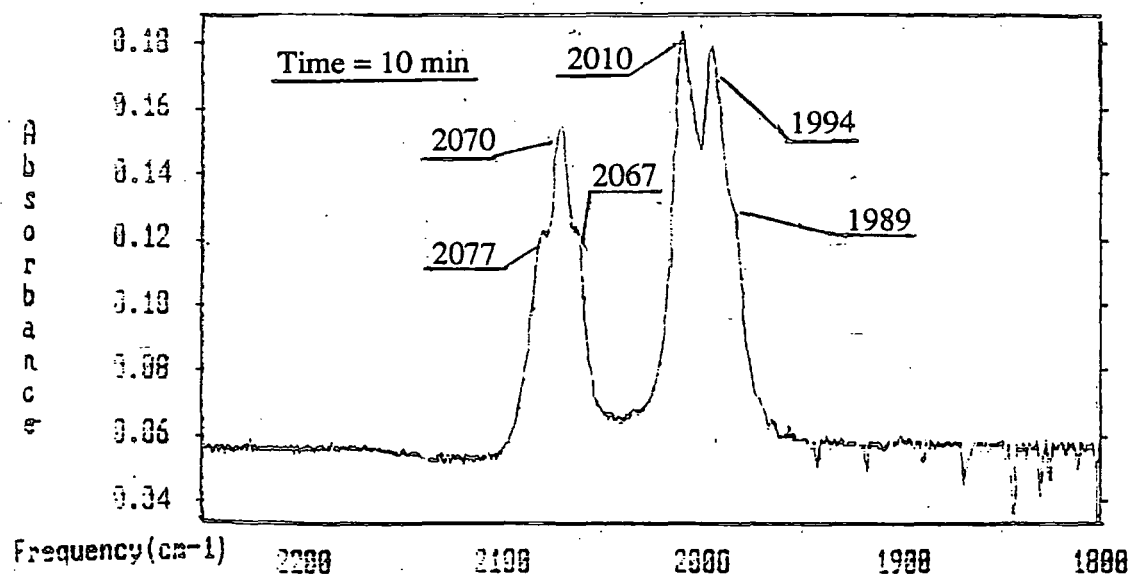
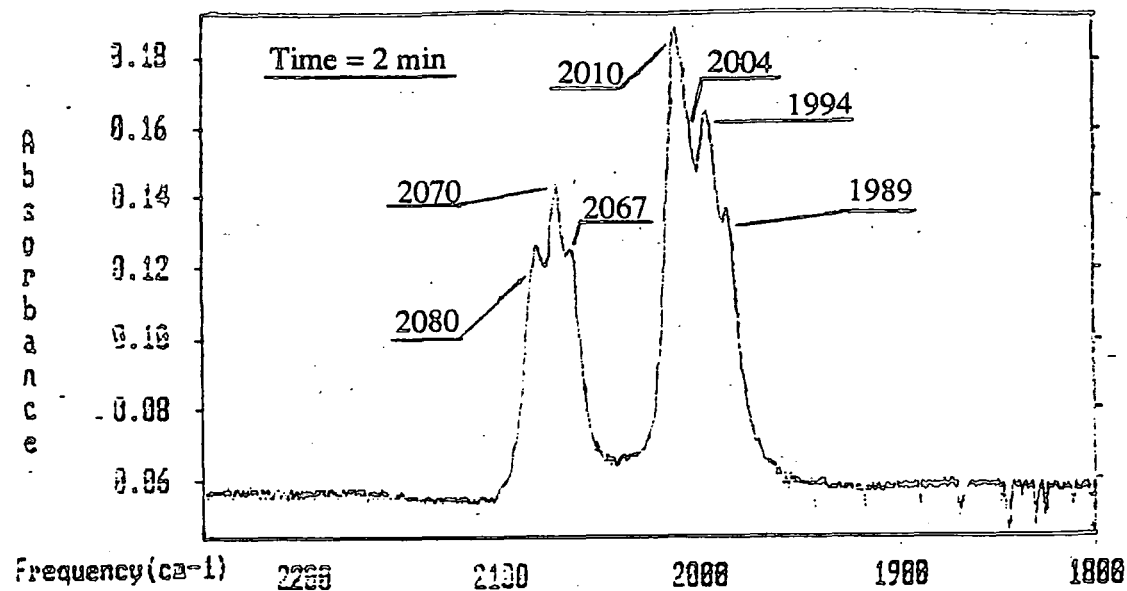
a - 11.30mg (0.029mmol) : 9.10mg (0.048mmol) : 12.30mg (0.054mmol), THF - 8ml

b - 12.30mg (0.032mmol) : 26.10mg (0.138mmol) : 1.40mg (0.063mmol), THF - 5ml

Notes

For Reactions 2.2.5.A and 2.2.5.B THF was added to a solid mixture of $\text{Rh}_2(\text{CO})_4\text{Cl}_2$, SnCl_2 and $\text{Bz}(\text{Et})_3\text{NCl}$.

Figure 2.4 Changes in the carbonyl absorptions for the 1:1:1 reaction of $\text{Rh}_2(\text{CO})_4\text{Cl}_2$ with SnCl_2 and $\text{Bz}(\text{Et})_3\text{NCl}$ in THF



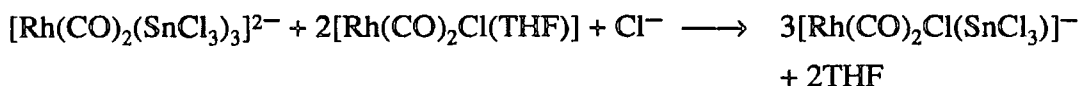
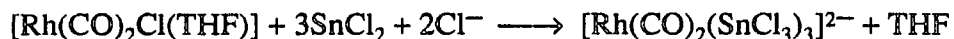
Reactions in THF

Table 2.8 summarises the infra-red data for the reactions of $\text{Rh}_2(\text{CO})_4\text{Cl}_2$ with $\text{Bz}(\text{Et})_3\text{NCl}$ and SnCl_2 carried out in THF at 20°C . Changes in the infra-red spectra in the carbonyl stretching region for Reaction 2.2.5.A are shown in Figure 2.4. A strong absorption at 2010cm^{-1} (Product A) was initially observed, along with weaker absorptions at 1994 and 2070cm^{-1} (Product C). Initial formation of $\text{Rh}(\text{CO})_2\text{Cl}(\text{THF})$ and $[\text{Rh}(\text{CO})_2\text{Cl}_2]^-$ also occurred, with their absorptions decreasing in intensity over 3 hours, as the intensity of the absorptions due to Product C increased. This increase in the amount of Product C during this period was also seemingly accompanied by a decrease in the intensity of the strong absorption at 2010cm^{-1} , assigned to Product A. Upon ageing (2 days) the absorptions at 1994 , 2011 and 2070cm^{-1} were completely lost, being replaced by absorptions due to $\text{Rh}(\text{CO})_2\text{Cl}(\text{THF})$ and $[\text{Rh}(\text{CO})_2\text{Cl}_2]^-$, consistent with loss of tin from the complexes.

The products absorbing at 2010 and at 1994 , 2070cm^{-1} appear on the basis of the data collected to be $\text{Rh}(\text{I})\text{-CO-SnCl}_3$ complexes, the first complex being the same as that observed in the reaction of $[\text{Rh}(\text{CO})_2\text{Cl}_2]^-$ with SnCl_2 in THF ($\nu(\text{CO}) - 2011/2013\text{cm}^{-1}$), assigned to Product A. As indicated in Table 2.1, the three Rh/Sn complexes $[\text{Rh}(\text{CO})(\text{SnCl}_3)_2\text{Cl}]^{2-}$, $[\text{Rh}(\text{CO})(\text{SnCl}_3)_4]^{3-}$ and $[\text{Rh}(\text{CO})_2(\text{SnCl}_3)_3]^{2-}$ have absorptions in the $2010\text{-}2013\text{cm}^{-1}$ region of the infra-red spectrum, and although the reaction was $1:1:1 \text{ Rh}:\text{Sn}:[\text{Bz}(\text{Et})_3\text{N}]^+$, the identity of the product cannot be categorically determined from the available infra-red data. The second product, assigned as Product C, has a pattern of $\nu(\text{CO})$ frequencies consistent with the formation of a $\text{Rh}(\text{I})$ cis-dicarbonyl complex of the type $[\text{Rh}(\text{CO})_2\text{XY}]^-$ where X and Y may be the same or different anionic groups. The data is consistent with both $[\text{Rh}(\text{CO})_2\text{Cl}(\text{SnCl}_3)]^-$ and $[\text{Rh}(\text{CO})_2(\text{SnCl}_3)_2]^-$, though the small increase in $\nu(\text{CO})$ compared with $[\text{Rh}(\text{CO})_2\text{Cl}_2]^-$ is more consistent with the former than the latter complex. Also, due to the presence of two bulky SnCl_3^- ligands $[\text{Rh}(\text{CO})_2(\text{SnCl}_3)_2]^-$ is most likely to prefer a square planar conformation with trans CO ligands. However, the identity of Product C cannot be categorically determined from infra-red data alone. Interestingly, the formation of Product C, at the apparent expense of Product A, could be explained by the following sequence of reactions:

1. Initial reaction favouring formation of $[\text{Rh}(\text{CO})_x(\text{SnCl}_3)_y]^{(y-1)-}$ ($x = 1, y = 3, 4; x = 2, y = 3$) or $[\text{Rh}(\text{CO})_x(\text{SnCl}_3)_y\text{Cl}_z]^{y+z-1}$ ($x = 2, y = 2, z = 1$).
2. Reaction of the complex formed in 1. with $[\text{Rh}(\text{CO})_2\text{Cl}_2]^-$ or $[\text{Rh}(\text{CO})_2\text{Cl}(\text{THF})]$ to form a complex having a lower $\text{Sn}:\text{Rh}$ ratio.

This may be illustrated as follows:



Though this remains purely speculative, and the precise identity of the complex cannot be determined from the available infra-red data, the model is consistent with the data.

When the reaction was undertaken using a 1:2:1 ratio of Rh:Sn:[Bz(Et)₃N]⁺ (Reaction 2.2.5.B), the only new carbonyl absorption observed was at 2011cm⁻¹. Product C was not observed. Reaction 2.2.5.B, however, gave a stronger absorption at 2011cm⁻¹ than Reaction 2.2.5.A and weaker absorptions due to [Rh(CO)₂Cl₂]⁻ and Rh(CO)₂Cl(THF). This is due to the increase in the amount of tin(II) chloride in the system, and implies that a Sn:Rh molar ratio of 2:1 favours completion of the reaction, and that the final complex contains Sn:Rh in a ratio of 2:1 or higher.

Reaction in CH₂Cl₂ and acetic acid

Reaction of Rh₂(CO)₄Cl₂ with SnCl₂ and Bz(Et)₃NCl was also undertaken using dichloromethane and acetic acid as solvents. Reaction in acetic acid gave no observed formation of a rhodium(I) carbonyl trichlorostannate complex, probably due to the poor solubility of SnCl₂. There was, however, chloride ion cleavage of the Rh-Cl-Rh bridges of Rh₂(CO)₄Cl₂ to form [Rh(CO)₂Cl₂]⁻ as indicated by the strong carbonyl absorptions at 2000 and 2076cm⁻¹. Data for the reaction of Rh₂(CO)₄Cl₂ with SnCl₂ and Bz(Et)₃NCl in CH₂Cl₂ is summarised in Table 2.9.

Table 2.9 Summary of infra-red data for the 1:1:1 reaction of $\text{Rh}_2(\text{CO})_4\text{Cl}_2^{\text{a}}$ with SnCl_2^{b} and $\text{Bz}(\text{Et})_3\text{NCl}^{\text{c}}$ in $\text{CH}_2\text{Cl}_2^{\text{d}}$ at 20°C

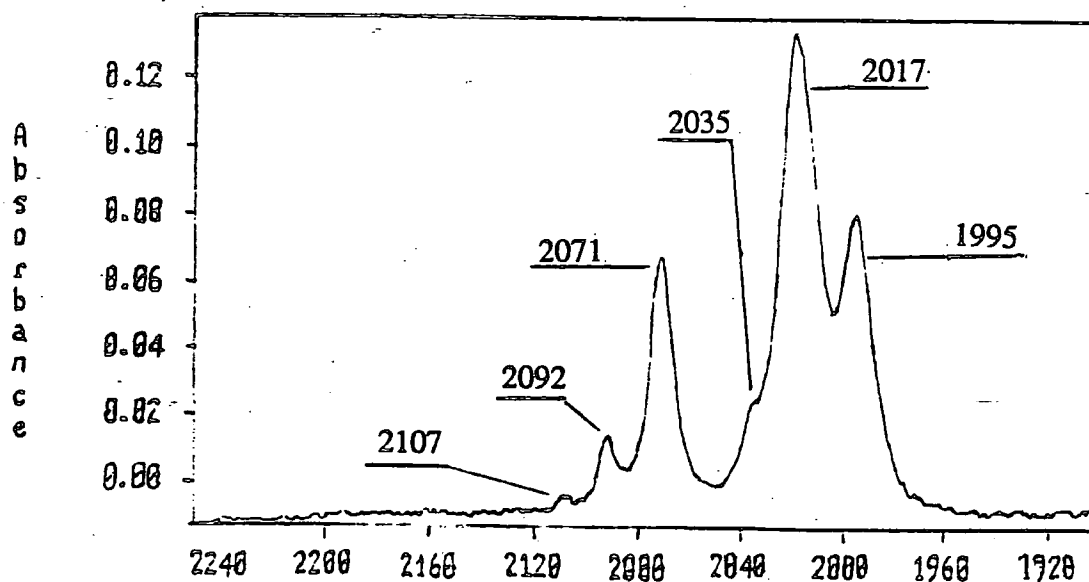
Reaction Code	Rh : Sn : $\text{Bz}(\text{Et})_3\text{NCl}$ Molar Ratio	Reaction Time	$\nu(\text{CO})/\text{cm}^{-1}$ Observed	Assignment
2.2.5.C	1 : 1 : 1	3 hours	1995 _m 2071 _m 2035 _w 2092 _w 2107 _{vw} 2017 _s	$[\text{Rh}(\text{CO})_2\text{Cl}_2]^-$ $\text{Rh}_2(\text{CO})_4\text{Cl}_2$ Product B

a - 5.4mg (0.014mmol) b - 6.5mg (0.034mmol) c - 7.4mg (0.032mmol) d - 3ml

Notes

1. For Reaction 2.2.5.C solid SnCl_2 and $\text{Bz}(\text{Et})_3\text{NCl}$ were added as a mixture to a solution of $\text{Rh}_2(\text{CO})_4\text{Cl}_2$ in CH_2Cl_2 .
2. The reaction was accompanied by a colour change from yellow to deep red over the 3 hour period of reaction.

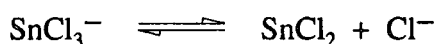
Figure 2.5 Infra-red spectrum for the 1:1:1 reaction of $\text{Rh}_2(\text{CO})_4\text{Cl}_2$ with SnCl_2 and $\text{Bz}(\text{Et})_3\text{NCl}$ in CH_2Cl_2 after 3 hours



Reaction 2.2.5.C gave a strong absorption at 2017cm⁻¹ which is consistent with the formation of Product B. Initially, strong absorptions at 1995 and 2071cm⁻¹ due to [Rh(CO)₂Cl₂]⁻ replaced absorptions due to the starting complex, and were then themselves steadily replaced by the strong absorption at 2017cm⁻¹. The weak intensity of the Rh₂(CO)₄Cl₂ carbonyl absorptions remained constant throughout the reaction, with the final spectrum after 3 hours showing trace amounts of Rh₂(CO)₄Cl₂ but residual [Bz(Et)₃N][Rh(CO)₂Cl₂] present (see Figure 2.5). The 1:1:1 Rh:Sn:[Bz(Et)₃N]⁺ ratio does not therefore correspond to the stoichiometry of the reaction taking place.

2.2.6 Reaction of Rh₂(CO)₄Cl₂ with [Bz(Et)₃N][SnCl₃]

There is a probability that Rh₂(CO)₄Cl₂ and SnCl₃⁻ will be present together at some stage during some rhodium-tin-chloride catalysed reactions to hydrocarbonylate ethene (see Chapter 4). Therefore, their reaction chemistry and the nature of the following equilibrium are of relevance, and are the subject of this section.



Reactions in THF

The data obtained for the reactions of Rh₂(CO)₄Cl₂ with [Bz(Et)₃N][SnCl₃] in THF are summarised in Table 2.10.

Table 2.10 Summary of infra-red data for the reactions of Rh₂(CO)₄Cl₂ with [Bz(Et)₃N][SnCl₃] in THF at 20°C

Reaction Code	Rh : Sn Molar Ratio	$\nu(\text{CO})/\text{cm}^{-1}$ Observed	Assignment
2.2.6.A	1 : 1 ^a	1984 _s 2062 _s 1995 _s 2070 _s 2011 _w	[Rh(CO) ₂ Cl ₂] ⁻ Product C Product A
2.2.6.B	1 : 3 ^b	1984 _s 2062 _s 1994 _{ms} 2070 _{ms} 2011 _m	[Rh(CO) ₂ Cl ₂] ⁻ Product C Product A

a - 8.7mg (0.022mmol) : 16.0mg (0.038mmol), THF - 5ml

b - 0.8mg (0.0021mmol) : 5.1mg (0.012mmol), THF - 4ml

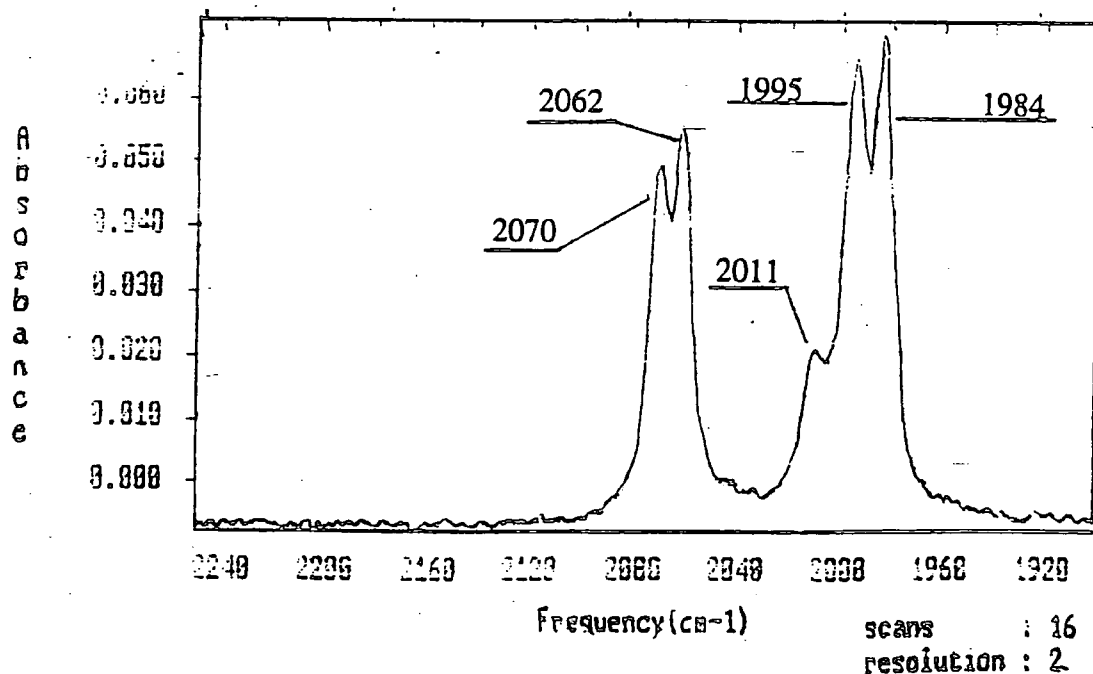
Notes:

- For Reactions 2.2.6.A and 2.2.6.B, THF was added to a mixture of [Bz(Et)₃N][SnCl₃] and Rh₂(CO)₄Cl₂ in the solid phase.

2. Reactions 2.2.6.A and 2.2.6.B were instantaneous, complete within 30 seconds, and were each accompanied by a colour change from yellow to orange.

The absorptions at 1994/5, 2011 and 2070 cm^{-1} in Reactions 2.2.6.A and 2.2.6.B have been observed before in Reaction 2.2.5.A and are assigned to the rhodium(I) carbonyl trichlorostannate complexes, Products A and C. The absorptions at 1995 and 2070 cm^{-1} are assigned to the same complex since a 3-fold molar increase of SnCl_3^- in the system, leads to a coupled decrease in their intensities as the absorption at 2011 cm^{-1} increases in intensity. In both reactions strong absorptions were observed at 1984 and 2062 cm^{-1} corresponding to $[\text{Rh}(\text{CO})_2\text{Cl}_2]^-$, but $\text{Rh}(\text{CO})_2\text{Cl}(\text{THF})$ was not observed. Figure 2.6 shows the infra-red absorptions observed for Reaction 2.2.6.A, upon completion.

Figure 2.6 Infra-red spectrum for the 1:1:1 reaction of $\text{Rh}_2(\text{CO})_4\text{Cl}_2$ with $\text{Bz}(\text{Et})_3\text{NSnCl}_3$ in THF



Interestingly the relative ratio of Product A:Product C has varied for reactions reported in this chapter. In some reactions A is the sole product and in others C is the

major product (Reactions 2.2.5.A, 2.2.6.A and 2.2.6.B). Products A and C, with other complexes, are believed to be related by a sequence of facile reactions (see later Chapter 3), and here reaction conditions appear critical in the formation of C rather than A.

Reaction in THF at low temperature

The reaction of $\text{Rh}_2(\text{CO})_4\text{Cl}_2$ with $[\text{Bz}(\text{Et})_3\text{N}][\text{SnCl}_3]$ in THF was also attempted at -78°C in an attempt to observe reaction intermediates, the method being as described in Section 2.2.2. The data obtained are summarised in Table 2.11.

Table 2.11 Summary of infra-red data for the reaction of $\text{Rh}_2(\text{CO})_4\text{Cl}_2$ with $[\text{Bz}(\text{Et})_3\text{N}][\text{SnCl}_3]$ in THF at -78°C

Reaction Code	Rh : Sn Molar Ratio	Reaction Time	$\nu(\text{CO})/\text{cm}^{-1}$ Observed	Assignment
2.2.6.C	1 : 1 ^c	3 hours	1984 _s 2062 _s 2005 _{ms} 2080 _m 2010 _m	$[\text{Rh}(\text{CO})_2\text{Cl}_2]^-$ $\text{Rh}(\text{CO})_2\text{Cl}(\text{THF})$ Product A

c - 20.5mg (0.053mmol) : 45.1mg (0.108mmol), THF - 5ml

Notes:

1. For Reaction 2.2.6.C, THF was added to a mixture of $[\text{Bz}(\text{Et})_3\text{N}][\text{SnCl}_3]$ and $\text{Rh}_2(\text{CO})_4\text{Cl}_2$ in the solid phase.
2. Reaction 2.2.6.C was accompanied by a colour change from yellow to orange

A gradual increase in the intensity of absorptions due to $[\text{Rh}(\text{CO})_2\text{Cl}_2]^-$ was observed with an increase in time. Also, an increase in the intensity of the absorption at 2010cm^{-1} (Product A) was accompanied by the steady decrease in the intensity of $\text{Rh}(\text{CO})_2\text{Cl}(\text{THF})$ absorptions. No reaction intermediates were observed, nor were absorptions at 1995 and 2070cm^{-1} (Product C), as observed in Reactions 2.2.6.A and 2.2.6.B.

A reaction of $\text{Rh}_2(\text{CO})_4\text{Cl}_2$ with a mixture of $\text{Bz}(\text{Et})_3\text{NCl}$ and $[\text{Bz}(\text{Et})_3\text{N}][\text{SnCl}_3]$ in THF was also explored in an attempt to investigate whether $\text{Rh}_2(\text{CO})_4\text{Cl}_2$ preferentially reacts with SnCl_3^- or the Cl^- anion. The data obtained for this reaction are summarised in Table 2.12.

Table 2.12 Summary of infra-red data for the 1:1:1 reaction of $\text{Rh}_2(\text{CO})_4\text{Cl}_2$ with $\text{Bz}(\text{Et})_3\text{NCl}$ and $[\text{Bz}(\text{Et})_3\text{N}][\text{SnCl}_3]$ in THF at 20°C

Reaction Code	Rh : Sn : $\text{Bz}(\text{Et})_3\text{NCl}$ Molar Ratio	Reaction Time	$\nu(\text{CO})/\text{cm}^{-1}$ Observed	Assignment
2.2.6.D	1 : 1 : 1 ^d	1 min	1984 _s , 2062 _s 2012 _m	$[\text{Rh}(\text{CO})_2\text{Cl}_2]^-$ Product A
		60 mins	As above	
		24 hours	1984 _s , 2062 _s 2011 _w	$[\text{Rh}(\text{CO})_2\text{Cl}_2]^-$ Product A

d - 11.8mg (0.030mmol) : 27.7mg (0.066mmol) : 13.4mg (0.059mmol), THF - 5ml

Notes:

1. A solid mixture of $\text{Bz}(\text{Et})_3\text{NCl}$ and $[\text{Bz}(\text{Et})_3\text{N}][\text{SnCl}_3]$ was added to a solution of $\text{Rh}_2(\text{CO})_4\text{Cl}_2$ in THF.
2. Reaction 2.2.6.D was accompanied by a colour change from yellow to orange.

The large amount of $[\text{Bz}(\text{Et})_3\text{N}][\text{Rh}(\text{CO})_2\text{Cl}_2]$ formed in Reaction 2.2.6.D indicates that $\text{Rh}(\text{CO})_2\text{Cl}(\text{THF})$ reacts with Cl^- in preference to SnCl_2 and SnCl_3^- under the conditions used here. The concentration of $[\text{Rh}(\text{CO})_2\text{Cl}_2]^-$ remains unchanged in the presence of an equi-molar proportion of SnCl_3^- over a long period.

The large amount of $[\text{Bz}(\text{Et})_3\text{N}][\text{Rh}(\text{CO})_2\text{Cl}_2]$ formed in the series of reactions 2.2.6.A-C confirms the existence of the following equilibrium in THF:



since it is the chloride ions generated which become bound to the metal by displacement of the THF ligand of $\text{Rh}(\text{CO})_2\text{Cl}(\text{THF})$.

Reactions in CH_2Cl_2 and acetic acid

Reaction of $\text{Rh}_2(\text{CO})_4\text{Cl}_2$ with $[\text{Bz}(\text{Et})_3\text{N}][\text{SnCl}_3]$ was undertaken in both acetic acid and CH_2Cl_2 . Reaction in acetic acid at room temperature yielded only chloride ion cleavage of the Cl-Rh-Cl bridges in $\text{Rh}_2(\text{CO})_4\text{Cl}_2$ to give $[\text{Rh}(\text{CO})_2\text{Cl}_2]^-$, with no formation of a Rh(I)-CO-SnCl₃ complex observed under these mild temperature conditions. Reaction did occur, however, in CH_2Cl_2 , as summarised in Table 2.13, to form Product B.

Table 2.13 Summary of infra-red data for the 1:1 reaction of $\text{Rh}_2(\text{CO})_4\text{Cl}_2$ with $[\text{Bz}(\text{Et})_3\text{N}][\text{SnCl}_3]$ in CH_2Cl_2 at 20°C

Reaction Code	Rh : Sn Molar Ratio	$\nu(\text{CO})/\text{cm}^{-1}$ Observed	Assignment
2.2.6.E	1 : 1 ^e	1994 _s 2071 _s 2035 _m 2092 _m 2107 _{vw} 2018 _{ms}	$[\text{Rh}(\text{CO})_2\text{Cl}_2]^-$ $\text{Rh}_2(\text{CO})_4\text{Cl}_2$ Product B

e - 9.4mg (0.024mmol) : 21.9mg (0.052mmol), CH_2Cl_2 - 5ml

Notes

1. Reaction 2.2.6.E was instantaneous, complete within 30 seconds, and was accompanied by a colour change from yellow to red.

2.2.7 Reaction of $\text{Rh}_2(\text{CO})_4\text{Cl}_2$ with SnCl_2 and $\text{HCl}_{(\text{g})}$

As discussed previously in this chapter, reactions involving hydrogen chloride are of relevance to chemistry which could occur in the catalytic work, which is the subject of Chapter 4. $\text{Rh}_2(\text{CO})_4\text{Cl}_2$, SnCl_2 and HCl are all species which may be present together at some stage during the heating process. The infra-red data obtained are summarised in Table 2.14.

Table 2.14 Summary of infra-red data for the reactions of $\text{Rh}_2(\text{CO})_4\text{Cl}_2$ with SnCl_2 and $\text{HCl}_{(\text{g})}$ in THF at 20°C

Reaction Code	Rh : Sn Molar Ratio	Reaction Time	$\nu(\text{CO})/\text{cm}^{-1}$ Observed	Assignment
2.2.7.A	1 : 1 ^a	1 min	1996 _s 2071 _s 2010 _m	Product C or $[\text{Rh}(\text{CO})_2\text{Cl}_2]^-$ Product A
2.2.7.B	1 : 1 ^b	1 min	2009 _s	Product A
2.2.7.C	1 : 1 ^c	1 min	2003 _{sh} 2084 _m 2009 _s 2035 _w 2094 _{sh}	$\text{Rh}(\text{CO})_2\text{Cl}(\text{THF})$ Product A $\text{Rh}_2(\text{CO})_4\text{Cl}_2$
		15 mins	2004 _s 2081 _s	$\text{Rh}(\text{CO})_2\text{Cl}(\text{THF})$

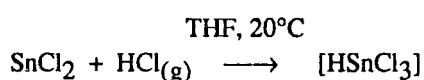
Notes:

a - 7.5mg (0.019mmol) : 7.5mg (0.040mmol), THF - 5ml

b - 17.8mg (0.046mmol) : 16.8mg (0.089mmol), THF - 6ml

c - 26.7mg (0.069mmol) : 27.4mg (0.144mmol), THF - 10ml

1. In Reaction 2.2.7.A a mixture of $\text{Rh}_2(\text{CO})_4\text{Cl}_2$ and SnCl_2 in THF was bubbled with $\text{HCl}_{(\text{g})}$.
2. In Reaction 2.2.7.B a solution of $\text{Rh}_2(\text{CO})_4\text{Cl}_2$ in THF was bubbled with $\text{HCl}_{(\text{g})}$, followed by dry nitrogen to remove excess $\text{HCl}_{(\text{g})}$, and then solid SnCl_2 was added.
3. In Reaction 2.2.7.C, the HSnCl_3 intermediate, a species previously prepared by Hutton⁽¹⁵⁾ and stable at room temperature, was synthesised using his method, by dissolving SnCl_2 in THF and bubbling hydrogen chloride through the resultant solution:



Excess $\text{HCl}_{(\text{g})}$ was removed by bubbling the solution with dry nitrogen, since its presence in solution would probably cause immediate cleavage of the Rh-Cl-Rh bridges in $\text{Rh}_2(\text{CO})_4\text{Cl}_2$. The solution of HSnCl_3 was then added to solid $\text{Rh}_2(\text{CO})_4\text{Cl}_2$.

4. Bubbling a THF solution of $\text{Rh}_2(\text{CO})_4\text{Cl}_2$ with $\text{HCl}_{(\text{g})}$ gave strong carbonyl absorptions at 1992 and 2069 cm^{-1} , assigned to $[\text{Rh}(\text{CO})_2\text{Cl}_2]^-$.

The absorptions at 2009 and 2010 cm^{-1} (Reactions 2.2.7.A and 2.2.7.B respectively) are consistent with the formation of the same Rh-CO-SnCl₃ species (Product A) as that formed in reactions of $[\text{Bz}(\text{Et})_3\text{N}][\text{Rh}(\text{CO})_2\text{Cl}_2]$ and $\text{Rh}_2(\text{CO})_4\text{Cl}_2$ with $\text{SnCl}_2/\text{SnCl}_3^-$. It is interesting that there is little change in the frequency of the Product A absorption upon replacing $[\text{Bz}(\text{Et})_3\text{N}]^+$ with $[\text{H}_{\text{solv}}]^+$, which suggests weak but similar bonding interactions between the Rh-SnCl₃ anionic complex (as in Product A), with each of the cations, either $[\text{H}_{\text{solv}}]^+$ or $[\text{Bz}(\text{Et})_3\text{N}]^+$.

Assignment of absorptions at 1996 and 2071 cm^{-1} (Reaction 2.2.7.A) to either Product C or $[\text{Rh}(\text{CO})_2\text{Cl}_2]^-$ may be possible through a consideration of previous infra-red data summarised in Table 2.15.

Table 2.15 Summary of infra-red data to aid the assignment of absorptions at 1996 and 2070 cm^{-1} for the reaction of $\text{Rh}_2(\text{CO})_4\text{Cl}_2$ with SnCl_2 and HCl

Reaction Code	Reagents	Solvent	$\nu(\text{CO})/\text{cm}^{-1}$	Assignment
2.2.5.A	$\text{Rh}_2(\text{CO})_4\text{Cl}_2$ SnCl_2 $\text{Bz}(\text{Et})_3\text{NCl}$	THF	1994 _m 2070 _m *	Product C
2.2.7.A	$\text{Rh}_2(\text{CO})_4\text{Cl}_2$ SnCl_2 HCl	THF	1996 _s 2071 _s	See below
—	$\dagger[\text{Rh}(\text{CO})_2\text{Cl}_2]^-$	THF	1984 _s 2062 _s	—
—	$\text{Rh}_2(\text{CO})_4\text{Cl}_2$ HCl	THF	1992 _s 2069 _s	$\diamond[\text{Rh}(\text{CO})_2\text{Cl}_2]^-$

$\dagger [\text{Bz}(\text{Et})_3\text{N}]^+$

* $[\text{Bz}(\text{Et})_3\text{N}][\text{Rh}(\text{CO})_2\text{Cl}_2]$ also present in solution

$\diamond [\text{H}_{\text{solv}}]^+$

The absorptions observed for Reaction 2.2.7.A are similar to those assigned to the Rh-SnCl_3 complex, Product C, in Reaction 2.2.5.A, but are also similar to those observed when a THF solution of $\text{Rh}_2(\text{CO})_4\text{Cl}_2$ is bubbled with HCl to yield $[\text{H}_{\text{solv}}][\text{Rh}(\text{CO})_2\text{Cl}_2]$. The absorptions observed for $[\text{Bz}(\text{Et})_3\text{N}][\text{Rh}(\text{CO})_2\text{Cl}_2]$ in THF are significantly lower than those for $[\text{H}_{\text{solv}}][\text{Rh}(\text{CO})_2\text{Cl}_2]$, suggesting that the bonding of $[\text{Bz}(\text{Et})_3\text{N}]^+$ to $[\text{Rh}(\text{CO})_2\text{Cl}_2]^-$ is significantly weaker than the bonding of $[\text{H}_{\text{solv}}]^+$ to $[\text{Rh}(\text{CO})_2\text{Cl}_2]^-$. Thus, the absorptions observed for Reaction 2.2.7.A may be due to:

1. Product C - This interpretation implies weak $[\text{H}_{\text{solv}}]^+$ bonding with the Rh-SnCl_3 anionic complex, and also that the bonding of $[\text{H}_{\text{solv}}]^+$ is similar to that of $[\text{Bz}(\text{Et})_3\text{N}]^+$, as in the case of Product C.
2. $[\text{Rh}(\text{CO})_2\text{Cl}_2]^-$ - This interpretation implies that $[\text{H}_{\text{solv}}]^+$ bonding to the anion is strong, and is significantly stronger than the bonding of $[\text{Bz}(\text{Et})_3\text{N}]^+$ to $[\text{Rh}(\text{CO})_2\text{Cl}_2]^-$, as indicated by the $\nu(\text{CO})$ frequencies.

The observed frequencies for Reaction 2.2.7.A fall very close to those of Product C, which contains SnCl_3^- ligands, and $[\text{H}_{\text{solv}}][\text{Rh}(\text{CO})_2\text{Cl}_2]$, the largest difference between observed frequencies being 4 cm^{-1} . Thus, it is not possible to differentiate

between the two possibilities, and indeed, both complexes may be present together in solution.

In Reaction 2.2.7.C absorptions corresponding to $\text{Rh}(\text{CO})_2\text{Cl}(\text{THF})$ and $\text{Rh}_2(\text{CO})_4\text{Cl}_2$ were observed after 1 minute, along with the absorption at 2009cm^{-1} (Product A). Upon standing only $\text{Rh}(\text{CO})_2\text{Cl}(\text{THF})$ remained. Further bubbling of this solution with $\text{HCl}_{(\text{g})}$ yielded absorptions at 1995 and 2071cm^{-1} due to $[\text{Rh}(\text{CO})_2\text{Cl}_2]^-$.

2.3 ^{119}Sn NMR Studies of Rhodium(I) Carbonyl Chloride/Tin Chloride Reaction solutions

2.3.1 Introduction

Tin has three naturally occurring isotopes of spin $1/2$, ^{115}Sn , ^{117}Sn and ^{119}Sn . Two of these, ^{117}Sn and ^{119}Sn are reasonably naturally abundant, (7.61 and 8.58% respectively) and are important in determining NMR spectra. Due to its high receptivity, however, ^{119}Sn is usually the isotope that is observed⁽¹⁶⁾.

^{119}Sn chemical shifts show a strong dependence on

1. Coordination number of tin
2. Temperature
3. Solvent
4. Bond angles at the tin atom

Information about the electron cloud surrounding the tin nucleus and thus the environment around the nucleus is obtained through the chemical shift by a consideration of the nuclear shielding. Following Ramsey's terminology⁽¹⁷⁾, the nuclear shielding σ , results from diamagnetic (σ_d) and paramagnetic (σ_p) components, where

$$\sigma = \sigma_d + \sigma_p$$

The shielding is mainly due to a sum of diamagnetic and paramagnetic local and non-local contributions:

$$\sigma = (\sigma_d^{\text{loc}} + \sigma_p^{\text{loc}}) + (\sigma_d^{\text{non-loc}} + \sigma_p^{\text{non-loc}})$$

The non-local contributions may include solvent molecules and other atoms in a molecule. Equations exist for the calculation of σ_p and σ_d , but Ramsey's theory has not yet been sufficiently developed such that reliable values can be calculated for heavy nuclei such as tin. In general terms, there is a shift of the ^{119}Sn resonance to lower frequency as the coordination of groups around tin is increased. There are, however, other factors to be considered. These are mainly due to the presence of low-lying excited states and to the effective nuclear charge of the tin atom. The aforementioned influences can mask each other, however, and their separation is difficult. As a result ^{119}Sn chemical shift data is qualitative at best. Tin coupling constants are much more useful in assigning structures to tin(II) complexes, depending strongly on the geometry of the metal complex. The one bond coupling constant $^1J(^{119}\text{SnM})$ (M=Transition metal) has been studied extensively for the complexes $\text{M-SnCl}_3^{(18)}$, the presence of $^1J(^{119}\text{SnM})$ demonstrating the kinetic stability of the M-Sn bond⁽¹⁶⁾. The magnitude of $^1J(^{119}\text{SnM})$ depends strongly upon the polarizability of the transition metal nucleus. Thus $^1J(^{119}\text{SnM})$ will increase with a decreasing trans influence and is therefore dependant on the ligand trans to the SnCl_3^- group.

However, the nature of the transition metal-tin bond depends on various factors which may be reflected by the magnitude of the $^1J(^{119}\text{Sn}, \text{M})$ coupling constant. Changes in coupling constants with large and polarizable nuclei are, however, difficult to interpret and predict.

2.3.2 ^{119}Sn NMR studies of the stability of SnCl_3^- in solution

The equilibrium



is of importance to the homogeneous rhodium-tin-chloride catalysed hydrocarbonylation of ethene described in Chapter 4 along with the reaction chemistry described in this chapter, and has thus been investigated using ^{119}Sn NMR spectroscopy. Studies were carried out in THF.

- (1) Table 2.16 ^{119}Sn NMR data for the addition of differing molar amounts of SnCl_2 to THF

Mole Fraction of SnCl_2	Shift δ/ppm
0.0590	-213.7
0.0390	-211.0
0.0294	-210.9
0.0196	-209.6
0.0098	-208.0

- (2) Table 2.17 ^{119}Sn NMR data for $\text{Bz}(\text{Et})_3\text{NCl}/\text{SnCl}_2$ mixtures in THF

Moles $\text{Bz}(\text{Et})_3\text{NCl}/\text{Moles SnCl}_2$	Shift δ/ppm
0.000	-209.7
0.190	-171.4
0.383	-131.0
0.577	-89.7
0.785	-44.1
0.976	-12.6
1.177	-10.4
1.369	-10.4

- (3) Table 2.18 ^{119}Sn NMR data for $\text{Bz}(\text{Et})_3\text{NCl}/[\text{Bz}(\text{Et})_3\text{N}][\text{SnCl}_3]$ mixtures in THF

Moles $\text{Bz}(\text{Et})_3\text{NCl}/\text{Moles Bz}(\text{Et})_3\text{NSnCl}_3$	Shift δ/ppm
0.000	-7.7
0.201	-7.5

Only single resonances were observed for each of the ^{119}Sn NMR spectra recorded indicating rapid exchange of the chloride ion in the equilibrium



A comparison of the results shown in Tables 2.17 and 2.18 shows that the equilibrium lies more or less totally in favour of the SnCl_3^- species when the $\text{SnCl}_2:\text{Cl}^-$ molar ratio is 1:1, with little change in the position of the signal as the chloride ion content is increased.

2.3.3 ^{119}Sn NMR solution studies of the reactions of Rhodium(I) Carbonyl Chlorides and Tin(II) Chlorides

^{119}Sn NMR spectroscopic studies were carried out for several of the reactions studied using FT-IR spectroscopy and reported earlier in this chapter. The data are summarised in Table 2.19.

2.3.4 Discussion of ^{119}Sn NMR Data

Success in obtaining good quality ^{119}Sn NMR spectra was limited, although a large number of reactions were attempted, and useful information was obtained only for those reactions reported in Table 2.19. The major problem was the decomposition of Rh-SnCl₃ complexes in solution over the long periods of time that were required for accumulation of spectra (usually around 12-24 hours). Poor signal to noise ratio was a notable feature which was difficult to improve. ^{119}Sn NMR spectra were recorded, however, for several solids isolated from the preparative reactions and are discussed in the context of the synthesis studies in Chapter 3.

It is notable that all of the spectra recorded in Table 2.19 consist of one doublet only, suggesting the formation of only a single Rh-SnCl₃ complex in solution for each of the reaction mixtures studied. Infra-red data indicated the formation of Rh(I)-CO-SnCl₃ complexes absorbing at 2011cm⁻¹ (Product A) and 1995, 2010cm⁻¹ (Product C) in THF (Reactions 2.3.3.A, C, D) and at 2017cm⁻¹ in CH₂Cl₂ (Product B) (Reaction 2.3.3.B). The ^{119}Sn NMR data provide further strong evidence which indicates that Products A and B, produced in THF and CH₂Cl₂ solutions respectively, are the same (similar chemical shifts and Rh/Sn coupling constants), and that the small differences arise from different solvent effects. No ^{119}Sn NMR data consistent with the formation of Product C was observed, indicating that conditions are critical for its formation, and that Products A and B are the favoured solution species. The ^{119}Sn NMR data also demonstrates that no non-carbonyl containing Rh-SnCl₃ complexes e.g. $[\text{Rh}(\text{SnCl}_3)_5]^{4-}$ are formed in solution. Thus, the product absorbing in THF at 2011cm⁻¹ (designated Product A) and in CH₂Cl₂ at 2017cm⁻¹ (designated Product B) are considered to be the same complex.

Table 2.19 Summary of ^{119}Sn NMR data for the reactions of rhodium(I) carbonyl chloride complexes with tin(II) chlorides at 25°C

Reaction Code	Reagents	Rh : Sn : (Bz(Et) ₃ NCl) Molar Ratio	Solvent	$\delta(^{119}\text{Sn})/\text{ppm}$	$^1J(^{103}\text{Rh}, ^{119}\text{Sn})$ /Hz	Assignment
2.3.3.A	*[Rh(CO) ₂ Cl ₂] ⁻ SnCl ₂	1 : 1 ^a	THF ^{a1}	92.5d	873	[Rh(CO) ₂ (SnCl ₃) ₃] ²⁻
2.3.3.B	*[Rh(CO) ₂ Cl ₂] ⁻ SnCl ₂	1 : 1 ^b	CH ₂ Cl ₂ ^{b1}	89.5d	876	[Rh(CO) ₂ (SnCl ₃) ₃] ²⁻
2.3.3.C	Rh ₂ (CO) ₄ Cl ₂ SnCl ₂ Bz(Et) ₃ NCl	1 : 1 : 1 ^c	THF ^{c1}	92.6d	960 [†]	[Rh(CO) ₂ (SnCl ₃) ₃] ²⁻
2.3.3.D	Rh ₂ (CO) ₄ Cl ₂ Bz(Et) ₃ NSnCl ₃	1 : 3 ^d	THF ^{d1}	92.2d	838	[Rh(CO) ₂ (SnCl ₃) ₃] ²⁻
2.3.3.E	◇ [Rh(COD)(SnCl ₃) ₃] ²⁻ CO	—	CH ₂ Cl ₂	89.7d	879	[Rh(CO) ₂ (SnCl ₃) ₃] ²⁻

[†] Estimated from a noisy spectrum having a low signal to noise ratio. Any discrepancy is accounted for by uncertainty in the position of the signal maxima.

* Cation = [Bz(Et)₃N]⁺, ◇ Cation = [PPN]⁺ a - 54.0mg (0.128mmol) : 28.9mg (0.152mmol), a1 - 5ml b - 52.1mg (0.123mmol) : 25.3mg (0.133mmol), b1 - 5ml
 c - 19.8mg (0.051mmol) : 20.1mg (0.106mmol), c1 - 4ml d - 20.5mg (0.064mmol) : 162mg (0.390mmol), d1 - 5ml

Notes:

- All of the above reactions 2.3.3.A-2.3.3.E were carried out under a nitrogen atmosphere in a 10mm NMR tube.
- All chemical shifts were measured relative to Me₄Sn as an external reference.
- The spectra were recorded on a Bruker AC-250 operating at 93.275MHz.
- No $^2J(^{119}\text{Sn}, ^{119}\text{Sn})$ or $^2J(^{119}\text{Sn}, ^{117}\text{Sn})$ coupling was observed for any of Reactions 2.2.3.A-E, possibly due to the poor signal to noise ratio.

However, it is of relevance that ^{119}Sn NMR data is accumulated over a 24 hour period whilst infra-red data is obtained over approximately a 1 minute scan. Thus, although the data obtained from the two techniques can be correlated to provide information about a particular reaction, there exists the possibility that some further chemistry may occur over the long period of time required for accumulation of ^{119}Sn NMR spectral data.

The ^{119}Sn NMR data for Reactions 2.3.3.A-E relates closely to Pregosin's data on the product of carbonylation of $[\text{Rh}(\text{COD})(\text{SnCl}_3)_3]^{2-}$ ($\delta(^{119}\text{Sn})/\text{ppm}$ 89.1d, $^1\text{J}(^{103}\text{Rh}, ^{119}\text{Sn})/\text{Hz}$ 864, CDCl_3 , RT ⁽⁷⁾), which using $^{117}\text{Sn}/^{119}\text{Sn}$ satellite data he assigned as $[\text{Rh}(\text{CO})_2(\text{SnCl}_3)_3]^{2-}$. On the basis of relative intensities of satellite signals, he eliminated complexes containing Rh:Sn ratios of 1:1, 1:2, 1:4 etc. and categorically assigned the solution species as the 1:3 complex. Though the signal to noise ratio did not allow observation of satellites for the reactions reported here, the close correspondence of ^{119}Sn NMR data obtained in this work, with Pregosin's data, leads to the conclusion that the doublets observed in Reactions 2.3.3.A-E are due to $[\text{Rh}(\text{CO})_2(\text{SnCl}_3)_3]^{2-}$.

The ^{119}Sn NMR single doublets observed indicate that either the Rh/Sn complex is fluxional, or equivalent trichlorostannate groups exist over the NMR time scale. Previous studies have indicated that ligands coordinated to transition metals are often mobile, and that 5-coordinate rhodium d^8 complexes are non-rigid on the NMR time scale, due to Berry pseudorotation^(19,20), which has activation energies of the order 7.5-12 kcal/mol for a rhodium(I) trichlorostannate system⁽²¹⁾. This pseudorotation of ligands is found to be rapid at room temperature and can still be observed at temperatures as low as -90°C . This implies that for the Rh/Sn complexes formed in this work, no distinction will be detected between trichlorostannate groups in different environments. Thus, the observed ^{119}Sn NMR signal and $^1\text{J}(^{103}\text{Rh}, ^{119}\text{Sn})$ coupling constant at room temperature will each be an average comprised of the component signals and coupling constants of the trichlorostannate ligands in their various positions. This seems to be the case for Reactions 2.3.3.A-E. Several of the ^{119}Sn NMR experiments were carried out at temperatures down to -50°C , in an attempt to remove the possibility of Berry pseudorotation, and thus distinguish between trichlorostannate groups which may be in different chemical environments. Both equatorial and axial ligands for example, are present in the trigonal bipyramidal complex $[\text{Rh}(\text{CO})(\text{SnCl}_3)_4]^{3-}$, synthesised and isolated in the crystal form, as described in Chapter 3, from the components used for Reaction 2.3.3.C. No ^{119}Sn NMR signals were observed at low temperature for any of the systems 2.2.3.A-E,

however, probably due to the relative insolubility at low temperature of both the starting materials and species formed in solution.

An additional ^{119}Sn NMR singlet was observed at -8.3 ppm for the reaction of $\text{Rh}_2(\text{CO})_4\text{Cl}_2$ and $[\text{Bz}(\text{Et})_3\text{N}][\text{SnCl}_3]$ (Reaction 2.3.3.D). A comparison of this value with data shown in Tables 2.17 and 2.18 for SnCl_3^- in THF, Section 2.3.2, indicated that this signal was due to $[\text{Bz}(\text{Et})_3\text{N}][\text{SnCl}_3]$, the starting material. Reaction appears not to have gone to completion. Free SnCl_3^- was not detected in solution for other reactions.

2.4 Discussion of Results

Infra-red and ^{119}Sn NMR studies described in this chapter have shown that the rhodium(I)-carbonyl-chlorides, $\text{Rh}_2(\text{CO})_4\text{Cl}_2$ and $[\text{Rh}(\text{CO})_2\text{Cl}_2]^-$, react with the tin(II) chlorides SnCl_2 and SnCl_3^- , to form rhodium(I)-carbonyl-trichlorostannate complexes. A summary of the data obtained for these reactions, along with assignments to Products A, B and C, is shown in Table 2.20, together with other data for Rh(I)-CO- SnCl_3 species of relevance to this work.

In THF, infra-red data indicate the formation of a complex absorbing at $2011/2010\text{cm}^{-1}$ (Product A), whilst in CH_2Cl_2 an absorption is observed at $2017/2018\text{cm}^{-1}$ (Product B). A very weak absorption $\{\nu(\text{CO})\ 2072\text{cm}^{-1}\}$ apparently due to the same complex as the absorption at $2010/2011\text{cm}^{-1}$ (Product A), was also observed on two occasions in THF (see Reactions 2.2.1.D and E). ^{119}Sn NMR data indicate the presence of one Rh- SnCl_3 complex only in each solvent, and the similar chemical shift and $^1J(^{103}\text{Rh}, ^{119}\text{Sn})$ coupling constants demonstrate that the complex in the two solvents is the same. The small difference in the strong $\nu(\text{CO})$ absorption in the two solvents is ascribed to solvent effects, comparable differences occurring for other complexes as illustrated for $[\text{Rh}(\text{CO})_2\text{Cl}_2]^-$ in Table 2.1. The ^{119}Sn NMR data relates closely to Pregosin's data on the product of carbonylation of $[\text{Rh}(\text{COD})(\text{SnCl}_3)_3]^{2-}$ (7), which using $^{117}\text{Sn}/^{119}\text{Sn}$ satellite data he assigned as $[\text{Rh}(\text{CO})_2(\text{SnCl}_3)_3]^{2-}$. On the basis of relative intensities of satellite signals, he eliminated complexes containing Rh:Sn ratios of 1:1, 1:2, 1:4 etc. and categorically assigned the solution species as the 1:3 complex. Though the signal to noise ratio did not allow observation of satellites for the reactions reported here, the close correspondence of ^{119}Sn NMR data obtained in this work, with Pregosin's data, along with $\nu(\text{CO})$ data leads to the conclusion that Product A/B is $[\text{Rh}(\text{CO})_2(\text{SnCl}_3)_3]^{2-}$. Unfortunately, the weak $\nu(\text{CO})$ stretching frequency at 2072cm^{-1} associated with

$[\text{Rh}(\text{CO})_2(\text{SnCl}_3)_3]^{2-}$ was not observed in most reactions, though it was frequently detected in work to be described in Chapter 3. The weak intensity of this absorption, and the presence of other complexes e.g. $[\text{Rh}(\text{CO})_2\text{Cl}_2]^-$, $\text{Rh}_2(\text{CO})_4\text{Cl}_2$ and $\text{Rh}(\text{CO})_2\text{Cl}(\text{THF})$ having absorptions in the same region all contributed to its lack of detection in both THF and CH_2Cl_2 .

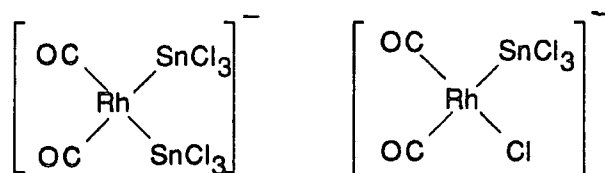
Table 2.20 Summary of infra-red and ^{119}Sn NMR data for the Rh(I)-CO-SnCl₃ complexes formed in solution, together with data for other species of relevance to this work

Reactants	Solvent	Data obtained for Rh(I)-CO-SnCl ₃ complexes formed		
		$\nu(\text{CO})/\text{cm}^{-1}$	$\delta(^{119}\text{Sn})/\text{ppm}$	$^1J(^{103}\text{Rh}, ^{119}\text{Sn})$
* $[\text{Rh}(\text{CO})_2\text{Cl}_2]^-$ SnCl ₂	THF	2011 Product A	92.5 d Product A	873
* $[\text{Rh}(\text{CO})_2\text{Cl}_2]^-$ SnCl ₂	CH ₂ Cl ₂	2017 Product B	89.5 d Product B	876
Rh ₂ (CO) ₄ Cl ₂ SnCl ₂ Bz(Et) ₃ NCl	THF	2010 Product A 1994 2070 Product C	92.6 d Product A	960 [†]
Rh ₂ (CO) ₄ Cl ₂ SnCl ₂ Bz(Et) ₃ NCl	CH ₂ Cl ₂	2017 Product B	—	—
Rh ₂ (CO) ₄ Cl ₂ *SnCl ₃ ⁻	THF	2011 Product A 1995 2070 Product C	92.2 d Product A	838
Rh ₂ (CO) ₄ Cl ₂ *SnCl ₃ ⁻	CH ₂ Cl ₂	2018 Product B	—	—
* $[\text{Rh}(\text{COD})(\text{SnCl}_3)_3]^{2-}$ CO	THF CH ₂ Cl ₂	2011 _s 2072 _{vw} 2018 _s 2069 _{vw}	91.6 d —	864 —
* $[\text{Rh}(\text{COD})(\text{SnCl}_3)_3]^{2-}$ CO	CH ₂ Cl ₂	2017 _s 2069 _{vw}	89.7 d	879
* $[\text{Rh}(\text{CO})(\text{SnCl}_3)_4]^{3-}$ (Chapter 3, Sec. 3.2.1)	Nujol	2012 _s	—	—
* $[\text{Rh}(\text{CO})(\text{SnCl}_3)_2\text{Cl}]^{2-}$ (Chapter 3, Sec. 3.2.2)	Nujol	2013 _s	—	—
* $[\text{Rh}(\text{CO})_2(\text{SnCl}_3)_3]^{2-}$ (7)	KBr	2010 2060	89.1 d(CDCl ₃)	864 $^2J(^{119}\text{Sn}, ^{117}\text{Sn}) =$ 9341
* $[\text{Rh}(\text{CO})_2(\text{SnCl}_3)_3]^{2-}$	Nujol	2016 _s 2065 _{vw}	89.4 d(CH ₂ Cl ₂)	879

[†] Estimated from a noisy spectrum (see Table 2.19). * [Bz(Et)₃N]⁺ ♦ [PPN]⁺

The data collected during the reaction studies are consistent with the favoured complex being $[\text{Rh}(\text{CO})_2(\text{SnCl}_3)_3]^{2-}$, the complex forming rapidly in THF from reaction of both $[\text{Rh}(\text{CO})_2\text{Cl}_2]^-$ and $\text{Rh}_2(\text{CO})_4\text{Cl}_2$ with $\text{SnCl}_2/\text{Cl}^-$ and SnCl_3^- . Though reactions were undertaken using a variety of molar ratios of Rh:Sn (i.e. 1:1 to 1:4), the sole product detected in THF solution for most reactions was $[\text{Rh}(\text{CO})_2(\text{SnCl}_3)_3]^{2-}$ irrespective of the Rh:Sn molar ratio of the starting complexes. Interestingly, a second species, Product C, was detected only in THF, from reaction of $\text{Rh}_2(\text{CO})_4\text{Cl}_2$ with SnCl_3^- or $\text{SnCl}_2/\text{Cl}^-$, and not in CH_2Cl_2 , and forms along with $[\text{Rh}(\text{CO})_2(\text{SnCl}_3)_3]^{2-}$, sometimes in a much greater quantity than this complex. It appears to predominate in reactions which are 1:1 Rh:Sn, but not exclusively. It is also detected as a major product in a 1:3 Rh:Sn reaction, and appears to be closely related to $[\text{Rh}(\text{CO})_2(\text{SnCl}_3)_3]^{2-}$, either as an intermediate in its formation, or as a product of its dissociation or decomposition, and is also observed to form on ageing of $[\text{Rh}(\text{CO})_2(\text{SnCl}_3)_3]^{2-}$ solutions. However, reaction to form Product C at room temperature was too fast to differentiate between the two routes, and infra-red studies at lower temperature also did not provide information about formation of Product C or indeed other reaction intermediates. Product C was not detected by ^{119}Sn NMR spectroscopy, and reactions to form it are not reproducible, with $[\text{Rh}(\text{CO})_2(\text{SnCl}_3)_3]^{2-}$ often formed as the sole product.

Product C has a pattern of $\nu(\text{CO})$ absorptions (1994_s , 2070_scm^{-1}) which is consistent with the formation of a cis-dicarbonyl complex of the type $[\text{Rh}(\text{CO})_2\text{XY}]^-$, where X and Y are either SnCl_3^- or Cl^- groups [c.f. $[\text{Bu}_4\text{N}][\text{Rh}(\text{CO})_2(\text{OAc})_2]$ $\nu(\text{CO})$ 1986, 2066cm^{-1} (terminal CO) in CH_2Cl_2 , and $n\text{-}[\text{Bu}_4\text{N}][\text{Rh}(\text{CO})_2(\text{OAc})\text{I}]$ $\nu(\text{CO})$ 1979, 2058cm^{-1} (terminal CO) in THF, reported by Maitlis et al⁽²²⁾]. The increase in the frequency of the carbonyl absorptions compared with those for $[\text{Rh}(\text{CO})_2\text{Cl}_2]^-$ (1984_s , 2062_scm^{-1}) indicate that the data is consistent with both $[\text{Rh}(\text{CO})_2(\text{SnCl}_3)\text{Cl}]^-$ and $[\text{Rh}(\text{CO})_2(\text{SnCl}_3)_2]^-$ in the square planar arrangements shown below, though the relatively small increase in $\nu(\text{CO})$ compared with $[\text{Rh}(\text{CO})_2\text{Cl}_2]^-$, is probably more consistent with the former than the latter complex. Also, since it has two bulky SnCl_3^- ligands, $[\text{Rh}(\text{CO})_2(\text{SnCl}_3)_2]^-$ is more likely to prefer a square planar conformation with CO ligands in positions trans to each other.

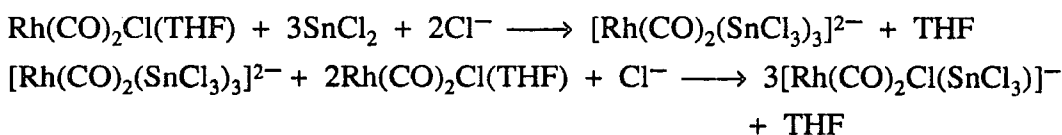


Unfortunately, however, it is not possible to differentiate between these two possibilities purely on the basis of solution infra-red data.

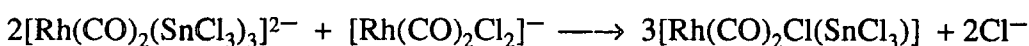
Reaction of $\text{Rh}_2(\text{CO})_4\text{Cl}_2$ with SnCl_2 and $\text{Bz}(\text{Et})_3\text{NCl}$ (see Section 2.2.5), indicated that Product C, although immediately formed in solution upon reaction, was also formed at the apparent expense of $[\text{Rh}(\text{CO})_2(\text{SnCl}_3)_3]^{2-}$. This could be explained by the following:

1. Initial reaction favouring formation of $[\text{Rh}(\text{CO})_2(\text{SnCl}_3)_3]^{2-}$.
2. Reaction of $[\text{Rh}(\text{CO})_2(\text{SnCl}_3)_3]^{2-}$ with $[\text{Rh}(\text{CO})_2\text{Cl}_2]^-$ or $\text{Rh}(\text{CO})_2\text{Cl}(\text{THF})$ to form product C.

The following series of reactions are an illustration of this:



or



The relative ratio of $[\text{Rh}(\text{CO})_2(\text{SnCl}_3)_3]^{2-}$:Product C varied from reaction to reaction, and reactions to give Product C were not reproducible. $[\text{Rh}(\text{CO})_2(\text{SnCl}_3)_3]^{2-}$ was often produced alone, but in some reactions (Reactions 2.2.5.A, 2.2.6.A, 2.2.6.B), C was the major product, and in Reaction 2.2.5.A was apparently formed at the expense of $[\text{Rh}(\text{CO})_2(\text{SnCl}_3)_3]^{2-}$. It was never observed in reactions of $[\text{Rh}(\text{CO})_2\text{Cl}_2]^-$ with SnCl_2 . $[\text{Rh}(\text{CO})_2(\text{SnCl}_3)_3]^{2-}$ and Product C, along with other $\text{Rh}(\text{I})\text{-CO-SnCl}_3$ complexes, are believed to be related by a series of facile reactions (see Chapter 3) involving the dissociation of SnCl_3^- and CO ligands. Here, the reaction conditions (e.g. temperature, concentration of species in solution) appear to be critical for its formation and $[\text{Rh}(\text{CO})_2(\text{SnCl}_3)_3]^{2-}$ appears to be the more favoured product in solution, which is in keeping with the recognised tendency of the SnCl_3^- ligand to stabilise 5-coordination⁽²³⁻²⁷⁾.

The reactions studied by infra-red and ^{119}Sn NMR spectroscopy were, in the main, extremely fast at room temperature, indicating that the rhodium(I) carbonyl chlorides are very reactive towards the tin(II) chlorides. Slower reactions were only afforded by the relative insolubility of the starting materials (usually those in CH_2Cl_2 in which SnCl_2 was taken into solution as the reactions progressed). Attempts to follow the reactions at -78°C using infra-red spectroscopy were not successful since no reaction intermediates were observed, suggesting that any such complexes formed in solution were short lived. Nevertheless, based on infra-red spectral data the reaction pathway shown in Figure 2.6 is proposed for the reactions carried out in THF.

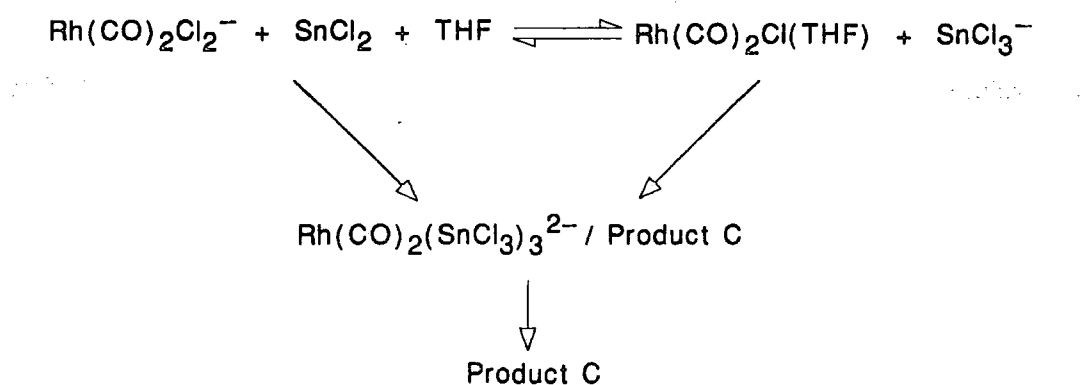


Figure 2.6 Proposed scheme for the reactions of rhodium(I) carbonyl chlorides with tin(II) chlorides in THF

The reactions of $[\text{Rh}(\text{CO})_2\text{Cl}_2]^-$ and $\text{Rh}_2(\text{CO})_4\text{Cl}_2$ with SnCl_2 and SnCl_3^- in THF may be explained as follows:

- (a) Reaction of $[\text{Rh}(\text{CO})_2\text{Cl}_2]^-$ with SnCl_2 which involves initial abstraction of a chloride ligand from $[\text{Rh}(\text{CO})_2\text{Cl}_2]^-$ by SnCl_2 , and the vacant coordination site taken by THF to form SnCl_3^- and $\text{Rh}(\text{CO})_2\text{Cl}(\text{THF})$ in solution ($\nu(\text{CO}) - 2004, 2081\text{cm}^{-1}$). Small quantities of $\text{Rh}(\text{CO})_2\text{Cl}(\text{THF})$ are always observed for reactions of $[\text{Rh}(\text{CO})_2\text{Cl}_2]^-$ with SnCl_2 in THF (see Reactions 2.2.1.A-D).
- (b) $\text{Rh}_2(\text{CO})_4\text{Cl}_2$ undergoes reaction to form $\text{Rh}(\text{CO})_2\text{Cl}(\text{THF})$ via cleavage of the Rh-Cl-Rh bridges by THF.

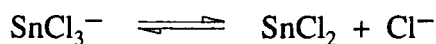
The reaction to form $[\text{Rh}(\text{CO})_2(\text{SnCl}_3)_3]^{2-}$ and Product C may then proceed by two separate routes from either $\text{Rh}(\text{CO})_2\text{Cl}(\text{THF})$ or $[\text{Rh}(\text{CO})_2\text{Cl}_2]^-$.

- Route I By ligand substitution involving displacement of THF and the chloride ligand by SnCl_3^- ligands.
- Route II By ligand migration such as insertion of SnCl_2 into the Rh-Cl bonds of $[\text{Rh}(\text{CO})_2\text{Cl}_2]^-$ or $\text{Rh}(\text{CO})_2\text{Cl}(\text{THF})$.

Each of the routes could possibly operate at the same time and may be competing with each other. The formation of Product C could occur by the series of insertion and displacement reactions described above, but the formation of $[\text{Rh}(\text{CO})_2(\text{SnCl}_3)_3]^{2-}$ via further reaction of SnCl_3^- with an initially formed complex, such as $[\text{Rh}(\text{CO})_2(\text{SnCl}_3)_2]^-$, consistent with Product C, seems more favourable, and is in keeping with the tendency of the SnCl_3^- ligand to stabilise 5-coordination⁽²³⁻²⁷⁾, along with the general preference for the formation of $[\text{Rh}(\text{CO})_2(\text{SnCl}_3)_3]^{2-}$ over Product C. A similar reaction scheme to that shown in Figure 2.6 is appropriate for reactions undertaken in CH_2Cl_2 , except that the solvent containing complex does not feature.

The formation of 5-coordinate complexes can be attributed to the strong π -acceptor ability of the SnCl_3^- group⁽¹¹⁻¹⁴⁾. This allows formation of such complexes by a large back donation of π -electron density from the occupied rhodium d-orbitals to the vacant tin 5d orbitals. Thus, the 5-coordinate state is 'stabilised' due to a strengthening of the metal-ligand bonds (i.e. increase in bond energy). Removal of electron density from the metal centre is favourable for a metal such as rhodium(I) in a low formal oxidation state, since electron density built up via the σ -system is dispersed through the π -system. The removal of π -electron density from rhodium effectively makes the metal centre more electropositive. Therefore, addition of further ligands becomes more favourable, and hence the ability of strong π -acceptor ligands such as SnCl_3^- to form 5-coordinate rhodium(I) complexes such as $[\text{Rh}(\text{CO})_2(\text{SnCl}_3)_3]^{2-}$. 5-coordination would not be favoured by chloride ligands, which are predominantly σ -donors.

^{119}Sn NMR data for $\text{SnCl}_2/\text{Cl}^-$ and $\text{SnCl}_3^-/\text{Cl}^-$ mixtures in THF (see Section 2.3.2), showed that the equilibrium:



lies more or less totally in favour of the SnCl_3^- ion when the $\text{Cl}^-:\text{SnCl}_2$ molar ratio is 1:1 or greater. However, reactions of $\text{Rh}_2(\text{CO})_4\text{Cl}_2$ with SnCl_3^- in both THF and

CH_2Cl_2 (see Reactions 2.2.6.A-E) resulted in the formation of $[\text{Rh}(\text{CO})_2\text{Cl}_2]^-$. Also, the same tin-containing complexes were obtained from the rhodium(I) carbonyl chloride complexes whether SnCl_2 or SnCl_3^- were used, demonstrating the importance of the equilibrium. This illustrates that both insertion of SnCl_2 into a Rh-Cl bond and ligand substitution, SnCl_3^- for Cl^- and THF, may lead to Rh(I)-CO- SnCl_3 complexes.

2.5 Conclusions

The rhodium(I) carbonyl chloride complexes, $[\text{Rh}(\text{CO})_2\text{Cl}_2]^-$ and $\text{Rh}_2(\text{CO})_4\text{Cl}_2$, react with the tin(II) chlorides, SnCl_2 and SnCl_3^- , in both THF and CH_2Cl_2 to form Rh(I)- SnCl_3 complexes. Infra-red and ^{119}Sn NMR data identified the 5-coordinate complex $[\text{Rh}(\text{CO})_2(\text{SnCl}_3)_3]^{2-}$ as the favoured species formed in solution. However, reactions of $\text{Rh}_2(\text{CO})_4\text{Cl}_2$ with $\text{SnCl}_2/\text{Cl}^-$ and SnCl_3^- in THF indicated that a 4-coordinate species, possibly either $[\text{Rh}(\text{CO})_2(\text{SnCl}_3)_2]^-$ or $[\text{Rh}(\text{CO})_2\text{Cl}(\text{SnCl}_3)]^-$, is also formed. The reaction conditions appear to be critical towards the formation and/or stability of this second product, which appears closely related to $[\text{Rh}(\text{CO})_2(\text{SnCl}_3)_3]^{2-}$, either as an intermediate in its formation, or as a product of its dissociation or decomposition.

2.6 References

1. N.J. Winter, Ph.D Thesis, University of Durham, 1991.
2. J.A. McCleverty, G. Wilkinson, *Inorg. Synth.*, **1966**, 8, 211.
3. L.M. Vallarino, *Inorg. Chem.*, **1965**, 4, 161.
4. M.J. Cleare, W.P. Griffith, *J. Chem. Soc. (A)*, **1970**, 2788.
5. J.F. Young, R.D. Gillard, G. Wilkinson, *J. Chem. Soc.*, **1964**, 5176.
6. J.V. Kingston, G.R. Scollary, *J. Chem. Soc. (A)*, **1971**, 3399.
7. M. Kretschmer, P.S. Pregosin, H. Rügger, *J. Organometal. Chem.*, **1983**, 241, 87.
8. L. Garlaschelli, M.C. Iapalucci, G. Longoni, M. Marchionna, *J. Organometal. Chem.*, **1989**, 378, 457.
9. K. Nakamoto, 'Infrared and Raman Spectra of Inorganic and Coordination Compounds', 4th Ed., J. Wiley & Sons, **1986**.
10. J.A. McCleverty, G. Wilkinson, *Inorg. Synth.*, **1966**, 8, 214.
11. W.A.G. Graham, *Inorg. Chem.*, **1968**, 7, 315.
12. W. Jetz, P.B. Simons, J.A.J. Thompson, W.A.G. Graham, *Inorg. Chem.*, **1966**, 5, 2217.
13. R.V. Lindsey Jr., G.W. Parshall, U.G. Stolberg, *J. Am. Chem. Soc.*, **1965**, 87, 658.
14. G.W. Parshall, *J. Am. Chem. Soc.*, **1966**, 88, 704.
15. R.E. Hutton, V. Oakes, *Adv. Chem.*, **1976**, 157, 123.
16. B. Wrackmayer, *Annual Reports in NMR Spectroscopy*, Ed. G.A. Webb, **1985**, 16, 73.
17. N.F. Ramsey, *Phys. Rev.*, **195**, 78, 689.
18. K.H.A.O. Starzewski, P.S. Pregosin, *Adv. Chem. Ser.*, **1982**, 196, 23.
19. M.A. Garralda, E. Pinilla, M.A. Monge, *J. Organometal. Chem.*, **1992**, 427, 193.
20. R. Uson, L.A. Oro, M.T. Pinillos, A. Arruebo, K.H.A.O. Starzewski, P.S. Pregosin, *J. Organometal. Chem.*, **1980**, 192, 227.
21. P. Meakin, J.P. Jesson, *J. Am. Chem. Soc.*, **1973**, 95, 7272.
22. A. Fulford, N.A. Bailey, H. Adams, P.M. Maitlis, *J. Organometal. Chem.*, **1991**, 417, 139.
23. P. Porta, H.M. Powell, R.J. Mawby, L.M. Venanzi, *J. Chem. Soc. (A)*, **1967**, 455.
24. M.R. Churchill, K.K.G. Lin, *J. Am. Chem. Soc.*, **1974**, 96, 76.
25. R.D. Cramer, R.V. Lindsay Jr., C.T. Prewitt, U.G. Stolberg, *J. Am. Chem. Soc.*, **1965**, 87, 658.

26. C.Y. Hsu, M. Orchin, *J. Am. Chem. Soc.*, 1975, 97, 3553.
27. R. Uson, L.A. Oro, M.T. Pinillas, A. Arruebo, K.H.A.O. Starzewski, P.S. Pregosin, *J. Organometal. Chem.*, 1980, 192, 227.

Chapter 3

Synthesis, Characterisation and Properties of Rhodium(I) - Trichlorostannate Complexes

3.1 Introduction

The studies reported in Chapter 2, relating to the fundamental chemistry occurring in solution between rhodium(I) carbonyl chlorides and tin(II) chlorides were extended to include the synthesis and characterisation of Rh(I)-SnCl₃ complexes, using standard laboratory techniques, with the aim of isolating species observed in solution by FT-IR and NMR spectroscopy. The complexes, along with other rhodium(I)-tin(II) complexes, synthesised by known methods, were later used to develop the catalytic process for the hydrocarbonylation of ethene (see Chapter 4). The synthesis and study of these complexes is necessary for further understanding of the chemistry occurring in the hydrocarbonylation process.

The synthesis, reaction chemistry and structural properties of complexes isolated may reveal much about the chemistry of the rhodium(I) carbonyl trichlorostannate complexes formed in solution (see Chapter 2), and may therefore provide information about the reaction chemistry occurring in the catalytic process, and the role of the trichlorostannate ligand in this reaction.

3.2 Experimental

All solvents used for the reactions described in this chapter were dried and degassed prior to use. Acetone was also distilled.

3.2.1 Preparation of [Bz(Et)₃N]₃[Rh(CO)(SnCl₃)₄]

Anhydrous tin(II) chloride(0.0102g, 0.054mmol) and solid benzyltriethylammonium chloride(0.0208g, 0.091mmol) were added to dichlorotetracarbonyldirrhodium(I) (0.0107g, 0.0275mmol) in 5ml of THF under dry nitrogen in a Schlenk tube at 20°C. An instantaneous colour change from orange to bright red was observed. The solution was stored at approximately 0°C for 24 hours, giving deposition of bright red crystals. The bulk of the solution was removed by syringe and the residual solvent removed under vacuum. The red crystals of [Bz(Et)₃N]₃[Rh(CO)(SnCl₃)₄] were then transferred and stored under a dry nitrogen atmosphere, although exposure to air suggested that they were not particularly air or moisture sensitive.

{Infra-red: $\nu(\text{CO})/\text{cm}^{-1}$ - 2012_s in nujol; Found: C 29.42, H 4.15, N 2.44%; [Bz(Et)₃N]₃[Rh(CO)(SnCl₃)₄] requires C 29.85, H 4.10, N 2.44%}

A crystal structure determination was carried out by Prof. J.A.K. Howard and J. Cole on a crystal of [Bz(Et)₃N]₃[Rh(CO)(SnCl₃)₄].

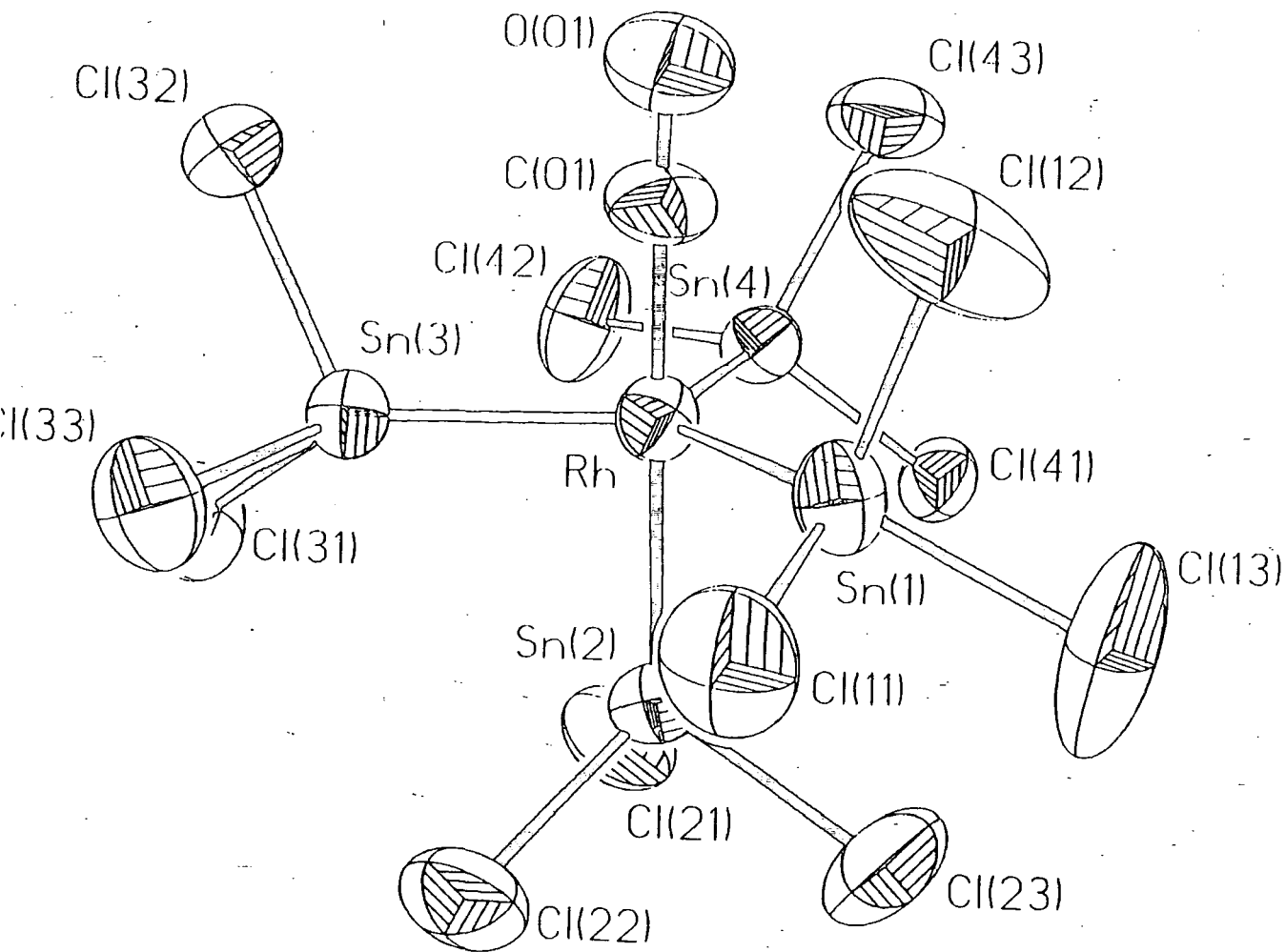
Structure Determination Summary

Empirical Formula	$C_{20}H_{32.5}Cl_6N_{1.5}O_{0.5}Rh_{0.5}Sn_2$
Formula Weight	803.5
Colour	Red
Space Group	$P3_2$, Trigonal
a	13.125(4)Å
b	13.125(4)Å
c	30.6114(5)Å
α	90°
β	90°
γ	120°
Volume	4566.8(13)Å ³
Temperature	298K
R	0.0390
Rw	0.0390
wR	0.0413
Goodness of fit	3.11
$N_{\text{parameters}}$ (Total)	420
$N_{\text{parameters}}$ (Max refined)	420
$N_{\text{reflections}}$	4306
Largest residual peak	0.60eÅ ⁻³
Largest residual trough	-0.51eÅ ⁻³

Figure 3.1 shows the solid state crystal structure of the anion $[Rh(CO)(SnCl_3)_4]^{3-}$ and Figure 3.2 shows the complete structure of $[Bz(Et)_3N]_3[Rh(CO)(SnCl_3)_4]$ with the spatial arrangement of the benzyltriethylammonium cations around the central rhodium anion.

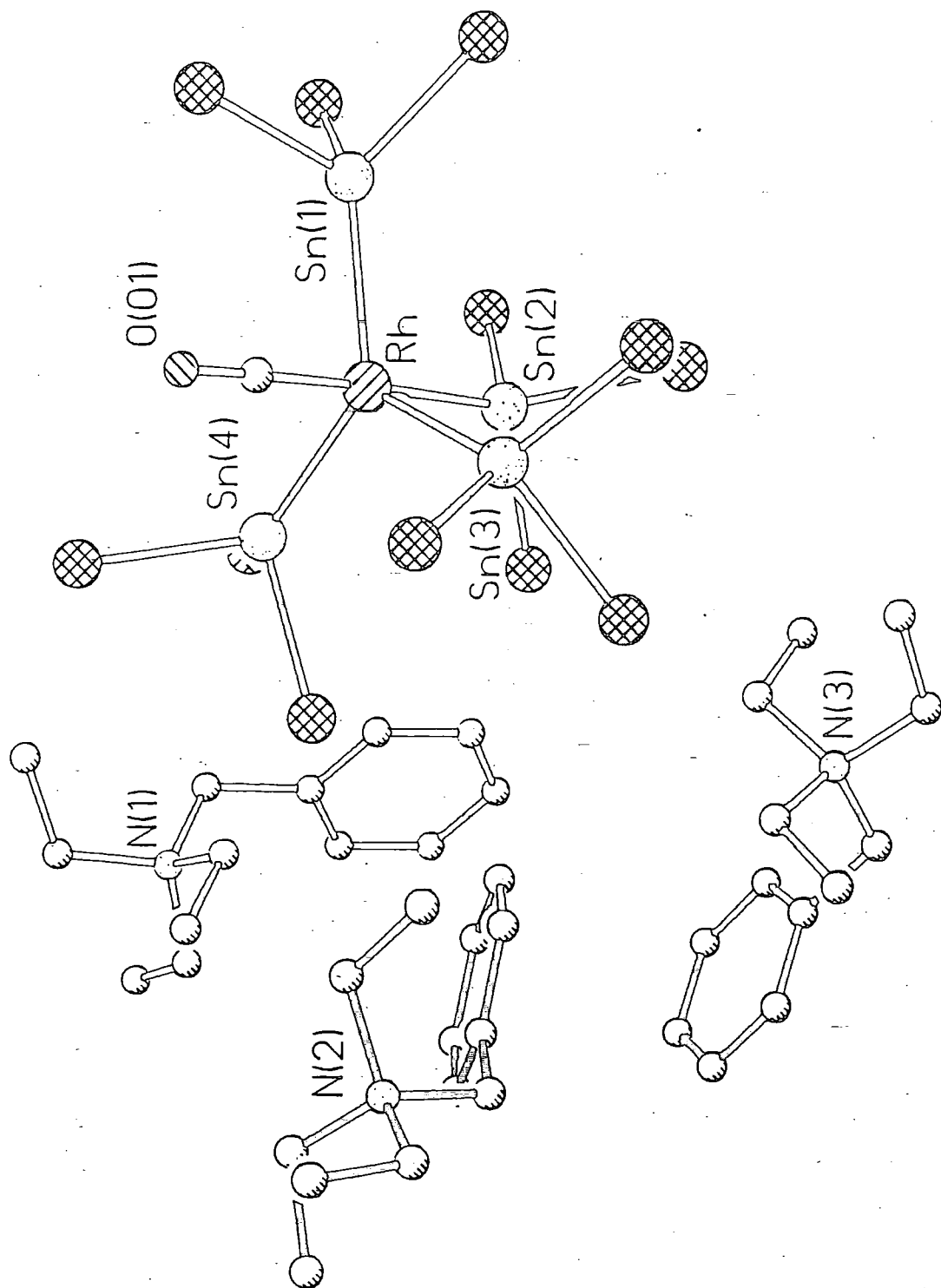
The anion is essentially trigonal bipyramidal in nature with three trichlorostannate ligands in equatorial positions and the other trichlorostannate ligand along with the carbon monoxide ligand in axial positions. Tables 3.1-3.2 summarise the atomic coordinates, bond lengths and bond angles of $[Bz(Et)_3N]_3[Rh(CO)(SnCl_3)_4]$.

Figure 3.1 Crystal structure of $[\text{Rh}(\text{CO})(\text{SnCl}_3)_4]^{3-}$



Prof. J.A.K. Howard and Jason Cole, unpublished data.

Figure 3.2 Crystal structure of $[\text{Bz}(\text{Et})_3\text{N}]_3[\text{Rh}(\text{CO})(\text{SnCl}_3)_4]$



Prof. J.A.K. Howard and J. Cole, unpublished data.

Table 3.1. Bond lengths (Å) for [Bz(Et)₃N]₃[Rh(CO)(SnCl₃)₄]

Rh-Sn(1)	2.553(2)	Rh-Sn(2)	2.559(2)
Rh-Sn(3)	2.543(1)	Rh-Sn(4)	2.535(2)
Rh-C(01)	1.840(18)	Sn(1)-Cl(13)	2.363(7)
Sn(1)-Cl(12)	2.348(6)	Sn(1)-Cl(11)	2.371(6)
Sn(2)-Cl(23)	2.351(7)	Sn(2)-Cl(22)	2.370(6)
Sn(2)-Cl(21)	2.374(5)	Sn(3)-Cl(33)	2.397(4)
Sn(3)-Cl(32)	2.390(7)	Sn(3)-Cl(31)	2.406(5)
Sn(4)-Cl(43)	2.361(6)	Sn(4)-Cl(42)	2.380(7)
Sn(4)-Cl(41)	2.394(3)	C(01)-O(01)	1.144(23)
N(1)-C(1)	1.516(25)	N(1)-C(17)	1.506(22)
N(1)-C(19)	1.529(15)	N(1)-C(111)	1.510(23)
C(1)-C(11)	1.518(20)	C(17)-C(18)	1.512(27)
C(19)-C(110)	1.544(28)	C(111)-C(112)	1.523(19)
N(2)-C(2)	1.555(21)	N(2)-C(27)	1.531(22)
N(2)-C(29)	1.509(18)	N(2)-C(211)	1.501(19)
C(2)-C(21)	1.504(20)	C(27)-C(28)	1.501(21)
C(29)-C(210)	1.505(26)	C(211)-C(212)	1.519(30)
N(3)-C(3)	1.528(20)	N(3)-C(37)	1.479(20)
N(3)-C(39)	1.501(29)	N(3)-C(311)	1.520(24)
C(3)-C(31)	1.507(18)	C(37)-C(38)	1.546(26)
C(39)-C(310)	1.497(29)	C(311)-C(312)	1.518(36)

Table 3.2 Bond angles (°) for [Bz(Et)₃N]₃[Rh(CO)(SnCl₃)₄]

Sn(1)-Rh-Sn(2)	91.1(1)	Sn(1)-Rh-Sn(3)	121.9(1)
Sn(2)-Rh-Sn(3)	90.9(1)	Sn(1)-Rh-Sn(4)	126.0(1)
Sn(2)-Rh-Sn(4)	88.4(1)	Sn(3)-Rh-Sn(4)	112.2(1)
Sn(1)-Rh-C(01)	89.9(7)	Sn(2)-Rh-C(01)	178.2(6)
Sn(3)-Rh-C(01)	89.8(5)	Sn(4)-Rh-C(01)	89.8(6)
Rh-Sn(1)-Cl(13)	128.2(2)	Rh-Sn(1)-Cl(12)	111.9(3)
Cl(13)-Sn(1)-Cl(12)	96.7(4)	Rh-Sn(1)-Cl(11)	123.5(2)
Cl(13)-Sn(1)-Cl(11)	92.9(3)	Cl(12)-Sn(1)-Cl(11)	96.9(3)
Rh-Sn(2)-Cl(23)	120.4(2)	Rh-Sn(2)-Cl(22)	121.2(2)
Cl(23)-Sn(2)-Cl(22)	97.1(3)	Rh-Sn(2)-Cl(21)	119.7(2)
Cl(23)-Sn(2)-Cl(21)	96.3(2)	Cl(22)-Sn(2)-Cl(21)	96.3(2)
Rh-Sn(3)-Cl(33)	125.7(2)	Rh-Sn(3)-Cl(32)	113.9(1)
Cl(33)-Sn(3)-Cl(32)	94.2(2)	Rh-Sn(3)-Cl(31)	125.5(1)
Cl(33)-Sn(3)-Cl(31)	94.3(2)	Cl(32)-Sn(3)-Cl(31)	95.4(2)
Rh-Sn(4)-Cl(43)	121.6(1)	Rh-Sn(4)-Cl(42)	117.2(1)
Cl(43)-Sn(4)-Cl(42)	96.0(2)	Rh-Sn(4)-Cl(41)	125.4(1)
Cl(43)-Sn(4)-Cl(41)	92.4(2)	Cl(42)-Sn(4)-Cl(41)	97.7(2)
Rh-C(01)-O(01)	176.7(10)	C(1)-N(1)-C(17)	109.5(13)
C(1)-N(1)-C(19)	108.0(12)	C(17)-N(1)-C(19)	111.0(12)
C(1)-N(1)-C(111)	110.9(13)	C(17)-N(1)-C(111)	108.2(13)
C(19)-N(1)-C(111)	109.2(12)	N(1)-C(1)-C(11)	117.0(12)
C(1)-C(11)-C(12)	119.9(7)	C(1)-C(11)-C(16)	120.0(6)
N(1)-C(17)-C(18)	115.1(15)	N(1)-C(19)-C(110)	113.6(14)
N(1)-C(111)-C(112)	114.3(14)	C(2)-N(2)-C(27)	109.5(14)
C(2)-N(2)-C(29)	105.9(10)	C(27)-N(2)-C(29)	112.1(10)
C(2)-N(2)-C(211)	109.4(11)	C(27)-N(2)-C(211)	106.8(11)
C(29)-N(2)-C(211)	113.0(14)	N(2)-C(2)-C(21)	117.0(11)
C(2)-C(21)-C(22)	121.9(9)	C(2)-C(21)-C(26)	118.1(8)
N(2)-C(27)-C(28)	115.0(12)	N(2)-C(29)-C(210)	114.0(12)
N(2)-C(211)-C(212)	115.5(13)	C(3)-N(3)-C(37)	105.3(12)
C(3)-N(3)-C(39)	110.2(15)	C(37)-N(3)-C(39)	111.6(12)
C(3)-N(3)-C(311)	113.0(11)	C(37)-N(3)-C(311)	112.4(16)
C(39)-N(3)-C(311)	104.5(13)	N(3)-C(3)-C(31)	117.3(11)
C(3)-C(31)-C(32)	119.0(9)	C(3)-C(31)-C(36)	120.9(9)
N(3)-C(37)-C(38)	114.2(14)	N(3)-C(39)-C(310)	117.0(16)
N(3)-C(311)-C(312)	114.2(15)		

3.2.2 Attempted preparation of [Bz(Et)₃N]₂[Rh(CO)(SnCl₃)₂Cl]

A method similar to that of Young et al⁽¹⁾ was used to prepare this complex. Solid anhydrous tin(II) chloride(0.277g, 1.46mmol) was added to a solution of dichlorotetracarbonyldirhodium(I) (0.1399g, 0.36mmol) in 15ml of absolute ethanol at 20°C under a nitrogen atmosphere. Stirring for 20 minutes afforded a colour

change from yellow/orange to deep red. Solid benzyltriethylammonium chloride (0.3306g, 1.45mmol) was then added to this solution giving immediate deposition of a red solid. This solid was removed by filtration under a nitrogen atmosphere, and, due to its instability to both air and vacuum was dried under a stream of nitrogen at atmospheric pressure. The orange/red product (0.25g, Yield 35%) was transferred and stored under a nitrogen atmosphere. Analysis of the product, however, did not correspond closely with the data expected for $[\text{Bz}(\text{Et})_3\text{N}]_2[\text{Rh}(\text{CO})(\text{SnCl}_3)_2\text{Cl}]$ {Found: C 34.23, H 4.86, N 2.90, Sn 23.16%; $[\text{Bz}(\text{Et})_3\text{N}]_2[\text{Rh}(\text{CO})(\text{SnCl}_3)_2\text{Cl}]$ requires C 32.36, H 4.39, N 2.80, Sn 23.72%}. However, the infra-red spectrum consisted of only one $\nu(\text{CO})$ absorption at 2013_scm^{-1} (nujol) which appears to be consistent with the published data value, $\{\nu(\text{CO}) - 2000\text{cm}^{-1}(\text{nujol})^{(1)}\}$, taking into account that the latter was recorded on a grating instrument, and the peak maximum determined from a chart. The 2013_scm^{-1} absorption band was symmetrical and sharp, with no shoulders. The major component is considered to be the desired complex though the reasons for the discrepancies in the analytical data are not obvious. Interestingly, Young's own sample, of $[\text{Me}_4\text{N}]_2[\text{Rh}(\text{CO})(\text{SnCl}_3)_2\text{Cl}]$, also gave poor analytical data { % Found(Calc) - C 13.6(14.5), H 3.0(3.2), N 3.5(2.2), Cl 34.3(33.2), Sn 35.6(31.1)}, indicating the possible presence of minor rhodium-carbonyl impurities which may not have been detected by the infra-red measurements.

The complex was stored with rigorous exclusion of air which led to rapid decomposition. Interestingly, in some attempts to synthesise this complex, a mixture of carbonyl products was obtained as indicated by a broad infra-red absorption at 2016_scm^{-1} (nujol) and associative weak absorptions at 2029, 2069 and 2079cm^{-1} , as shown in Figure 3.3. Carbonyl absorptions for $[\text{Rh}(\text{CO})_2(\text{SnCl}_3)_3]^{2-}$ are observed at 2017_s , $2069_{\text{vw}}(\text{CH}_2\text{Cl}_2)$, 2016_s , $2065_{\text{vw}}\text{cm}^{-1}$ (nujol) (see Section 3.2.5), and are reported by Pregosin et al at 2010 2060cm^{-1} (KBr)⁽²⁾. The major component of these mixtures is considered to be $[\text{Bz}(\text{Et})_3\text{N}]_2[\text{Rh}(\text{CO})_2(\text{SnCl}_3)_3]$, although the presence of $[\text{Bz}(\text{Et})_3\text{N}]_2[\text{Rh}(\text{CO})(\text{SnCl}_3)_2\text{Cl}]$ and/or $[\text{Bz}(\text{Et})_3\text{N}]_3[\text{Rh}(\text{CO})(\text{SnCl}_3)_4]$ is also likely because of the broadness of the 2016cm^{-1} absorption. Thus Young's preparation can lead to both $[\text{Bz}(\text{Et})_3\text{N}]_2[\text{Rh}(\text{CO})(\text{SnCl}_3)_2\text{Cl}]$ and $[\text{Bz}(\text{Et})_3\text{N}]_2[\text{Rh}(\text{CO})_2(\text{SnCl}_3)_3]$. The 2029 and 2079cm^{-1} absorptions remain unattributed.

In an attempt to obtain further information on the components of the above product a ^{119}Sn NMR spectrum (see Table 3.3 and Figure 3.4) was recorded using a mixed

solvent system of CH₂Cl₂/CDCl₃ at 298K. The solution was maintained under a nitrogen atmosphere throughout the acquisition time.

Table 3.3 ¹¹⁹Sn NMR data* for the mixture of complexes isolated from the reaction of Rh₂(CO)₄Cl₂ with SnCl₂ and Bz(Et)₃NCl

δ(¹¹⁹ Sn)/ppm	Multiplicity	Relative intensity	¹ J(¹⁰³ Rh, ¹¹⁹ Sn)/Hz
93.9	Doublet	2	872
61.2	Doublet	1	804

* Solvent : CH₂Cl₂/CDCl₃ mixture.

The doublet observed at 93.9 ppm is assigned to [Bz(Et)₃N]₂[Rh(CO)₂(SnCl₃)₃] by reference to data for the authentic material prepared by the method of Pregosin et al⁽²⁾ {δ(¹¹⁹Sn) 89.1ppm, ¹J(¹¹⁹Sn, ¹⁰³Rh) 864Hz, CDCl₃, RT}. The doublet observed at 61.2 ppm indicates coupling to rhodium but remains unassigned. The relative intensity indicates that this doublet is associated with a species present in a lower concentration than that of [Bz(Et)₃N]₂[Rh(CO)₂(SnCl₃)₃]. Since minor products are also indicated by the infra-red absorptions at 2029 and 2079cm⁻¹, the 61.2 ppm signal along with either or both of these infra-red absorptions may arise from the same complex. Alternatively, a non-carbonyl containing Rh-SnCl₃ species such as [Rh(SnCl₃)₅]⁴⁻ (3) or either of [Rh(CO)(SnCl₃)₂Cl]²⁻ and [Rh(CO)(SnCl₃)₄]³⁻ may be assigned to the signal at 61.2 ppm.

Thus, Young's method for preparing [Rh(CO)(SnCl₃)₂Cl]⁻ appears not to be a reliable route for the synthesis of this complex alone, and complexes other than the target material are obtained, sometimes with none of the desired complex apparently present. Even for the most successful preparations, it has not proved possible to obtain a material which analyses precisely for the desired complex.

3.2.3 Preparation of [PPN]₂[Rh(COD)(SnCl₃)₃]

This complex was prepared by the method of Pregosin et al⁽²⁾. Tin(II) chloride(0.0785g, 0.41mmol) was added to a suspension of dichlorobis(1,5-cyclooctadiene)dirhodium(I), Rh₂(COD)₂Cl₂(0.0509g, 0.10mmol) in 10ml of acetone. Stirring of this mixture at room temperature for 15 minutes resulted in a

Figure 3.3 Infra-red spectrum showing the carbonyl absorptions as a nujol mull for a mixture of complexes isolated from an attempted preparation of $[\text{Rh}(\text{CO})(\text{SnCl}_3)_2\text{Cl}]^{2-}$

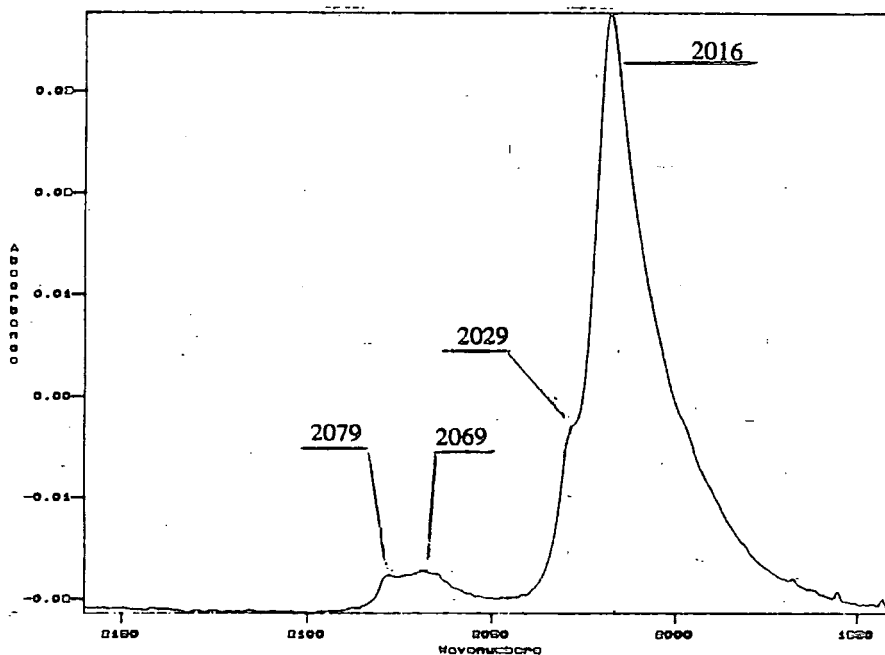
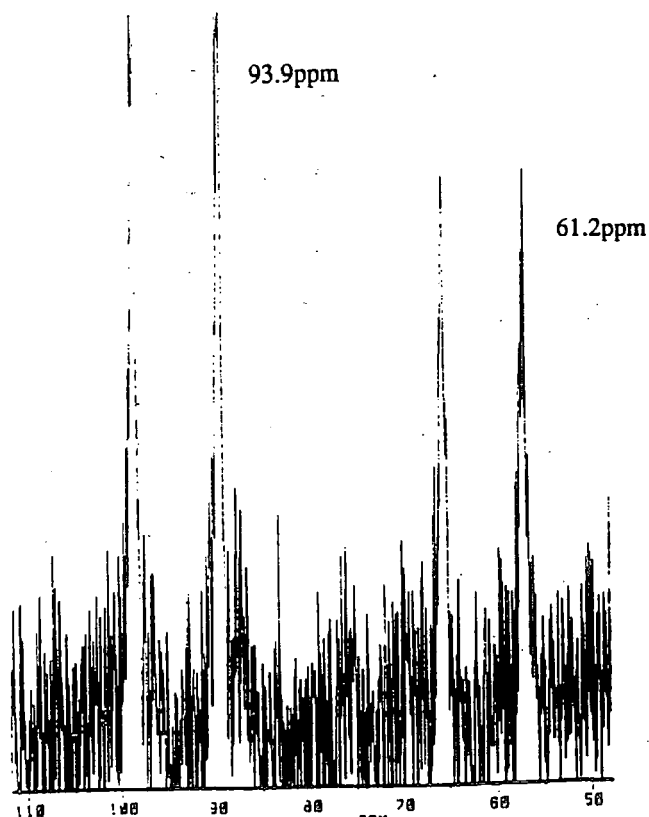


Figure 3.4 ^{119}Sn NMR spectrum recorded in $\text{CH}_2\text{Cl}_2/\text{CDCl}_3$ at 298K of a mixture of complexes isolated from an attempted preparation of $[\text{Rh}(\text{CO})(\text{SnCl}_3)_2\text{Cl}]^{2-}$



deep red solution. A solution of bis(triphenylphosphoranylidene)ammonium chloride, PPNCl(0.1254g, 0.22mmol) in 5ml of acetone and 1ml of dichloromethane was added by syringe, with the deep red colouration still persisting. Approximately half of the solvent was removed under vacuum and 5ml of methanol added slowly, giving deposition of a deep red solid. The red solid $[\text{PPN}]_2[\text{Rh}(\text{COD})(\text{SnCl}_3)_3]$ (2.29g) was removed by filtration, washed with methanol, and dried under vacuum. The complex was recrystallised from acetone-dichloromethane mixtures.

Data

Yield	:	72%
Found:		C 48.29, H 4.22, N 1.25, Cl 16.23%;
$[\text{PPN}]_2[\text{Rh}(\text{COD})(\text{SnCl}_3)_3]$ requires:		C 48.89, H 3.67, N 1.43, Cl 16.25%
^{119}Sn NMR	:	δ /ppm in CH_2Cl_2 - 23.4 Doublet
		$^1\text{J}(\text{}^{103}\text{Rh}, \text{}^{119}\text{Sn})$ - 664 Hz
Data reported by Pregosin et al ⁽²⁾ :		$\delta(\text{}^{119}\text{Sn})$ in CDCl_3 28.7 ppm,
		$^1\text{J}(\text{}^{103}\text{Rh}, \text{}^{119}\text{Sn})$ 651Hz,
		$^2\text{J}(\text{}^{119}\text{Sn}, \text{}^{117}\text{Sn})$ 1681Hz

The ^{119}Sn NMR data appears in good agreement with that of Pregosin et al⁽²⁾ indicating formation of the desired complex $[\text{PPN}]_2[\text{Rh}(\text{COD})(\text{SnCl}_3)_3]$. ^{117}Sn satellites were not observed, probably due to poor S/N ratio. However, data reported by Pregosin et al⁽²⁾ revealed that the relative intensities of the ^{117}Sn satellites and the main ^{119}Sn signal were consistent with the formation of the tri- SnCl_3 complex in solution. The reaction of $\text{Rh}_2(\text{CO})_2\text{Cl}_2$ with SnCl_2 and PPNCl:



probably occurs via cleavage of the Rh-Cl-Rh bridges during or after which tin coordinates to rhodium. Attempts to form mono- or bis-trichlorostannate complexes using the appropriate stoichiometric amounts of SnCl_2 were unsuccessful, ^{119}Sn NMR spectra and microanalytical data being consistent with the formation only of $[\text{PPN}]_2[\text{Rh}(\text{COD})(\text{SnCl}_3)_3]$, both in solution and in the solid state. The various equilibria present in solution therefore seem to favour the formation of the tri- SnCl_3 complex. This is in keeping with the known tendency of SnCl_3^- to stabilise 5-coordinate complexes.⁽⁴⁻⁸⁾

The preparation of $[\text{Bz}(\text{Et})_3\text{N}]_2[\text{Rh}(\text{COD})(\text{SnCl}_3)_3]$ was carried out in the same way giving formation of a paler red solid (1.87g) {Yield: 91%; Found: C 31.31, H 4.37, N 1.87%; $[\text{Bz}(\text{Et})_3\text{N}]_2[\text{Rh}(\text{COD})(\text{SnCl}_3)_3]$ requires C 32.10, H 4.41, N 2.20%}.

3.2.4 Preparation of $\text{Rh}(\text{COD})_2\text{SnCl}_3$

This complex was prepared by the method used by Pregosin et al⁽²⁾. Tin(II) chloride(1.24g, 0.27mmol) was added to a suspension of $\text{Rh}_2(\text{COD})_2\text{Cl}_2$ (0.15g, 0.30mmol) and 6ml of 1,5-cyclooctadiene in 25ml of absolute ethanol, giving an immediate red colouration. The mixture was refluxed at 85°C for 15 minutes until a clear orange/red solution was formed. This was allowed to cool and then filtered under nitrogen to remove unreacted $\text{Rh}_2(\text{COD})_2\text{Cl}_2$. The volume of the solution was then reduced under vacuum by approximately a half, giving deposition of a bright red solid which was removed by filtration and dried under vacuum. The complex was not found to be air or moisture sensitive. Attempts to recrystallise the material were unsuccessful because of its poor solubility at room temperature. At higher temperatures loss of SnCl_2 occurs resulting in the partial reformation of the starting complex and cyclooctadiene. {Yield: 30%; Found: C 33.86, H 4.33, N 0, Cl 20.20%; $\text{Rh}(\text{COD})_2(\text{SnCl}_3)$ requires C 35.27, H 4.41, N 0, Cl 18.34%}. The product is considered to be mainly composed of $\text{Rh}(\text{COD})_2(\text{SnCl}_3)$ with probable contamination from very small amounts of $\text{Rh}_2(\text{COD})_2\text{Cl}_2$ and SnCl_2 explaining the discrepancies in the microanalytical data.

3.2.5 Preparation of $[\text{PPN}]_2[\text{Rh}(\text{CO})_2(\text{SnCl}_3)_3]$

This was prepared by a method similar to that used by Pregosin et al⁽²⁾. $[\text{PPN}]_2[\text{Rh}(\text{COD})(\text{SnCl}_3)_3]$ (0.97g, 0.494mmol) was dissolved in 20ml of dichloromethane to give a cherry red solution. This was bubbled with carbon monoxide for 30 minutes to give an orange solution. The reaction was monitored by FT-IR spectroscopy. $\nu(\text{CO})$ absorptions, observed at 2017_s and 2069_wcm⁻¹ (see Figure 3.5), gradually increased in intensity as the reaction progressed and the cyclooctadiene ligand was displaced, to give $[\text{Rh}(\text{CO})_2(\text{SnCl}_3)_3]^{2-}$. When no further increase in intensity of $\nu(\text{CO})$ absorptions was detected 30ml of hexane was added to the orange solution to give deposition of bright orange/red crystals upon cooling in ice. The remaining solution was then removed by syringe. The crystals were washed with hexane, and dried under a stream of nitrogen. The dry orange/red crystals (0.84g) were stored under nitrogen, although prolonged exposure to the atmosphere did not indicate that they were either air or moisture sensitive. Attempts

to follow the procedure of Pregosin et al by evaporating the dichloromethane solution of $[\text{PPN}]_2[\text{Rh}(\text{CO})_2(\text{SnCl}_3)_3]$ to dryness yielded only formation of a red oil.

Attempts to isolate $[\text{Bz}(\text{Et})_3\text{N}]_2[\text{Rh}(\text{CO})_2(\text{SnCl}_3)_3]$ in the solid state by the same method were unsuccessful, yielding only a red oil. However, reaction of $[\text{Bz}(\text{Et})_3\text{N}]_2[\text{Rh}(\text{COD})(\text{SnCl}_3)_3]$ with CO leads to the apparent formation of $[\text{Bz}(\text{Et})_3\text{N}]_2[\text{Rh}(\text{CO})_2(\text{SnCl}_3)_3]$ in solution $\{\nu(\text{CO})\text{-}2018_{\text{s}}, 2069_{\text{vw}}\text{cm}^{-1}(\text{CH}_2\text{Cl}_2), 2011_{\text{s}}, 2072_{\text{vw}}\text{cm}^{-1}(\text{THF})\}$. The identical frequencies of the carbonyl absorptions for $[\text{PPN}]^+$ and $[\text{Bz}(\text{Et})_3\text{N}]^+$ salts of $[\text{Rh}(\text{CO})_2(\text{SnCl}_3)_3]^{2-}$ in CH_2Cl_2 indicates that anion-cation interactions are similar, in agreement with studies reported in Chapter 2 where interactions of $\text{Rh}(\text{I})\text{-CO-SnCl}_3$ anions with counter ions are concluded to be weak.

Data for reaction of $[\text{PPN}]_2[\text{Rh}(\text{COD})(\text{SnCl}_3)_3] + \text{CO}$ in CH_2Cl_2 , Reaction 3.2.5

Infra-red	:	$\nu(\text{CO})/\text{cm}^{-1}$ -	2017 _s , 2069 _w (see Figure 3.5)
^{119}Sn NMR	:	δ/ppm , 298K -	89.7 Doublet
		$^1\text{J}(\text{Rh}, \text{Sn})/\text{Hz}$ -	879

Pregosins data for $[\text{PPN}]_2[\text{Rh}(\text{CO})_2(\text{SnCl}_3)_3]^{(2)}$:

$\nu(\text{CO})/\text{cm}^{-1}$ -	2010, 2060 (KBr)
$\delta(^{119}\text{Sn})$	89.1ppm in CDCl_3 at RT,
$^1\text{J}(\text{Rh}, \text{Sn})$	864Hz, $^2\text{J}(\text{Sn}, \text{Sn})$ 9341Hz

Data for the solid product obtained from Reaction 3.2.5

Found: C 45.43, H 3.19, N 1.28, Cl 17.05%; $[\text{PPN}]_2[\text{Rh}(\text{CO})_2(\text{SnCl}_3)_3]$ requires C 46.46, H 3.14, N 1.46, Cl 16.69%

Infra-red	:	$\nu(\text{CO})/\text{cm}^{-1}$ -	1989 _s , 2016 _{sh} , 2039 _{mw} , 2065 _{vw} in nujol
			(see Figure 3.6)

This solid is named SAMPLE 1 for later reference

^{119}Sn NMR	:	δ/ppm in CH_2Cl_2 , 298K-	89.4 Doublet
		$^1\text{J}(\text{Rh}, \text{Sn})/\text{Hz}$	879

Pregosins data for $[\text{PPN}]_2[\text{Rh}(\text{CO})_2(\text{SnCl}_3)_3]^{(2)}$:

$\nu(\text{CO})/\text{cm}^{-1}$ -	2010, 2060 (KBr)
$\delta(^{119}\text{Sn})$	89.1ppm in CDCl_3 at RT,
$^1\text{J}(\text{Rh}, \text{Sn})$	864Hz, $^2\text{J}(\text{Sn}, \text{Sn})$ 9341Hz

Figure 3.6 shows the carbonyl absorptions as a nujol mull for the solid product precipitated from the reaction of $[\text{PPN}]_2[\text{Rh}(\text{COD})(\text{SnCl}_3)_3]$ with CO in CH_2Cl_2 , Reaction 3.2.5. A crystal structure determination was carried out by Prof J.A.K.

Howard and J. Cole on a crystal of $[\text{PPN}]_2[\text{Rh}(\text{CO})_2(\text{SnCl}_3)_3] \cdot \text{CH}_2\text{Cl}_2$, obtained from the isolated sample. The following is a summary of the data obtained.

Structure Determination Summary

Empirical Formula	$\text{C}_{75}\text{H}_{64}\text{Cl}_{11}\text{N}_2\text{O}_2\text{P}_4\text{RhSn}_3$
Formula Weight	1998.1
Space Group	$\text{P}2_1/\text{n}$ Monoclinic
a	18.184(4)Å
b	18.661(4)Å
c	25.086(5)Å
α	90°
β	90°
γ	106.32(3)°
Volume	8169(3)Å ³
Temperature	298K
R	0.0532
Rw	0.0547
wR	0.0612
Goodness of Fit	1.47
$N_{\text{parameters}}$ (Total)	878
$N_{\text{parameters}}$ (Max refined)	520
$N_{\text{reflections}}$	8110
Largest Residual Peak	1.39eÅ ⁻³
Largest Residual Trough	-1.58Å ⁻³

The solvent molecule present (CH_2Cl_2) was found to be highly disordered and hence remains undefined. Figure 3.7 shows the solid state crystal structure of the $[\text{Rh}(\text{CO})_2(\text{SnCl}_3)_3]^{2-}$ anion and Figure 3.8 shows the complete structure of $[\text{PPN}]_2[\text{Rh}(\text{CO})_2(\text{SnCl}_3)_3]$, (CH_2Cl_2 not included). The anion is essentially square pyramidal in shape with two CO ligands and two trichlorostannate ligands forming the square base. The rhodium atom sits slightly above the plane of the square base, essentially in a central position. The third trichlorostannate ligand is at the apex of the pyramid directly above the rhodium atom. The structure seems to be borne out of distortion of a trigonal bipyramidal arrangement, with the CO ligands bent slightly from axial positions. The Sn(1)-Rh(1)-Sn(2) bond angle is higher than the 120° expected for atoms in the trigonal arrangement, with Sn(1)-Rh(1)-Sn(3) and Sn(2)-Rh(1)-Sn(3) angles smaller as a result. Tables 3.4-3.5 summarise the atomic coordinates, bond lengths and bond angles for the complex.

Figure 3.5 Infra-red spectrum showing the carbonyl absorptions observed in the reaction of $[\text{PPN}]_2[\text{Rh}(\text{COD})(\text{SnCl}_3)_3]$ with CO in CH_2Cl_2 at room temperature

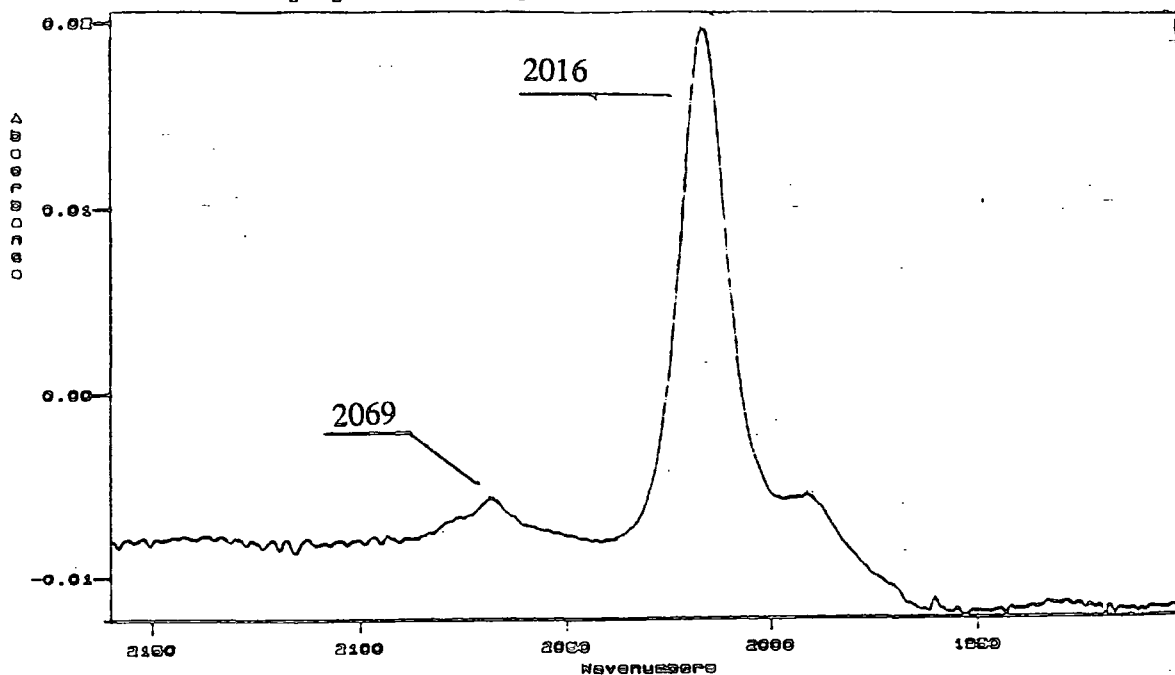


Figure 3.6 Infra-red spectrum in nujol showing the carbonyl absorptions for the solid product isolated from the reaction of $[\text{PPN}]_2[\text{Rh}(\text{COD})_2(\text{SnCl}_3)_3]$ with CO in CH_2Cl_2 (Reaction 3.2.5)

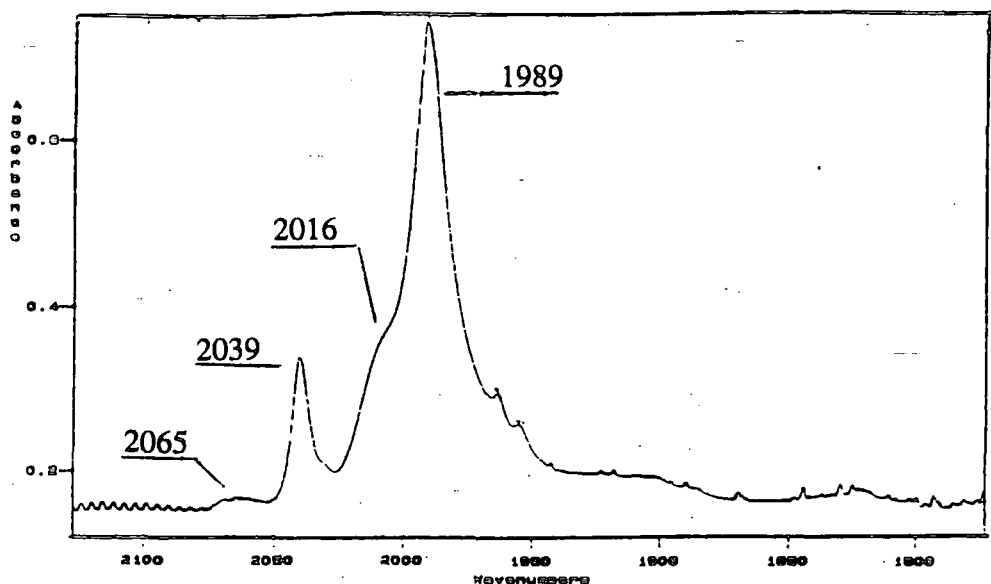
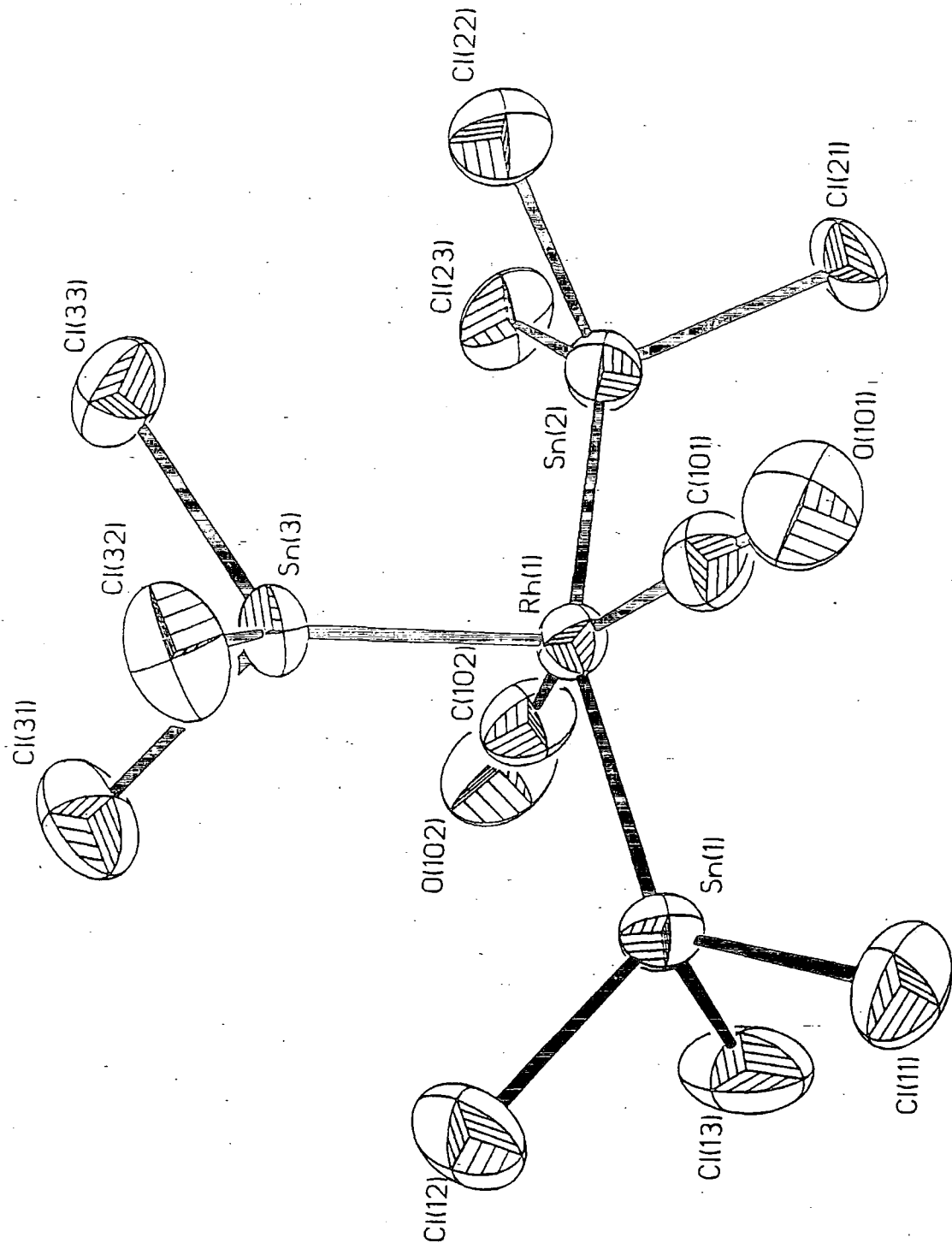
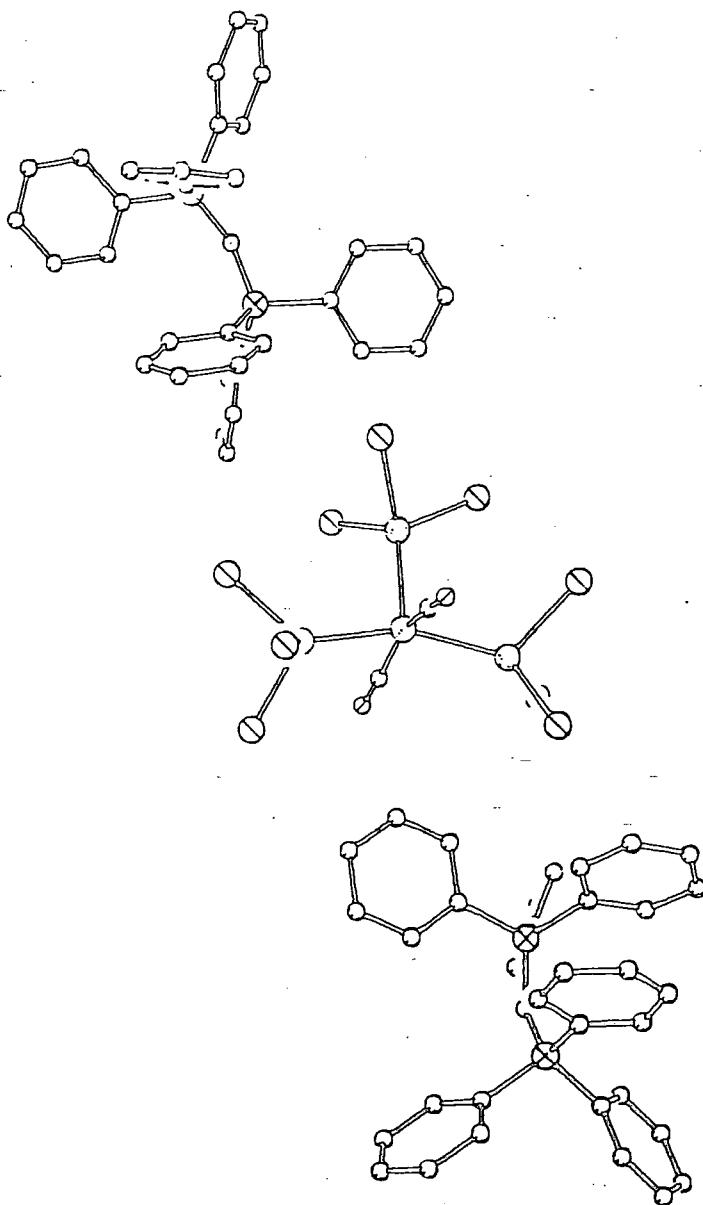


Figure 3.7 Crystal Structure of $[\text{Rh}(\text{CO})_2(\text{SnCl}_3)_3]^{2-}$



Prof. J. A. K. Howard and Jason Cole, unpublished data.

Figure 3.8 Crystal Structure of $[\text{PPN}]_2[\text{Rh}(\text{CO})_2(\text{SnCl}_3)_3]$



Prof. J. A. K. Howard and Jason Cole, unpublished data.

Table 3.4 Bond lengths (Å) for [PPN]₂[Rh(CO)₂(SnCl₃)₃]

Rh(1)-Sn(1)	2.547(1)	Rh(1)-Sn(2)	2.540(1)
Rh(1)-Sn(3)	2.605(1)	Rh(1)-C(101)	1.877(12)
Rh(1)-C(102)	1.895(14)	Sn(1)-Cl(11)	2.355(4)
Sn(1)-Cl(12)	2.357(3)	Sn(1)-Cl(13)	2.358(5)
Cl(31)-Sn(3)	2.404(4)	Cl(32)-Sn(3)	2.385(3)
Cl(33)-Sn(3)	2.399(3)	Sn(2)-Cl(21)	2.359(7)
Sn(2)-Cl(2A)	2.357(7)	Sn(2)-Cl(22)	2.365(8)
Sn(2)-Cl(2B)	2.353(6)	Sn(2)-Cl(23)	2.352(6)
Sn(2)-Cl(2C)	2.363(7)	Cl(21)-Cl(2A)	0.309(11)
Cl(22)-Cl(2B)	0.831(10)	Cl(23)-Cl(2C)	0.856(11)
C(101)-O(101)	1.151(15)	C(102)-O(102)	1.144(18)
P(1)-N(1)	1.577(7)	P(1)-C(1)	1.810(10)
P(1)-C(7)	1.808(9)	P(1)-C(25)	1.808(10)
P(2)-N(1)	1.580(7)	P(2)-C(13)	1.800(8)
P(2)-C(19)	1.803(10)	P(2)-C(31)	1.809(9)
C(1)-C(2)	1.399(13)	C(1)-C(6)	1.356(15)
C(2)-C(3)	1.386(17)	C(3)-C(4)	1.353(20)
C(4)-C(5)	1.359(19)	C(5)-C(6)	1.405(17)
C(7)-C(8)	1.379(13)	C(7)-C(12)	1.383(12)
C(8)-C(9)	1.401(14)	C(9)-C(10)	1.343(16)
C(10)-C(11)	1.383(16)	C(11)-C(12)	1.379(15)
C(13)-C(14)	1.392(14)	C(13)-C(18)	1.391(13)
C(14)-C(15)	1.375(13)	C(15)-C(16)	1.374(15)
C(16)-C(17)	1.380(16)	C(17)-C(18)	1.386(13)
C(19)-C(20)	1.385(13)	C(19)-C(24)	1.382(14)
C(20)-C(21)	1.372(17)	C(21)-C(22)	1.370(16)
C(22)-C(23)	1.379(17)	C(23)-C(24)	1.391(18)
C(25)-C(26)	1.371(15)	C(25)-C(30)	1.396(12)
C(26)-C(27)	1.398(16)	C(27)-C(28)	1.355(16)
C(28)-C(29)	1.376(20)	C(29)-C(30)	1.394(16)
C(31)-C(32)	1.369(13)	C(31)-C(36)	1.383(14)
C(32)-C(33)	1.369(15)	C(33)-C(34)	1.365(17)
C(34)-C(35)	1.379(16)	C(35)-C(36)	1.381(16)
P(3)-N(2)	1.580(7)	P(3)-C(37)	1.816(10)
P(3)-C(61)	1.795(8)	P(3)-C(67)	1.796(10)



P(4)-N(2)	1.569(7)	P(4)-C(43)	1.802(10)
P(4)-C(49)	1.817(9)	P(4)-C(55)	1.799(10)
C(37)-C(38)	1.381(12)	C(37)-C(42)	1.370(14)
C(38)-C(39)	1.392(17)	C(39)-C(40)	1.378(20)
C(40)-C(41)	1.335(17)	C(41)-C(42)	1.404(17)
C(43)-C(44)	1.373(15)	C(43)-C(48)	1.417(13)
C(44)-C(45)	1.406(16)	C(45)-C(46)	1.378(17)
C(46)-C(47)	1.369(18)	C(47)-C(48)	1.379(16)
C(49)-C(50)	1.377(15)	C(49)-C(54)	1.397(13)
C(50)-C(51)	1.399(14)	C(51)-C(52)	1.381(17)
C(52)-C(53)	1.359(18)	C(53)-C(54)	1.391(13)
C(55)-C(56)	1.402(12)	C(55)-C(60)	1.379(15)
C(56)-C(57)	1.395(16)	C(57)-C(58)	1.371(18)
C(58)-C(59)	1.347(15)	C(59)-C(60)	1.409(17)
C(61)-C(62)	1.381(15)	C(61)-C(66)	1.392(15)
C(62)-C(63)	1.372(15)	C(63)-C(64)	1.382(19)
C(64)-C(65)	1.341(17)	C(65)-C(66)	1.387(13)
C(67)-C(68)	1.399(13)	C(67)-C(72)	1.389(14)
C(68)-C(69)	1.366(15)	C(69)-C(70)	1.378(17)
C(70)-C(71)	1.365(16)	C(71)-C(72)	1.395(16)
Cl(2S)-C(1S)	1.622(17)	Cl(1S)-C(1S)	1.778(20)

Table 3.5 Bond angles (°) for [PPN]₂[Rh(CO)₂(SnCl₃)₃]

Sn(1)-Rh(1)-Sn(2)	155.8(1)	Sn(1)-Rh(1)-Sn(3)	102.7(1)
Sn(2)-Rh(1)-Sn(3)	101.5(1)	Sn(1)-Rh(1)-C(101)	87.6(3)
Sn(2)-Rh(1)-C(101)	86.5(3)	Sn(3)-Rh(1)-C(101)	104.9(3)
Sn(1)-Rh(1)-C(102)	86.3(4)	Sn(2)-Rh(1)-C(102)	90.1(4)
Sn(3)-Rh(1)-C(102)	97.9(3)	C(101)-Rh(1)-C(102)	157.2(5)
Rh(1)-Sn(1)-Cl(11)	119.1(1)	Rh(1)-Sn(1)-Cl(12)	120.2(1)
Cl(11)-Sn(1)-Cl(12)	100.7(1)	Rh(1)-Sn(1)-Cl(13)	116.7(1)
Cl(11)-Sn(1)-Cl(13)	97.9(1)	Cl(12)-Sn(1)-Cl(13)	97.9(2)
Rh(1)-Sn(2)-Cl(21)	120.3(2)	Rh(1)-Sn(2)-Cl(2A)	117.4(2)
Cl(21)-Sn(2)-Cl(2A)	7.5(3)	Rh(1)-Sn(2)-Cl(22)	116.7(2)
Cl(21)-Sn(2)-Cl(22)	96.1(3)	Cl(2A)-Sn(2)-Cl(22)	92.0(3)
Rh(1)-Sn(2)-Cl(2B)	129.3(2)	Cl(21)-Sn(2)-Cl(2B)	98.6(3)
Cl(2A)-Sn(2)-Cl(2B)	96.9(3)	Cl(22)-Sn(2)-Cl(2B)	20.3(2)
Rh(1)-Sn(2)-Cl(23)	124.5(2)	Cl(21)-Sn(2)-Cl(23)	96.7(2)
Cl(2A)-Sn(2)-Cl(23)	103.5(2)	Cl(22)-Sn(2)-Cl(23)	96.5(3)
Cl(2B)-Sn(2)-Cl(23)	76.2(3)	Rh(1)-Sn(2)-Cl(2C)	113.7(2)
Cl(21)-Sn(2)-Cl(2C)	89.3(2)	Cl(2A)-Sn(2)-Cl(2C)	96.7(2)
Cl(22)-Sn(2)-Cl(2C)	116.8(3)	Cl(2B)-Sn(2)-Cl(2C)	96.6(3)
Cl(23)-Sn(2)-Cl(2C)	20.9(3)	Sn(2)-Cl(21)-Cl(2A)	85.9(17)
Sn(2)-Cl(2A)-Cl(21)	86.6(17)	Sn(2)-Cl(22)-Cl(2B)	79.0(7)
Sn(2)-Cl(2B)-Cl(22)	80.7(6)	Sn(2)-Cl(23)-Cl(2C)	80.2(6)
Sn(2)-Cl(2C)-Cl(23)	78.9(6)	Rh(1)-Sn(3)-Cl(31)	119.5(1)
Rh(1)-Sn(3)-Cl(32)	122.4(1)	Cl(31)-Sn(3)-Cl(32)	98.7(1)
Rh(1)-Sn(3)-Cl(33)	119.7(1)	Cl(31)-Sn(3)-Cl(33)	95.1(1)
Cl(32)-Sn(3)-Cl(33)	95.5(1)	Rh(1)-C(101)-O(101)	177.2(10)
Rh(1)-C(102)-O(102)	176.7(11)	N(1)-P(1)-C(1)	116.5(4)
N(1)-P(1)-C(7)	109.4(4)	C(1)-P(1)-C(7)	107.6(5)
N(1)-P(1)-C(25)	108.5(4)	C(1)-P(1)-C(25)	106.5(4)
C(7)-P(1)-C(25)	107.9(4)	N(1)-P(2)-C(13)	109.7(4)
N(1)-P(2)-C(19)	113.2(4)	C(13)-P(2)-C(19)	106.8(4)
N(1)-P(2)-C(31)	111.6(4)	C(13)-P(2)-C(31)	106.2(4)
C(19)-P(2)-C(31)	108.9(4)	P(1)-N(1)-P(2)	138.6(6)
P(1)-C(1)-C(2)	118.2(8)	P(1)-C(1)-C(6)	121.8(7)
C(2)-C(1)-C(6)	120.0(9)	C(1)-C(2)-C(3)	118.9(11)
C(2)-C(3)-C(4)	120.7(11)	C(3)-C(4)-C(5)	120.6(12)

C(4)-C(5)-C(6)	119.8(12)	C(1)-C(6)-C(5)	119.8(10)
P(1)-C(7)-C(8)	120.3(7)	P(1)-C(7)-C(12)	120.0(7)
C(8)-C(7)-C(12)	119.7(9)	C(7)-C(8)-C(9)	119.5(9)
C(8)-C(9)-C(10)	119.9(10)	C(9)-C(10)-C(11)	121.4(10)
C(10)-C(11)-C(12)	119.2(10)	C(7)-C(12)-C(11)	120.3(9)
P(2)-C(13)-C(14)	119.5(6)	P(2)-C(13)-C(18)	121.4(7)
C(14)-C(13)-C(18)	118.9(8)	C(13)-C(14)-C(15)	120.2(9)
C(14)-C(15)-C(16)	120.9(11)	C(15)-C(16)-C(17)	119.6(9)
C(16)-C(17)-C(18)	120.1(9)	C(13)-C(18)-C(17)	120.3(10)
P(2)-C(19)-C(20)	121.1(7)	P(2)-C(19)-C(24)	118.3(8)
C(20)-C(19)-C(24)	120.0(10)	C(19)-C(20)-C(21)	118.6(9)
C(20)-C(21)-C(22)	121.3(10)	C(21)-C(22)-C(23)	120.9(12)
C(22)-C(23)-C(24)	117.9(11)	C(19)-C(24)-C(23)	121.1(10)
P(1)-C(25)-C(26)	119.1(6)	P(1)-C(25)-C(30)	120.4(8)
C(26)-C(25)-C(30)	120.5(9)	C(25)-C(26)-C(27)	119.6(9)
C(26)-C(27)-C(28)	120.7(12)	C(27)-C(28)-C(29)	119.8(12)
C(28)-C(29)-C(30)	121.1(10)	C(25)-C(30)-C(29)	118.3(10)
P(2)-C(31)-C(32)	120.8(7)	P(2)-C(31)-C(36)	119.5(7)
C(32)-C(31)-C(36)	119.5(9)	C(31)-C(32)-C(33)	119.4(10)
C(32)-C(33)-C(34)	122.3(10)	C(33)-C(34)-C(35)	118.5(10)
C(34)-C(35)-C(36)	120.0(10)	C(31)-C(36)-C(35)	120.3(9)
N(2)-P(3)-C(37)	110.8(4)	N(2)-P(3)-C(61)	114.6(4)
C(37)-P(3)-C(61)	106.6(4)	N(2)-P(3)-C(67)	109.2(4)
C(37)-P(3)-C(67)	106.1(4)	C(61)-P(3)-C(67)	109.2(4)
N(2)-P(4)-C(43)	111.2(5)	N(2)-P(4)-C(49)	113.0(4)
C(43)-P(4)-C(49)	108.9(4)	N(2)-P(4)-C(55)	109.2(4)
C(43)-P(4)-C(55)	107.4(4)	C(49)-P(4)-C(55)	107.0(4)
P(3)-N(2)-P(4)	143.0(5)	P(3)-C(37)-C(38)	118.3(8)
P(3)-C(37)-C(42)	120.0(7)	C(38)-C(37)-C(42)	121.5(10)
C(37)-C(38)-C(39)	118.4(10)	C(38)-C(39)-C(40)	120.2(10)
C(39)-C(40)-C(41)	120.6(13)	C(40)-C(41)-C(42)	120.9(12)
C(37)-C(42)-C(41)	118.4(9)	P(4)-C(43)-C(44)	119.9(7)
P(4)-C(43)-C(48)	121.3(8)	C(44)-C(43)-C(48)	118.8(9)
C(43)-C(44)-C(45)	120.9(9)	C(44)-C(45)-C(46)	119.0(11)
C(45)-C(46)-C(47)	120.9(11)	C(46)-C(47)-C(48)	120.5(10)

C(43)-C(48)-C(47)	119.8(10)	P(4)-C(49)-C(50)	117.0(7)
P(4)-C(49)-C(54)	122.4(7)	C(50)-C(49)-C(54)	120.6(8)
C(49)-C(50)-C(51)	118.6(10)	C(50)-C(51)-C(52)	120.7(12)
C(51)-C(52)-C(53)	120.4(10)	C(52)-C(53)-C(54)	120.3(10)
C(49)-C(54)-C(53)	119.5(10)	P(4)-C(55)-C(56)	118.3(8)
P(4)-C(55)-C(60)	122.3(7)	C(56)-C(55)-C(60)	119.4(9)
C(55)-C(56)-C(57)	119.0(10)	C(56)-C(57)-C(58)	120.0(9)
C(57)-C(58)-C(59)	122.2(11)	C(58)-C(59)-C(60)	118.8(12)
C(55)-C(60)-C(59)	120.7(9)	P(3)-C(61)-C(62)	123.4(8)
P(3)-C(61)-C(66)	118.3(7)	C(62)-C(61)-C(66)	118.2(8)
C(61)-C(62)-C(63)	120.6(11)	C(62)-C(63)-C(64)	119.8(12)
C(63)-C(64)-C(65)	121.0(10)	C(64)-C(65)-C(66)	119.5(11)
C(61)-C(66)-C(65)	120.8(10)	P(3)-C(67)-C(68)	120.1(8)
P(3)-C(67)-C(72)	120.6(7)	C(68)-C(67)-C(72)	119.2(9)
C(67)-C(68)-C(69)	120.6(10)	C(68)-C(69)-C(70)	119.8(10)
C(69)-C(70)-C(71)	120.8(11)	C(70)-C(71)-C(72)	120.3(10)
C(67)-C(72)-C(71)	119.3(9)	Cl(2S)-C(1S)-Cl(1S)	116.2(10)

Thus, infra-red data indicates that $[A]_2[Rh(COD)(SnCl_3)_3]$ reacts with CO to form $[A]_2[Rh(CO)_2(SnCl_3)_3]$ (where $A = [Bz(Et)_3N]^+$ or $[PPN]^+$) as the favoured complex in solution, no changes being observed in the carbonyl stretching region of the infra-red spectrum over a lengthy period of time (ca. 24 hours). The data is in close agreement with that reported by Pregosin et al⁽²⁾ for this complex. ^{119}Sn NMR data collected are also in extremely close agreement to those of Pregosin et al⁽²⁾, confirming the formation and apparent stability of this tri-tin complex in solution. Through a comparison of the relative intensities of the ^{117}Sn satellites and the main ^{119}Sn signal Pregosin categorically assigned the complex as the tri-tin species⁽²⁾.

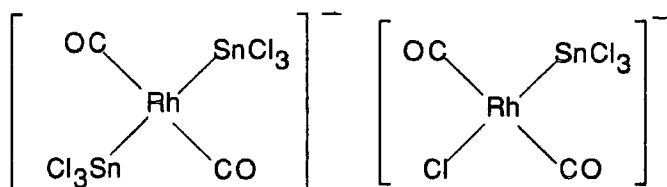
^{119}Sn NMR data in CH_2Cl_2 at 25°C for the solid product precipitated from the reaction of $[PPN]_2[Rh(COD)(SnCl_3)_3]$ with CO (Sample 1, Reaction 3.2.5), consisted of only one doublet, indicating the presence of only one Rh(I)- $SnCl_3$ complex in solution. The frequencies and coupling constant are very similar to data assigned to $[PPN]_2[Rh(CO)_2(SnCl_3)_3]$ reported by Pregosin et al⁽²⁾, thus confirming it as apparently the only Rh(I)- $SnCl_3$ complex in solution. The formula is consistent with the recognised tendency of the $SnCl_3^-$ ligand to stabilise 5-coordination⁽⁴⁻⁸⁾. An infra-red spectrum of this solution was also consistent with the presence of $[PPN]_2[Rh(CO)_2(SnCl_3)_3]$ $\{\nu(CO)- 2017_s, 2069_{vw}cm^{-1}$ in CH_2Cl_2 ; 2010 2060 cm^{-1} (KBr)⁽²⁾, as the sole $[PPN]_2[Rh(CO)_2(SnCl_3)_3]$ complex in solution.

However, further infra-red studies of samples of the solid isolated from the solution state, indicate that the chemistry is more complex than that indicated by Pregosin et al⁽²⁾, and that $[\text{Rh}(\text{CO})_2(\text{SnCl}_3)_3]^{2-}$ is not the only component of the samples. Infra-red data for a sample of the solid as a nujol mull (Sample 1, see page 96) showed 4 carbonyl absorption bands (1989_{s} , 2016_{sh} , 2039_{mw} , $2069_{\text{vw}}\text{cm}^{-1}$, see Figure 3.6). Also, addition of separate samples of the same batch of solid to CH_2Cl_2 resulted in differences in the observed carbonyl absorptions e.g.:

Sample 2	$\nu(\text{CO})/\text{cm}^{-1}$	1991_{s} , 2016_{m} , 2044_{w} , 2069_{ms}
Sample 3	$\nu(\text{CO})/\text{cm}^{-1}$	2016_{s} , 2069_{vw}

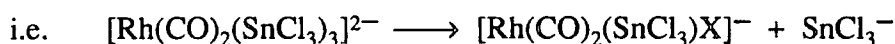
The infra-red data for the solid as a nujol mull ($\nu(\text{CO})/\text{cm}^{-1}$ - 1989_{s} , 2016_{sh} , 2039_{mw} , 2065_{vw} (Sample 1)) was clearly consistent with a mixture of complexes, the weaker absorptions at 2016 and 2065cm^{-1} arising from $[\text{PPN}]_2[\text{Rh}(\text{CO})_2(\text{SnCl}_3)_3]$ as the minor component. The infra-red data obtained when a further sample of this solid (Sample 2) is added to CH_2Cl_2 is consistent with that obtained for Sample 1, with $[\text{PPN}]_2[\text{Rh}(\text{CO})_2(\text{SnCl}_3)_3]$ again implicated as the minor component. However, infra-red data obtained for another sample of the same batch of solid added to CH_2Cl_2 (Sample 3) showed only two carbonyl absorptions, which were consistent with $[\text{PPN}]_2[\text{Rh}(\text{CO})_2(\text{SnCl}_3)_3]$ as the only Rh(I)-CO complex present in solution.

Clearly, infra-red data for Sample 1 indicates that precipitation of a solid from a solution of $[\text{PPN}]_2[\text{Rh}(\text{CO})_2(\text{SnCl}_3)_3]$ in CH_2Cl_2 has resulted in the formation of a second rhodium-carbonyl complex. Initial microanalytical data on the product were consistent with $[\text{PPN}]_2[\text{Rh}(\text{CO})_2(\text{SnCl}_3)_3]$ and were certainly not in keeping with it being the minor component of a mixture as indicated by the infra-red data for Sample 1. However, microanalyses of further portions of this sample were more consistent with a mixture, the carbon content being lower than found for previous samples. On the basis of microanalytical data it is not possible to determine the identity of the complex having carbonyl absorptions at 1989_{s} , $2039_{\text{w}}\text{cm}^{-1}$ in nujol and 1991_{s} , $2044_{\text{w}}\text{cm}^{-1}$ in CH_2Cl_2 , but they appear to originate from the dissociation or decomposition of $[\text{Rh}(\text{CO})_2(\text{SnCl}_3)_3]^{2-}$. These absorptions appear to arise from the same complex and not two different rhodium monocarbonyl complexes. The pattern of $\nu(\text{CO})$ frequencies, compared with those for $[\text{Rh}(\text{CO})_2(\text{SnCl}_3)_3]^{2-}$ (in CH_2Cl_2 both are lower than the respective higher and lower frequencies of $[\text{Rh}(\text{CO})_2(\text{SnCl}_3)_3]^{2-}$ by an almost identical value), would be consistent with the formation of one of the Rh(I)- SnCl_3 trans-dicarbonyl complexes shown below,



Infra-red data reported for samples of this mixture of solids in CH_2Cl_2 (Samples 2 and 3) implies that the conditions are critical for the formation and stability in solution of the complex having absorptions at 1991 and 2044 cm^{-1} . The relative ratio of the intensities of these absorptions to those of $[\text{Rh}(\text{CO})_2(\text{SnCl}_3)_3]^{2-}$ varies. In one case $[\text{Rh}(\text{CO})_2(\text{SnCl}_3)_3]^{2-}$ is the minor component (Sample 2), but in most cases studied it is the sole component (e.g. Sample 3). Interestingly, upon addition of either Sample 2 or 3 to CH_2Cl_2 , the initial infra-red spectrum obtained is not followed by any subsequent change in either the relative intensities or the frequency positions of the absorptions.

Thus, in attempting to isolate $[\text{Rh}(\text{CO})_2(\text{SnCl}_3)_3]^{2-}$ from solution, it appears that tin is lost from the complex by some means to form the 4-coordinate complex $[\text{Rh}(\text{CO})_2(\text{SnCl}_3)\text{X}]^-$ ($\text{X} = \text{Cl}^-$ or SnCl_3^-):



3.2.6 Reaction of $[\text{Bz}(\text{Et})_3\text{N}][\text{Rh}(\text{CO})_2\text{Cl}_2]$ and SnCl_2 in THF

$[\text{Bz}(\text{Et})_3\text{N}][\text{Rh}(\text{CO})_2\text{Cl}_2]$ (0.2632g, 0.623mmol) was dissolved in 10ml of dry THF under a nitrogen atmosphere to give a yellow solution. Solid anhydrous tin(II) chloride (0.3736g, 1.97mmol) was then added to this solution at room temperature. A clear deep red solution was formed almost instantaneously upon stirring. Addition of hexane (7ml) to the solution and cooling to 0°C , gave a red oil over 2 days. The remaining solution was removed from the oil by syringe and stored in a Schlenk tube under nitrogen. 3ml of methanol was added to the red oil causing it to solidify. The red solid (0.45g), called Product A, was then removed by filtration, washed with a small amount of hexane, and dried under vacuum.

Data for Product A

Analysis % : C 28.40, H 4.09, N 2.35, Sn 27.10, Rh 7.91
 Infra-red : $\nu(\text{CO})/\text{cm}^{-1}$ - 2013_s in nujol

The solvent was removed from the remaining orange solution leaving an orange/red residue which was extracted with 5ml of methanol and the solution filtered. Addition of hexane to the filtrate gave separation of a red solid, Product B, which was filtered under nitrogen and dried under vacuum.

Data for Product B

Analysis % : C 27.25, H 3.69, N 2.70
 Infra-red : $\nu(\text{CO})/\text{cm}^{-1}$ - 2016_s, 2028_w, 2070_{vw}, 2079_w in nujol

Product A was formed upon repetition of this reaction, but more usually Product B was the sole product. Product B was isolated from the reaction irrespective of the original Rh:Sn molar ratio (ranging from 1:1 to 1:4) employed. Table 3.6 summarises the infra-red and microanalytical data for materials isolated from further reactions of $[\text{Bz}(\text{Et})_3\text{N}][\text{Rh}(\text{CO})_2\text{Cl}_2]$ with SnCl_2 in THF Products C, D and E), along with calculated microanalytical data and infra-red frequencies for relevant Rh(I)-CO-SnCl₃ complexes.

Infra-red and microanalytical data are consistent with Products A and C being $[\text{Bz}(\text{Et})_3\text{N}]_3[\text{Rh}(\text{CO})(\text{SnCl}_3)_4]$, and Products B, D and E being $[\text{Bz}(\text{Et})_3\text{N}]_2[\text{Rh}(\text{CO})_2(\text{SnCl}_3)_3]$ as the main product. By examination of the infra-red data and expected microanalytical data for pure samples of $[\text{Bz}(\text{Et})_3\text{N}]_3[\text{Rh}(\text{CO})(\text{SnCl}_3)_4]$ and $[\text{Bz}(\text{Et})_3\text{N}]_2[\text{Rh}(\text{CO})_2(\text{SnCl}_3)_3]$ the difficulties encountered in establishing the nature of Rh(I)-CO-SnCl₃ products are readily appreciated. On the basis of the broad non-symmetrical carbonyl absorption at 2016 cm^{-1} it is not possible to eliminate with confidence either $[\text{Rh}(\text{CO})(\text{SnCl}_3)_4]^{3-}$ or $[\text{Rh}(\text{CO})(\text{SnCl}_3)_2\text{Cl}]^{2-}$ as minor components of Products B, D and E, since both of these complexes have a carbonyl absorption in this region at an almost identical frequency. Furthermore, the benzyltriethylammonium salts of $[\text{Rh}(\text{CO})(\text{SnCl}_3)_4]^{3-}$, $[\text{Rh}(\text{CO})_2(\text{SnCl}_3)_3]^{2-}$ and $[\text{Rh}(\text{CO})(\text{SnCl}_3)_2\text{Cl}]^{2-}$ give similar C, H, N and Cl microanalytical data, and consequently, it is difficult to derive further information about possible Rh(I)-CO-SnCl₃ product mixtures by assessment of such data. Theoretically, rhodium analysis could differentiate between the possible complexes, and tin analysis should distinguish $[\text{Rh}(\text{CO})(\text{SnCl}_3)_2\text{Cl}]^{2-}$ from $[\text{Rh}(\text{CO})(\text{SnCl}_3)_4]^{3-}$ and $[\text{Rh}(\text{CO})_2(\text{SnCl}_3)_3]^{2-}$. However, microanalytical data for these elements is not sufficiently reliable for this purpose. Other techniques used to analyse these solids, such as ¹¹⁹Sn and ¹³C NMR spectroscopy generally did not provide any useful information due to either the insolubility or decomposition of species in solution over the long periods of time necessary to acquire spectra.

Table 3.6 Infra-red and microanalytical data for Rh(I)-CO-SnCl₃ products and calculated data for relevant complexes

Product code	Rh:Sn ratio of reagents	$\nu(\text{CO})/\text{cm}^{-1}$ in nujol	% C	H	N	Cl	Sn	Rh
			Found					
C	1:2	2016 _s 2028 _w 2079 _w	27.89	3.83	2.29	-	27.86	-
D	1:4	2016 _s 2028 _w 2067 _{vw} 2078 _{vw}	27.26	3.83	2.25	-	28.91	9.15
E	1:4	2016 _s 2028 _w 2068 _{vw} 2079 _{vw}	25.87	3.48	2.12	-	-	-
Complex			Calculated values					
*[Rh(CO)(SnCl ₃) ₄] ³⁻ See section 3.2.1		2012 nujol	29.84	4.10	2.61	26.45	29.52	6.40
*[Rh(CO) ₂ (SnCl ₃) ₃] ²⁻ See section 3.2.5		2011 _s 2072 _{vw} THF 2018 _s 2069 _{vw} CH ₂ Cl ₂ 2016 _s 2065 _{vw} nujol †	27.57	3.61	2.30	26.18	29.22	8.45
◊[Rh(CO) ₂ (SnCl ₃) ₃] ²⁻ See section 3.2.5		2017 _s 2069 _{vw} CH ₂ Cl ₂ 2016 _s 2065 _w nujol	—	—	—	—	—	—
*[Rh(CO)(SnCl ₃) ₂ Cl] ²⁻ See section 3.2.2		2013 nujol	32.36	4.39	2.80	24.79	23.72	10.3

* [Bz(Et)₃N]⁺

◊ [PPN]⁺

† The infra-red data for solid [Bz(Et)₃N]₂[Rh(CO)₂(SnCl₃)₃] as a nujol mull is derived from that assigned to solid [PPN]₂[Rh(CO)₂(SnCl₃)₃] as a nujol mull, since the benzyltriethylammonium salt of [Rh(CO)₂(SnCl₃)₃]²⁻ has not been isolated as a pure solid. There is no change in the positions of the carbonyl absorptions for [Rh(CO)₂(SnCl₃)₃]²⁻ in CH₂Cl₂ with either [PPN]⁺ or [Bz(Et)₃N]⁺ as the counter ion. Therefore, the carbonyl absorptions for solid [Bz(Et)₃N]₂[Rh(CO)₂(SnCl₃)₃] as a nujol mull are expected at 2016 and 2065cm⁻¹ i.e. at the same frequencies as those for [PPN]₂[Rh(CO)₂(SnCl₃)₃] as a nujol mull.

However, a ¹¹⁹Sn NMR spectrum in CH₂Cl₂/CDCl₃ was obtained for an apparently identical product (on the basis of infra-red and microanalytical data) to Products B, D and E (see Section 3.2.2), thus confirming the presence in solution of [Bz(Et)₃N]₂[Rh(CO)₂(SnCl₃)₃] as the major component. A weaker signal consistent with a further Rh-SnCl₃ complex was also observed, and could possibly be assigned to either [Bz(Et)₃N]₂[Rh(CO)(SnCl₃)₂Cl] or [Bz(Et)₃N]₃[Rh(CO)(SnCl₃)₄]. Consequently, infra-red and microanalytical data, along with ¹¹⁹Sn NMR data for an apparently identical product appear to be consistent with Products B, D and E containing [Bz(Et)₃N]₂[Rh(CO)₂(SnCl₃)₃] as the main component, although the presence of a further Rh-SnCl₃ complex e.g. [Bz(Et)₃N]₂[Rh(CO)(SnCl₃)₂Cl] and

$[\text{Bz}(\text{Et})_3\text{N}]_3[\text{Rh}(\text{CO})(\text{SnCl}_3)_4]$, purely on the basis of such data, is also likely. Mass spectroscopic studies did not provide any useful information about these products, or indeed any of the other products reported in this chapter.

3.2.7 Reaction of $[\text{Bz}(\text{Et})_3\text{N}][\text{Rh}(\text{CO})_2\text{Cl}_2]$ with $[\text{Bz}(\text{Et})_3\text{N}][\text{SnCl}_3]$ and 37% $\text{HCl}_{(\text{aq})}$ in acetic acid

This experiment was carried out in an attempt to investigate the chemistry which occurs between species known to be present in the rhodium-tin-chloride catalytic reaction, described in Chapter 4.

$[\text{Bz}(\text{Et})_3\text{N}][\text{Rh}(\text{CO})_2\text{Cl}_2]$ (0.105g, 0.25mmol) was dissolved in 10ml of acetic acid at 50°C under a nitrogen atmosphere to give a pale yellow solution. $[\text{Bz}(\text{Et})_3\text{N}][\text{SnCl}_3]$ (0.2845g, 0.682mmol) was dissolved in a mixture of 7ml of acetic acid and 0.5ml of 37% $\text{HCl}_{(\text{aq})}$ and added by syringed to the warm solution of $[\text{Bz}(\text{Et})_3\text{N}][\text{Rh}(\text{CO})_2\text{Cl}_2]$. Immediate precipitation of an orange/red solid occurred, which was separated by filtration of the warm mixture under nitrogen, and then dried under vacuum. The orange/red product (0.08g), which decomposed in air to give a black solid, was transferred and handled under nitrogen. {Found C 28.21, H 3.83, N 2.20, Sn 29.79%; $[\text{Bz}(\text{Et})_3\text{N}]_2[\text{Rh}(\text{CO})_2(\text{SnCl}_3)_3]$ requires C 27.57, H 3.61, N 2.30, Sn 29.22%; Infra-red : $\nu(\text{CO})/\text{cm}^{-1}$ - 1997_w, 2016_s, 2028_w, 2068_{vw}, 2079_w}.

Infra-red and microanalytical data for this product are similar to those reported in previous reactions, and indicate that it is $[\text{Bz}(\text{Et})_3\text{N}]_2[\text{Rh}(\text{CO})_2(\text{SnCl}_3)_3]$, with slight contamination from a complex or complexes absorbing at 1997, 2028 and 2079 cm^{-1} .

In the absence of 37% aqueous HCl from the reaction in acetic acid, decomposition of the carbonyl complex occurred to form a brown/black non-carbonyl solid at temperatures close to 50°C.

3.2.8 Reaction of $\text{Rh}_2(\text{CO})_4\text{Cl}_2$ and $[\text{Bz}(\text{Et})_3\text{N}][\text{SnCl}_3]$ in acetic acid

As for Reaction 3.2.7 this was attempted to determine the chemistry which occurs in the rhodium-tin-chloride catalytic process to hydrocarbonylate ethene (described in chapter 4).

$[\text{Bz}(\text{Et})_3\text{N}][\text{SnCl}_3]$ (0.3346g, 0.802mmol) in 8ml of acetic acid was heated to 80°C under a nitrogen atmosphere until it dissolved to give a pale yellow solution. The solution was allowed to cool and then added to a warm solution of $\text{Rh}_2(\text{CO})_4\text{Cl}_2$

(0.0496g, 0.128mmol) in 5ml of acetic acid. Immediate precipitation of the red/orange solid $[\text{Bz}(\text{Et})_3\text{N}]_2[\text{Rh}(\text{CO})_2(\text{SnCl}_3)_3]$ occurred, which was separated by filtration of the warm mixture under a nitrogen atmosphere and then dried under vacuum. The product (0.31g) was transferred and handled under a nitrogen atmosphere. {Found : C 29.47, H 4.13, N 2.49, Sn 29.90%; $[\text{Bz}(\text{Et})_3\text{N}]_2[\text{Rh}(\text{CO})_2(\text{SnCl}_3)_3]$ requires C 27.57, H 3.61, N 2.30, Sn 29.22%; Infra-red : $\nu(\text{CO})/\text{cm}^{-1}$ - 2000_w, 2014_m, 2028_{sh}, 2068_w, 2078_w}.

Reactions of $\text{Rh}_2(\text{CO})_4\text{Cl}_2$ with SnCl_3^- or $\text{SnCl}_2/\text{Cl}^-$, and $[\text{Rh}(\text{CO})_2\text{Cl}_2]^-$ with SnCl_3^- apparently produce the same complex, $[\text{Rh}(\text{CO})_2(\text{SnCl}_3)_3]^{2-}$ having absorptions at 2016_s / 2014_s, 2068_w cm^{-1} .

3.3 Discussion

3.3.1 Crystal Structure Information

Table 3.7 summarises the relevant bond lengths for the two complexes discussed in this chapter for which X-ray crystal structures have been determined by Prof. J.A.K. Howard and J. Cole (Department of Chemistry, Durham University), and also for other reported Rh-CO and Rh-SnCl₃ complexes.

The Rh-CO bond lengths for $[\text{PPN}]_2[\text{Rh}(\text{CO})_2(\text{SnCl}_3)_3]$ are longer than those for the rhodium-carbonyl-halide complexes $\text{Rh}_2(\text{CO})_4\text{Cl}_2$ and $[\text{Rh}(\text{CO})_2\text{Cl}_2]^-$ and also for the $[\text{Rh}(\text{CO})_2(\text{OAc})_2]^-$ complex. The distances found are shorter than the Rh-CO distance of 1.92Å (CO trans to SnCl_3^-) in $\text{Rh}_2\text{Sn}_2(\text{CO})_2\text{Cl}_6[\mu-(\text{Ph}_2\text{P})_2\text{py}]_2$. The long length of the Rh-Carbon bonds for $[\text{Rh}(\text{CO})_2(\text{SnCl}_3)_3]^{2-}$ is consistent with the trichlorostannate ligand being a strong π -acceptor and certainly a stronger π -acceptor than carbon monoxide. In general a shortening of the Rh-CO bond would be the consequence of attachment of an additional ligand to convert a 16e⁻ e.g. planar complex, to an 18e⁻ complex. Clearly, in the square pyramidal arrangement of the $[\text{Rh}(\text{CO})_2(\text{SnCl}_3)_3]^{2-}$ anion there will be strictly speaking no direct trans influence since there are no SnCl_3^- or CO ligands directly trans to each other, and thus competition for π -electron density will not involve all the same orbitals. The Rh-CO bond lengths obtained will reflect an effect from all the trichlorostannate groups present competing for π -electron density from metal orbitals. Although there will be no single large contribution of π -electron density from one particular metal orbitals to an empty 5d orbital of a trichlorostannate ligand, the net contribution of π -electron density from several metal orbitals to the vacant tin 5d orbital of more than one trichlorostannate group is enough to cause an increase in the Rh-CO bond

length. The short Rh-Sn distances for the trichlorostannate ligands which form the square base of the pyramid with the two carbonyl ligands (Rh-Sn : 2.547(1), 2.540(1)Å) are indicative of groups strongly withdrawing electron density from the metal orbitals to a greater extent than the trichlorostannate group above the plane of the square base, which has a significantly longer Rh-Sn bond length of 2.605(1)Å.

Table 3.7 Summary of the relevant bond lengths for various Rh-CO and Rh-SnCl₃ complexes.

Complex	Rh-CO/Å	Rh-Sn/Å	Reference
*[Rh(CO)(SnCl ₃) ₄] ³⁻	1.840(18)	2.553(2) 2.559(2) 2.543(1) 2.535(2)	Section 3.2.1
◇[Rh(CO) ₂ (SnCl ₃) ₃] ²⁻	1.877(12) 1.895(14)	2.547(1) 2.540(1) 2.605(1)	Section 3.2.5
Rh ₂ (CO) ₄ Cl ₂	1.841 1.854	—	9
[n-Bu ₄ N][Rh(CO) ₂ (OAc) ₂]	1.826 1.817	—	10
Rh(CO) ₂ Cl ₂ ⁻	1.800	—	11
Rh ₂ Sn ₂ (CO) ₂ Cl ₆ [μ-(Ph ₂ P) ₂ py] ₂	1.850 1.920	2.601 m 2.588 m 2.587	12
mer[{Rh(CNC ₈ H ₉) ₃ (SnCl ₃) (μ-SnCl ₂) ₂ }]	—	2.606 2.645 b 2.616 b	13
Rh(SnCl ₃)(NBD)(dppp)	—	2.637	14

* = [Bz(Et)₃N]⁺ ◇ = [PPN]⁺ b - Bridging m - in macrocycle

The Rh-CO bond length (1.840(18)Å) in the trigonal bipyramidal anionic complex [Rh(CO)(SnCl₃)₄]³⁻ is longer than those in the [Rh(CO)₂Cl₂]⁻ and [Rh(CO)₂(OAc)₂]⁻ complexes but is similar in length to those in Rh₂(CO)₄Cl₂ and considerably shorter than the Rh-CO bond length for the carbonyl group trans to a trichlorostannate group in Rh₂Sn₂(CO)₂Cl₆[μ-(Ph₂P)₂py]₂ (1.920Å). The Rh-CO bond length of 1.840(18)Å in [Rh(CO)(SnCl₃)₄]³⁻ is, however, subject to a

significant error, with the actual length possibly being approximately $\pm 0.05 \text{ \AA}$ of this quoted value. Nevertheless, the quoted value does indicate an increase in the Rh-CO bond length compared with the anionic complexes $[\text{Rh}(\text{CO})_2\text{Cl}_2]^-$ and $[\text{Rh}(\text{CO})_2(\text{OAc})_2]^-$, although possibly not as much as for $[\text{Rh}(\text{CO})_2(\text{SnCl}_3)_3]^{2-}$. Further, it is also indicative of the SnCl_3^- ligand being a strong π -acceptor and exerting a significant trans influence. In this case the shortening of the Rh-CO bond length is caused by a single trichlorostannate ligand trans to the carbonyl ligand, and competition for π -electron density between these ligands. The trichlorostannate ligand, being a stronger π -acceptor than the carbonyl ligand will remove a greater share of electron density from the metal and thus causes a lengthening of the Rh-CO bond.

The Rh-Sn bond length of the trichlorostannate group trans to the carbonyl ligand is $2.559(2) \text{ \AA}$ whilst those in the equatorial positions are $2.553(2)$, $2.543(1)$ and $2.535(2) \text{ \AA}$. Thus, there is no shortening of the Rh-Sn bond of the trichlorostannate ligand trans to CO, compared with the other Rh-Sn distances, although all of the Rh-Sn distances in this complex are significantly shorter than those quoted for other complexes in Table 3.7. Bonds to ligands in axial positions are normally longer than those to equatorial ligands and the fact that similar Rh-Sn lengths in both axial and equatorial positions are observed may reflect the enhanced π -bonding contribution to the bonding of the trichlorostannate ligand in the axial position.

A general feature of SnCl_3^- ligands coordinated to transition metals is that M-Sn-Cl bond angles are greater than the ideal tetrahedral value of 109.4° and that Cl-Sn-Cl angles are smaller than 109.4° ^(13,15,16). This is interpreted as being due to a greater s orbital character in the M-Sn bonding orbitals than in the Sn-Cl bonding orbitals, which have a greater p orbital character and consequently Cl-Sn-Cl angles are smaller.

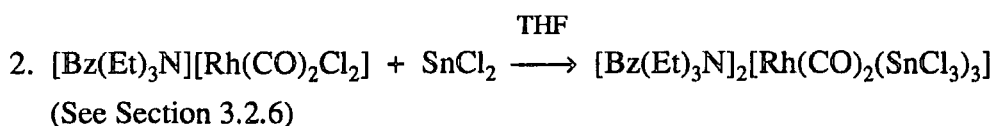
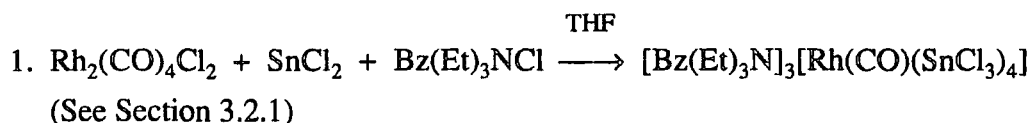
This bond angle trend is upheld for the complexes reported in this chapter. The Rh-Sn-Cl bond angles in $[\text{Rh}(\text{CO})_2(\text{SnCl}_3)_3]^{2-}$ range from $129.3(2)^\circ$ to $113.7(2)^\circ$, whilst the Cl-Sn-Cl angles range from $107.7(1)^\circ$ to $95.5(1)^\circ$. The Rh-Sn-Cl bond angles in $[\text{Rh}(\text{CO})(\text{SnCl}_3)_4]^{3-}$ range from $128.2(2)^\circ$ to $111.9(3)^\circ$, whilst the Cl-Sn-Cl angles range from $97.7(2)^\circ$ to $92.4(2)^\circ$.

3.3.2 Rationalisation of the formation of complexes isolated from solution

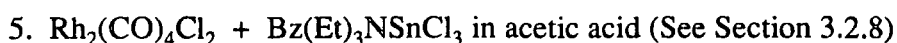
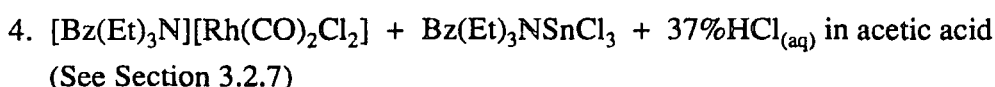
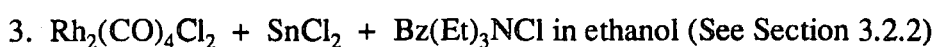
The 5-coordinate rhodium(I) complexes $[\text{Rh}(\text{CO})_2(\text{SnCl}_3)_3]^{2-}$ and $[\text{Rh}(\text{CO})(\text{SnCl}_3)_4]^{3-}$, isolated from reactions of rhodium(I) carbonyl chloride complexes and tin(II) chlorides, and reported in this chapter, are in keeping with the well documented ability of the SnCl_3^- ion to form and stabilise such 18-electron 5-coordinate transition metal complexes⁽⁴⁻⁸⁾. This is supported by the fact that the 5-coordinate Rh(I)- SnCl_3 complexes formed are extremely air and moisture stable species, whereas the 4-coordinate Young's complex $[\text{Rh}(\text{CO})(\text{SnCl}_3)_2\text{Cl}]^{2-}$ is very unstable and decomposes quickly when exposed to the atmosphere. Even when stored under apparent anaerobic conditions in a glove box this complex will decompose over one week. The formation of the 5-coordinate complexes can be attributed to the strong π -acceptor ability of the trichlorostannate group⁽¹⁷⁻¹⁸⁾, which is confirmed from infra-red studies reported in Chapter 2 and crystal structure data in Section 3.2.1. This allows formation of 5-coordinate complexes by a large back donation of π -electron density from the occupied rhodium d-orbitals to the vacant tin 5d orbitals. Thus, the 5-coordinate state is stabilised due to a strengthening of the metal ligand bonds, i.e. an increase in bond energy. Removal of electron density from the metal centre is favourable for a system containing a metal in a low formal oxidation state such as Rh(I), since electron density built up via the σ -system can be dispersed through the π -system. The removal of π -electron density from rhodium effectively makes the metal more electropositive. Therefore, addition of further ligands becomes more favourable and hence, the ability of strong π -acceptor ligands such as SnCl_3^- to form 5-coordinate 18 electron rhodium(I) complexes such as $[\text{Rh}(\text{CO})_2(\text{SnCl}_3)_3]^{2-}$ and $[\text{Rh}(\text{CO})(\text{SnCl}_3)_4]^{3-}$. This 5-coordination is not favoured by an arrangement of chloride ligands which are primarily σ -donors and have no π -acceptor ability.

The reactions described in this chapter have been studied in solution using FT-IR and NMR spectroscopy, and the chemistry reported in detail in Chapter 2. Infra-red and ^{119}Sn NMR studies indicate that $[\text{Rh}(\text{CO})_2(\text{SnCl}_3)_3]^{2-}$ is the favoured species formed in solution. However, in some circumstances a 4-coordinate complex, either $[\text{Rh}(\text{CO})_2(\text{SnCl}_3)_2]^-$ or $[\text{Rh}(\text{CO})_2(\text{SnCl}_3)\text{Cl}]^-$, is formed in THF. This complex appears to be closely related to $[\text{Rh}(\text{CO})_2(\text{SnCl}_3)_3]^{2-}$, either as an intermediate in its formation or as a product of its decomposition. The π -acceptor properties of the SnCl_3^- ligand explain its ability to form 5-coordinate 18-electron rhodium(I) complexes, such as $[\text{PPN}]_2[\text{Rh}(\text{CO})_2(\text{SnCl}_3)_3]$ and $[\text{Bz}(\text{Et})_3\text{N}]_3[\text{Rh}(\text{CO})(\text{SnCl}_3)_4]$, isolated and characterised in this work. However, although $[\text{Rh}(\text{CO})_2(\text{SnCl}_3)_3]^{2-}$ is the predominant species in solution, it appears to be related, probably by a series of

equilibria, to other Rh-SnCl₃ complexes. The conditions, i.e. temperature, amount of solvent, concentration of reactants in solution, removal of solvent, appear critical towards the isolation of other complexes. For instance, for the apparently similar reactions, shown below, which both form [Rh(CO)₂(SnCl₃)₃]²⁻ in solution, different solid complexes were isolated.



The isolation of [Bz(Et)₃N]₂[Rh(CO)₂(SnCl₃)₃] from Reaction 2 as a single species was unusual, since a mixture of rhodium carbonyl products was usually obtained. Infra-red, ¹¹⁹Sn NMR and microanalytical data indicated that this mixture, along with the products of Reactions 3-5 shown below



contained [Bz(Et)₃N]₂[Rh(CO)₂(SnCl₃)₃] as the main component, together with small quantities of [Bz(Et)₃N]₃[Rh(CO)(SnCl₃)₄] and/or [Bz(Et)₃N]₂[Rh(CO)(SnCl₃)₂Cl]. ¹¹⁹Sn NMR data in CDCl₃/CH₂Cl₂ for the solid product obtained from Reaction 3 were consistent with the presence of an additional Rh(I)-SnCl₃ complex together with than [Bz(Et)₃N]₂[Rh(CO)₂(SnCl₃)₃]. The additional signal may be due to the Rh-CO species giving the weak infra-red absorptions at 2028 and 2079cm⁻¹, to [Rh(CO)(SnCl₃)₄]³⁻ or [Rh(CO)(SnCl₃)₂Cl]²⁻, or to a non-carbonyl containing complex such as [Rh(SnCl₃)₅]⁴⁻⁽³⁾. It is relevant that Reaction 3, on several attempts, formed the desired Young's complex [Bz(Et)₃N]₂[Rh(CO)(SnCl₃)₂Cl] rather than the mixture of species described above, demonstrating that the same reaction may lead to different products.

Consequently, since similar reactions of rhodium(I) carbonyl chlorides with tin(II) chlorides give the formation of different solid Rh(I)-CO-SnCl₃ complexes, and in

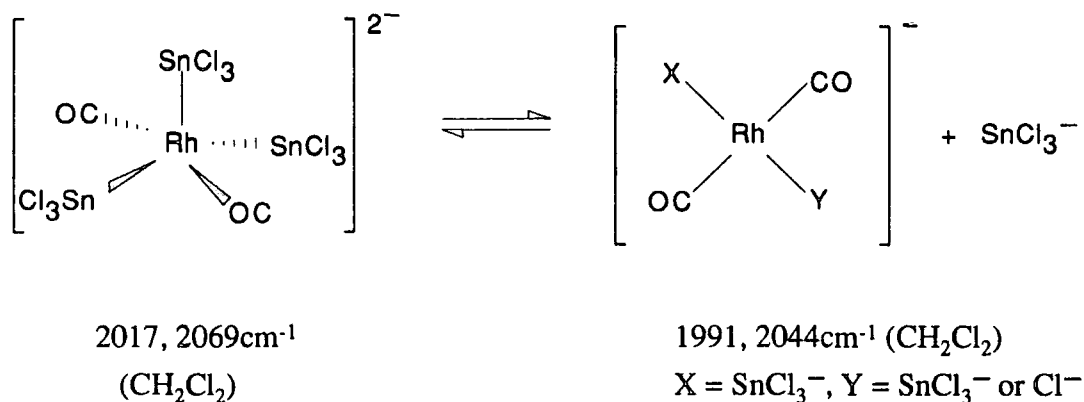
The influence of the π -electron acceptor properties of SnCl_3^- on the formation of a particular complex can be illustrated by a consideration of the equilibrium (given below) between $[\text{Rh}(\text{CO})(\text{SnCl}_3)_4]^{3-}$ and $[\text{Rh}(\text{CO})_2(\text{SnCl}_3)_3]^{2-}$. The π -electron acceptor properties of SnCl_3^- will favour 5-coordination, and complexes containing many SnCl_3^- ligands, since higher numbers of SnCl_3^- groups coordinated to rhodium would be expected to remove more π -electron density from the occupied rhodium(I) d-orbitals and offset the σ -donation from the five ligands. This therefore implies that an equilibrium between the two would be in favour of the tetra-tin complex:



However, increasing numbers of SnCl_3^- groups attached to rhodium may also decrease the strength of the Rh- SnCl_3 and Rh-CO bonds, since there is increased competition for π -electron density from the same rhodium d-orbitals, e.g. the 3 equatorial SnCl_3^- groups in $[\text{Rh}(\text{CO})(\text{SnCl}_3)_4]^{3-}$ will compete for π -electron density from the same occupied rhodium d-orbitals. Thus, a balance exists between maximising the number of π -acceptor ligands and the weakening effect on metal-ligand bonds of strong competition between ligands. Therefore, although the strong π -acceptor ability of SnCl_3^- may weaken the Rh-CO bonds of $[\text{Rh}(\text{CO})_2(\text{SnCl}_3)_3]^{2-}$, thus labilising CO and promoting formation of $[\text{Rh}(\text{CO})(\text{SnCl}_3)_4]^{3-}$, the indication is that $[\text{Rh}(\text{CO})_2(\text{SnCl}_3)_3]^{2-}$ formation is preferred, probably because the increased ability of SnCl_3^- ligands to labilise each other in a complex such as $[\text{Rh}(\text{CO})(\text{SnCl}_3)_4]^{3-}$ has a greater destabilising effect. The ability of SnCl_3^- to labilise other SnCl_3^- and CO ligands, and hence favour the formation of one complex over another, is most likely dependant on the geometry of the species, i.e. the arrangement of the occupied rhodium d-orbitals with respect to the position of the SnCl_3^- groups. However, the above equilibrium must be disturbed during precipitation since $[\text{Bz}(\text{Et})_3\text{N}]_3[\text{Rh}(\text{CO})(\text{SnCl}_3)_4]$ is the only solid complex produced in Reaction 3.2.1.

The formation of $[\text{PPN}]_2[\text{Rh}(\text{CO})_2(\text{SnCl}_3)_3]$ by reaction of $[\text{PPN}]_2[\text{Rh}(\text{COD})(\text{SnCl}_3)_3]$ with CO (Section 3.2.5) is also a reflection of the ability of SnCl_3^- to form 5-coordinate 18-electron Rh(I)-CO- SnCl_3 complexes. This complex was identified by comparison of infra-red and ^{119}Sn NMR spectral data with that reported by Pregosin et al⁽²⁾. However, although reaction with CO favoured the initial formation of the 5-coordinate complex $[\text{Rh}(\text{CO})_2(\text{SnCl}_3)_3]^{2-}$ in THF and

CH₂Cl₂, the complex appears to change upon an attempt to precipitate it, and [Rh(CO)₂(SnCl₃)₃]²⁻ along with either a single rhodium(I) dicarbonyl complex or two rhodium(I) monocarbonyl complexes is precipitated from CH₂Cl₂, as indicated by infra-red spectroscopy {ν(CO) (nujol) 1989_s, 2016_{sh}, 2039_{mw}, 2065_{vw} cm⁻¹}. Infra-red studies of the behaviour of the solid product upon addition of CH₂Cl₂ (Section 3.2.5) indicate that the solution species produced is determined by the conditions. [Rh(CO)₂(SnCl₃)₃]²⁻ is usually the sole species, but in one case the species with the absorptions at 1991 and 2044cm⁻¹ in CH₂Cl₂, usually the minor species, predominated. Although the absorptions at 1991 and 2044cm⁻¹ may be due to two different rhodium monocarbonyl complexes, the infra-red pattern is consistent with a single trans-dicarbonyl rhodium(I) 4-coordinate complex. [Rh(CO)₂(SnCl₃)₃]²⁻ appears to be related to the complex having absorptions at 1991 and 2044cm⁻¹, which seems to be formed at its expense upon precipitation. Consequently, [Rh(CO)₂(SnCl₃)₃]²⁻ and the 4-coordinate rhodium(I) complex are possibly related by the following equilibrium:



Precipitation of this apparently 4-coordinate complex over [Rh(CO)₂(SnCl₃)₃]²⁻ was favoured under particular conditions, indicating that such species can also exist in a stable solid form. The results suggest that although [Rh(CO)₂(SnCl₃)₃]²⁻ is the species initially favoured in solution, the position of the equilibrium can be disturbed upon precipitation or removal of solvent, and dissociation of SnCl₃⁻ occurs, resulting in formation of the 4-coordinate complex.

Reaction of [Rh(COD)(SnCl₃)₃]²⁻ with CO in CH₂Cl₂ would be expected to initially give adjacent carbonyl groups upon displacement of the 1,5-cyclooctadiene ligand. However, the carbonyl absorptions observed at 2016_s and 2065_{vw}cm⁻¹ in CH₂Cl₂ suggest rapid isomerisation to give a complex containing trans carbonyl groups, possibly in a trigonal bipyramidal arrangement with CO groups in axial positions.

The precipitation of the $[\text{Rh}(\text{CO})_2(\text{SnCl}_3)_3]^{2-}$ complex in the square pyramidal arrangement shown in Figure 3.8 (p 99) ($\nu(\text{CO}) - 2016_{\text{sh}} 2065_{\text{vw}} \text{cm}^{-1}$, see Section 3.2.5), suggests that such an arrangement will be thermodynamically preferred in the solid state. This structural conformation is consistent with bulky SnCl_3^- groups preferring not to be adjacent to each other.

The difficulties involved in distinguishing between the possible $\text{Rh}(\text{I})\text{-CO-SnCl}_3$ products $[\text{Rh}(\text{CO})_2(\text{SnCl}_3)_3]^{2-}$, $[\text{Rh}(\text{CO})(\text{SnCl}_3)_4]^{3-}$ and $[\text{Rh}(\text{CO})(\text{SnCl}_3)_2\text{Cl}]^{2-}$ purely on the basis of the frequencies of their infra-red carbonyl absorptions and microanalytical data were discussed in Section 3.2.6. In Table 3.8 their similar carbonyl absorptions are illustrated.

Complex	$\nu(\text{CO})/\text{cm}^{-1}$ in nujol
* $[\text{Rh}(\text{CO})(\text{SnCl}_3)_4]^{3-}$	2012
* $[\text{Rh}(\text{CO})(\text{SnCl}_3)_2\text{Cl}]^{2-}$	2013
† $[\text{Rh}(\text{CO})_2(\text{SnCl}_3)_3]^{2-}$	2016 2065

* Cation = $[\text{Bz}(\text{Et})_3\text{N}]^+$ † Cation = $[\text{PPN}]^+$

Table 3.8 Frequencies of carbonyl absorptions for isolated $\text{Rh}(\text{I})\text{-CO-SnCl}_3$ complexes recorded with a resolution of 2cm^{-1}

The carbonyl frequencies shown in Table 3.8 indicate that the number of SnCl_3^- groups attached to rhodium has little effect on $\nu(\text{CO})$ positions, the data being in agreement also with that obtained for the series of monocarbonyl $\text{Rh}(\text{I})\text{-CO-SnCl}_3$ complexes obtained from the reactions of $[\text{Rh}(\text{CO})_2\text{Cl}_2]^-$ with SnCl_2 as reported by Kingston et al⁽¹⁹⁾ (Table 3.9).

Rh:Sn molar ratio of reactants	Complex formed	$\nu(\text{CO})/\text{cm}^{-1}$ KBr	$\nu(\text{CO})/\text{cm}^{-1}$ CH_2Cl_2
1:1	^a $[\text{Rh}(\text{CO})(\text{SnCl}_3)\text{Cl}_2]^{2-}$	2005	—
1:2	^b $[\text{Rh}(\text{CO})(\text{SnCl}_3)_2\text{Cl}]^{2-}$	2005	—
1:3	^a $[\text{Rh}(\text{CO})(\text{SnCl}_3)_3]^{2-}$	2005	
	^c $[\text{Rh}(\text{CO})(\text{SnCl}_3)_3]^{2-}$	2005 2060 _w	2010 2064 _w

a $[\text{Et}_4\text{N}]^+$ b $[\text{Me}_4\text{N}]^+$ c $[\text{Ph}_4\text{As}]^+$

Table 3.9 Infra-red data for a series of $\text{Rh}(\text{I})\text{-CO-SnCl}_3$ complexes obtained from reactions of $[\text{Rh}(\text{CO})_2\text{Cl}_2]^-$ with SnCl_2 reported by Kingston et al⁽¹⁹⁾

Generally, an increase in the number of SnCl_3^- groups attached to rhodium is expected to increase the frequency of the carbonyl absorption for a monocarbonyl complex due to a weakening of the Rh-CO bond. However, this is based on the assumption that each attached SnCl_3^- group will receive the same amount of π -electron density for d_π - d_π backbonding from filled rhodium d-orbitals which also contribute π -electron density to Rh-CO d_π - d_π backbonding. The extent of Rh-Sn π -bonding, and therefore competition with carbonyl groups, will depend on the extent of d_π - d_π overlap, which will also depend on the geometry of the complex i.e. the degree of π -electron donation to SnCl_3^- groups from filled rhodium d-orbitals also contributing to Rh-CO backbonding, will be dependant on the geometry of the complex and the positions of the tin 5d orbitals relative to the relevant filled rhodium d-orbitals. It is therefore possible that contribution of π -electron density to Rh-SnCl₃ bonding from filled rhodium d-orbitals also contributing to Rh-CO backbonding, will vary from an important contribution down to little contribution at all, depending on the geometry of the complex. The latter is governed by factors such as thermodynamic stability and steric crowding. As a result the position of the carbonyl frequency will depend on the net overall contribution of π -electron density from filled rhodium d-orbitals also involved in Rh-CO backbonding, to all of the coordinated SnCl_3^- groups. In the case of $[\text{Rh}(\text{CO})(\text{SnCl}_3)_2\text{Cl}]^{2-}$ and $[\text{Rh}(\text{CO})(\text{SnCl}_3)_4]^{3-}$ the overall contributions seem to be similar and suggest similar Rh-CO bond strengths.

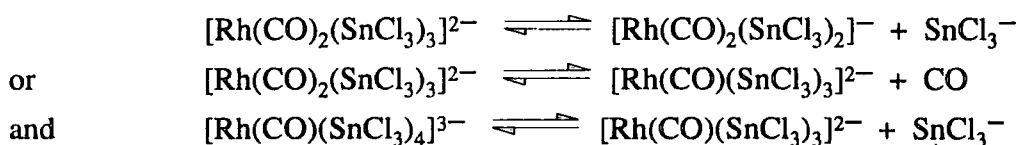
The data reported by Kingston also indicated that the Rh:Sn stoichiometry of each product was directly proportional to the Rh:Sn molar ratio of the reactants, thus indicating that a 1:1 reaction was complete before the 1:2 reaction commenced. Data reported here and in Chapter 2 is in disagreement with this feature, and indicates that $[\text{Rh}(\text{CO})_2(\text{SnCl}_3)_3]^{2-}$ forms irrespective of the Rh:Sn molar ratio of the reactants. Also, the assignment of infra-red data reported by Kingston to salts of $[\text{Rh}(\text{CO})(\text{SnCl}_3)_3]^{2-}$, is questioned. The frequencies of the two carbonyl absorptions for the $[\text{Ph}_4\text{As}]^+$ salt indicate that their product is in fact $[\text{Rh}(\text{CO})_2(\text{SnCl}_3)_3]^{2-}$ which cannot be easily distinguished from the monocarbonyl complex by the limited analysis above. Also, the isolation of the $[\text{Et}_4\text{N}]^+$ salt of $[\text{Rh}(\text{CO})_2(\text{SnCl}_3)_3]^{2-}$ must be questioned, a more likely interpretation being that $[\text{Rh}(\text{CO})_2(\text{SnCl}_3)_3]^{2-}$ was formed. The weak absorption at 2060cm^{-1} , expected for $[\text{Rh}(\text{CO})_2(\text{SnCl}_3)_3]^{2-}$, was not observed, not surprisingly as the sensitivity of the infra-red spectrometer used was poor. Since the formation of $[\text{Rh}(\text{CO})(\text{SnCl}_3)_3]^{2-}$ by Kingston is doubtful, it has

not been proposed as a possible component of the mixtures of solid species isolated in this work.

3.4 Conclusions

The reactions of rhodium(I) carbonyl chlorides with tin(II) chlorides have led to the isolation and characterisation of $[\text{Bz}(\text{Et})_3\text{N}]_3[\text{Rh}(\text{CO})(\text{SnCl}_3)_4]$ and $[\text{PPN}]_2[\text{Rh}(\text{CO})_2(\text{SnCl}_3)_3]$ as stable 5-coordinate 18-electron rhodium(I) complexes in the solid state. The production of these complexes is in keeping with the recognised ability of SnCl_3^- , as a π -acceptor ligand, to stabilise such 5-coordinate species. Bond length data for crystals of $[\text{Bz}(\text{Et})_3\text{N}]_3[\text{Rh}(\text{CO})(\text{SnCl}_3)_4]$ and $[\text{PPN}]_2[\text{Rh}(\text{CO})_2(\text{SnCl}_3)_3]$ confirmed the significant π -acceptor ability of SnCl_3^- . Infra-red and NMR data for solution studies of reactions of rhodium(I) carbonyl chlorides with tin(II) chlorides, reported in Chapter 2, indicated that $[\text{Rh}(\text{CO})_2(\text{SnCl}_3)_3]^{2-}$ was the favoured species formed in solution, but that it was also closely related to a 4-coordinate Rh(I)-CO-SnCl₃ complex, which was formed either as an intermediate in the formation of $[\text{Rh}(\text{CO})_2(\text{SnCl}_3)_3]^{2-}$ or as a product of its dissociation or decomposition. Further, the isolation of solid materials from these solutions indicates that although $[\text{Rh}(\text{CO})_2(\text{SnCl}_3)_3]^{2-}$ is isolated in significant quantities, it is related by a series of equilibria to other Rh(I)-SnCl₃ complexes. The other species which precipitate include $[\text{Rh}(\text{CO})(\text{SnCl}_3)_4]^{3-}$, $[\text{Rh}(\text{CO})(\text{SnCl}_3)_2\text{Cl}]^{2-}$, and a species consistent with the 4-coordinate rhodium(I) dicarbonyl complex $[\text{Rh}(\text{CO})_2(\text{SnCl}_3)\text{X}]^-$ ($\text{X}=\text{SnCl}_3^-$ or Cl^-), and are obtained often as mixtures along with $[\text{Rh}(\text{CO})_2(\text{SnCl}_3)_3]^{2-}$.

Although $[\text{Rh}(\text{CO})_2(\text{SnCl}_3)_3]^{2-}$ is isolated in the crystalline form, it does not appear to be wholly robust in solution e.g. $[\text{Rh}(\text{CO})(\text{SnCl}_3)_4]^{3-}$ and $[\text{Rh}(\text{CO})_2(\text{SnCl}_3)_3]^{2-}$ are possibly linked by related equilibria such as those shown below, and indeed the same reaction procedure leads to either product.



The isolation of solid material from solution relies upon the disturbance of the equilibria in favour of one particular product complex, and therefore conditions of temperature, solvent, concentration of species in solution, history of the solution (i.e.

loss of dissolved carbon monoxide, loss of SnCl_3^- ligands by aerial/glass hydrolysis) etc. all contribute to the nature of the product material. The results are therefore consistent with the main solution species being $[\text{Rh}(\text{CO})_2(\text{SnCl}_3)_3]^{2-}$, but also with the lability of the SnCl_3^- ligand.

3.5 References

1. J.F. Young, R.D. Gillard, G. Wilkinson, *J. Chem. Soc.*, 1964, 5176.
2. M. Kretschmer, P.S. Pregosin, H. Rügger, *J. Organometal. Chem.*, 1983, 241, 87.
3. H. Moriyama, T. Aoki, S. Shinoda, Y. Saito, *J. Chem. Soc. Dalton. Trans.*, 1981, 639.
4. P. Porta, H.M. Powell, R.J. Mawby, L.M. Venanzi, *J. Chem. Soc. (A)*, 1967, 455.
5. M.R. Churchill, K.K.G. Lin, *J. Am. Chem. Soc.*, 1974, 96, 76.
6. R.D Cramer, R.V. Lindsey Jr., C.T. Prewitt, U.G. Stolberg, *J. Am. Chem. Soc.*, 1965, 87, 658.
7. C.Y. Hsu, M. Orchin, *J. Am. Chem. Soc.*, 1975, 97, 3553.
8. R. Uson, L.A. Oro, M.T. Pinillos, A. Arruebo, K.H.A.O. Starzewski, P.S. Pregosin, *J. Organometal. Chem.*, 1980, 192, 227.
9. L. Walz, P. Scheer, *Acta. Cryst.*, 1991, C47, 640.
10. A. Fulford, N.A. Bailey, H. Adams, P.M. Maitlis, *J. Organometal. Chem.*, 1991, 417, 139.
11. A. Backson, J.A. Osborn, P.H. Bird, A.V. Peters, *J. Chem. Soc. Chem. Commun.*, 1984, 72.
12. A.L. Balch, H. Hope, F.E. Wood, *J. Am. Chem. Soc.*, 1985, 107, 6936.
13. S.G. Bott, J.C. Machell, D.M.P. Mingos, M.J. Watson, *J. Chem. Soc. Dalton. Trans.*, 1991, 859.
14. M.A. Garralda, E. Pinilla, M.A. Monge, *J. Organometal. Chem.*, 1992, 427, 193.
15. M.S. Holt, W.L. Wilson, J.H. Nelson, *Chem. Rev.*, 1989, 89, 11.
16. B.Y.K. Ho, J.J. Zuckerman, *J. Organometal. Chem.*, 1973, 49, 1.
17. G.W. Parshall, *J. Am. Chem. Soc.*, 1966, 88, 704.
18. W. Jetz, P.B. Simons, J.A.J. Thompson, W.A.G. Graham, *Inorg. Chem.*, 1966, 5, 2217.
19. J.V. Kingston, G.R. Scollary, *J. Chem. Soc. (A)*, 1971, 3399.

Chapter 4

The Hydrocarbonylation of Ethene Using Rhodium(I)-Tin(II) Catalytic Systems

4.1 Introduction

The ability of the trichlorostannate anion SnCl_3^- to act as a co-catalyst with transition metal complexes has been studied previously and is reported in detail in Chapter 1. Recent studies⁽¹⁾, the details of which are shown in Table 4.1, have shown that rhodium(III) chloride trihydrate is an active catalytic precursor for the hydrocarbonylation of ethene to form propanoic acid, but only when tin(II) chloride is present as a co-catalyst.

A comparison of Reactions 1 and 2 in Table 4.1 shows that addition of an alkyl ammonium salt, benzyltriethylammonium chloride, to the rhodium-tin catalytic system, led to an approximate six-fold enhancement in the rate of propanoic acid production. There was only a small difference, however, in the total amount of propanoic acid produced. Reactions 3,4 and 5 in Table 4.1 show that optimum rates and selectivities for propanoic acid were achieved for the rhodium/tin systems when a 1:2 molar ratio of rhodium:tin was employed, as in Reactions 2 and 4. Lower tin content leads to a decrease in rate and higher tin content lowers both the rate and selectivity. The data obtained for Reactions 6,7 and 8 also show that the optimum temperature for propanoic acid production was 180°C. At temperatures of 150°C or less the reactions were shown to be 90-95% selective for butyl compounds. It is interesting to note that in Reactions 2 and 4, both of which were carried out in the same reaction vessel and which are apparently identical systems, the rate of gas uptake and selectivity observed for Reaction 4 are significantly lower than those observed for Reaction 2, but the rate of propanoic acid production is strangely higher for Reaction 4 than for Reaction 2. Studies also showed that no catalytic activity occurred in the absence of HCl from the systems, and once again it is stressed that no activity was found to occur for a rhodium-chloride catalytic system in the absence of tin(II) chloride, although no data has been made available.

The data obtained under the optimum conditions clearly suggested a synergy between rhodium and tin. The nature of the active catalyst was, however, unclear, and the role of the tin was speculative. The aim of the work reported in this chapter was, initially, to duplicate previous work carried out on this process in order to test the authenticity of the results obtained, and then to improve upon and explore the catalytic process utilising previous knowledge and known chemical processes.

Table 4.1 A summary of the important features of the rhodium-tin-chloride catalysed hydrocarbonylation of ethene taken from the data obtained by a previous worker⁽¹⁾

Moles of propanoic acid produced	Rate bar.hr ⁻¹	Rate of propanoic acid production mol.kg ⁻¹ .hr ⁻¹	% Selectivity for propanoic acid	Rh:Sn :Bz(Et) ₃ NCl Molar Ratio	Temperature °C
1. Components:		RhCl ₃ .3H ₂ O, SnCl ₂ .2H ₂ O, 37%HCl _(aq) , CH ₃ COOH, CO, C ₂ H ₄			
0.101	21.0	0.89	80.1	1:2:0	180
2. Components:		RhCl ₃ .3H ₂ O, SnCl ₂ .2H ₂ O, Bz(Et) ₃ NCl, 37%HCl _(aq) , CH ₃ COOH, CO, C ₂ H ₄ *			
0.121	137	5.4	88.6	1:2:3	180
3. Components:		Same as Reaction 2			
0.115	63.0	2.97	91.4	1:1:3	180
4. Components:		Same as Reaction 2*			
0.116	88.0	5.72	79.6	1:2:3	180
5. Components:		Same as Reaction 2			
0.016	160	1.69	50.7	1:4:3	180
6. Components:		RhCl ₃ .3H ₂ O, SnCl ₂ .2H ₂ O, Bu ₄ NCl, 37%HCl _(aq) , CH ₃ COOH, CO, C ₂ H ₄			
0.088	220	8.97	44.2	1:2:2	180
7. Components:		Same as Reaction 6			
6 x 10 ⁻⁴	240	0.097	0.5	1:3:2	150
8. Components:		Same as Reaction 6			
5.6 x 10 ⁻³	102	0.17	10.1	1:3:2	120

For Reactions 1-8 CO pressure = 40 bar, C₂H₄ pressure = 40 bar

* Reactions 2 and 4 are essentially the same, carried out with similar quantities of reagents and in the same reaction vessel.

4.2 Experimental procedures, summary of data obtained, and calculation of rate data, propanoic acid production and selectivity for propanoic acid

Table 4.2 summarises the quantities of reagents used, and the data obtained for all of the high pressure catalytic runs described throughout this chapter.

4.2.1 Experimental procedures

The high pressure reactions described in this chapter were carried out in a 120 ml Hastalloy C autoclave which is described in detail in Appendix 2. The same autoclave was used for previous studies of similar systems⁽¹⁾, the results of which are summarised in Table 4.1.

In all reactions degassed glacial acetic acid (99-100%) was used as solvent, the volume of which was measured by syringe, to an estimated precision of +/- 0.3 ml. In most cases, except for the odd exceptions which are noted throughout this chapter, a small volume of 37% $\text{HCl}_{(\text{aq})}$ (either 2.4 ml or 1.2 ml), was added to each system, since previous studies⁽¹⁾ showed that the presence of HCl was a necessary requirement for hydrocarbonylation to occur. The volume of 37% $\text{HCl}_{(\text{aq})}$ was measured by pipette. Acetic and hydrochloric acid used throughout the work were taken from the same batches of chemical which were restricted for the use of high pressure catalytic runs.

The same batch of rhodium(III) chloride trihydrate as supplied by Johnson Matthey plc was used for all of the reactions. Anhydrous tin(II) chloride, 99.99% purity, supplied by the Aldrich Chemical Co., was taken similarly from the same batch throughout the series of reactions shown in Table 4.2.

For each reaction the reagents were loaded via the inlet at the head of the autoclave. The solid reagents were added first, followed by the liquid reagents, usually acetic acid and concentrated hydrochloric acid. After sealing, the autoclave was flushed by pressurising the vessel twice with nitrogen and once with carbon monoxide. It was then pressurised with the appropriate amounts of reactant gases, in most cases 30 bar of ethene followed by 30 bar of carbon monoxide to give a total pressure of 60 bar. The autoclave was stirred at the same preset speed for all reactions using an internal magnetic follower and heated by a thermocouple controlled external heater to a temperature of 180°C. The reactions were followed by manual reading of gas uptake using pressure gauges. Upon reaching a temperature of 180°C, each reaction was

monitored for a period of 1 hour, with a pressure reading normally taken after 5 minute periods. After 1 hour, the heater was turned off and the autoclave allowed to cool to room temperature. A final pressure reading was recorded at a temperature of 25°C. Any remaining pressure due to unreacted gases was released from the autoclave and the liquid contents were removed by syringe and stored in a sealed container.

Experimental restrictions meant that the autoclave could not be dismantled for cleaning purposes upon completion of every reaction. Thus, an alternative method for removing non-liquid residues and general cleaning was developed, and was used after every catalytic run; The autoclave was stirred overnight with approximately 50ml of acetone in order to dissolve any solid residues. Upon removal of these washings the autoclave was repeatedly washed with further amounts of acetone until the washings removed were completely colourless. Prior to each catalytic run, the remaining traces of acetone were removed from the system by flushing it with a pressure of nitrogen gas. Additionally, after approximately every ten catalytic runs, the autoclave was washed for a period of 24 hours with a mixture of acetic and hydrochloric acid maintained at a temperature of 180°C.

Reaction Code	Reagents	Temperature/ °C	Rate (A) bar.hr ⁻¹	Rate (B) Mol.Kg ⁻¹ .hr ⁻¹	Moles of propanoic acid produced	% Selectivity for propanoic acid
4.6	RhCl ₃ .3H ₂ O 0.103 mmol SnCl ₂ 0.103 mmol	180	26	1.45	0.044	85.6
4.7	RhCl ₃ .3H ₂ O 0.103 mmol SnCl ₂ 0.206 mmol	180	52	2.71	0.104	85.1
4.8	RhCl ₃ .3H ₂ O 0.105 mmol SnCl ₂ 0.331 mmol	180	50	2.06	0.079	77.5
4.9	RhCl ₃ .3H ₂ O 0.103 mmol SnCl ₂ 0.220 mmol Bz(Et) ₃ NCl 0.312 mmol	180	58	2.73	0.105	73.0
4.10	RhCl ₃ .3H ₂ O 0.107 mmol Bz(Et) ₃ NCl 0.0319 mmol	180	28	1.58	0.061	88.8
4.11	*[Rh(CO) ₂ Cl ₂] ⁻ 0.133 mmol	180	26	1.48	0.057	95.1
4.12	*[Rh(CO) ₂ Cl ₂] ⁻ 0.108 mmol SnCl ₂ 0.215 mmol	180	61	3.33	0.128	72.0
4.13	*[Rh(CO) ₂ Cl ₂] ⁻ 0.106 mmol *[SnCl ₃] ⁻ 0.105 mmol	180	30	1.50	0.058	97.6

Reaction Code	Reagents	Temperature/ °C	Rate (A) bar.hr ⁻¹	Rate (B) Mol.Kg ⁻¹ .hr ⁻¹	Moles of propanoic acid produced	% Selectivity for propanoic acid
4.14	*[Rh(CO) ₂ Cl ₂] ⁻ 0.108 mmol *[SnCl ₃] ⁻ 0.206 mmol	180	72	1.66	0.064	65.8
4.15	*[Rh(CO) ₂ Cl ₂] ⁻ 0.106 mmol *[SnCl ₃] ⁻ 0.527 mmol	180	6 ^a	0.16	0.006	10.2
4.16	*[Rh(CO) ₂ Cl ₂] ⁻ 0.105 mmol SnCl ₂ 0.217 mmol CO 30 bar C ₂ H ₄ 20 bar	180	24	1.15	0.044	97.6
4.17	*[Rh(CO) ₂ Cl ₂] ⁻ 0.105 mmol SnCl ₂ 0.217 mmol CO 30 bar C ₂ H ₄ 25 bar	180	43	2.14	0.082	98.0
4.18	*[Rh(CO) ₂ Cl ₂] ⁻ 0.111 mmol SnCl ₂ 0.217 mmol CO 30 bar C ₂ H ₄ 30 bar	180	66	2.83	0.109	96.4
4.19	*[Rh(CO) ₂ Cl ₂] ⁻ 0.106 mmol SnCl ₂ 0.217 mmol CO 30 bar C ₂ H ₄ 40 bar	180	78	2.76	0.106	68.7

Reaction Code	Reagents	Temperature/ °C	Rate (A) bar.hr ⁻¹	Rate (B) Mol.Kg ⁻¹ .hr ⁻¹	Moles of propanoic acid produced	% Selectivity for propanoic acid	
4.20 ^b	RhCl ₃ .3H ₂ O SnCl ₂ Bz(Et) ₃ NCl 37%DCl _(aa) in D ₂ O (99%D)	0.111 mmol 0.219 mmol 0.332 mmol 2.4 ml	180	46	1.26	0.049	19.8
4.21 ^c	RhCl ₃ .3H ₂ O SnCl ₂ Bz(Et) ₃ NCl 37%DCl _(aa) in D ₂ O (99%D) CH ₃ COOD CO C ₂ H ₄	0.061 mmol 0.129 mmol 0.181 mmol 1.2 ml 17 ml 20 bar 20 bar	180	20	1.77	0.036	96.0
4.22 ^d	RhCl ₃ .3H ₂ O SnCl ₂ 37%HCl _(aa)	0.628mmol 1.200mmol 9 ml	180	35	1.03	0.146	82.8
4.23 ^d	*[Rh(CO) ₂ Cl ₂] ⁻ SnCl ₂ 37%HCl _(aa) H ₂ O	0.298mmol 0.708mmol 5ml 5ml	180	42	0.087	0.029	19.7

Reaction Code	Reagents	Temperature/ °C	Rate (A) bar.hr ⁻¹	Rate (B) Mol.Kg ⁻¹ .hr ⁻¹	Moles of propanoic acid produced	% Selectivity for propanoic acid	
4.24 ^d	*[Rh(CO) ₂ Cl ₂] ⁻ SnCl ₂ 37% HCl _(aq)	0.600mmol 1.270mmol 9ml	180	43	1.120	0.158	77.2
4.25	Rh(COD) ₂ (SnCl ₃) 37% HCl _(aq) CH ₃ COOH	0.054 mmol 1.2 ml 17 ml	180	14	1.51	0.029	84.3
4.26	*[Rh(CO)(SnCl ₃) ₂ Cl] ²⁻	0.108 mmol	180	24	1.08	0.042	91.8
4.27	Rh(I)-CO-SnCl ₃ mixture (see Section 3.2.2)	122.8 mg	180	46	2.35	0.090	97.3
4.28	*[Rh(COD)(SnCl ₃) ₃] ²⁻	0.103 mmol	180	47	2.99	0.115	99.2
4.29	◇ [Rh(COD)(SnCl ₃) ₃] ²⁻	0.102 mmol	180	71	2.43	0.093	87.0
4.30	◇ [Rh(CO) ₂ (SnCl ₃) ₃] ²⁻ 37% HCl _(aq) CH ₃ COOH	0.042 mmol 1.2 ml 17 ml	180	16	0.65	0.025	89.3

Reaction Code	Reagents	Temperature/ °C	Rate (A) bar.hr ⁻¹	Rate (B) Mol.Kg ⁻¹ .hr ⁻¹	Moles of propanoic acid produced	% Selectivity for propanoic acid
4.31	Rh ₂ (C ₂ H ₄) ₄ Cl ₂ 0.057 mmol	180	33	1.39	0.054	81.2
4.32 ^e	Rh-CO-SnCl ₃ mix H ₂ O 121.7 mg 2.4 ml	180	0	0	0	—
4.33	RhCl ₃ .3H ₂ O Ph ₃ SnCl Bz(Et) ₃ NCl 0.106 mmol 0.194 mmol 0.305 mmol	180	45	2.46	0.095	80.0
4.34	RhCl ₃ .3H ₂ O Ph ₄ Sn Bz(Et) ₃ NCl 0.104 mmol 0.207 mmol 0.302 mmol	180	33	2.14	0.082	88.0
4.35	RhCl ₃ .3H ₂ O SnCl ₂ Bz(Et) ₃ NCl CH ₃ COOH CH ₂ Cl ₂ 0.105 mmol 0.225 mmol 0.325 mmol 10 ml 24 ml	180	8	0.82	0.032	89.1
4.36	RhCl ₃ .3H ₂ O SnBr ₂ 0.114mmol 0.229mmol	180	72	2.87	0.110	97.8

4.2.2 Calculation of selectivity for propanoic acid and amount of propanoic acid production

The solutions obtained from the reactions carried out in this chapter were analysed by Gas Chromatography, enabling the selectivity for propanoic acid and the amount of propanoic acid produced to be calculated. Non-volatile reaction products were removed by vacuum distillation prior to GC analysis. A sealed system under a static vacuum was used to ensure that the more volatile components were not lost, and a quantitative transfer of volatile components was achieved. Analar grades of propanoic and acetic acids, and ethyl acetate were used as standards to determine response factors, in order to enable the reaction mixtures to be analysed quantitatively. Since a known volume (and therefore mass) of acetic acid was used for each reaction, it is possible to calculate the amount of propanoic acid produced. The same approach was used to obtain yield data for other components. This method was also used to calculate propanoic acid production and selectivity data in previous work⁽¹⁾. Response factors were checked regularly by using the standard solutions. Taking into account errors due to syringe technique, and the changes in the response of the GC equipment to repeated injections of the same volume of either acetic and propanoic acid, maximum errors of approximately +/- (5-10)% are estimated. Values of peak area for propanoic and acetic acid for reaction solutions were obtained by GC analysis, and therefore the total amount of propanoic acid produced for a particular reaction was easily calculated using standard solutions of acetic and propanoic acid. Bearing in mind the observed changes in the response of the equipment to repeated injection of the same known volume of acids, the errors in the calculated values for % selectivity for propanoic acid, moles of propanoic acid produced, and rate of propanoic acid production, are estimated to be approximately +/- 5%, and certainly no greater than +/- 10%. Several reaction mixtures were repeatedly injected and the errors in response found to be within these values.

As with previous work⁽¹⁾ the percentage selectivity for propanoic acid is expressed as the percentage of propanoic acid produced in relation to all liquid organic products. Propanoic acid derivatives such as ethyl propanoate, which is formed in some reactions, were not classified as propanoic acid when calculating percentage selectivity.

4.2.3 Calculation of rates of reaction

Rate (A) / bar.hr⁻¹

The data summarised for all of the catalytic runs recorded in Table 4.2, show a value for rate expressed in bar.hr⁻¹. This rate was calculated directly by monitoring the amount of gas uptake for a reaction over a period of 1 hour after reaching a temperature of 180°C. The minimal errors involved in pressurisation with the required amount of reactant gases, and in taking readings from pressure gauges as reactions proceed is expected to cause very small random errors of approximately +/- 3 bar.hr⁻¹ in the quoted rates of reaction. Systematic errors may be greater because of the nature of the operation of the gauges, but are eliminated to some extent by calculating differences in pressure. It must be stressed that Rate (A) is a measure of the total gas uptake for each reaction not the rate of propanoic acid production. Thus, comparing rates of gas uptake for various reactions cannot be taken as a reliable criterion for comparing the activity of various systems towards the production of propanoic acid. Even though the stirring system was maintained at a preset speed, there will still be variations in the rate of mixing of the reactant gases with the solution when using a magnetic follower. This may also be partly responsible for variations in the rate of gas uptake and rate of propanoic acid production for reactions recorded in this chapter.

Rate (B) / Mol.Kg⁻¹.hr⁻¹

Rate (A) in bar.hr⁻¹ cannot be used as an expression for the rate of propanoic acid production since the reactant gases, CO and ethene, may be incorporated into other products formed during the catalytic reactions. Thus, Rate (A) would only be a reliable indicator for the rate of propanoic acid production if all of the reactions were 100% selective for propanoic acid. GC analysis reported in this chapter, and in previous studies⁽¹⁾ show that this is not the case. Consequently, it was necessary to formulate an expression for the rate of production of propanoic acid based on the total amount formed, which was calculated from GC analytical data, as explained in Section 4.2.2. Hence, Rate (B), in Mol.Kg⁻¹.hr⁻¹, gives the moles of propanoic acid produced per kilogramme of initial solution per hour of reaction. A value has been calculated for each of the reactions recorded in Table 4.2. This gives a more reliable measurement for the rate of propanoic acid production, and is thus a very useful criterion for comparing the activities of various catalytic systems towards the production of propanoic acid. In using the data, however, due regard must be given to the parameters used in their calculation. All reactions were monitored for a period of 1 hour upon reaching a temperature of 180°C and the rate of propanoic acid

production, Rate (B), is quoted over this one hour period before the heater is switched off. Production of propanoic acid may, however, occur before the reaction temperature is reached, and may continue for a short while when the heater is turned off, assuming that all of the gas has not been consumed during the reaction period. The calculation of Rate (B) does not taken these latter factors into account. The amount of propanoic acid produced outside of the period in which the reactions are monitored is difficult to assess, and will vary from system to system, i.e. some reactions are virtually complete after 1 hour, whereas some are still progressing at a significant rate according to gas uptake measurements. To an extent, the errors in the rate of propanoic acid production should be minimised, however, since studies outlined in Table 4.1, indicate that little production occurs below 180°C.

4.3 'Blank' Reactions

Reactions 4.1, 4.2, and 4.3 (see Table 4.2 for experimental details)

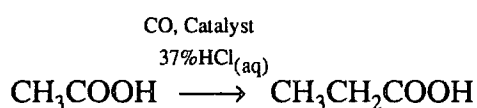
<i>Components:</i>	<i>4.1</i>	<i>SnCl₂, CH₃COOH, 37%<i>HCl</i>_(aq), CO, C₂H₄</i>
	<i>4.2</i>	<i>CH₃COOH, 37%<i>HCl</i>_(aq), CO, C₂H₄</i>
	<i>4.3</i>	<i>RhCl₃·3H₂O, SnCl₂, Bz(<i>Et</i>)₃NCl, 37%<i>HCl</i>_(aq) CH₃COOH, CO</i>

Batch reactions were carried out firstly in the absence of rhodium(III) chloride trihydrate (Reaction 4.1), and then in the absence of both rhodium(III) chloride trihydrate and tin(II) chloride (Reaction 4.2). The aim was to investigate whether in Reaction 4.1 any catalytic activity would occur in the presence of only tin(II) chloride as a metal precursor and in Reaction 4.2 whether any catalytic activity would occur in the absence of any metal precursors. These reactions are also a test for 'carry-over', the transfer of residues from a previous reaction, such as rhodium and tin containing solids, to the components of subsequent reactions.

The data obtained for these 'blank' reactions show that no catalytic hydrocarbonylation occurs when rhodium(III) chloride trihydrate is not added to the reaction mixture. Total gas pressure is essentially maintained over 1 hour at 180°C. GC data confirmed that no propanoic acid or any other organic products were formed in either of Reactions 4.1 or 4.2. Further analysis by GCMS did, however, indicate an extremely small quantity of chloroethane for Reaction 4.2, not significant enough to be detected by the standard equipment normally used for analysis. This suggests that tin(II) chloride does have the capability to promote formation of chloroethane possibly via initial formation of C₂H₅SnCl₃ in solution.

The lack of propanoic acid formation for Reactions 4.1 and 4.2 demonstrates that acid production requires a rhodium precursor. Interestingly, the general absence of by-products in these reactions, suggests that they generally form at the catalytically active rhodium centre. The data obtained for Reactions 4.1 and 4.2 also supports the method employed to clean the autoclave described in Section 4.2.1, as catalytic material from extraneous sources, i.e. previous reactions, appears to be absent.

A further reaction (Reaction 4.3), was carried out in the absence of ethene to test whether any catalytic reaction to form propanoic acid would still occur, chiefly by the following homologation reaction:



and also to explore the possibility of the formation of products in the absence of ethene. The data in Table 4.2 indicated a complete lack of activity and suggests that ethene is necessary for any organic product-forming reaction to occur, since there was no formation of propanoic acid or other organic products.

4.4 Rhodium(III) chloride trihydrate as a catalytic precursor in the absence of tin

Previous work⁽¹⁾ has shown that in the absence of tin(II) chloride, rhodium(III) chloride trihydrate is a completely ineffective catalytic precursor for the hydrocarbonylation of ethene. This observation is somewhat surprising considering the fact that rhodium(III) chloride trihydrate is a highly effective catalytic precursor for the iodide promoted hydrocarbonylation of ethene⁽¹⁾, forming $[\text{Rh}(\text{CO})_2\text{I}_2]^-$ as the active catalyst. $[\text{Rh}(\text{CO})_2\text{Cl}_2]^-$ readily forms from rhodium(III) chloride, and although some decrease in rate would be expected, since Rh-Cl bonds are stronger than Rh-I bonds, making the chloride ligand less labile than an iodide ligand, some catalysis by $[\text{Rh}(\text{CO})_2\text{Cl}_2]^-$ may still be expected. Therefore, the reaction in the absence of tin(II) chloride was repeated, using similar quantities of reagents and the same autoclave as used in previous work, in order to check the validity of previous results.

Reactions 4.4 and 4.5 (see Table 4.2 for experimental details)

Components: 4.4 $RhCl_3 \cdot 3H_2O$, 37% $HCl_{(aq)}$, CH_3COOH , CO , C_2H_4
4.5☆ Same as Reaction 4.4

☆ A cleaning run with CH_3COOH and 37% $HCl_{(aq)}$ was carried out prior to this reaction.

An assessment of the data in Table 4.2 for the identical reactions 4.4 and 4.5 shows little variation between the two reactions in the amount and rate of propanoic acid production, or in the percentage selectivity for propanoic acid. These data confirm the reproducibility of this particular experiment. The similar data obtained for Reactions 4.4 and 4.5 also justifies the method used to clean the autoclave after catalytic runs.

Reaction Code	Moles of propanoic acid produced	Rate of propanoic acid production $Mol.Kg^{-1}.hr^{-1}$	% Selectivity
4.4	0.072	1.88	95.0
4.5	0.073	1.89	91.0

Thus, rhodium(III) chloride trihydrate is itself a catalytic precursor for the production of propanoic acid in the absence of tin(II) chloride. The results are in disagreement with those obtained in previous studies⁽¹⁾ when no reaction was found to occur in the absence of tin(II) chloride. There is, however, no doubt about the validity of the results obtained for Reactions 4.4 and 4.5. The rate of production of propanoic acid for Reactions 4.4 and 4.5 is, in fact, double that observed for the rhodium-tin-chloride promoted system studied previously⁽¹⁾, using the same autoclave though not necessarily the same stirring speed, where the rate was calculated as $0.89 \text{ Mol.Kg}^{-1}.hr^{-1}$ (see Reaction 1, Table 4.1). Consequently, there must be some doubt over results obtained from previous studies of these systems, and the promotional ability of tin(II) chloride is brought into question.

Gas Chromatograph Mass Spectroscopic analysis of the solutions from Reactions 4.4 and 4.5 showed the major by-product to be ethyl propanoate in both cases, along with very small quantities (< 1%) of ethyl acetate and chloroethane.

4.5 Addition of Tin(II) chloride to the rhodium-chloride catalytic system

The reactions described in Section 4.4 showed that a rhodium-chloride system is catalytically active for the hydrocarbonylation of ethene in the absence of tin(II) chloride, and gives a higher rate of propanoic acid production than the optimum rhodium-tin-chloride system in previous studies⁽¹⁾. In the light of these differing results a further series of reactions was carried out with the addition of anhydrous tin(II) chloride to the catalytic system, to investigate whether it actually is a promoter for the rhodium-chloride catalysed hydrocarbonylation of ethene, or whether previous results⁽¹⁾ merely reflected the activity of a rhodium-chloride system alone. As with previous studies⁽¹⁾, the reactions employed various rhodium to tin molar ratios in an attempt to discover the optimum catalytic conditions.

Reactions 4.6, 4.7 and 4.8 (see Table 4.2 for experimental details)

Components:	4.6	<i>RhCl₃·3H₂O, SnCl₂, 37% HCl_(aq), CH₃COOH, CO, C₂H₄</i>		
	4.7	<i>Same as Reaction 4.6</i>		
	4.8	<i>Same as Reaction 4.6</i>		

Reaction Code	4.6	4.7	4.8
Rh:Sn Molar Ratio	1:1	1:2	1:3
Rate of propanoic acid production/mol.Kg⁻¹.hr⁻¹	1.45	2.71	2.06
% Selectivity	85.6	85.1	77.5

Reaction 4.6 employing a tin:rhodium molar ratio of 1:1 gave a rate of propanoic acid production of 1.45 Mol.Kg⁻¹.hr⁻¹ which was lower than those obtained for the rhodium-chloride catalytic systems in the absence of tin(II) chloride, [Reactions 4.4 and 4.5 (1.88 and 1.89 Mol.Kg⁻¹.hr⁻¹ respectively)]. Reaction 4.7 employing a tin:rhodium molar ratio of 2:1 gave a rate of propanoic acid production of 2.71 Mol.Kg⁻¹.hr⁻¹, which was an approximate 50% improvement on the non-tin containing systems (Reactions 4.4 and 4.5). A reaction employing a 3:1 tin:rhodium molar ratio, (Reaction 4.8), had a similar rate of gas uptake to Reaction 4.7, but a lower rate of propanoic acid production (2.06 Mol.Kg⁻¹.hr⁻¹), which was only a marginal improvement on the non-tin systems. Selectivity was also reduced. Also, tin(II) chloride appears to lower the selectivity compared with non-tin systems and increasing amounts of it are accompanied by a decrease in the selectivity for propanoic acid, in agreement with previous work in this area⁽¹⁾. GCMS analysis showed that the by-products for Reactions 4.6, 4.7 and 4.8 were chloroethane, ethyl

acetate and ethyl propanoate. In Reaction 4.7 there was also a small amount of diethyl ether produced.

From the data obtained, that tin(II) chloride appears to have a promotional effect on the rhodium-chloride catalysed hydrocarbonylation of ethene to form propanoic acid, but only when used in a Sn:Rh molar ratio of 2:1. Two of the rhodium-tin-chloride systems studied (Reactions 4.6 and 4.8) showed no improvement in the catalytic activity towards production of propanoic acid, and one of them (Reaction 4.6), showed that a small amount of tin(II) chloride actually appears to inhibit the production of propanoic acid, the activity being less than that observed for a $\text{RhCl}_3 \cdot 3\text{H}_2\text{O}$ system alone.

4.6 Addition of benzyltriethylammonium chloride to rhodium-chloride and rhodium-tin-chloride catalytic systems

Previous work⁽¹⁾ highlighted the effects of adding quaternary ammonium salts and alkali metal salts to the rhodium-tin-chloride catalytic system. Particular attention focused on the addition of benzyltriethylammonium chloride (see Table 4.1, Reaction 2) which led to a six-fold increase in the rate of propanoic acid production when added to a rhodium-tin-chloride catalytic system. In view of the various differences observed so far in catalytic activity between present and previous work, it was also necessary to study the effect of adding benzyltriethylammonium chloride to rhodium-chloride and rhodium-tin-chloride systems to test the validity of past results.

Reactions 4.9 and 4.10 (see Table 4.2 for experimental details)

Components: 4.9[☆] $\text{RhCl}_3 \cdot 3\text{H}_2\text{O}$, SnCl_2 , $\text{Bz}(\text{Et})_3\text{NCl}$, 37% $\text{HCl}_{(\text{aq})}$, CH_3COOH , CO , C_2H_4

4.10 $\text{RhCl}_3 \cdot 3\text{H}_2\text{O}$, $\text{Bz}(\text{Et})_3\text{NCl}$, 37% $\text{HCl}_{(\text{aq})}$, CH_3COOH , CO , C_2H_4

☆ A cleaning run with CH_3COOH and 37% $\text{HCl}_{(\text{aq})}$ was carried out prior to this reaction

Reaction Code	4.9	4.10
Rh:Sn:Bz(Et)₃NCl Molar Ratio	1:2:3	1:0:3
Rate of propanoic acid production/Mol.Kg⁻¹.hr⁻¹	2.73	1.58
% Selectivity	73.0	88.8

The data in Table 4.2 showed that benzyltriethylammonium chloride had neither a significant beneficial or detrimental effect on the rate of propanoic acid production [c.f. Reaction 4.7 (Rate = 2.71 Mol.Kg⁻¹.hr⁻¹, % Selectivity = 85.1)]. As the data indicates, however, addition of benzyltriethylammonium chloride caused a marked decrease in selectivity. The results are in contrast to previous work⁽¹⁾ (see Table 4.1), which reported a large increase in the rate of propanoic acid production and an increase in the percentage selectivity, upon addition of benzyltriethylammonium chloride to a rhodium-tin-chloride catalytic system.

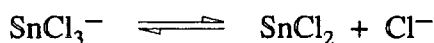
Using benzyltriethylammonium chloride in the absence of tin(II) chloride (reaction 4.10), comparison of the data obtained shows that benzyltriethylammonium chloride has no promotional effect on the rate of propanoic acid production in the absence of tin(II) chloride. In fact, the rate of propanoic acid production and selectivity are slightly less than those obtained using rhodium chloride alone. Clearly, the ability of the benzyltriethylammonium cation to form ion-pairs with rhodium containing species has little effect on the catalytic hydrocarbonylation reaction.

From the data obtained it is impossible to reach any conclusion about the possible role, if any, of the benzyltriethylammonium cation in the catalytic process. Clearly, there must be some doubt over the validity of previous work, as no evidence was found in the present work for an enhancement in the reactivity of catalytic species in the mixture upon the introduction of the benzyltriethylammonium cation. Indeed, the addition of benzyltriethylammonium chloride, far from being beneficial, actually seems to reduce the efficiency of the reaction by lowering the selectivity for propanoic acid.

4.7 Catalytic activity of model rhodium(I) carbonyl chloride complexes

During the heating process, such as for Reactions 4.4, 4.5 and 4.10, rhodium(III) chloride trihydrate reacts with carbon monoxide at approximately 90°C to form dichlorotetracarbonyldirrhodium(I), Rh₂(CO)₄Cl₂⁽²⁾. Under the reaction conditions employed, however, this will quickly react with chloride ions, present in a large molar excess from the hydrochloric acid used, to form the dichlorodicarbonylrhodium(I) anionic species, [Rh(CO)₂Cl₂]⁻, via cleavage of the Rh-Cl-Rh bridges of Rh₂(CO)₄Cl₂. This has been confirmed by high pressure infra-red studies of the same systems as used for Reactions 4.4 and 4.5, ν(CO) bands being observed at 2004 and 2079cm⁻¹ {ν(CO) of [Bz(Et)₃N][Rh(CO)₂Cl₂] in acetic

acid are at 2001 and 2076cm⁻¹). In the presence of a large alkylammonium cation such as benzyltriethylammonium chloride, e.g. Reaction 4.10, some formation of [Bz(Et)₃N⁺][Rh(CO)₂Cl₂⁻] ion-pairs will probably occur in solution. Tin(II) chloride present in solution with a large molar excess of chloride ions will react to form the trichlorostannate anionic species SnCl₃⁻ as follows:



but the equilibrium nature of this reaction should not be overlooked. ¹¹⁹Sn NMR studies (see Chapter 2), have shown that the equilibrium favours the trichlorostannate species when the chloride ion to tin ratio is 1:1 or greater. Studies reported also in Chapter 2 indicate that changes in the equilibrium position are effected during reaction with [Rh(CO)₂Cl₂]⁻ or Rh₂(CO)₄Cl₂. In the presence of a large amount of chloride ions however, as is the case in the catalytic process, the SnCl₃⁻ ion is expected to dominate.

Taking into account the ready formation of [Rh(CO)₂Cl₂]⁻ and Rh₂(CO)₄Cl₂ under conditions similar to those used for catalysis, any active rhodium-tin catalyst will probably be formed via reaction of [Rh(CO)₂Cl₂]⁻ with SnCl₃⁻ or SnCl₂ (see Chapter 2 for a detailed study of this reaction chemistry). To investigate this aspect [Bz(Et)₃N][Rh(CO)₂Cl₂] was prepared by the method of Cleare et al⁽³⁾, and used in place of rhodium(III) chloride trihydrate as the catalytic precursor for the hydrocarbonylation of ethene.

Reactions 4.11 and 4.12 (see Table 4.2 for experimental details)

Components: 4.11 [Bz(Et)₃N][Rh(CO)₂Cl₂], 37% HCl_(aq), CH₃COOH, CO, C₂H₄
 4.12 [Bz(Et)₃N][RhCO)₂Cl₂], SnCl₂, 37% HCl_(aq), CH₃COOH, CO, C₂H₄
Rh:Sn Molar Ratio = 1:2

<i>Reaction Code</i>	<i>4.4</i>	<i>4.5</i>	<i>4.10</i>	<i>4.11</i>
<i>Rate of propanoic acid prodⁿ/Mol.Kg⁻¹.hr⁻¹</i>	<i>1.88</i>	<i>1.89</i>	<i>1.58</i>	<i>1.48</i>
<i>% Selectivity</i>	<i>95.0</i>	<i>95.1</i>	<i>88.8</i>	<i>95.1</i>

The data in Table 4.2 shows that for Reaction 4.11 carried out in the absence of tin(II) chloride, the rate of propanoic acid production (1.48 Mol.Kg⁻¹.hr⁻¹), was lower than when the rhodium(III) chloride precursor was used [Reactions 4.4 and 4.5 (1.88

and 1.89 Mol.Kg⁻¹.hr⁻¹ respectively)]. Taking into account experimental errors, there was however no significant difference in the percentage selectivity for Reaction 4.11 compared with Reactions 4.4 and 4.5. The approximate 20% decrease in the rate of propanoic acid production suggests that, although [Rh(CO)₂Cl₂]⁻ may be the active catalytic species for the rhodium-chloride systems (Reactions 4.4, 4.5 and 4.10), direct addition of it to a high pressure system may lead to some loss, possibly through decomposition during the heating process, by reaction with chloride ions, or reaction with CO to form Rh(CO)₃Cl, identified previously by high pressure infra-red spectroscopic studies⁽¹⁾. Indeed, HPIR studies have shown that the concentration of [Rh(CO)₂Cl₂]⁻ decreases as the reaction temperature is maintained at 180°C. Conversely, however, the presence of CO should help to stabilise [Rh(CO)₂Cl₂]⁻ as the active catalyst at high temperatures. GCMS analysis of the final solution indicated that chloroethane which was the main by-product for Reaction 4.11. Interestingly, GCMS data was also consistent with the formation of a very small amount of CH₃COCH=C(CH₃)₂, although the route by which this species is formed is unclear.

<i>Reaction Code</i>	<i>4.7</i>	<i>4.9</i>	<i>4.12*</i>
<i>Rate of propanoic acid prodⁿ/Mol.Kg⁻¹.hr⁻¹</i>	<i>2.71</i>	<i>2.73</i>	<i>3.33</i>
<i>% Selectivity</i>	<i>85.1</i>	<i>73.0</i>	<i>72.0</i>

* Reaction 4.12 was repeated (see later Section 4.9). Rate of propanoic acid production = 2.83 Mol.Kg⁻¹.hr⁻¹.

Addition of tin(II) chloride to the same system (Reaction 4.12), in a Sn:Rh molar ratio of 2:1, gave a rate of propanoic acid production of 3.33 Mol.Kg⁻¹.hr⁻¹ which was more than two-fold higher than that for the system in the absence of tin(II) chloride [Reaction 4.11, (1.48 Mol.Kg⁻¹.hr⁻¹)]. However, unlike the differences in rates between Reactions 4.4 and 4.7, and Reactions 4.9 and 4.10, the observed difference in rates here on adding SnCl₂ (Reactions 4.11 and 4.12), is much more pronounced, clearly showing that tin(II) chloride does, in the present circumstances, have a clear promotional effect on the catalytic process. The exceptionally high rate of propanoic acid production for Reaction 4.12, may in some part be due to production of propanoic acid outside the monitored reaction period, since assessment of data in Table 4.2 showed that the rate of gas uptake for this reaction over 1 hour was not dissimilar to those for other systems (Reactions 4.7 and 4.9) containing a Sn:Rh molar ratio of 2:1. The errors due to GC analysis are not significant enough to explain such a large difference in propanoic acid production, but the effect of a change in the stirring rate is a possible but unlikely explanation.

In common with other rhodium-tin-chloride systems discussed previously, Reaction 4.12 has its limitations, being much less selective towards propanoic acid (72.0%) than the reaction containing no tin [Reaction 4.11 (95.1%)]. GCMS analysis of the final solution showed that the main by-product was chloroethane along with a very small amount of $\text{CH}_3\text{COCH}=\text{C}(\text{CH}_3)_2$. There was no apparent formation of ethyl acetate or ethyl propanoate in either of Reactions 4.11 or 4.12.

4.8 Addition of benzyltriethylammonium trichlorostannate to a rhodium-chloride catalytic system

During the heating process of a catalytic reaction in which tin(II) chloride is present, reaction occurs with chloride ions to form the trichlorostannate species, SnCl_3^- , and in the presence of the benzyltriethylammonium cation the ion-pair $[\text{Bz}(\text{Et})_3\text{N}][\text{SnCl}_3]$ may form. Hence, the preformed benzyltriethylammonium trichlorostannate species $[\text{Bz}(\text{Et})_3\text{N}][\text{SnCl}_3]$ (see Appendix 1 for experimental details), was used in the catalytic system, and the effect of various rhodium to tin molar ratios on the hydrocarbonylation process investigated.

Reactions 4.13, 4.14 and 4.15 (see Table 4.2 for experimental details)

Components: 4.13 $[\text{Bz}(\text{Et})_3\text{N}][\text{Rh}(\text{CO})_2\text{Cl}_2]$, $\text{Bz}(\text{Et})_3\text{NSnCl}_3$, 37% $\text{HCl}_{(\text{aq})}$,
 CH_3COOH , CO , C_2H_4
 4.14 Same as Reaction 4.13
 4.15 Same as Reaction 4.13

<i>Reaction Code</i>	<i>4.13</i>	<i>4.14</i>	<i>4.15</i>
<i>Rh:Sn Molar Ratio</i>	<i>1:1</i>	<i>1:2</i>	<i>1:5</i>
<i>Rate of propanoic acid prodⁿ/Mol.Kg⁻¹.hr⁻¹</i>	<i>1.5</i>	<i>1.66</i>	<i>0.16</i>
<i>% Selectivity</i>	<i>97.6</i>	<i>65.8</i>	<i>10.2</i>

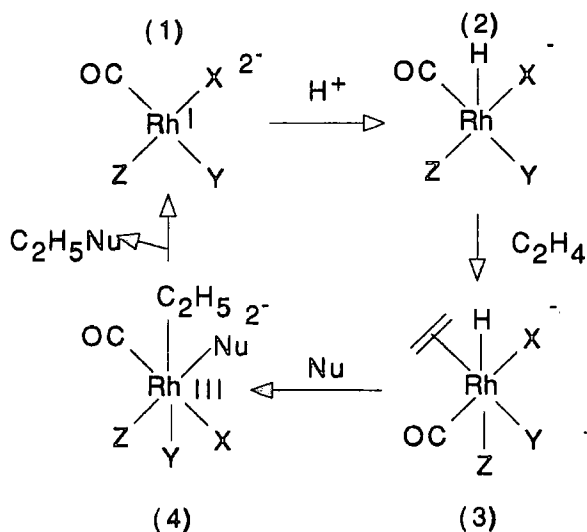
The data in Table 4.2 shows that the highest rate of propanoic acid production was achieved for Reaction 4.14 (1.66 Mol.Kg⁻¹.hr⁻¹), where a Sn:Rh molar ratio of 2:1 was employed. Reaction 4.13 employing a Sn:Rh molar ratio of 1:1, gave no improvement in the rate of propanoic acid production (1.50 Mol.Kg⁻¹.hr⁻¹) compared with Reaction 4.11 (1.48 Mol.Kg⁻¹.hr⁻¹) which employed no tin but only the rhodium complex $[\text{Bz}(\text{Et})_3\text{N}][\text{Rh}(\text{CO})_2\text{Cl}_2]$. In the case of Reaction 4.15 which employed a Sn:Rh molar ratio of 5:1 the rate of propanoic acid production was extremely low (0.16 Mol.Kg⁻¹.hr⁻¹).

In agreement with earlier studies⁽¹⁾ (see Reactions 3, 4 and 5 in Table 4.1), the calculated data again show that tin(II) chloride contents corresponding to Sn:Rh molar ratios higher than 1:1 lead to a decrease in the percentage selectivity for propanoic acid. Reaction 4.14 shows only a small increase in rate compared with the use of $[\text{Bz}(\text{Et})_3\text{N}][\text{Rh}(\text{CO})_2\text{Cl}_2]$ alone (Reactions 4.11). The reason for this is not totally clear but possibly relates to the poor selectivity for propanoic acid. Other Sn:Rh 2:1 systems (Reactions 4.7, 4.9, 4.12 and 4.18) had significantly higher rates of reaction than rhodium-chloride systems. The rate of gas uptake for Reaction 4.14 was high compared with rhodium-chloride systems (e.g. Reaction 4.4: $33\text{bar}\cdot\text{hr}^{-1}$ and Reaction 4.11: $26\text{bar}\cdot\text{hr}^{-1}$), clearly showing that tin has a promotional effect on the reaction. However, the selectivity for propanoic acid was unusually low for some reason, and possibly explains the observed rate. Reaction 4.15 which had a selectivity of only 10.2% gave reaction at temperatures much lower than 180°C , as indicated by a steady decrease in pressure from a temperature of 130°C upwards. Reaction stopped soon after the temperature reached 180°C indicating decomposition of catalytic species. GCMS analysis of the reaction solution confirmed the formation of substantial amounts of ethyl acetate and ethyl propanoate. This suggests that the formation of products other than propanoic acid may primarily occur at temperatures lower than 180°C , before the optimum reaction temperature for hydrocarbonylation is reached. The formation of butyl moieties such as butyl acetate, butyl propanoate and 2-chlorobutane, which had been detected in very small amounts in previous studies⁽¹⁾, was not apparent for any of the reactions discussed in this chapter, suggesting that the ethyl group was removed from the metal centre before oligomerisation reactions occurred.

From the data available, there appears to be a link between the formation of ethyl derivatives and the amount of tin(II) chloride present in the catalytic system, with large amounts of tin(II) chloride giving an increase in the amounts of these species produced.

A tentative explanation for the formation of by-products such as ethyl acetate and ethyl propanoate is based on a consideration of the proposed oxidative addition process shown in Figure 4.1, which leads to initial production of chloroethane, via chemistry occurring at the catalytically active rhodium centre. Here it is assumed that the catalytically active complex is based on $[\text{Rh}(\text{CO})\text{XYZ}]^{2-}$, where X, Y and Z may be Cl^- or SnCl_3^- .

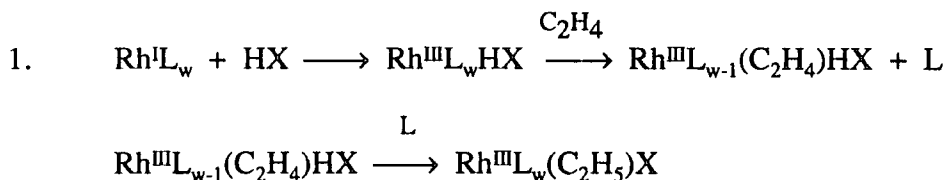
The initial step of any oxidative addition process in this highly acidic system is likely to be the addition of a proton to the catalytically active rhodium(I) species (1) to form complex (2). This could then be followed by addition of ethene leading to cis hydride and ethene ligands as in complex (3). The process is then completed by proton migration on to ethene accompanied by addition of a further ligand such as CH_3COOH , SnCl_3^- or Cl^- to occupy the vacant site, giving the rhodium(III) complex (4). Chloroethane may then be formed as a by-product via reductive elimination, prior to carbonylation at the rhodium centre.



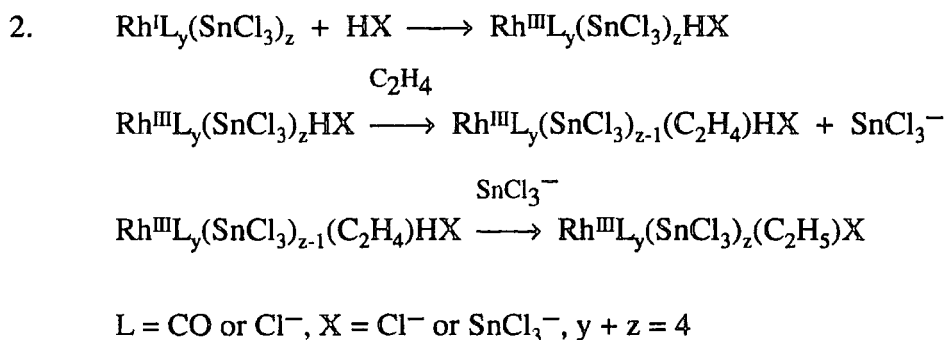
X, Y, Z = Cl^- or SnCl_3^- , Nu = Cl^- , SnCl_3^- , CH_3COOH etc.

Figure 4.1 Proposed oxidative addition step for a rhodium monocarbonyl complex containing chloride and/or trichlorostannate ligands

Slight variations in the reaction scheme shown in Figure 4.1 may occur as follows:



L = CO or Cl^- , w = 4, X = Cl^- or SnCl_3^-



Reaction 1 differs from Figure 4.1 in that it involves oxidative addition of HCl or HSnCl₃ to a rhodium(I) carbonyl chloride complex as the initial step. Reaction 2 involves a similar process but this time with oxidative addition of HCl or HSnCl₃ to a trichlorostannate complex as the initial step. It is also possible that either C₂H₅Cl or C₂H₅SnCl₃ could add directly to a 16e⁻ rhodium(I) catalytic complex, but it is not clear whether they will be formed from the initial reagents under the reaction conditions employed.

Ethyl acetate may be formed from chloroethane by known organic chemistry, via an S_N2 esterification reaction involving nucleophilic attack of acetic acid on the alkyl halide. The formation of ethyl propanoate can also be explained in this way following completion of the catalytic hydrocarbonylation process to produce propanoic acid. Figure 4.2 shows a proposed hydrocarbonylation process to produce propanoic acid based on the results presented in this chapter, and based on dichlorodicarbonylrhodium(I) as the active catalyst in the absence of tin(II) chloride.

Initial cis oxidative addition, Steps A, B, and C is then followed by cis migratory insertion of a carbonyl group in Step D, along with addition of free CO to occupy the vacant site generated. Finally, Step E involves cis reductive elimination of C₂H₅COCl to regenerate the active catalyst [Rh(CO)₂Cl₂]⁻. The acid chloride C₂H₅COCl will be quickly hydrolysed by the large amount of water present in the system to give the main product, propanoic acid.

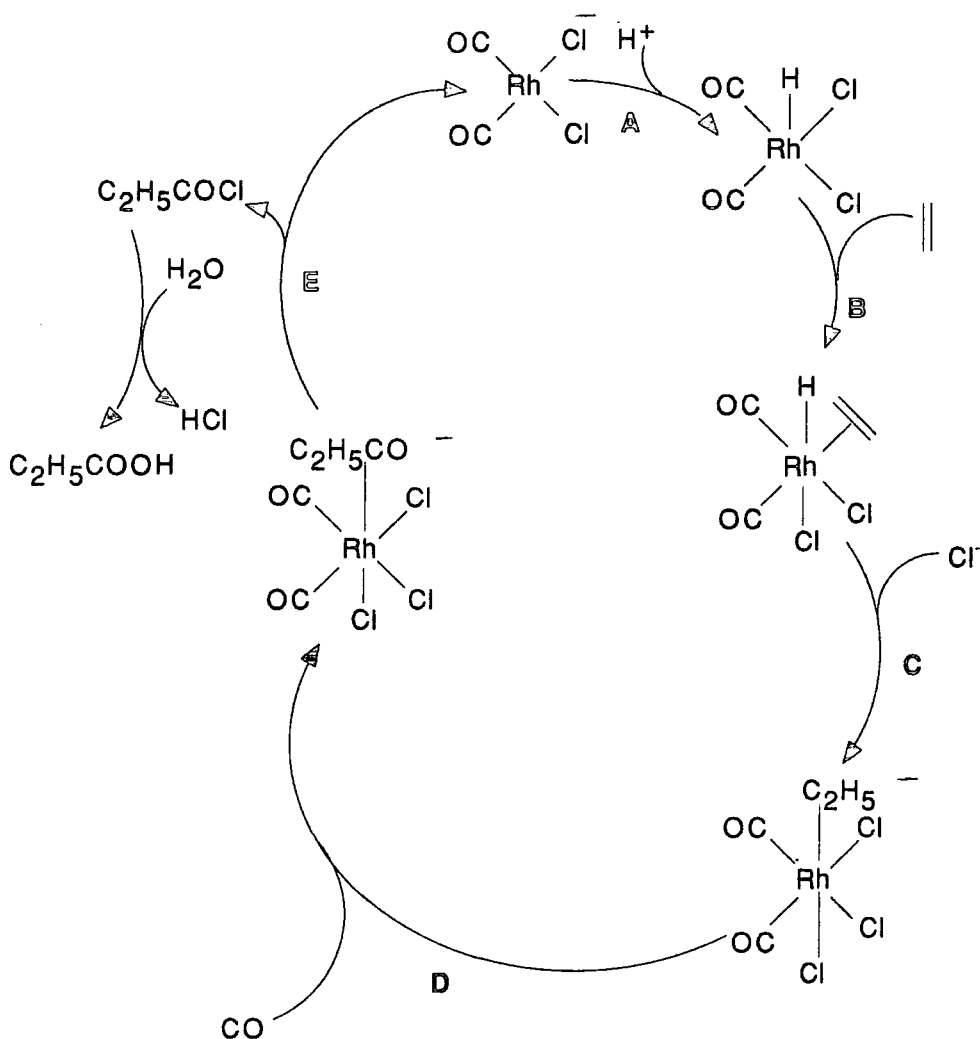


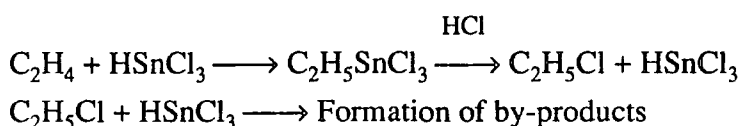
Figure 4.2 Proposed catalytic scheme for the rhodium-chloride catalyzed hydrocarbonylation of ethene

The reaction between benzyltriethylammonium dichlorodicarbonylrhodium(I) and benzyltriethylammonium trichlorostannate, used as catalytic precursors (Reactions 4.13-15), has also been studied under milder conditions in acetic acid in the presence of concentrated aqueous hydrochloric acid (see Chapter 3 for experimental details), in an attempt to determine the chemistry which may be occurring between these species under non-catalytic conditions. Infra-red and ^{119}Sn NMR data indicated that $[\text{Bz}(\text{Et})_3\text{N}]_2[\text{Rh}(\text{CO})_2(\text{SnCl}_3)_3]$ was formed as the major component, with the possibility that $[\text{Bz}(\text{Et})_3\text{N}]_3[\text{Rh}(\text{CO})(\text{SnCl}_3)_4]$ and/or $[\text{Bz}(\text{Et})_3\text{N}]_2[\text{Rh}(\text{CO})(\text{SnCl}_3)_2\text{Cl}]$ were also present in much smaller quantities. Very small quantities of other, as yet assigned, rhodium carbonyl containing complexes were also present. In the case of the first two complexes, which are 18-electron systems, there is a possibility that they may be formed in the hydrocarbonylation reaction and

may be important catalytic precursors (see HPIR studies in Chapter 5 for further details). The ability of 18-electron systems to generate 16-electron complexes, normally required for catalytic activity, is well documented e.g. the catalytic precursors $\text{RhH}(\text{CO})(\text{PPh}_3)_3$, $\text{RuHCl}(\text{PPh}_3)_3$ and $\text{IrH}(\text{CO})(\text{PPh}_3)_3$ each lose a PPh_3 group to generate catalytically active 16-electron complexes, as the first step of the catalytic cycle for the hydrogenation and isomerisation of alk-1-enes⁽⁴⁾. Dissociation of SnCl_3^- and CO from $[\text{Rh}(\text{CO})_2(\text{SnCl}_3)_3]^{2-}$ is known to occur under room temperature conditions, with several 18-electron 5-coordinate and 16-electron 4-coordinate Rh(I)-CO-SnCl₃ complexes apparently related by a sequence of facile reactions (see Chapters 2 and 3), and therefore dissociation of ligands most surely occurs under catalytic conditions. Since $[\text{Rh}(\text{CO})_2(\text{SnCl}_3)_3]^{2-}$ initially forms on mixing the reagents for the Reactions 4.13-15, it is reasonable to consider that the active catalytic species may be either $[\text{Rh}(\text{CO})_2(\text{SnCl}_3)_2]^-$, $[\text{Rh}(\text{CO})_2(\text{SnCl}_3)\text{Cl}]^-$ or $[\text{Rh}(\text{CO})(\text{SnCl}_3)_2\text{Cl}]^{2-}$. Infra-red data at room temperature for the reaction of rhodium(I) carbonyl chlorides and tin(II) chlorides relevant to catalysis were consistent with the formation of either of the first two complexes by dissociation/decomposition of $[\text{Rh}(\text{CO})_2(\text{SnCl}_3)_3]^{2-}$ (see Chapter 2), and $[\text{Rh}(\text{CO})(\text{SnCl}_3)_2\text{Cl}]^{2-}$ has been isolated from a reaction of rhodium(I) carbonyl chlorides and tin(II) chlorides relevant to catalysis (see Section 3.2.2, Chapter 3).

The increase in the amount of ethyl by-products formed as the amount of tin(II) chloride present is increased (as in Reaction 4.15), may be due to the formation of rhodium(I) complexes containing several SnCl_3^- ligands. Trichlorostannate ligands favour the formation of 5-coordinate 18-electron rhodium(I) complexes containing several SnCl_3^- ligands⁽⁵⁻⁹⁾, e.g. $[\text{Rh}(\text{CO})_2(\text{SnCl}_3)_3]^{2-}$ and $[\text{Rh}(\text{CO})(\text{SnCl}_3)_4]^{3-}$ (see Chapters 2 and 3). Under catalytic conditions, large amounts of tin(II) chlorides may favour the formation of 18-electron rhodium(I) trichlorostannate complexes, or 16-electron complexes containing several SnCl_3^- ligands, and as a consequence may enhance the amount of cis reductive elimination of chloroethane from a species such as complex (4), Figure 4.1, prior to the start of hydrocarbonylation. This can be attributed to the strong π -acceptor and trans effect properties of the SnCl_3^- ligand⁽¹⁰⁻¹⁴⁾. Large amounts of tin(II) chlorides may even lead to catalyst inactivity towards hydrocarbonylation via displacement of carbonyl groups and the formation of species such as $[\text{Rh}(\text{SnCl}_3)_5]^{4-}$. The ability of trichlorostannate ligands to form 18-electron 5-coordinate rhodium(I) systems, will make oxidative addition reactions, as shown in Figure 4.1, more unfavourable as the tin(II) chloride content in the system is increased above an optimum level.

An alternative mechanism operating for the formation of by-products may involve the direct generation of chloroethane or ethyltin moieties in solution, with no participation of the rhodium complex. The 'blank' reaction, 4.2, indicated that this does not occur to any significant extent, but Reaction 4.1, where trace amounts of chloroethane were detected, suggests that formation of an ethyltin intermediate in solution may occur. It is possible that, under the catalytic conditions, ethene will react with HSnCl_3 formed in solution to generate $\text{C}_2\text{H}_5\text{SnCl}_3$. This could then react with chloride ions present in a large molar excess to form chloroethane, and hence other organic by-products. Ethene does not normally react with HSnCl_3 generated in solution, at either room temperature or with gentle heating, with olefins usually requiring a carbonyl group adjacent to the double bond for such a reaction to occur⁽¹⁵⁾. However, Reaction 4.1 demonstrates that under pressure at high temperatures, reaction does occur, albeit to an extremely small extent.

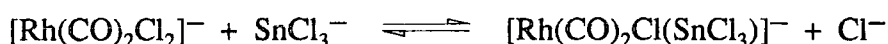


Higher tin content is expected to promote such a process, and will contribute in part towards the decrease in selectivity for propanoic acid when the Sn:Rh molar ratio is higher than 2:1. However, the possible contribution of this route to by-product formation is considered to be small, with the majority of evidence indicating that by-product formation occurs at a rhodium centre, which is probably not the active hydrocarbonylation catalyst. The abrupt change in rate which occurs at $\geq 180^\circ\text{C}$ suggests a change in the nature of the rhodium complex at and above this temperature.

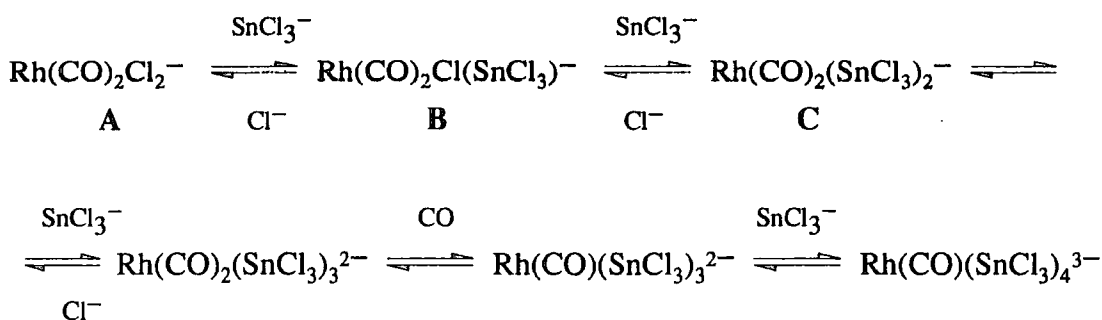
From the data obtained it is possible to provide some rationalisation as to the role of $\text{SnCl}_2/\text{SnCl}_3^-$ in the rhodium-chloride catalysed hydrocarbonylation of ethene to form propanoic acid. After due consideration of the experimental errors already discussed in detail in this chapter, it is clear that SnCl_2 has an effect on the catalytic process, and when systems having a Sn:Rh molar ratio of 2:1 are employed it has a significant promotional effect on the rate of propanoic acid production [e.g. Reactions 4.7, 4.9, 4.12 and 4.18 (Section 4.9)]. There is a strong possibility that more than one active catalytic species is present in the rhodium-tin-chloride catalytic systems discussed so far, with both $[\text{Rh}(\text{CO})_2\text{Cl}_2]^-$ and Rh-Sn species being present. Evidence to support this is provided by high pressure infra-red studies of a 2:1 Sn:Rh catalytic system discussed in Chapter 5, for which carbonyl stretches, assigned to a $\text{Rh}(\text{I})\text{-CO-SnCl}_3$ complex, are observed, along with equally strong

absorbance bands assigned to $[\text{Rh}(\text{CO})_2\text{Cl}_2]^-$, a proven catalyst in its own right. The occurrence of a mixture of rhodium species is not unexpected considering the large amount of chloride ions present in the systems. Infra-red studies reported in Chapter 7 have shown that addition of chloride ions to solutions of rhodium-tin complexes leads to displacement of the trichlorostannate ligands to form $[\text{Rh}(\text{CO})_2\text{Cl}_2]^-$.

No enhancement of catalytic activity occurs for 1:1 Sn:Rh systems probably because an equilibrium between $[\text{Rh}(\text{CO})_2\text{Cl}_2]^-$ and an active 16-electron Rh(I)-CO-SnCl₃ complex, for example,



will be highly in favour of $[\text{Rh}(\text{CO})_2\text{Cl}_2]^-$ in the presence of a high Cl⁻ concentration. This effectively leads to activity similar to that of a rhodium-chloride complex alone. For 2:1 Sn:Rh systems the increase in the rate of propanoic acid production is probably a consequence of the movement of the equilibrium to the right, towards the formation of a rhodium-tin complex. However, the promotional effect of SnCl₂ would probably be much more pronounced were it not for the presence of large amounts of $[\text{Rh}(\text{CO})_2\text{Cl}_2]^-$. For Sn:Rh molar ratios greater than 2:1 the propanoic acid production is inhibited by the higher amounts of tin, probably due to a lowering of the concentration of the active species by the processes discussed earlier. A 3:1 Sn:Rh reaction (Reaction 4.8) had a rate of gas-uptake similar to that of a 2:1 Sn:Rh system (Reaction 4.7), showing that the rate enhancement caused by tin(II) chloride was maintained, but selectivity towards propanoic acid production decreased. Thus, selectivity is highest when tin is absent, yet rate is highest for reactions having a Sn:Rh ratio of 2:1. The catalysis appears to be dependant on the nature of the rhodium species present and their relative proportions, several of the complexes themselves being catalytically active. Thus, a possible explanation for the results may be the occurrence in solution of an equilibrium such as the following:



Species to the left are proposed as active catalysts, selectivity being favoured by movement to the left. However, rate is enhanced by movement of the equilibria to the right, but only by a small degree, possibly to favour **B** and **C**. Too great a movement to the right through the use of high SnCl_3^- concentrations decreases catalytic activity markedly. Thus, differences found for the catalysis, (Table 4.2), appear to be more a direct consequence of the position of the equilibrium (i.e. the proportion of **A**, **B**, and **C**) present, rather than to factors relating to the generation of a single catalytic species. $[\text{Rh}(\text{CO})(\text{SnCl}_3)_2\text{Cl}]^{2-}$ may also be an active catalytic component in an equilibrium such as the one shown above.

The identification of one Rh-Sn species under catalytic conditions has not been achieved, though many attempts have been made. Acetic acid, the solvent, makes IR studies particularly difficult in the $2300\text{-}1800\text{cm}^{-1}$ region. HPIR studies under the temperature and pressure conditions used for catalysis, described in Chapter 5, indicated that it was difficult to differentiate between the following Rh/Sn complexes, each of which have a strong absorption in the region where a carbonyl band was observed: $[\text{Rh}(\text{CO})_2(\text{SnCl}_3)_3]^{2-}$, $[\text{Rh}(\text{CO})_2(\text{SnCl}_3)_3]^{2-}$, $[\text{Rh}(\text{CO})(\text{SnCl}_3)_2\text{Cl}]^{2-}$ and $[\text{Rh}(\text{CO})(\text{SnCl}_3)_4]^{3-}$. However, studies of the reaction chemistry of rhodium(I) carbonyl chlorides with tin(II) chlorides under more ambient conditions (see Chapters 2 and 3) indicated that $[\text{Rh}(\text{CO})(\text{SnCl}_3)_4]^{3-}$ and $[\text{Rh}(\text{CO})_2(\text{SnCl}_3)_3]^{2-}$ are possible 18-electron catalytic precursors.

Previous studies, along with work reported in Chapters 2 and 3, have established SnCl_3^- as a weak σ -donor and a strong π -acceptor ligand⁽¹⁰⁻¹⁴⁾. Thus, the role of SnCl_2 as a co-catalyst and promoter will probably relate to the properties of the SnCl_3^- ligand (SnCl_2 in $\text{HCl}_{(\text{aq})}$ rapidly forms $\text{SnCl}_3^-_{(\text{aq})}$), and the changes in π -electron acceptor and trans effect properties when SnCl_3^- replaces chloride ligand(s) in a rhodium complex. These properties will affect the processes occurring at an active Rh(I) centre during the catalytic cycle, and the high trans effect of the SnCl_3^- ligand, is a likely cause of the increase in the rate of propanoic acid production. For instance, the π -acceptor properties of the SnCl_3^- ligand may make a rhodium(I) complex more susceptible to addition of an electron donating group, such as the olefin double bond (see Figure 4.1), by removing electron density from the metal centre. This removal of electron density from the rhodium centre may also help to stabilise catalytically active rhodium(I) complexes. The trans effect properties of SnCl_3^- could also influence the final step of the catalytic process, reductive elimination, by promoting the loss of $\text{C}_2\text{H}_5\text{COX}$, where $\text{X}=\text{Cl}^-$ or SnCl_3^- (see Figure

4.2). Alternatively, the promotional effect of SnCl_2 may be partly due to chemistry which does not occur at the active catalyst, such as formation of $\text{C}_2\text{H}_5\text{SnCl}_3$ in solution, although this seems to be unlikely based on previous work⁽¹⁾, and work reported in this chapter.

4.9 Effect of Ethene on Reactivity

A series of reactions were carried out to investigate the effect of changing the pressure of ethene on the rate of reaction for the catalytic process, and thus to provide some information on mechanistic aspects of the catalytic process.

Reactions 4.16, 4.17, 4.18 and 4.19 (see Table 4.2 for experimental details)

*Components: 4.16 [Bz(Et)₃N][Rh(CO)₂Cl₂], SnCl₂, 37% HCl_(aq),
CH₃COOH, CO, C₂H₄*

4.17, 4.18, 4.19 Same as Reaction 4.16

Rh:Sn Molar Ratio was 1:2 in all cases

<i>Reaction code</i>	<i>4.16</i>	<i>4.17</i>	<i>4.18</i>	<i>4.19</i>
<i>CO pressure/bar</i>	30	30	30	30
<i>C₂H₄ pressure/bar</i>	20	25	30	40
<i>Rate/bar.hr⁻¹</i>	24	43	66	78
<i>Rate/Mol.Kg⁻¹.hr⁻¹</i>	1.15	2.14	2.83	2.76

As can be seen from Figure 4.3 an increase in the initial pressure of ethene leads to an increase in the rate of gas uptake for the catalytic reaction. Figure 4.3 also indicates that initial ethene pressures which are less than approximately 15 bar will render the hydrocarbonylation process inactive. A progressive increase in the initial pressure of ethene also leads to a progressive increase in the rate of propanoic acid production. The graph in Figure 4.3 approximates to a linear increase in rate for ethene pressures up to 30 bar, but the rate becomes slightly lower when the ethene pressure is 40 bar. Since there was initially a higher partial pressure of ethene than CO for Reaction 4.19, some ethene may be left unused at the end of the reaction. Consequently this may explain the similar rates of propanoic acid production for Reactions 4.18 and 4.19. However, the higher rate of gas uptake for Reaction 4.19 compared with Reaction 4.18 did suggest reaction of the excess ethene in Reaction 4.19 to form by-products. Indeed, examination of GC data indicated a higher selectivity for chloroethane ($\approx 15\%$) than for Reactions 4.16-18. Small amounts of ethyl acetate and ethyl propanoate were also produced. The maximum rate of gas

Figure 4.3 Dependence of rate of reaction on the pressure of ethene

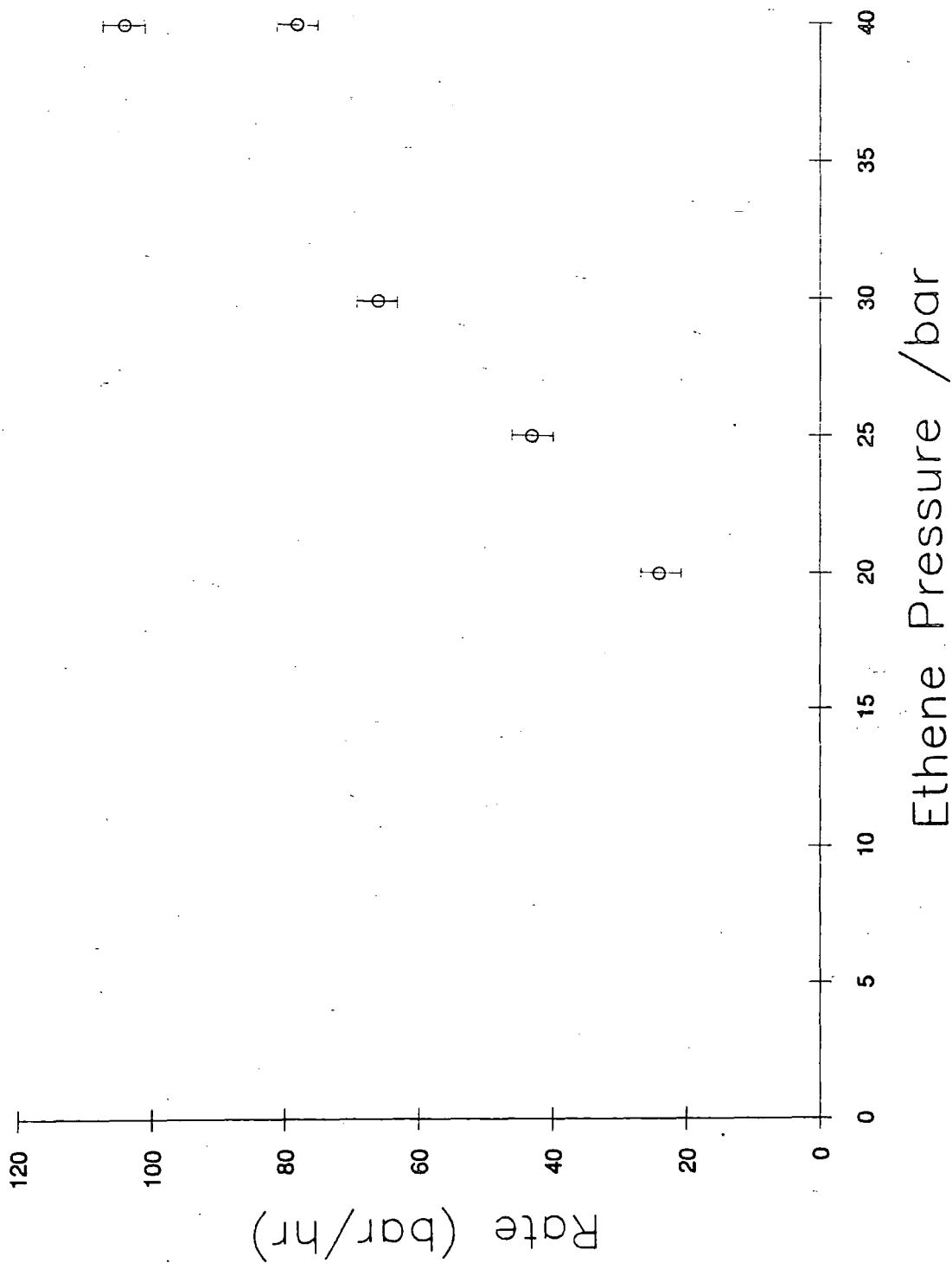
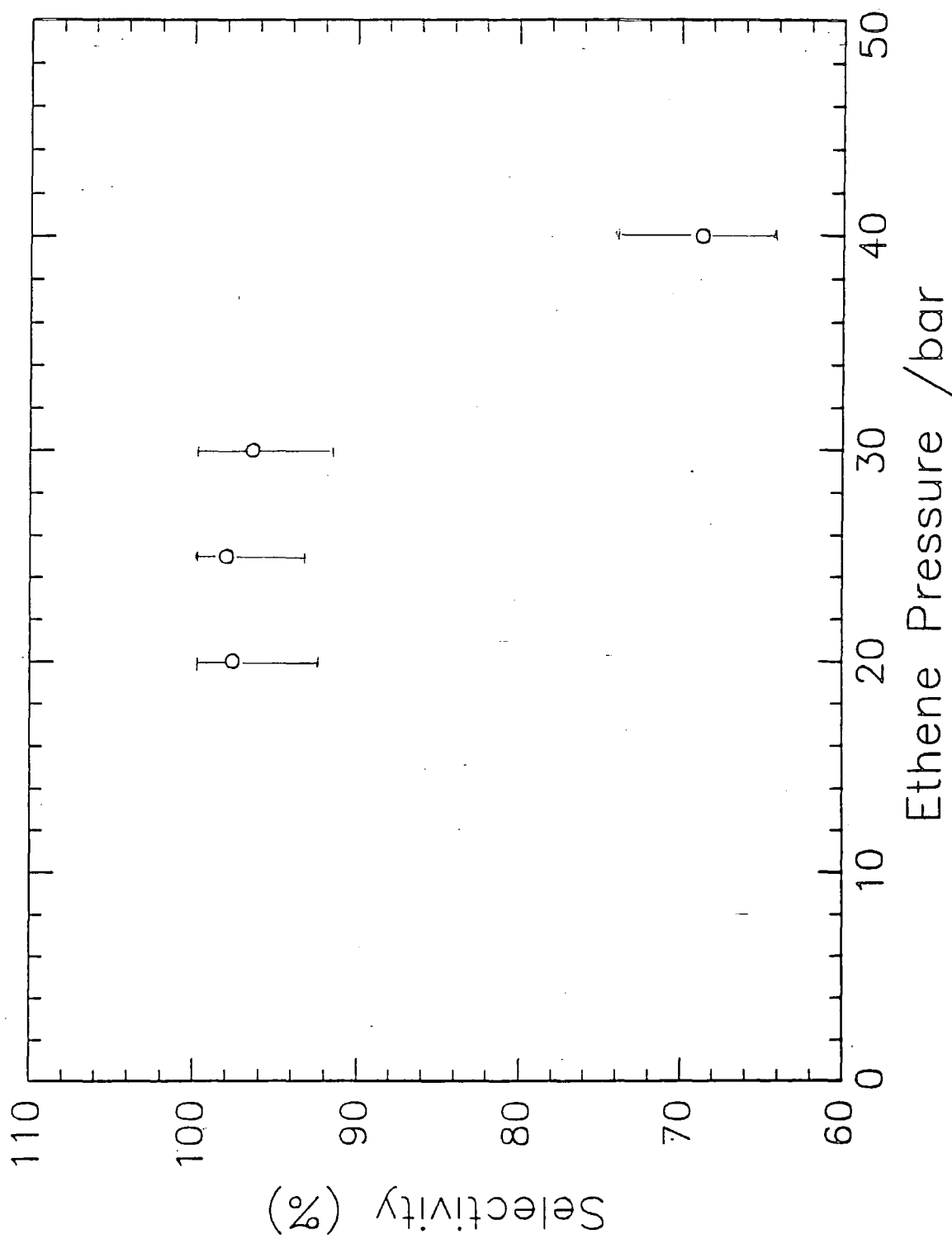


Figure 4.4 Effect of ethene pressure on the percentage selectivity for propanoic acid



uptake for Reaction 4.19, taken over a 10 minute period at the start of the reaction (CO and C₂H₄ are 30 and 40 bar respectively) is 104 bar.hr⁻¹. The graph shown in Figure 4.3 approximates closely to a straight line if a rate of 104 bar.hr⁻¹ rather than 78 bar.hr⁻¹ is plotted as the rate of reaction for Reaction 4.19. Thus, the rate of reaction is envisaged to be first order with respect to the pressure of ethene, with Reaction 4.19 only obeying the first order rate law in its early stages. Indeed, ethene pressures higher than 40 bar may not obey the first order rate law.

The data shows that the extra ethene present in Reaction 4.19 gave no increase in the rate of propanoic acid production (2.76 Mol.Kg⁻¹.hr⁻¹), over the 1 hour period, and the amount of propanoic acid produced (0.1060 moles), compares closely with the amount formed in Reaction 4.18 (2.83 Mol.Kg⁻¹.hr⁻¹, 0.1085 moles). However, Figure 4.4 shows that an ethene pressure of 40 bar leads to a significant decrease in the selectivity for propanoic acid and substantial formation of chloroethane, with Reaction 4.19 having a selectivity for propanoic acid of only 68.7% compared with Reactions 4.16-4.18 where the selectivity was greater than 90% in each case.

4.10 Isotopic Exchange Experiments

In the Monsanto process involving the homogeneous carbonylation of methanol to form acetic acid⁽¹⁶⁾, the rate determining step for the reaction was found to be the oxidative addition of methyl iodide to the catalytically active rhodium species [Rh(CO)₂I₂]⁻, with the rate equation

$$\text{Rate} = k[\text{Rh}]^1[\text{I}]^1[\text{MeOH}]^0[\text{CO}]^0$$

independent of the two reactants carbon monoxide and methanol.

The discussion in this chapter, which concerns the hydrocarbonylation of ethene to form propanoic acid, has centred around an initial oxidative addition reaction, followed by generation of an ethyl-rhodium species. The initial step is considered to be addition of a proton to the rhodium centre, followed by coordination of ethene and finally proton migration on to ethene to give an ethyl group. Work carried out by Forster on hydrogen iodide and ethyl iodide addition^(17,18) suggests that, like the Monsanto process, the oxidative addition step is likely also to be rate limiting for the hydrocarbonylation process.

As a consequence a series of experiments (Reactions 4.20 and 4.21) were carried out to investigate the possible steps operating in the hydrocarbonylation of ethene. These were carried out using a deuterium labelling technique. 37% $\text{HCl}_{(\text{aq})}$ in the $\text{RhCl}_3 \cdot 3\text{H}_2\text{O}/\text{SnCl}_2/\text{Bz}(\text{Et})_3\text{NCl}$ system (Reaction 4.9) was replaced by 37% $\text{DCl}_{(\text{aq})}$ in D_2O (99%D) for each of the catalytic runs, the aim being to investigate the number and the position of the deuterium atoms in the final propanoic acid product, and thus to gain information about the addition of ethene to the catalytic rhodium species. Reaction 4.20 was carried in the presence of CH_3COOH while Reaction 4.21 was carried out in the presence of CH_3COOD . The effect on the overall rate of the reaction was also monitored.

Reactions 4.20 and 4.21 (see Table 4.2 for experimental details)

Components: 4.20 $\text{RhCl}_3 \cdot 3\text{H}_2\text{O}$, SnCl_2 , $\text{Bz}(\text{Et})_3\text{NCl}$, CH_3COOH - 34ml,
37%DCl in D_2O (99%D) - 2.4ml, CO - 30 bar,
 C_2H_4 - 30 bar
4.21 $\text{RhCl}_3 \cdot 3\text{H}_2\text{O}$, SnCl_2 , $\text{Bz}(\text{Et})_3\text{NCl}$, CH_3COOD - 17ml,
37%DCl in D_2O (99%D) - 1.2ml, CO - 20 bar,
 C_2H_4 - 20 bar

Notes:

1. The amounts of $\text{RhCl}_3 \cdot 3\text{H}_2\text{O}$, SnCl_2 and $\text{Bz}(\text{Et})_3\text{NCl}$ used for Reaction 4.21 were approximately half those used for Reaction 4.20.
2. The volumes of 37%DCl_(aq) and solvent used for Reaction 4.21 were half those used for Reaction 4.20. This was due to the limited availability of CH_3COOD .

Reaction Code	Rate of gas uptake/bar.hr ⁻¹	Rate of propanoic acid production/ Mol.Kg ⁻¹ .hr ⁻¹	Moles of propanoic acid produced	% Selectivity
4.20	◆46	1.26	0.049	19.2
4.21	20	1.77	0.036	96.0
4.9	58	2.73	0.105	73.0

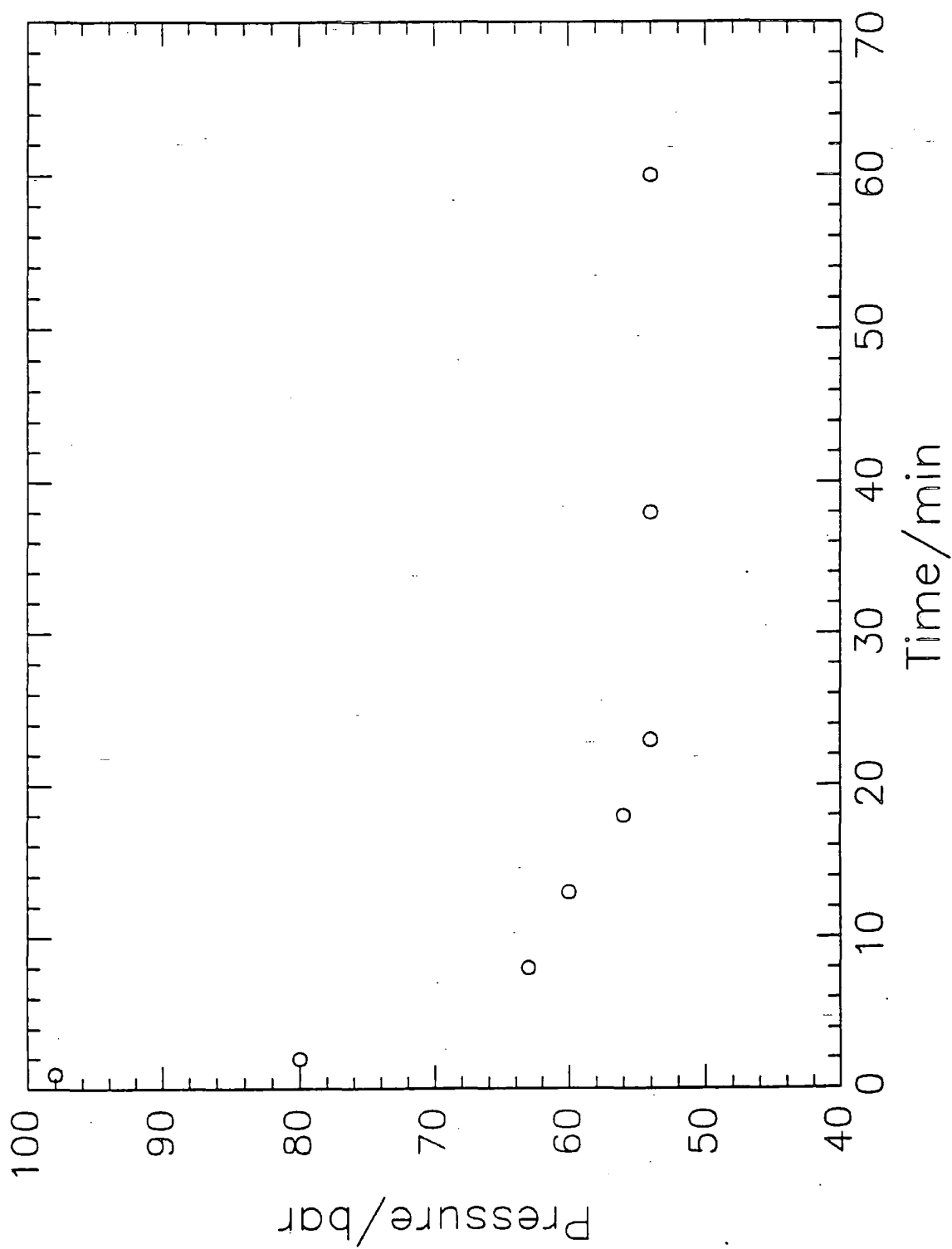
◆ There was no increase in pressure as the temperature was increased from 140-180°C indicating that reaction had begun at this stage. The rate of gas uptake was, however, monitored over a one hour period after the temperature reached 180°C and the value of 46 bar.hr⁻¹ is quoted over this period. The reaction stopped, however, after 18 minutes with a pressure drop of 37 bar during the first 8 minutes. This is consistent with a rate of gas uptake of 277 bar.hr⁻¹ in the early stages of the reaction i.e. the first 18 minutes. A pressure/time profile for Reaction 4.20 is shown in Figure 4.5.

The rate of gas uptake observed in the early stages of Reaction 4.20 (277 bar.hr⁻¹, over an 18 minute period), was much higher than for any previous reaction described in this chapter, where a steady drop in pressure generally occurred over a one hour period, with a maximum rate usually occurring between 20 and 40 minutes. Gas uptake for Reaction 4.20 also occurred at a lower temperature than for previous systems. Reaction 4.9, carried out with 37% HCl_(aq) rather than 37% DCl_(aq), but otherwise having identical stoichiometric amounts of components to Reaction 4.20, gave a steady drop in pressure upon reaching 180°C, with a rate of gas uptake of 58 bar.hr⁻¹ over a 1 hour period. The observed initial rate of gas uptake for Reaction 4.20 does indicate that the introduction of 37% DCl_(aq) increases the rate of gas uptake, causing reaction to occur at a lower temperature, but the amount of propanoic acid produced and selectivity for propanoic acid are much lower than for Reaction 4.9. Experience has shown that reaction temperatures below 180°C do not favour propanoic acid production (see Table 4.1), and in Reaction 4.20 gas uptake below 180°C appears to be the cause of the large yield of other organic products, namely chloroethane and ethyl acetate.

The increase in rate in the presence of DCl rather than HCl could possibly be due to an inverse isotope effect. During oxidative addition the rate of addition of D⁺ to an active rhodium complex is expected to be higher than the rate of addition of H⁺, since DCl has a higher acid dissociation constant than HCl. This may effectively cause the formation of a [Rh-Ethyl] complex at a lower temperature than 180°C, since the energy required to form C-D bonds is lower than the energy required to form C-H bonds. The apparent lack of further reaction with CO to yield propanoic acid at temperatures lower than 180°C increases the probability of reductive elimination of chloroethane, and hence reaction with acetic acid to form ethyl acetate. This seems to be the case for Reaction 4.20. However, the observed increase in rate for Reaction 4.12 was only accompanied by approximately 30% incorporation of deuterium into propanoic acid. ¹H NMR analysis showed a large proportion of the propanoic acid to contain no deuterium. As a consequence this proposed rationalisation of rates in terms of isotopic effects remains speculative.

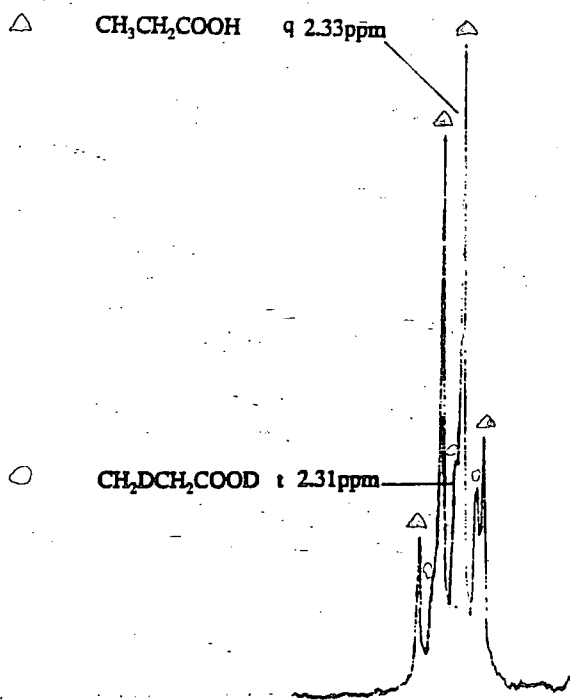
An experiment (Reaction 4.21) undertaken using CH₃COOD as the solvent gave results contrasting with those for Reaction 4.20, in terms of reaction temperature, initial rate, overall rate and selectivity. Examination of the propanoic acid produced, however, gave strange results, and consequently the data is considered unreliable,

Figure 4.5 Pressure-Time profile for Reaction 4.20



though no obvious explanation can be given at present. ^1H NMR analysis showed a large proportion of the propanoic acid to contain no deuterium (see Figure 4.6), though the reaction was undertaken in D_2O and CH_3COOD . The source of the protons required to produce the quantity of propanoic acid obtained is not known, the obvious sources having been checked, and consequently Reaction 4.21 must be disregarded.

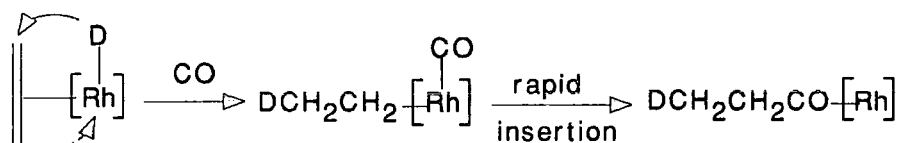
The organic products obtained for Reactions 4.20 and 4.21 were separated by distillation under a nitrogen atmosphere and a ^1H NMR spectrum of the propanoic acid species was recorded. Figure 4.6 shows the $-\text{CH}_2-$ region of the spectrum for Reaction 4.21. The ^1H NMR spectrum for Reaction 4.20 is similar to that shown for Reaction 4.21 in Figure 4.6. The approximate 30% deuterium incorporation in the propanoic acid produced in Reaction 4.20 is not altogether unexpected, since deuterium will exchange with the proton on the OH group of the solvent, CH_3COOH . No evidence of CH-CD coupling is observed for any of the ^1H NMR spectra. This would cause each signal in the CH_2 triplet to split into a further triplet, but since the coupling constant would only be expected to be of the order of 1 Hz, the only effect seen at the resolution used would be line broadening.



Data: $\delta(^1\text{H})/\text{ppm}$ (in CDCl_3 , 25°C , ^1H coupled): 1.12 t, $^1J[\text{CH}_3-\text{CH}_2] = 7.45\text{Hz}$;
2.31 t, $^1J[\text{CH}_2-\text{CH}_2\text{D}] = 7.50\text{Hz}$; 2.33 q, $^1J[\text{CH}_2-\text{CH}_3] = 7.09\text{Hz}$; 10.75 s

Figure 4.6 ^1H NMR showing the CH_2 region of $\text{CH}_2\text{DCH}_2\text{COOD}$ and $\text{CH}_3\text{CH}_2\text{COOH}$, both of which are products of Reaction 4.21

The formation of $\text{CH}_2\text{DCH}_2\text{COOD}$ in Reaction 4.20 indicates that the oxidative addition step of the catalytic process will involve migration of a single proton or deuterium atom onto the coordinated ethene group, and that this process will be irreversible, since there is no evidence for any deuterium incorporation into the CH_2 group of propanoic acid. Since only one deuterium atom is incorporated into the propanoate group i.e. $\text{CH}_2\text{DCH}_2\text{COOD}$, this implies that the carbonylation step of the catalytic reaction involves rapid migratory insertion of CO into the rhodium-ethyl bond:



4.11 Catalyst Injection Techniques

The rhodium-chloride and rhodium-tin-chloride catalysed hydrocarbonylation of ethene to form propanoic acid also gives formation of smaller amounts of other organic products, the main ones being chloroethane, ethyl acetate and ethyl propanoate. These products may be formed during the heating process of the reaction, before the reaction temperature of 180°C is reached, during the reaction itself, or during the cooling period when the heating has been switched off. Consequently, experiments were carried out to investigate the formation of by-products below 180°C . This was carried out by adding the active catalyst when the reaction temperature of 180°C had been reached.

This work was carried out at BP Chemicals Ltd., Hull, using a Hastalloy B2 autoclave (Parr, U.S.A) of 300ml capacity which had a maximum working pressure of 200 bar and a maximum working temperature of 250°C . The autoclave had a glandless stirring system, a thermowell and five ports. In addition the equipment had the following facilities:

1. Catalyst injection.
2. Gas sampling.
3. Ballast vessel operation.

All reactants were loaded into the autoclave via an inlet port at the head, except for reactions involving use of the catalyst inject system, when the rhodium precursor was omitted. In such cases the rhodium precursor was first of all dissolved in approximately 10ml of solvent, in this case acetic acid, and the solution syringed into

the inject vessel, which was connected to a gas inlet system. The autoclave was sealed, flushed with carbon monoxide and then pressurised with carbon monoxide and ethene. The autoclave was stirred at a preset speed using a mechanical stirrer. After heating to the desired reaction temperature of 180°C the solution of rhodium complex was injected into the system using a mixture of carbon monoxide and ethene at a pressure which was slightly higher than the pressure in the autoclave. Thus, it was possible to ensure that all of the catalyst was successfully transferred from the injector. The gas uptake during the reaction was measured by computer monitoring of digital pressure gauges.

The following catalytic reaction was first undertaken without the use of the injection facility, in order to standardise the equipment for a rhodium-tin-chloride catalytic system:

Reaction 4.22 (see Table 4.2 for experimental details)

Components: $RhCl_3 \cdot 3H_2O$, $SnCl_2$, 37% $HCl_{(aq)}$, CH_3COOH , CO , C_2H_4
Rh:Sn Molar Ratio = 1:2

<i>Rate bar.hr⁻¹</i>	<i>Rate of propanoic acid production/Mol.Kg⁻¹.hr⁻¹</i>	<i>Moles of propanoic acid produced</i>	<i>% Selectivity</i>
35	1.03	0.146	82.8

The following reactions were carried out using the catalyst inject facility. The effect on rate and selectivity of varying the amount of 37% $HCl_{(aq)}$ in the system was also investigated.

Reactions 4.23 and 4.24 (see Table 4.2 for experimental details)

Components: 4.23 $[Bz(Et)_3N][Rh(CO)_2Cl_2]$, $SnCl_2$, CH_3COOH , CO , C_2H_4
 4.24 Same as Reaction 4.23

The Rh:Sn Molar Ratio was 1:2 for Reactions 4.23 and 4.24

<i>Reaction Code</i>	<i>37%$HCl_{(aq)}$ /ml</i>	<i>H_2O /ml</i>	<i>Rate of propanoic acid production/ Mol.Kg⁻¹.hr⁻¹</i>	<i>Moles of propanoic acid produced</i>	<i>% Selectivity</i>
4.23	5	5	0.087	0.029	19.7
4.24	9	0	1.120	0.158	77.2

The data obtained for Reactions 4.23 and 4.24 indicates that although formation of by-products such as ethyl acetate may occur during the heating process of the

catalytic reaction, it also seems to occur at the reaction temperature of 180°C, the temperature at which the catalyst was added. The selectivity for the reaction using the catalyst inject system (Reaction 4.24) is actually less than that for Reaction 4.22 carried out without the use of the catalyst inject facility, clearly suggesting that injecting the catalytic precursor at 180°C does not enhance the selectivity for propanoic acid. There is, however, no information available to rule out the formation of by-products as the system is cooled at the end of the reaction period, although this is considered to be unlikely. The findings conclusively show that by-products may be formed in substantial quantity at 180°C, and do not relate exclusively to chemistry taking place prior to achieving the preferred reaction temperature.

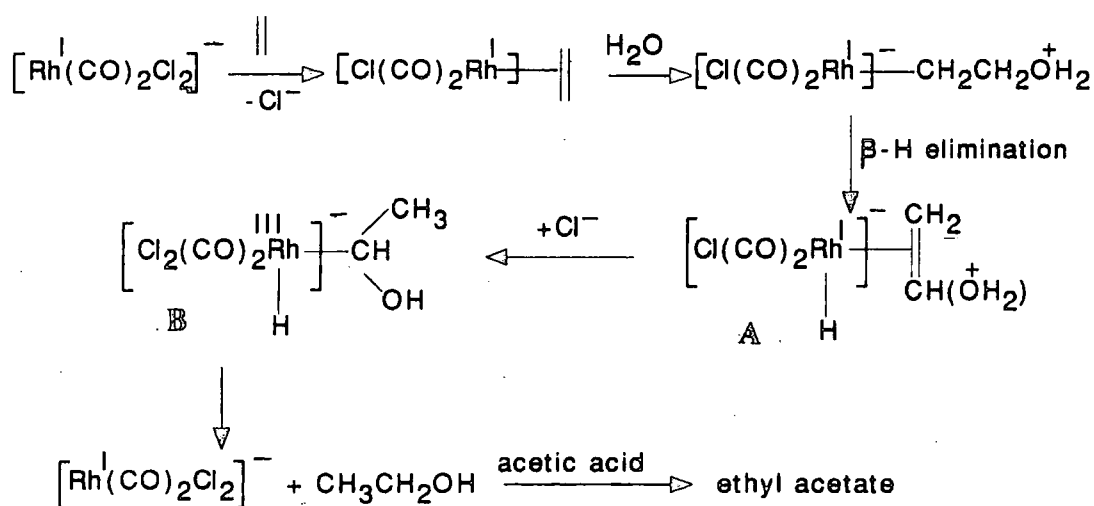
Reactions 4.23 and 4.24 also demonstrate that a decrease in the concentration of $\text{HCl}_{(\text{aq})}$ or an effective increase in the amount of water has a detrimental effect on the rate and selectivity for the formation of propanoic acid. This is consistent with previous studies⁽¹⁾, where a decrease in the HCl concentration accompanied by an increase in the amount of water in the system, led to a decrease in the rate of propanoic acid production (see Table 4.3 below). A completely anhydrous system gave an extremely fast though poorly-selective reaction⁽¹⁾ (see Table 4.3 below):

Table 4.3 The effect of the concentration of HCl on the rate of propanoic acid production and on the selectivity for propanoic acid (data taken from ref. 1)

	Moles of propanoic acid produced	Rate/ bar.hr ⁻¹	Rate of propanoic acid production/ Mol.Kg ⁻¹ .hr ⁻¹	% Selectivity
1.	Components: 2.4ml.2M.HCl _(aq)			
	0.047	66.2	0.97	88.1
2.	Components: 2.4ml.2M.HCl _(aq) + 7.6ml H ₂ O			
	0.013	15.0	0.27	†
3.	Components: HCl _(g)			
	0.053	236	5.55	46.5

Standard components for each reaction were RhCl₃.3H₂O, SnCl₂.2H₂O, Bz(Et)₃NCl, CH₃COOH - 34ml, CO - 40bar, C₂H₄ - 40bar. Reaction 3 also contained (CH₃CO)₂O to maintain anhydrous conditions. † The sensitivity of the GC equipment did not allow a reliable value for the percentage selectivity to be calculated.

The results in Table 4.3 indicate that an amount of water is detrimental to the yield of acid, but is beneficial to achieve a highly selective production of propanoic acid. However, increasing this amount of water above a certain volume, i.e. lowering the $\text{HCl}_{(\text{aq})}$ concentration, lowers the selectivity for propanoic acid, and leads to an increase in the formation of other organic products. A large amount of ethyl acetate (0.104 moles) was formed in Reaction 4.23. The selectivity for ethyl acetate was approximately 78%, with the overall rate of gas uptake ($42 \text{ bar}\cdot\text{hr}^{-1}$) almost identical to that of Reaction 4.24 ($43 \text{ bar}\cdot\text{hr}^{-1}$). The main by-product for Reaction 4.24 was also ethyl acetate (0.018 moles). Clearly, a decrease in the concentration of aqueous HCl causes an increase in by-product formation, namely ethyl acetate, at the expense of significantly lowering the rate and selectivity for propanoic acid. Aqueous HCl is known to be in equilibrium with HCl gas⁽¹⁹⁾. Therefore, a decrease in the concentration of HCl may lower the proton availability, due to an increase in the amount of aquated HCl, and consequently the formation of a rhodium hydride species, the expected initial step of the catalytic process (see Figure 4.2), will become less favourable. As a result, coordination of ethene to a catalytic species such as $[\text{Rh}(\text{CO})_2\text{Cl}_2]^-$ as the initial step of the catalytic cycle, which is not expected to occur in the presence of concentrated HCl, will become more likely. Therefore, the following mechanism is proposed to explain the formation of ethyl acetate. It is based on $[\text{Rh}(\text{CO})_2\text{Cl}_2]^-$ as the active catalyst, and is similar to that for the Wacker reaction involving the palladium(II) halide catalysed reaction of substituted alkenes and water to form substituted aldehydes/alcohols⁽²⁰⁾.



Initial coordination of ethene to the metal, which is known to occur in the Wacker reaction⁽²⁰⁾ and in the formation of Zeise's salt $[(C_2H_4)PtCl_3]^-$ from the platinum(II) complex $PtCl_4^{2-}$ ⁽²¹⁾, is followed by nucleophilic attack at the double bond by water. This is followed by β -hydrogen elimination to generate a rhodium-hydride intermediate (A). A rearrangement of the organic group, and addition of Cl^- to rhodium is then envisaged to occur, to generate an 18-electron rhodium(III) species (B). The cycle is then completed by cis reductive elimination to regenerate the catalyst $[Rh(CO)_2Cl_2]^-$, and form ethanol. Under the reaction conditions, ethanol will undergo an esterification reaction with the solvent, acetic acid, to form ethyl acetate.

GC analysis followed by computer fitting of the GC peaks with known reagents also suggested the formation of very small quantities of acetic anhydride in Reactions 4.22, 4.23 and 4.24, which is very surprising considering the hydrous conditions employed. Formation of acetic anhydride, implies the consumption of water, which is conceivable via the Water Gas Shift reaction, but is very unusual for such systems. Alternatively, dehydration during the analytical procedures, and erroneous computer fitting, may explain the apparent presence of acetic anhydride.

4.12 Hydrocarbonylation using model Rhodium-Tin complexes

Reactions previously described in this chapter, were carried out with addition of either $SnCl_2$ or $Bz(Et)_3NSnCl_3$ to a rhodium-chloride compound using a variety of reaction conditions in order to gain information about the catalysis taking place. A series of reactions were also carried out using model rhodium-tin complexes and the results compared with other rhodium/tin systems described in this chapter, in an attempt to gain information about the possible effect of the trichlorostannate ligand, and the type of chemistry which may occur in rhodium-tin-chloride catalytic processes. The effect on catalytic activity of differing numbers of trichlorostannate groups coordinated to the rhodium centre, was also of interest, bearing in mind the changes in activity observed when the Rh:Sn molar ratio is changed (see Section 4.5).

Table 4.4 Catalytic data for model rhodium/tin precursors

Reaction Code	Rh-Sn Precursor	Rate of gas uptake/ bar.hr ⁻¹	Rate of propanoic acid production/ Mol.Kg ⁻¹ .hr ⁻¹	% Selectivity
4.25	$Rh(COD)_2SnCl_3$	14	1.51	84.3
4.26	$*[Rh(CO)(SnCl_3)_2Cl]^{2-}$	24	1.08	91.8
4.27	$*Rh(I)-CO-SnCl_3$ mix	46	2.35	97.3
4.28	$*[Rh(COD)(SnCl_3)_3]^{2-}$	47	2.99	99.2
4.29	$\diamond [Rh(COD)(SnCl_3)_3]^{2-}$	71	2.43	87.0
4.30	$\diamond [Rh(CO)_2(SnCl_3)_3]^{2-}$	16	1.30	89.3
4.31	$Rh_2(C_2H_4)_4Cl_2$	33	1.39	81.2

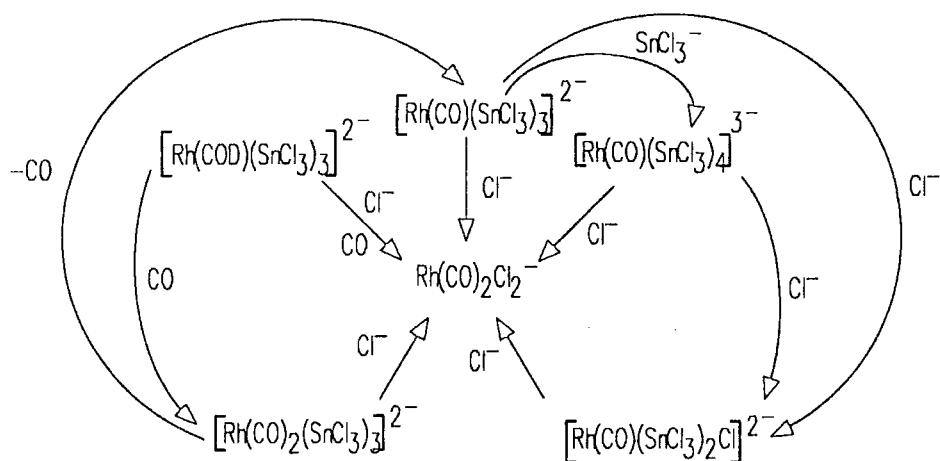
* Cation = $[Bz(Et)_3N]^+$

\diamond Cation = $[PPN]^+$

Notes:

1. Reactions 4.25-4.31 (see Table 4.2 for experimental details)
2. Reactions 4.25 and 4.30 both contained 1.2ml of 37% $HCl_{(aq)}$ and 17ml of CH_3COOH whilst the other reactions each contained 2.4ml of 37% $HCl_{(aq)}$ and 34ml of CH_3COOH .
3. Reactions 4.25-4.31 were carried out under a pressure of 30 bar CO and 30 bar C_2H_4 .
4. It should be noted that each 1,5-cyclooctadiene ligand, present in complexes used in Reactions 4.25, 4.28 and 4.29 is readily replaced by two CO ligands upon pressurisation⁽²²⁾ (see Chapter 3). This has been confirmed by FT-IR studies of solutions of these complexes in acetic acid under a pressure of CO.
5. The mixture used in Reaction 4.27 was synthesised as outlined in Chapter 3, Section 3.2.2 and mainly consists of $[Bz(Et)_3N]_2[Rh(CO)_2(SnCl_3)_3]$, probably along with much smaller amounts of $[Bz(Et)_3N]_3[Rh(CO)(SnCl_3)_4]$ and $[Bz(Et)_3N]_2[Rh(CO)(SnCl_3)_2Cl]$, and very small quantities of unidentified rhodium carbonyl containing complexes. See Chapter 3 for details of the synthesis of the other complexes used in Reactions 4.25-31.

Cyclooctadiene ligands will each be replaced in the complexes recorded above by two carbonyl groups, but further reactions may occur under the reaction conditions employed. For instance, in the presence of a large amount of 37% $HCl_{(aq)}$, it is entirely possible that one or more of the trichlorostannate ligands will be displaced by a Cl^- ligand (see Chapter 7). Work described in Chapters 2, 3 and 7 using dichloromethane and THF as solvents indicated that the following transformations are possible in the reaction mixtures used in the high pressure processes:



Conversely, however, it has been possible to isolate rhodium(I)- SnCl_3 species, namely $[\text{Rh}(\text{CO})_2(\text{SnCl}_3)_3]^{2-}$, $[\text{Rh}(\text{CO})(\text{SnCl}_3)_4]^{3-}$ and $[\text{Rh}(\text{CO})(\text{SnCl}_3)_2\text{Cl}]^{2-}$, in acetic acid, in the presence of excess 37% $\text{HCl}_{(\text{aq})}$, from the reaction of $[\text{Bz}(\text{Et})_3\text{N}][\text{Rh}(\text{CO})_2\text{Cl}_2]$ with $[\text{Bz}(\text{Et})_3\text{N}][\text{SnCl}_3]$, described in Chapter 3, Section 3.2.2, indicating that Rh(I)- SnCl_3 complexes can be formed in the presence of a large amount of HCl . The isolation of particular Rh(I)- SnCl_3 complexes from solution, reported in Chapter 3, may be a feature of their relative insolubility compared with the corresponding chloro- complexes, and in solution at high pressure and high temperature it is highly probable that equilibria exist between several chloro- and trichlorostannate-rhodium(I) complexes, as indicated by high pressure infra-red studies (see Chapter 5) and studies in solution at ambient temperature and pressure (see Chapters 2 and 3):



Thus, catalytic systems containing active Rh(I)- SnCl_3 complexes will probably also contain $[\text{Rh}(\text{CO})_2\text{Cl}_2]^-$ as an active catalyst. Even initial loss of trichlorostannate ligands would not rule out further reaction of the ligand with the rhodium species as the reaction conditions are changed.

The catalytic precursors used in Reactions 4.25 $\{\text{Rh}(\text{COD})_2\text{SnCl}_3\}$, 4.26 $\{[\text{Rh}(\text{CO})(\text{SnCl}_3)_2\text{Cl}]^{2-}\}$ and 4.31 $\{\text{Rh}_2(\text{C}_2\text{H}_4)_4\text{Cl}_2\}$, each have a lower rate of propanoic acid production than Reactions 4.4 and 4.5 (1.88 and 1.89 $\text{Mol.Kg}^{-1}.\text{hr}^{-1}$ respectively) which were carried out in the absence of SnCl_2 , with $\text{RhCl}_3.3\text{H}_2\text{O}$ used as the sole catalytic precursor. In the case of Reaction 4.26 this may have been due to either the instability of the air sensitive $16e^-$ $[\text{Bz}(\text{Et})_3\text{N}]_2[\text{Rh}(\text{CO})(\text{SnCl}_3)_2\text{Cl}]$ complex under the catalytic conditions or its poor solubility in acetic acid. The poor

activity of $\text{Rh}(\text{COD})_2\text{SnCl}_3$ as a precursor, Reaction 4.25, is most likely due to a smaller volume of acetic acid than usual present in the catalytic system (17 ml as opposed to 34 ml). This appears to lead to a low rate of gas uptake ($14 \text{ bar}\cdot\text{hr}^{-1}$), and hence will lead to a lower rate of propanoic acid production.

The $\text{Rh}(\text{I})\text{-SnCl}_3$ precursors used for Reactions 4.27 ($\text{Rh}(\text{I})\text{-CO-SnCl}_3$ mixture), 4.28 $\{[\text{Bz}(\text{Et})_3\text{N}]_2[\text{Rh}(\text{COD})(\text{SnCl}_3)_3]\}$ and 4.29 $\{[\text{PPN}]_2[\text{Rh}(\text{COD})(\text{SnCl}_3)_3]\}$ each gave a higher rate of propanoic acid production than the rhodium-chloride catalytic systems employed in Reactions 4.4 and 4.5 (1.88 and $1.89 \text{ Mol}\cdot\text{Kg}^{-1}\cdot\text{hr}^{-1}$ respectively), with the values obtained not dissimilar to those obtained for the rhodium-tin-chloride catalytic systems which employed a Sn:Rh molar ratio of 2:1, Reactions 4.7 and 4.17 (2.71 and $2.14 \text{ Mol}\cdot\text{Kg}^{-1}\cdot\text{hr}^{-1}$ respectively). This is an indication of the ability of the trichlorostannate ligand to lead, in some circumstances, to an increase in the activity of the catalytic systems towards propanoic acid production, chiefly when the Sn:Rh molar ratio is 2:1. Unfortunately, the data obtained does not allow conclusions to be made about the formulation of one $\text{Rh}(\text{I})\text{-SnCl}_3$ complex as either the main catalytic precursor or the active catalyst. It is entirely possible that in each of Reactions 4.27, 4.28 and 4.29, the $\text{Rh}(\text{I})\text{-SnCl}_3$ complexes will react with the large amount of chloride ions present in the systems to form $[\text{Rh}(\text{CO})_2\text{Cl}_2]^-$, which is catalytically active in its own right.

Interestingly, $[\text{PPN}]_2[\text{Rh}(\text{CO})_2(\text{SnCl}_3)_3]$ (Reaction 4.30) only gave a rate of propanoic acid production of $1.30 \text{ Mol}\cdot\text{Kg}^{-1}\cdot\text{hr}^{-1}$. A possible reason for this may be the relative insolubility of this complex in acetic acid. Indeed, the activity of all of Reactions 4.25-4.30 may be affected, to some degree, by the solubility of the catalytic precursor in acetic acid. It is also possible that insoluble rhodium-tin species may be formed for other rhodium-tin systems reported in this chapter, and that consequently the activity of the systems may be affected.

Previous work⁽¹⁾ has shown that in the absence of HCl from the catalytic system, but with water present, hydrocarbonylation does not occur, and catalyst inject work (Reaction 4.23) indicated that lower concentrations of $37\% \text{HCl}_{(\text{aq})}$ give a decrease in the formation of propanoic acid. A reaction was carried out using the same mixture of $\text{Rh}(\text{I})\text{-SnCl}_3$ complexes as that used for Reaction 4.27. $37\% \text{HCl}_{(\text{aq})}$ was replaced by the same volume of water, to investigate whether HCl was still necessary to produce propanoic acid.

Reaction 4.32 (see Table 4.2 for experimental details)

Components: 4.32 Rh-SnCl₃ mixture, H₂O, CH₃COOH, CO, C₂H₄

There was no production of propanoic acid nor any other products from this reaction, thus proving that the presence of HCl is necessary for catalytic activity.

The presence of HCl is necessary to facilitate the initial step of the catalytic process, the formation of a rhodium hydride, as in the proposed catalytic scheme shown in Figure 4.2. Without the free protons available from HCl for initial protonation of an active catalyst e.g. $[\text{Rh}(\text{CO})_2\text{Cl}_2]^-$, subsequent reaction steps cannot occur. Protons are less likely to be available from acetic acid and water since they have a lower acid dissociation constant than HCl. It is possible that lower concentrations of HCl will decrease the rate of propanoic acid production by slowing down the oxidative addition process, due to an effective decrease in the availability of protons as HCl becomes more aquated. However, this should only be apparent with extremely low concentrations of HCl. Beyond a certain point the concentration should not significantly affect the rate of gas uptake. For example, there is no significant change in the rate of gas uptake upon changing the HCl concentration for Reactions 4.23 and 4.24, since in both systems HCl is present in a much greater molar amount than the rhodium catalyst. The significant effect of higher concentrations of 37% HCl_(aq) for these reactions seems to be reduction of side reactions, thus increasing the selectivity for propanoic acid and the amount of propanoic acid produced. Previous studies also indicated that the chloride ion is necessary for catalytic activity⁽¹⁾, since no reaction was observed upon addition of HBF₄ as a proton source in place of HCl. Chloride ions are possibly required for addition to the metal in order to generate a 6-coordinate rhodium(III) complex upon the completion of oxidative addition, as shown in Figure 4.2.

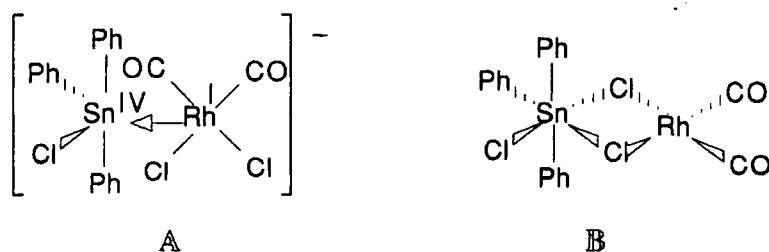
4.13 Promotional Effect of Tin(IV) Species

Tin(IV) species are known to form complexes with rhodium(I)⁽²³⁾ and previous work⁽¹⁾ has indicated that $[\text{Bz}(\text{Et})_3\text{N}]_2[\text{SnCl}_6]$ has a promotional effect on the rate of reaction for the hydrocarbonylation of ethene, although the rate of reaction was lower than for the rhodium-chloride catalytic systems (Reactions 4.4 and 4.5) described in this chapter. This observation has been tested further with other tin(IV) compounds, Ph₃SnCl and Ph₄Sn.

Reactions 4.33 and 4.34 (see Table 4.2 for experimental details)

Components: 4.33 $RhCl_3 \cdot 3H_2O$, Ph_3SnCl , $Bz(Et)_3NCl$, $37\%HCl_{(aq)}$,
 CH_3COOH , CO , C_2H_4
 4.34 $RhCl_3 \cdot 3H_2O$, Ph_4Sn , $Bz(Et)_3NCl$, $37\%HCl_{(aq)}$,
 CH_3COOH , CO , C_2H_4
Rh:Sn molar ratio = 1:2 in both reactions

There is no evidence to suggest that tetraphenyltin has a promotional effect on the catalytic process with the rate of propanoic acid production and selectivity (2.14 Mol.Kg⁻¹.hr⁻¹ and 88.0%) similar to those obtained for the rhodium-chloride catalytic systems in Reactions 4.4 and 4.5 (1.88 Mol.Kg⁻¹.hr⁻¹ and 91.0% for Reaction 4.5). Triphenyltin chloride gave a rate of propanoic acid production of 2.46 Mol.Kg⁻¹.hr⁻¹ which was higher than the rhodium-chloride systems but not as good as the optimum rhodium/SnCl₂ catalytic systems employing a Sn:Rh molar ratio of 2:1. It is therefore conceivable that Ph₃SnCl does have an effect on the catalytic process. The possibility exists that Ph₃SnCl will form an adduct or a bridging species with the catalytic rhodium-chloride complex [Rh(CO)₂Cl₂]⁻ as speculated below:



However, it is not likely that any interactions of both of these types would have a promotional effect on the hydrocarbonylation process. Indeed, the 5-coordination around the rhodium centre in A would be more likely to hinder the formation of an active catalytic species. B could conceivably have a promotional effect in removal of chloride ions from rhodium and generation of free coordination sites, but this remains pure speculation. Any promotional effect is more probably caused by reaction of Ph₃SnCl to form the trichlorostannate species SnCl₃⁻ in solution.

4.14 Dichloromethane as a co-solvent

In previous work⁽¹⁾ a mixed solvent system of acetic acid/dichloromethane, 5/12 v/v, was used for high pressure infra-red studies of the rhodium-tin-chloride promoted systems for the hydrocarbonylation of ethene, but limited catalytic information is available for this combination of solvents. Thus, a reaction was carried out using an

acetic acid/dichloromethane mixture, 5/12 v/v, to determine the effect of dichloromethane on the catalytic activity of the system.

Reaction 4.35 (see Table 4.2 for experimental details)

Components: 4.35 $RhCl_3 \cdot 3H_2O$, $SnCl_2$, $Bz(Et)_3NCl$, CH_3COOH , CH_2Cl_2 ,
 CO , C_2H_4

Rh:Sn:Bz(Et)₃NCl molar ratio = 1:2:3

The data obtained for Reaction 4.35 show that when dichloromethane is used as a co-solvent with acetic acid a very poor rate of gas uptake ($8 \text{ bar}\cdot\text{hr}^{-1}$) and rate of propanoic acid production ($0.82 \text{ Mol}\cdot\text{Kg}^{-1}\cdot\text{hr}^{-1}$) was found to occur, suggesting that dichloromethane is not a suitable solvent for the hydrocarbonylation process. The reason probably relates to the reduced ability of the Brønsted acid, acetic acid, due to a decrease in concentration, to promote the CO migratory insertion step of the catalytic cycle, and thus enhance the rate of CO uptake by the active rhodium complex. It has been postulated that the basis for this enhancement in the migratory insertion reaction is due to protonation/hydrogen bonding with a metal-carbonyl oxygen⁽²⁴⁾. A correlation has been observed between acidity and rate enhancement, with stronger acids giving a higher degree of rate enhancement. CCl_2HCOOH will increase the rate by a factor of 2.4 compared with the same concentration of acetic acid, whereas CF_3COOH increases the rate by a factor of 9.4. Thus, it is not surprising that rates of reaction are low when CH_2Cl_2 is used as a co-solvent. These results must be borne in mind when interpreting the results obtained in previous studies⁽¹⁾ when the hydrocarbonylation reactions were monitored using HPIR spectroscopy. When this mixed solvent system is used for such studies it is conceivable that carbonyl absorptions observed will be due to species which are formed in dichloromethane but are not participating as active species in the hydrocarbonylation of ethene. Consequently, such a mixed solvent system using CH_2Cl_2 as a dilutant, appears not to be appropriate for HPIR studies directed towards identifying species active in catalysis.

4.15 Tin(II) Bromide as a Promoter

The catalytic hydrocarbonylation of ethene was carried out with tin(II) bromide used as a promoter, in place of tin(II) chloride, in an attempt to investigate whether changing the substituent halogen groups attached to tin(II) had any effect on the rate and selectivity of the reaction.

Reaction code 4.36 (see Table 4.2 for experimental details)

*Components: 4.36 RhCl₃.3H₂O, SnBr₂, 37% HCl_(aq), CH₃COOH, CO,
C₂H₄*

Rh:Sn molar ratio = 1:2

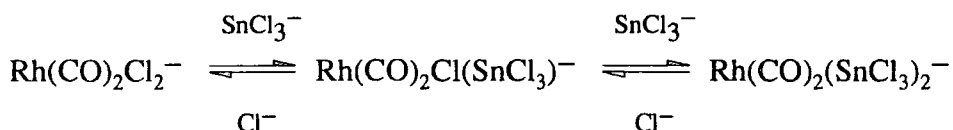
The rate of gas uptake was much higher for the rhodium-tin-bromide system [Reaction 4.36 (72 bar.hr⁻¹)] than for the rhodium-tin-chloride system [Reaction 4.7 (52 bar.hr⁻¹)]. The reason for this is unclear, however, since it is not reflected in the rate of propanoic acid production of 2.87 Mol.Kg⁻¹.hr⁻¹, which was not significantly higher than for the equivalent rhodium-tin-chloride catalytic system, [Reaction 4.7], which had a rate of 2.71 Mol.Kg⁻¹.hr⁻¹ and was also less selective towards production of propanoic acid. The rate difference is within the estimated experimental error of 5-10%. The results of Reaction 4.36 are not dissimilar to those obtained when using SnCl₂, suggesting that bromide may be displaced by the large amount of chloride ions in the system, and that activity may essentially be due to a rhodium-tin-chloride system. Bromide systems were not followed further, however.

4.16 Conclusions

[Rh(CO)₂Cl₂]⁻ was shown to be an active catalyst for the hydrocarbonylation of ethene to form propanoic acid, and is probably an active component also in the catalyst systems containing tin(II) chloride species (see HPIR studies in Chapter 5). Tin(II) chloride as a co-catalyst was shown to have an effect on the rhodium-chloride catalytic process, but a clear increase in the rate of propanoic acid production only occurs for systems employing a Sn:Rh molar ratio of 2:1. The full potential of SnCl₂ to promote rhodium-chloride catalysis has not been achieved, probably because of the tendency of the rhodium-tin complexes formed to revert to [Rh(CO)₂Cl₂]⁻ in large quantities, in the presence of the high concentration of chloride ions. However, HCl is necessary for catalytic activity, with lower concentrations of HCl_(aq) giving a decrease in the production of propanoic acid, but an increase in by-product formation, chiefly ethyl acetate. The role of HCl is attributed to the generation of an intermediate rhodium hydride by oxidative addition. Contrary to previous work⁽¹⁾ (see Table 4.1), introduction of benzyltriethylammonium chloride to rhodium-tin-chloride systems gave no enhancement in the catalytic activity, clearly indicating that the ability of [Bz(Et)₃N]⁺ to form ion-pairs with active species has little effect on the reaction.

Catalysis appears to be dependant on the nature of the rhodium species in solution, and their relative proportions, with $[\text{Rh}(\text{CO})_2\text{Cl}_2]^-$ and several $\text{Rh}(\text{I})\text{-CO-SnCl}_3$ complexes possibly related by a series of equilibria involving dissociation of SnCl_3^- and CO. Dissociation of SnCl_3^- and CO ligands from rhodium(I) trichlorostannate complexes has been shown to occur at room temperature (see Chapters 2 and 3), and therefore can most surely occur under high pressure, high temperature conditions. $[\text{Rh}(\text{CO})_2(\text{SnCl}_3)_3]^{2-}$ and $[\text{Rh}(\text{CO})(\text{SnCl}_3)_4]^{3-}$ are possible 18-electron precursors (see HPIR studies in Chapter 5), which are likely to form 16-electron catalytically active species via ligand dissociation.

In the presence of a high Cl^- concentration a Sn:Rh 1:1 catalytic system probably favours $[\text{Rh}(\text{CO})_2\text{Cl}_2]^-$ as an active species, with a low concentration of active Rh-Sn species. For 2:1 Sn:Rh systems the increase in the rate of propanoic acid production is probably a consequence of an increase in the concentration of active Rh-Sn species in solution. However, $[\text{Rh}(\text{CO})_2\text{Cl}_2]^-$ is probably still active in a 2:1 Sn:Rh system (the presence of both $[\text{Rh}(\text{CO})_2\text{Cl}_2]^-$ and $\text{Rh}(\text{I})\text{-CO-SnCl}_3$ complex(es) in solution has been reported for a 2:1 Sn:Rh system, see HPIR studies in Chapter 5). This can be illustrated by the equilibria shown below, which relate $[\text{Rh}(\text{CO})_2\text{Cl}_2]^-$ to possible catalytically active 16-electron $\text{Rh}(\text{I})\text{-SnCl}_3$ complexes such as $[\text{Rh}(\text{CO})_2\text{Cl}(\text{SnCl}_3)]^-$ and $[\text{Rh}(\text{CO})_2(\text{SnCl}_3)_2]^-$. Addition of tin favours a movement of the equilibrium to the right.



However, Sn:Rh molar ratios higher than 2:1 decrease activity and selectivity for propanoic acid, probably because the formation of 18-electron 5-coordinate rhodium(I) complexes containing several SnCl_3^- ligands becomes more favourable. Such complexes are not normally associated with catalytic activity.

Catalyst injection studies showed no improvement in the selectivity for propanoic acid when the active rhodium species was added at 180°C. Thus, while formation of by-products can occur during the heating process of the reaction, by-products form also during hydrocarbonylation, and are accentuated by low concentrations of $\text{HCl}_{(\text{aq})}$ and increasing amounts of tin(II) chloride beyond a Sn:Rh ratio of 2:1. The by-products commonly formed were chloroethane, ethyl propanoate, and ethyl acetate. The amounts formed varied, depending on the particular catalytic system.

The rate of catalytic reaction was shown to be dependant on the pressure of ethene in the system, with a possible first order relationship applying. The data for a series of experiments involving the use of deuterated liquid reagents were consistent with the protonation of rhodium species occurring during oxidative addition. The results of these experiments also indicate that the carbonylation step occuring during catalysis is rapid.

The significant differences between the results reported here, and those for rhodium-tin-chloride systems in previous studies⁽¹⁾, using the same autoclave and similar quantities of reagents for duplicated reactions, are difficult to quantify, although differences in stirring rate, or contamination from extraneous sources in previous work, remain the most likely explanations.

Further work in this area involving the use of catalyst injection equipment to provide further information about the formation of by-products at various temperatures during the heating process, would be extremely useful towards the understanding of the catalytic systems. Further studies of the effects of changing the amount of water and the concentration of HCl, should also provide further information about the changes in the by-product formation when these species are varied.

4.17 References

1. N.J. Winter, Ph.D. Thesis, University of Durham, 1991.
2. J.A. McCleverty, G. Wilkinson, *Inorg. Synth.*, 1960, 8, 711.
3. M.J. Cleare, W.P. Griffith, *J. Chem. Soc. (A)*, 1970, 2788.
4. F.A. Cotton, G. Wilkinson, *Advanced Inorganic Chemistry*, 5th Ed., J. Wiley & Sons, 1988.
5. R. Porta, H.M. Powell, R.J. Mawby, L.M. Venanzi, *J. Chem. Soc. (A)*, 1967, 455.
6. M.R. Churchill, K.K.G. Lin, *J. Am. Chem. Soc.*, 1974, 96, 76.
7. R.D. Cramer, R.V. Lindsey Jr., C.T. Prewitt, U.G. Stolberg, *J. Am. Chem. Soc.*, 1965, 87, 658.
8. C.Y. Hsu, M. Orchin, *J. Am. Chem. Soc.*, 1975, 97, 3553.
9. R. Uson, L.A. Oro, M.T. Pinillas, A. Arruebo, K.H.A.O. Starzewski, P.S. Pregosin, *J. Organometal. Chem.*, 1980, 192, 227.
10. W.A.G. Graham, *Inorg. Chem.*, 1968, 7, 315.
11. W. Jetz, P.B. Simons, J.A.J. Thompson, W.A.G. Graham, *Inorg. Chem.*, 1966, 5, 2217.
12. R.V. Lindsey Jr., G.W. Parshall, U.G. Stolberg, *J. Am. Chem. Soc.*, 1965, 87, 658.
13. G.W. Parshall, *J. Am. Chem. Soc.*, 1966, 88, 704.
14. R.C. Taylor, J.F. Young, G. Wilkinson, *Inorg. Chem.* 1966, 5, 20.
15. R.E. Hutton, V. Oakes, *Adv. Chem.*, 1976, 157, 123.
16. (a) J.F. Roth, *Chem. Tech.*, 1971, 1, 600.
(b) F.E. Paulik, U.S. Patent, 3 769 329, 1973.
17. D. Forster, *Adv. Organometal. Chem.*, 1978, 17, 255.
18. D. Forster, A. Hershman, D.E. Morris, *Catal. Rev. Sci. Eng.*, 1981, 23, 89.
19. J.F. Zemaitis, Jr., D.M. Clark, M. Rabal, N.C. Scrivner, *Handbook of Aqueous Electrolyte Thermodynamics*, Pub. American Institute of Chemical Engineers, New York, 1986, 841.
20. *Comprehensive Organometallic Chemistry*, Ed. G. Wilkinson, F.G.A. Stone, E.W. Abel, Pergamon Press, 1st Edition, 1982, 8, 882; *Organopalladium Compounds in Organic Synthesis and Catalysis*, B.M. Trost, T.R. Vehoeven.
21. R.D. Cramer, E.L. Jenner, R.V. Lindsey Jr., U.G. Stolberg, *J. Am. Chem. Soc.*, 1963, 85, 1691.
22. M. Kretschmer, *J. Organometal. Chem.*, 1983, 241, 87.
23. 'Chemistry of Tin', P.G. Harrison, 1989, Blackie & Sons, (Glasgow).
24. C.P. Horwitz, D.F. Shriver, *Adv. Organometal. Chem.*, 1984, 23, 219.

Chapter 5

High Pressure Infra - Red Studies of Rhodium - Tin - Chloride Catalytic Systems

5.1 Introduction

Chapter 2 was concerned with the use of Fourier Transform Infra-Red spectroscopy to probe the reaction chemistry between rhodium(I) carbonyl chloride complexes and tin(II) chlorides. Whilst this gave much information about the fundamental chemistry and provided information about the type of chemistry that could occur in the catalytic rhodium-tin systems described in Chapter 4, the hydrocarbonylation of ethene, it is not possible to predict with certainty whether the species formed at room temperature are the same as those which form under catalytic conditions. Thus, the species observed using Fourier Transform Infra-Red spectroscopy to probe a high pressure autoclave reaction should reveal much about the chemistry and the nature of the transformations occurring prior to, or during the catalytic process.

There are several aspects of the catalytic systems described in Chapter 4 which require investigation. The occurrence of a rhodium hydride species would establish the role of hydrogen chloride as it has been described in Chapter 4. The observation of rhodium(III) species by monitoring the position of the rhodium-carbonyl infra-red stretches would also provide information about an oxidative addition process. It is unclear, however, whether a species such as a $[\text{Rh-C}_2\text{H}_5]$ complex, would remain present for long enough in solution, in order to be observed, or whether migratory insertion of CO followed by reductive elimination to reform a rhodium(I) catalytic species would occur too quickly. Such a rhodium(III) species may also be formed in low concentrations, insufficient for carbonyl absorptions to be observed.

Of special interest is the hope of correlating, using the positions of the carbonyl absorptions, some of the known Rh(I)-CO-SnCl_3 complexes reported in Chapters 2 and 3 with any which may be observed by HPIR spectroscopy under catalytic conditions.

The reactions reported in this chapter by Fourier Transform Infra-Red spectroscopy were carried out in a Hastalloy C infra-red cell. This equipment is described in detail in Appendix 2, along with a full description of the experimental procedures in for this work.

Previous high pressure FT-IR studies of the rhodium-tin-chloride catalytic system⁽¹⁾ indicated that carboxylic acids were poor solvents for infra-red studies in the 1800-2300 cm^{-1} region, giving poor signal to noise ratio upon subtraction of the background. Therefore, most reactions were carried out in a mixed solvent system of

acetic acid/dichloromethane 5/12 v/v, which was found to improve spectral quality. These reactions generated many unidentified carbonyl absorptions, but did also show formation of the ion-pair $[A^+][Rh(CO)_2Cl_2]^-$ (where A^+ is the appropriate cation), and the occurrence of carbonyl absorptions likely to be due to Rh(I)-CO-SnCl₃ species, although no assignment to a particular complex was made.

Details of all reaction compositions used in this chapter are outlined in Section 5.7. All pressure values are quoted in psi, the units of the pressure gauge. [1 bar \equiv 14.50 psi]

Glacial acetic acid was degassed, and dichloromethane dried over molecular sieve and degassed, prior to use for all of the reactions described in this chapter.

5.2 RhCl₃/SnCl₂/Bz(Et)₃NCl as Catalytic Precursors under a Pressure of CO

The reactions were carried out in a mixed solvent system of acetic acid and dichloromethane. Reaction 5.2.1 detailed below, consists of the rhodium-tin-chloride catalytic system found to be active towards propanoic acid formation (see Section 4.6, Chapter 4), with RhCl₃, SnCl₂ and Bz(Et)₃NCl employed as the catalytic precursors, in a 1:2:3 molar ratio.

The two strong carbonyl absorptions at 2004 and 2079cm⁻¹, observed between 100 and 180°C, indicate the formation of $[Rh(CO)_2Cl_2]^-$ $\{[Bz(Et)_3N][Rh(CO)_2Cl_2] \nu(CO) - 2000, 2075cm^{-1}$ in CH₃COOH, see Table 2.1, Chapter 2}. A weak absorption at 2049cm⁻¹ was observed during the heating process and, although it remains unassigned, it is likely to be due to a rhodium(I) carbonyl chloride complex. A weak absorption was also observed at 2137cm⁻¹, and is possibly due to the rhodium(III) species Rh(CO)Cl₃ $\{\nu(CO) 2135cm^{-1}$ (KBr)}⁽²⁾. Rh(CO)Cl₃ is formed as an intermediate in the conversion of RhCl₃.3H₂O to Rh₂(CO)₄Cl₂. It is possible that Rh(CO)Cl₃ and the complex which has an absorption at 2049cm⁻¹ will affect the potential catalytic activity of the system. Between 170 and 180°C a carbonyl absorption appeared at 2012cm⁻¹ (see Figure 5.1), the position suggesting that formation of a rhodium(I) trichlorostannate species had occurred. An absorption at 1990cm⁻¹ was also observed at this temperature, and remains unassigned. The broadness and poor resolution of the carbonyl absorption in the regions 1980-2040cm⁻¹ meant that it was difficult to distinguish the absorption at 2004cm⁻¹,

attributed to $[\text{Rh}(\text{CO})_2\text{Cl}_2]^-$, but the persistence of this ion at 180°C was demonstrated by the associated absorption at 2079 cm^{-1} .

Reaction Code	Reagents	Rh:Sn: Bz(Et) ₃ NCl Molar Ratio	Temperature/ °C	$\nu(\text{CO})/\text{cm}^{-1}$ Observed	Assignment
5.2.1	RhCl ₃ .3H ₂ O SnCl ₂ Bz(Et) ₃ NCl 37%HCl _(aq) CO CH ₂ Cl ₂ CH ₃ COOH	1 : 2 : 3	100	2004 _w 2079 _w	$[\text{Rh}(\text{CO})_2\text{Cl}_2]^-$
			120	2004 _s 2079 _s 2049 _w 2137 _s	$[\text{Rh}(\text{CO})_2\text{Cl}_2]^-$ Unassigned Rh(CO)Cl ₃
			140-160	2004 _s 2079 _s	$[\text{Rh}(\text{CO})_2\text{Cl}_2]^-$
			170	2007 _s 2080 _s 2017 _{sh}	$[\text{Rh}(\text{CO})_2\text{Cl}_2]^-$ Rh-Sn species
			180	1990 _s 2012 _m 2049 _w 2079 _s 2137 _w	Unassigned Rh-Sn species Unassigned $[\text{Rh}(\text{CO})_2\text{Cl}_2]^-$ Rh(CO)Cl ₃
			45 (Upon cooling)	1983 _w 2018 _w 2044 _s	Unassigned Rh-Sn species Unassigned

The nature of the reaction conditions and the solvent system employed, mean that it is very difficult to accurately assign the positions of the carbonyl absorptions observed. This is mainly due to severe broadening of absorptions and poor signal to noise ratio, which prevents a clear distinction between absorptions which are close to each other, and also prevents the observation of weak absorptions. The error associated with identifying the position of the maximum of a peak is also increased.

There was a gradual decrease in the intensity of all the carbonyl absorptions on maintaining the temperature at 180°C for a period of 1 hour. This indicated that catalyst decomposition slowly occurs throughout the period of catalysis and may contribute to the usual decrease observed in the rate of propanoic acid production towards the end of the reaction period.

Based on the data available, the absorptions observed at 2004 and 2079 cm^{-1} could be due to either $[\text{H}_{\text{solv}}^+][\text{Rh}(\text{CO})_2\text{Cl}_2^-]$ or $[\text{Bz}(\text{Et})_3\text{N}][\text{Rh}(\text{CO})_2\text{Cl}_2]$. Studies reported in Chapter 2 have shown that both complexes have similar carbonyl frequencies in THF, with those for $[\text{H}_{\text{solv}}^+][\text{Rh}(\text{CO})_2\text{Cl}_2^-]$ approximately 8 cm^{-1} higher than those for $[\text{Bz}(\text{Et})_3\text{N}^+][\text{Rh}(\text{CO})_2\text{Cl}_2^-]$:

<u>Rh Complex</u>	<u>$\nu(\text{CO})/\text{cm}^{-1}$ in THF</u>
$[\text{H}_{\text{solv}}^+][\text{Rh}(\text{CO})_2\text{Cl}_2^-]$	1992 _s 2070 _s
$[\text{Bz}(\text{Et})_3\text{N}^+][\text{Rh}(\text{CO})_2\text{Cl}_2^-]$	1984 _s 2062 _s

Since the frequencies observed at 2004 and 2079 cm^{-1} in $\text{CH}_2\text{Cl}_2/\text{CH}_3\text{COOH}$ are higher by 4 cm^{-1} than those expected for $[\text{Bz}(\text{Et})_3\text{N}][\text{Rh}(\text{CO})_2\text{Cl}_2]$ in acetic acid ($\nu(\text{CO}) - 2000, 2075\text{cm}^{-1}$), on comparison with infra-red data in THF it is conceivable that both $[\text{H}_{\text{solv}}^+][\text{Rh}(\text{CO})_2\text{Cl}_2^-]$ and $[\text{Bz}(\text{Et})_3\text{N}][\text{Rh}(\text{CO})_2\text{Cl}_2]$ may exist in solution, or alternatively that the mixed solvent system causes the observed differences in frequencies.

Following the studies described in Chapters 2 and 3, the absorption at 2012 cm^{-1} is assigned to a Rh(I)-CO-SnCl₃ complex, although the broadness of the absorption prevents the specific complex from being identified. $[\text{Rh}(\text{CO})_2(\text{SnCl}_3)_3]^{2-}$, $[\text{Rh}(\text{CO})(\text{SnCl}_3)_2\text{Cl}]^{2-}$, $[\text{Rh}(\text{CO})(\text{SnCl}_3)_4]^{3-}$ and $[\text{Rh}(\text{CO})(\text{SnCl}_3)_3]^{2-}$ are possibilities based on the known infra-red data shown below:

<u>Rh(I)-SnCl₃ Complex</u>	<u>$\nu(\text{CO})/\text{cm}^{-1}$</u>	<u>Reference</u>
$[\text{Rh}(\text{CO})(\text{SnCl}_3)_3]^{2-}$	2005 _s (KBr)	3
$[\text{PPN}]_2[\text{Rh}(\text{CO})_2(\text{SnCl}_3)_3]$	2010 _s 2060 _w (CH_2Cl_2)	4
$[\text{Bz}(\text{Et})_3\text{N}]_2[\text{Rh}(\text{CO})_2(\text{SnCl}_3)_3]$	2018 _s 2069 _w (CH_2Cl_2)	Chapter 3
$[\text{Bz}(\text{Et})_3\text{N}]_2[\text{Rh}(\text{CO})(\text{SnCl}_3)_2\text{Cl}]$	2013 _s (nujol)	Chapter 3
$[\text{Bz}(\text{Et})_3\text{N}]_3[\text{Rh}(\text{CO})(\text{SnCl}_3)_4]$	2012 _s (nujol)	Chapter 5

$[\text{Rh}(\text{CO})_2(\text{SnCl}_3)_3]^{2-}$ and $[\text{Rh}(\text{CO})(\text{SnCl}_3)_4]^{3-}$ were isolated from the reactions of rhodium(I) carbonyl chlorides with tin(II) chlorides (see Chapters 2 and 3), are both highly likely catalytic precursors. Data reported in Chapters 2 and 3 indicated that they are closely related to each other and to other rhodium (I) carbonyl trichlorostannate complexes e.g. $[\text{Rh}(\text{CO})(\text{SnCl}_3)_2\text{Cl}]^{2-}$, $[\text{Rh}(\text{CO})_2(\text{SnCl}_3)_2]^-$ and $[\text{Rh}(\text{CO})_2\text{Cl}(\text{SnCl}_3)]^-$ by a sequence of facile reactions involving dissociation of SnCl_3^- and CO. These results indicate that possible

Figure 5.1 Infra-Red carbonyl absorptions observed at 180°C for a $\text{RhCl}_3 \cdot 3\text{H}_2\text{O}/\text{SnCl}_2/\text{Bz}(\text{Et})_3\text{NCl}$ catalytic system under CO pressure in acetic acid/ CH_2Cl_2 and c.HCl (Reaction 5.2.1)

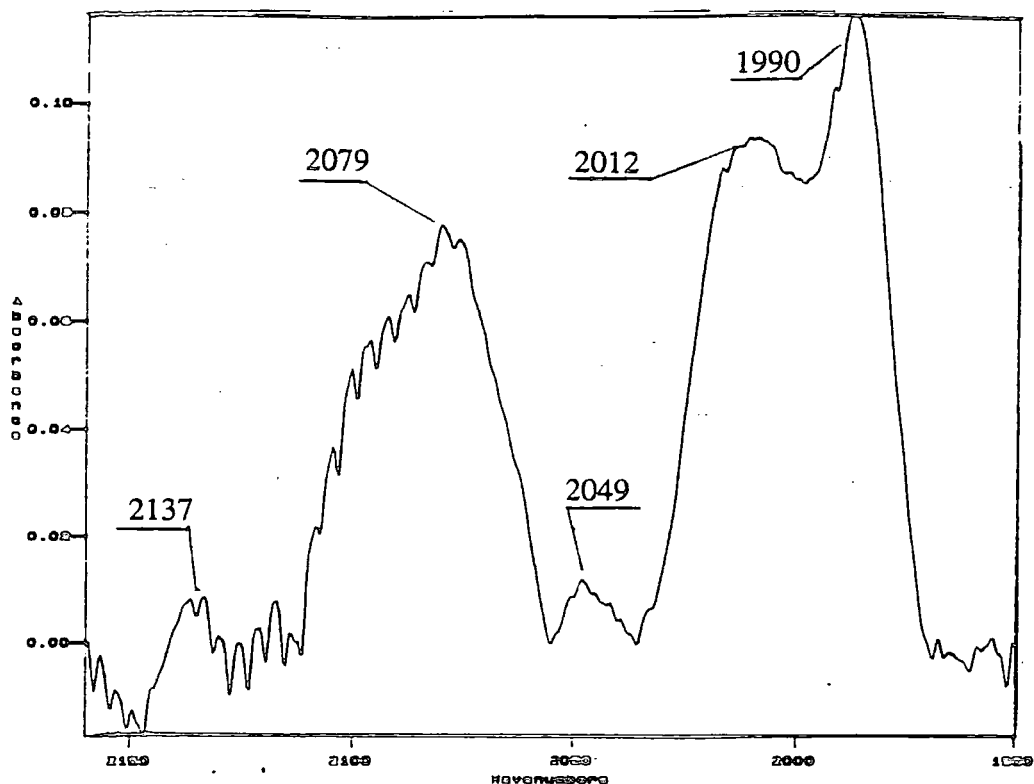
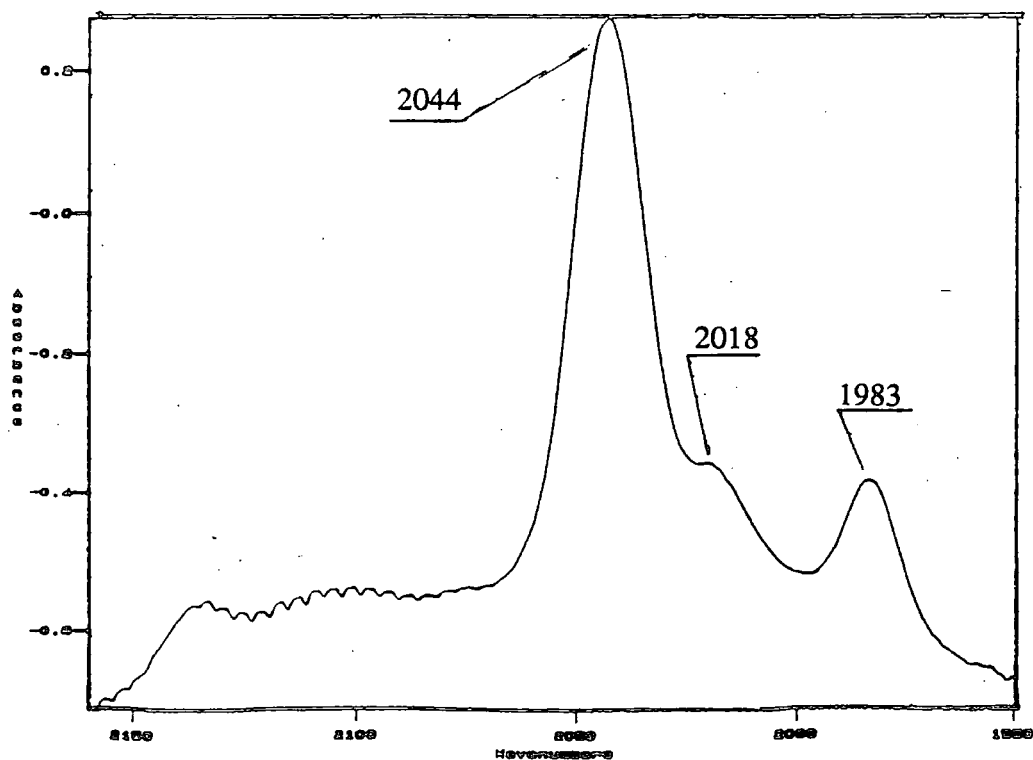
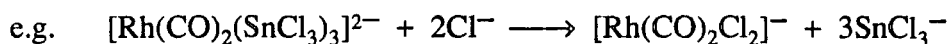


Figure 5.2 Infra-Red carbonyl absorptions observed upon cooling Reaction 5.2.1 to 45°C



18-electron precursors such as $[\text{Rh}(\text{CO})_2(\text{SnCl}_3)_3]^{2-}$ and $[\text{Rh}(\text{CO})(\text{SnCl}_3)_4]^{3-}$ will, under high pressure and high temperature conditions, undergo ligand dissociation to form 16-electron complexes normally associated with catalytic activity. There is also the possibility that more than one Rh(I)-CO-SnCl₃ complex will be present in solution at a particular time. Therefore, it is possible that more than one Rh-Sn complex can be catalytically active in rhodium-tin-chloride systems. Since absorptions due to $[\text{Bz}(\text{Et})_3\text{N}][\text{Rh}(\text{CO})_2\text{Cl}_2]^-$, which is an active catalyst in its own right (see Chapter 4), are also observed in Reaction 5.2.1, it is likely that both $[\text{Rh}(\text{CO})_2\text{Cl}_2]^-$, and rhodium(I)-trichlorostannate species will both be catalytically active for the 2:1 Sn:Rh system.

Chloride ions have been shown to displace SnCl_3^- from 5-coordinate rhodium(I) carbonyl trichlorostannate complexes in solution (see Chapter 7, Section 7.2.5),



and since aqueous HCl is present in the catalytic system this is probably the reason why the concentration of Rh-Sn species in Reaction 5.2.1 is not more pronounced. Also, since in Reaction 5.2.1 $[\text{Rh}(\text{CO})_2\text{Cl}_2]^-$ is present in a higher concentration than the Rh(I)-CO-SnCl₃ species [$\nu(\text{CO})$ 2012cm⁻¹], this may explain why the promotional effect of SnCl₂, reported in Chapter 4, when the Sn:Rh molar ratio is 2:1, is not greater, and probably also accounts for the fact that no promotional effect is observed with a Sn:Rh molar ratio of 1:1 i.e. very low concentrations of active Rh/Sn species but a high concentration of $[\text{Rh}(\text{CO})_2\text{Cl}_2]^-$. The high reaction temperature may also inhibit the formation of SnCl_3^- complexes.

Upon cooling Reaction 5.2.1 to 45°C, carbonyl absorptions were observed at 1983, 2018 and 2044cm⁻¹ (Figure 5.2). The absorptions at 1983cm⁻¹ (45°C, see Figure 5.2) and 1990cm⁻¹ (180°C, see Figure 5.1) are probably due to the same complex. These absorptions, along with the absorption at 2044cm⁻¹, remain uncharacterised. The pattern of absorptions at 1983_w and 2044_scm⁻¹ observed at 45°C is not consistent with them arising from the same species in solution, and consequently the absorptions observed at 1990 and 2049cm⁻¹ at 180°C are also unlikely to be due to the same species. The absorption at 1990cm⁻¹ does not appear until the temperature approaches 180°C, whereas the absorption at 2049cm⁻¹ is seen throughout the heating process.

5.3 RhCl₃/SnCl₂/Bz(Et)₃NCl as Catalytic Precursors under a Pressure of CO and C₂H₄

As a continuation of Reaction 5.2.1 a consideration of a rhodium-tin-chloride catalytic system under a pressure of CO and C₂H₄ was necessary, because although a rhodium(I) carbonyl trichlorostannate species was identified in Reaction 5.2.1, ethene was not present in the system, and therefore strict catalytic conditions did not apply.

Reaction Code	Reagents	Rh:Sn: Bz(Et) ₃ NCl Molar Ratio	Temperature/ °C	$\nu(\text{CO})/\text{cm}^{-1}$ Observed	Assignment
5.3.1	RhCl ₃ .3H ₂ O SnCl ₂ Bz(Et) ₃ NCl 37% HCl _(aq) CO C ₂ H ₄ CH ₂ Cl ₂ CH ₃ COOH	1 : 2 : 3	120-170 180	2003 _s , 2080 _s , 2052 _w 1988 _w , 2003 _s , 2080 _s , 2017 _w , 2045 _w	[Rh(CO) ₂ Cl ₂] ⁻ Unassigned Unassigned [Rh(CO) ₂ Cl ₂] ⁻ Rh-Sn species Unassigned

The frequencies of the carbonyl absorptions, observed during the heating process of Reaction 5.3.1, were similar to those observed for Reaction 5.2.1, with no further absorptions observed upon introduction of ethene to the system. Repetition of this reaction gave similar results, with no rhodium(I) or rhodium(III) species consistent with the presence of complexes containing the ethene ligand or an ethyl group being observed. Indeed, for some reason which has not been established, the introduction of C₂H₄ to the system generally leads to a decrease in spectral quality, with problems arising from gas bubbles displacing the solution from between the CaF₂ windows of the autoclave.

Upon cooling to 40°C only the strong absorption at 2045cm⁻¹ was observed.

5.4 Studies of Systems Containing Model Rhodium(I) Carbonyl Chloride Complexes

[Bz(Et)₃N][Rh(CO)₂Cl₂] was shown to be a catalytically species in the homogeneous catalysed hydrocarbonylation of ethene reported in Chapter 4. It has not been conclusively proven, however, whether this is the solitary active catalytic species in

the absence of tin(II) chloride, or whether other species are formed throughout the heating process of the reaction. A series of studies were carried out under high pressure conditions, monitored by FT-IR spectroscopy, to establish the role of $[\text{Bz}(\text{Et})_3\text{N}][\text{Rh}(\text{CO})_2\text{Cl}_2]^-$. In doing so it was hoped that the positions of its carbonyl absorptions in the mixed solvent would further confirm the presence of $[\text{Rh}(\text{CO})_2\text{Cl}_2]^-$ in Reactions 5.2.1 and 5.3.1.

Reaction Code	Reagents	Temperature/ °C	$\nu(\text{CO})/\text{cm}^{-1}$ Observed	Assignment
5.4.1	* $[\text{Rh}(\text{CO})_2\text{Cl}_2]^-$ 37% $\text{HCl}_{(\text{aa})}$ CO CH_2Cl_2 CH_3COOH	100-180 25 (Upon cooling)	2009 _s 2082 _s 2002 _m 2077 _m 2043 _s 2137 _s	$[\text{Rh}(\text{CO})_2\text{Cl}_2]^-$ $[\text{Rh}(\text{CO})_2\text{Cl}_2]^-$ Unassigned $\text{Rh}(\text{CO})\text{Cl}_3$

* Cation = $[\text{Bz}(\text{Et})_3\text{N}]^+$

The absorptions observed at 2009 and 2082 cm^{-1} started to form at 100°C and steadily increased in intensity as the temperature was increased to 180°C, but then began to decrease in intensity with time, as this temperature was maintained. No other absorptions were observed until the reaction mixture was cooled to 25°C, when strong absorptions were observed at 2043 cm^{-1} and 2137 cm^{-1} ($\text{Rh}(\text{CO})\text{Cl}_3$ $\nu(\text{CO})$ (KBr) 2135 cm^{-1})⁽²⁾ along with absorptions at 2002 and 2077 cm^{-1} arising from $[\text{Rh}(\text{CO})_2\text{Cl}_2]^-$.

The absorptions observed in Reaction 5.4.1 show that $[\text{Rh}(\text{CO})_2\text{Cl}_2]^-$ is the predominant species in solution under catalytic conditions and is most likely the catalytically active species in the hydrocarbonylation of ethene, in the absence of tin(II) chloride (see Chapter 4). No other carbonyl absorptions are observed.

Reaction 5.4.1 was also carried out under a mixed pressure of CO and C_2H_4 . No additional carbonyl absorptions were observed, however, with those formed assigned to the same complexes as for Reaction 5.4.1. Both CH_3COOH and $\text{C}_2\text{H}_5\text{COOH}$ have absorptions in the region 1500-1750 cm^{-1} , and absorptions for a $[\text{Rh}-\text{COC}_2\text{H}_5]$ complex are also expected to occur in this region. Such a moiety will form upon migration of an ethyl group onto an adjacent CO ligand which is coordinated to rhodium. No absorptions consistent with a $[\text{Rh}-\text{COC}_2\text{H}_5]$ complex were detected, however, upon subtraction of CH_3COOH and $\text{C}_2\text{H}_5\text{COOH}$ absorptions. GC analysis of the solutions obtained from this reaction and Reaction 5.4.1 did, however,

confirm the formation of propanoic acid as a reaction product, suggesting that a $[\text{Rh}-\text{COC}_2\text{H}_5]$ complex was either formed in too low a concentration to be observed, or that insertion and elimination reactions occur rapidly in solution..

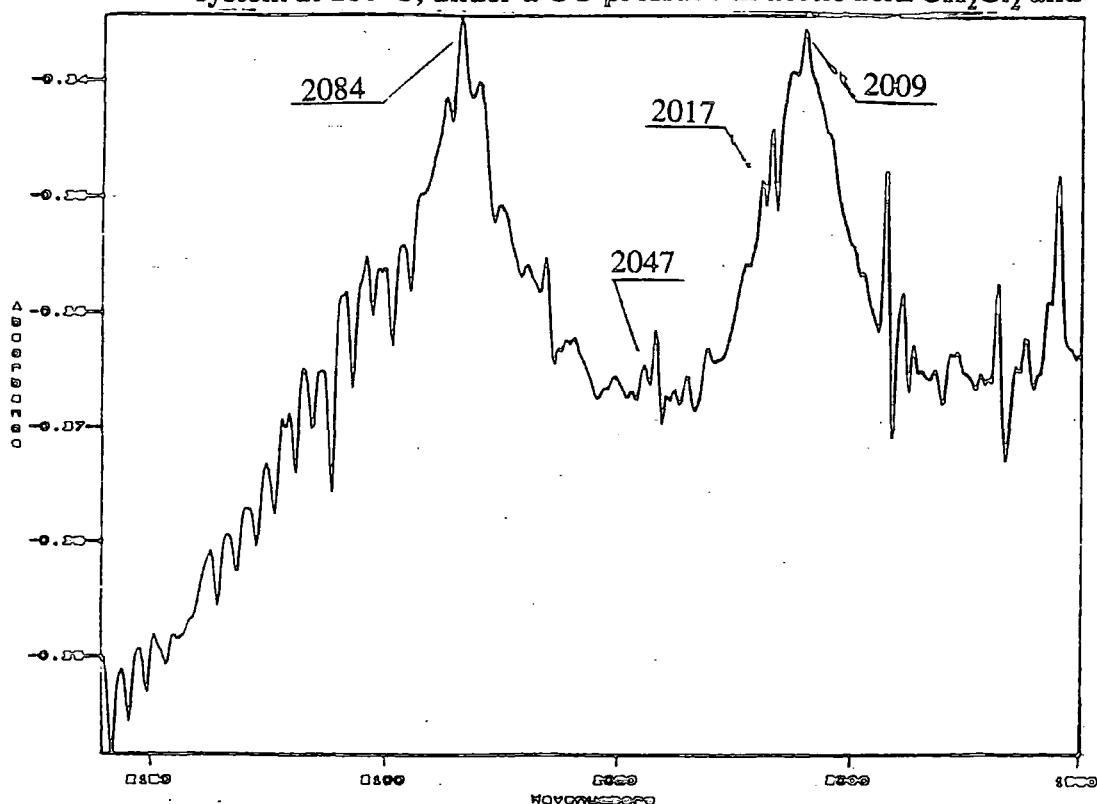
The effect of adding tin(II) chloride to Reaction 5.4.1 was also investigated.

Reaction Code	Reagents	Rh:Sn Molar Ratio	Temperature/ °C	$\nu(\text{CO})/\text{cm}^{-1}$ Observed	Assignment
5.4.2	* $[\text{Rh}(\text{CO})_2\text{Cl}_2]^-$ SnCl ₂ 37% $\text{HCl}_{(\text{aq})}$ CO CH ₂ Cl ₂ CH ₃ COOH	1 : 2	140-180	2009 _s 2084 _s 2017 _w 2047 _w	$[\text{Rh}(\text{CO})_2\text{Cl}_2]^-$ Rh-Sn species Unassigned

* Cation = $[\text{Bz}(\text{Et})_3\text{N}]^+$

In theory, the species observed for Reaction 5.4.2 should be the same as those observed for Reaction 5.2.1, since formation of $[\text{Rh}(\text{CO})_2\text{Cl}_2]^-$ occurs at approximately 100°C (Reaction 5.2.1). Indeed, the carbonyl absorptions observed for Reaction 5.4.2 were similar in frequency to those observed for Reaction 5.2.1, albeit the spectral quality was very poor in acetic acid. Changes in the absorptions for Reaction 5.4.2 started to occur at 140°C, with the appearance of a weak absorption at 2017 cm^{-1} consistent with the formation of Rh(I)-CO-SnCl₃ complex. The absorptions observed at 180°C are shown in Figure 5.3. All of the absorptions gradually decreased in intensity upon reaching the favoured catalytic reaction temperature of 180°C, similar to other reactions described in this chapter.

Figure 5.3 Carbonyl absorptions observed for a $[\text{Rh}(\text{CO})_2\text{Cl}_2]^-/\text{SnCl}_2$ system at 180°C , under a CO pressure in acetic acid/ CH_2Cl_2 and



A reaction was also undertaken starting with a rhodium(I) carbonyl trichlorostannate product isolated as described in Chapter 3, Section 3.2.2 from the reaction of $\text{Rh}_2(\text{CO})_4\text{Cl}_2$ with SnCl_2 and $\text{Bz}(\text{Et})_3\text{NCl}$, and found to be catalytically active (Chapter 4). The product contained $[\text{Bz}(\text{Et})_3\text{N}]_2[\text{Rh}(\text{CO})_2(\text{SnCl}_3)_3]$ as the main component, along with probable smaller quantities of $[\text{Bz}(\text{Et})_3\text{N}]_4[\text{Rh}(\text{CO})(\text{SnCl}_3)_4]$ and $[\text{Bz}(\text{Et})_3\text{N}]_2[\text{Rh}(\text{CO})(\text{SnCl}_3)_2\text{Cl}]$. Unidentified rhodium carbonyl containing species were also present in small quantities.

Reaction Code	Reagents	Temperature/ °C	$\nu(\text{CO})/\text{cm}^{-1}$ Observed	Assignment
5.4.3	$*[\text{Rh}(\text{CO})_2(\text{SnCl}_3)_3]^{2-}$ (Major component) $*[\text{Rh}(\text{CO})(\text{SnCl}_3)_4]^{3-}$ $*[\text{Rh}(\text{CO})(\text{SnCl}_3)_2\text{Cl}]^{2-}$ (Minor components) 37% $\text{HCl}_{(\text{aq})}$ CO CH_2Cl_2 CH_3COOH	140-180 180 (30mins)	1986 _w 2013 _w 2045 _{vw} 2080 _w 1988 _s 2044 _s	Unassigned Rh-Sn species Unassigned $[\text{Rh}(\text{CO})_2\text{Cl}_2]^-?$ Unassigned Unassigned

* Cation = $[\text{Bz}(\text{Et})_3\text{N}]^+$

The spectra obtained for Reaction 5.4.3 were of very poor quality, but the weak absorptions observed between 140 and 180°C (Figure 5.4) were similar to those observed for other rhodium-tin-halide systems reported in this chapter (Reactions 5.2.1 and 5.2.4). An unassigned absorption at 1986cm⁻¹ was also observed, and the absorption at 2080cm⁻¹ remains a mystery, since the absence of a band at around 2000cm⁻¹ suggests that it cannot be assigned to [Rh(CO)₂Cl₂]⁻. The absorption at 2013cm⁻¹ indicates that a rhodium(I) carbonyl trichlorostannate species remains in solution. Maintaining the temperature at 180°C for a 30 minute period led to complete loss of the absorption at 2013cm⁻¹, suggesting that this catalytic system will only be active over a short time period.

On cooling to 50°C absorptions were observed at 1985_w, 2019_m, 2044_s and 2137_m cm⁻¹ (see Figure 5.5). It is interesting that spectral quality is better for most reactions described in this chapter, upon cooling of the solutions, with high temperatures leading to poor spectral quality.

5.5 Studies with Acetic Acid as a Single Solvent

A reaction described in Chapter 4 showed that catalytic activity was much less when a mixed solvent system of acetic acid/dichloromethane 5/12 v/v was used than when acetic acid was used alone. Thus, the possibility arises that rhodium complexes formed in dichloromethane may be different from those formed in acetic acid, and consequently the catalytic activity of the system affected. Studies under atmospheric pressure conditions, reported in Chapter 2, did not indicate extreme variations in chemistry upon changing solvents, but since catalytic activity takes place under different conditions, differences in chemistry under these different conditions cannot be ruled out.

Spectral quality was poor for reactions in acetic acid as a single solvent. Tests carried out on the FT-IR spectrometer showed that when neat acetic acid was used as solvent, the signal at the detector was extremely low, due to acetic acid being a very strongly absorbing species in the infra-red region. In most reactions attempted, no signal at all was detected. The signal was only slightly better for a mixed CH₂Cl₂/CH₃COOH solvent system, and is probably one reason why weak, poor quality spectra were observed for most of the reactions. The signal voltage is an inherent property of the spectrometer and cannot be easily adjusted without major modifications. The length of cell path and the design of the light path to the

Figure 5.4 Carbonyl absorptions observed between 140 and 180°C for Reaction 5.4.3

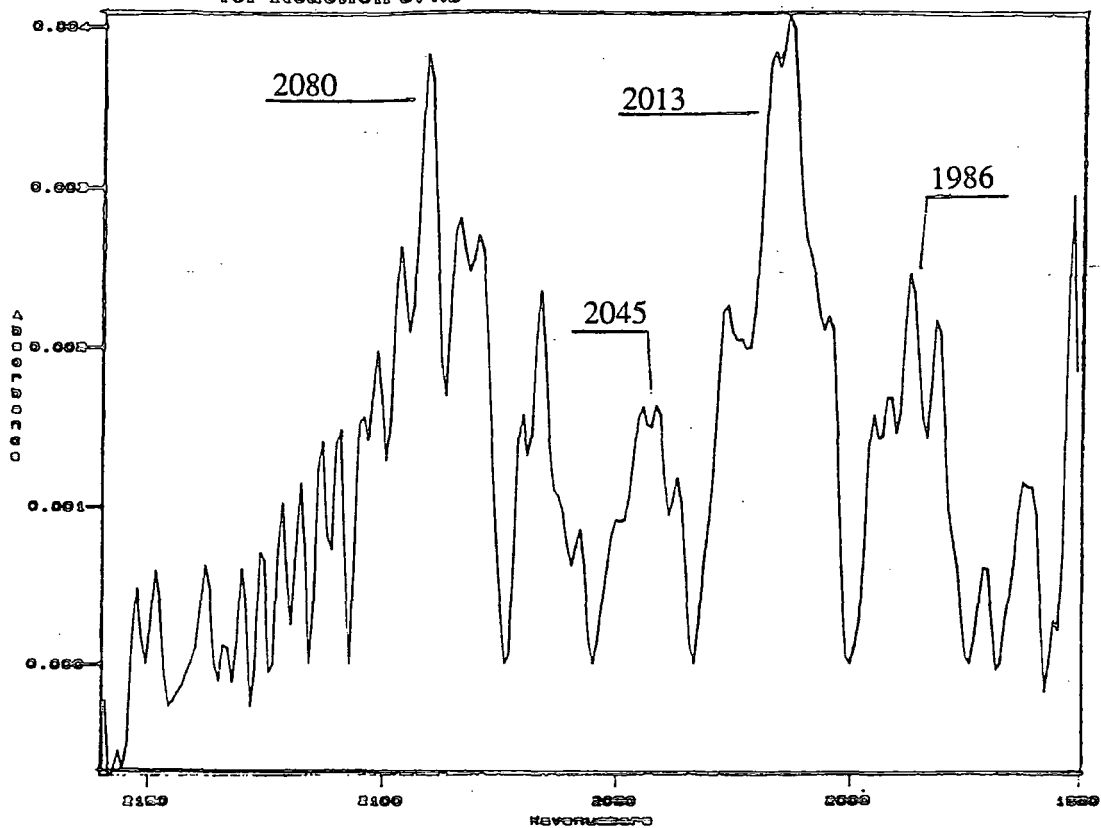
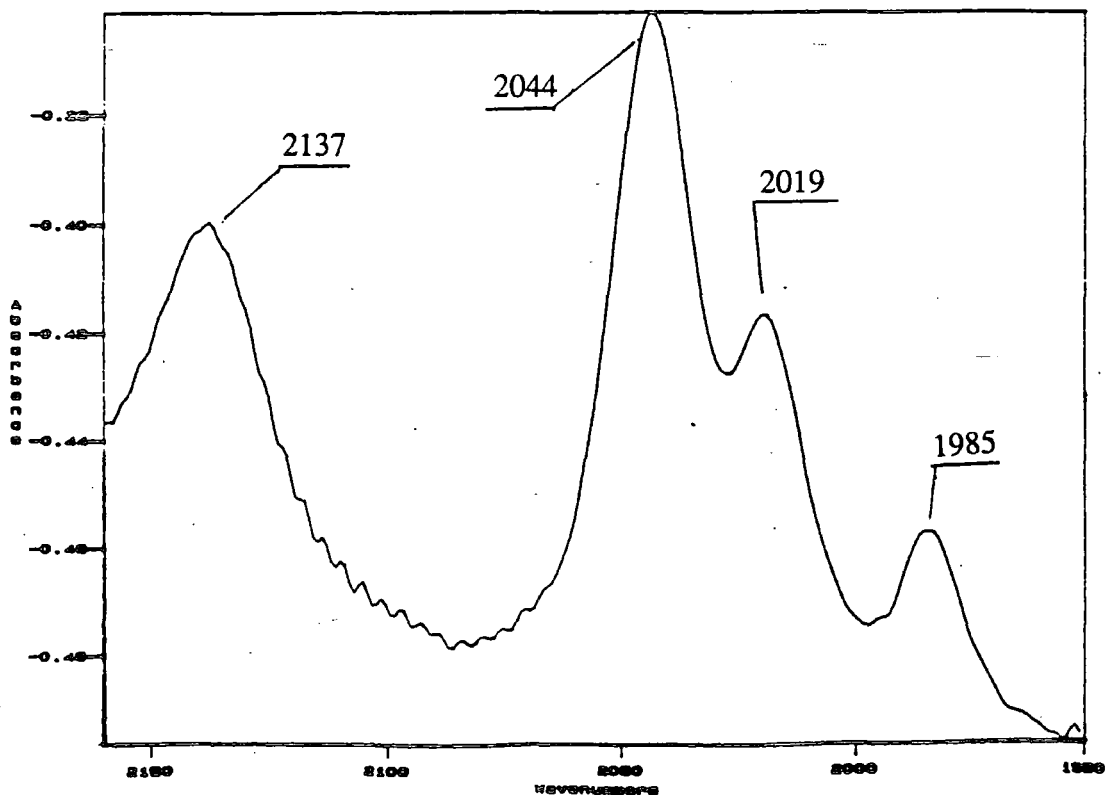


Figure 5.5 Carbonyl absorptions observed upon cooling Reaction 5.4.3 to 50°C



windows, along with the relatively thick CaF₂ windows, all necessary for high pressure studies, clearly do not assist the possibility of achieving a higher signal intensity. As a result, further experiments in neat acetic acid were abandoned. Nevertheless, because of the need to monitor high pressure, high temperature reactions, initial attempts were made as described below:

5.5.1 [Bz(Et)₃N][Rh(CO)₂Cl₂]/SnCl₂/CO/C₂H₄/37%HCl_(aq)/CH₃COOH

5.5.2 RhCl₃.3H₂O/SnCl₂/Bz(Et)₃NCl/CO/C₂H₄/38%HCl_(aq)/CH₃COOH

5.5.3 [Bz(Et)₃N][Rh(CO)₂Cl₂]/Bz(Et)₃NSnCl₃/CO/37%HCl_(aq)/CH₃COOH

For Reaction 5.5.1 carbonyl absorptions at 2004 and 2078cm⁻¹, assigned to [Rh(CO)₂Cl₂]⁻, appeared from a temperature of 50°C upwards. These became very weak, broad, and poorly resolved at temperatures greater than 100°C, and new ν(CO) absorptions were not detected. Upon cooling, the unassigned strong absorption at 2043cm⁻¹ was observed, and is consistent with a rhodium-monocarbonyl complex. Spectral quality was very poor for Reactions 5.5.2 and 5.5.3 and no ν(CO) absorptions were detected. Within the limitations of the measurements, the change in solvent system did not seem to lead to any major change in the chemistry taking place during the heating process, though observation of absorptions for Reaction 5.5.1 was clearly difficult. Thus, the decrease in catalytic activity, reported in Chapter 4 using a mixed CH₃COOH/CH₂Cl₂ solvent system rather than CH₃COOH alone is probably due to other factors, one of which is the electronic effects caused by acetic acid forming a hydrogen bond with the oxygen atom of a carbonyl group attached to rhodium, thereby promoting migratory insertion⁽⁵⁾. Ideally, however, high pressure infra-red studies should be carried out in the absence of CH₂Cl₂ to give an accurate representation of the catalytic system.

The observation of high quality spectra is clearly hampered by the constraints placed on the systems discussed in this chapter. Problems caused by the solvent system and the reaction conditions used, affect the spectral quality, but the present specifications of the spectrometer and the experimental set-up seem unsuitable for observation of reactions carried out in acetic acid. Thus, the generation of further useful results using FT-IR spectroscopy as an experimental probe for this type of catalytic reaction in highly polar media, is likely to be minimal unless major modifications are made to the design of the equipment.

5.6 Conclusions

The results reported in this chapter have indicated the formation of several rhodium(I) species relevant to the hydrocarbonylation of ethene. $[\text{Rh}(\text{CO})_2\text{Cl}_2]^-$, formed in solution as a salt with either $[\text{H}_{\text{soln}}]^+$ and/or $[\text{Bz}(\text{Et})_3\text{N}]^+$ counter ions, has been detected under most conditions. Addition of tin(II) chloride to the rhodium-chloride systems causes formation of a Rh(I)-CO-SnCl₃ species under the temperature and pressure conditions used for catalysis, with the infra-red data obtained consistent with formation of either of the following complexes: $[\text{Rh}(\text{CO})_2(\text{SnCl}_3)_3]^{2-}$, $[\text{Rh}(\text{CO})(\text{SnCl}_3)_2\text{Cl}]^{2-}$, $[\text{Rh}(\text{CO})(\text{SnCl}_3)_4]^{3-}$ and $[\text{Rh}(\text{CO})(\text{SnCl}_3)_3]^{2-}$. The $\nu(\text{CO})$ data did not allow differentiation between these possibilities, all of which have a strong absorption in the region 2005-2018cm⁻¹. Data reported in Chapters 2 and 3 indicated that the above Rh-SnCl₃ complexes are related by a series of facile reactions, and it is therefore conceivable that several Rh-SnCl₃ complexes will be present in solution at high temperature and high pressure. High pressure infra-red data strongly indicate that in the rhodium-tin-chloride catalytic systems reported in Chapter 4, rhodium(I) trichlorostannate species and $[\text{Rh}(\text{CO})_2\text{Cl}_2]^-$ will both be present in solution under catalytic conditions, and it is therefore conceivable that both Rh/Cl and Rh/SnCl₃ species are catalytically active in a rhodium-tin-chloride system.

Several unexplained absorptions were also observed, which demonstrate that the chemistry occurring under high pressure and high temperature conditions can differ, although not markedly so, from reactions carried out under atmospheric pressure conditions at room temperature (see Chapter 2). Generally, on maintaining the reactions reported in this chapter at the normal hydrocarbonylation temperature of 180°C, there was a gradual decrease in the intensity of carbonyl absorptions associated with catalytically active species, over a short time period e.g. 1 hour, with some absorptions completely disappearing. The data therefore indicates that these systems will only remain catalytically active for a short time period.

There is no evidence in this work for species containing coordinated H, C₂H₄, C₂H₅ or C₂H₅CO ligands, suggesting that intermediate complexes incorporating them as ligands were either too short lived or formed in too low a concentration to be observed.

5.7 Summary of Reagents and Reaction Conditions

* Cation = [Bz(Et)₃N]⁺

Reaction Code	Reagents	Solvents	Temperature Range/°C	Pressure Range/psi	Gases
5.2.1	RhCl ₃ ·3H ₂ O 0.190mmol SnCl ₂ 0.374mmol Bz(Et) ₃ NCl 0.527mmol 37%HCl _(aq) 0.75ml	CH ₃ COOH 5ml CH ₂ Cl ₂ 12ml	20-180	600-1050	CO - 600psi
5.3.1	RhCl ₃ ·3H ₂ O 0.186mmol SnCl ₂ 0.374mmol Bz(Et) ₃ NCl 0.546mmol 37%HCl _(aq) 0.75ml	CH ₃ COOH 5ml CH ₂ Cl ₂ 12ml	20-180	800-1350	CO - 450psi C ₂ H ₄ - 350psi
5.4.1	*[Rh(CO) ₂ Cl ₂] ⁻ 0.165mmol 37%HCl _(aq) 0.75ml	CH ₃ COOH 5ml CH ₂ Cl ₂ 12ml	20-180	1000-1400	CO - 1000psi
5.4.2	*[Rh(CO) ₂ Cl ₂] ⁻ 0.187mmol SnCl ₂ 0.374mmol 37%HCl _(aq) 0.75ml	CH ₃ COOH 5ml CH ₂ Cl ₂ 12ml	20-180	600-975	CO - 600psi
5.4.3	Rh-SnCl ₃ mixture 136.4mg 37%HCl _(aq) 0.75ml	CH ₃ COOH 5ml CH ₂ Cl ₂ 12ml	20-180	700-1100	CO - 700psi

5.8 References

1. N.J. Winter, Ph.D Thesis, University of Durham, 1991.
2. R. Colton, R.H. Farthing, J.E. Knapp, *Australian J. Chem.*, 1970, 23, 1351.
3. J.V. Kingston, G.R. Scollary, *J. Chem. Soc. (A)*, 1971, 3399.
4. M. Kretschmer, P.S. Pregosin, H. Rüegger, *J. Organometal. Chem.*, 1983, 241, 87.
5. C.P. Horwitz, D.F. Shriver, *Adv. Organometal. Chem.*, 1984, 23, 219.

Chapter 6

Studies of the Role of Triphenylphosphine and
Zinc(II) Chloride as co-catalysts in the Rhodium
Catalysed Hydrocarbonylation of Ethene
and
The Hydrocarbonylation of Alkenes Other than
Ethene

6.1 Introduction

This chapter describes the synthesis of several known rhodium(I) trichlorostannate complexes containing triphenylphosphine as a ligand, and a study of their effectiveness as catalysts in the homogeneous catalysed hydrocarbonylation of ethene. Platinum-phosphine complexes in conjunction with tin(II) chloride have been used previously to homogeneously catalyse both hydrogenation and hydroformylation reactions⁽¹⁻¹³⁾. Of particular use are metal complexes of low symmetry containing mixed ligands which exhibit variable steric and electronic parameters. Excellent results have also been achieved using a palladium complex⁽¹⁴⁾. The catalytic activity is dependant on the size and electronic character of the phosphine, the cone angle, the base strength, and the nature of the substituents attached to the phosphine⁽¹⁵⁾. The degree of steric crowding around the metal centre, which depends on the nature of the phosphine, and the actual position of the phosphine ligand in the coordination complex has enabled the synthesis of catalysts which are selective towards the hydrogenation and hydroformylation of particular alkenes^(3,16). Studies involving more bulky phosphine ligands such as bis(diphenylphosphino)butane (DPPB), have indicated that the rigid skeletons of these groups and the large metallocycles formed increase the instability of the metal-chelate ring and thus promote dissociation of the phosphorus group trans to the SnCl_3^- ligand, providing a vacant coordination site^(13,17,18). The use of chiral phosphines as ligands has enabled the asymmetric hydroformylation of olefins^(12,19,20). Less well known, however, is the catalytic activity of mixed rhodium-phosphine-trichlorostannate ligand systems. Recent studies⁽²¹⁾ have shown that tin(II) chloride acts as a promoter for the rhodium-chloride catalysed hydrocarbonylation of ethene to form propanoic acid. Studies reported in Chapter 4 showed that although tin(II) chloride can play a promotional role in this process, its effect is not as great as previous studies indicated. It is not known, however, whether phosphines, in this case triphenylphosphine, will promote the hydrocarbonylation of ethene and whether replacing, for instance, a trichlorostannate ligand with a triphenylphosphine ligand in the model complexes described in Chapter 4, will lead to an increase or decrease in catalytic activity. The aim of this chapter is to study such systems, since increases in catalytic activity caused by the presence of a phosphine group would open up a whole new area of chemistry, with the possibility of looking at the effect of more complex and unusual phosphines upon catalytic activity.

This chapter also includes a brief investigation of the ability of zinc(II) chloride to promote the rhodium catalysed hydrocarbonylation of ethene, a system which has

been briefly explored previously⁽²¹⁾, and a discussion of the attempts made to catalyse the hydrocarbonylation of other alkenes such as 1-hexene and 1,5-cyclooctadiene.

6.2 Synthesis

The following sections describe the synthesis and characterisation of several rhodium(I) complexes which were used as catalytic precursors in the homogeneous rhodium catalysed hydrocarbonylation of ethene, described later in this chapter, and used for studies of their reaction chemistry, described in Chapter 7. All solvents used were dried and degassed prior to use. Acetone was also distilled prior to use.

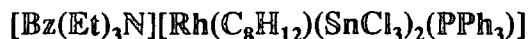
6.2.1 Preparation of Chlorobis(triphenylphosphine)carbonyl rhodium(I) - $\text{Rh}(\text{PPh}_3)_2(\text{CO})\text{Cl}$

This was prepared by a standard method⁽²²⁾ from $\text{RhCl}_3 \cdot 3\text{H}_2\text{O}$, $\{\nu(\text{CO}) \text{ nujol: } 1975\text{cm}^{-1}, \text{ lit. } 1977\text{cm}^{-1}(22)\}$.

6.2.2 Preparation of Chloro-1,5-cyclooctadienetriphenylphosphinerhodium(I) - $\text{Rh}(\text{C}_8\text{H}_{12})(\text{PPh}_3)\text{Cl}$

This complex was prepared by the method of Chatt and Venanzi⁽²³⁾. μ, μ' -dichloro-1,5-cyclooctadienedirhodium(I), $\text{Rh}_2(\text{C}_8\text{H}_{12})_2\text{Cl}_2$ (0.33g, 0.67mmol), prepared by a standard method described in Appendix 1, and triphenylphosphine (0.38g, 1.43mmol) were reacted together in 12ml of dichloromethane at room temperature, in a round bottom flask under a nitrogen atmosphere. The resultant yellow solution was evaporated to dryness to give fine yellow crystals. The crystals were washed with 3ml of methanol, filtered and dried under vacuum to give a pale yellow solid $\text{Rh}(\text{C}_8\text{H}_{12})(\text{PPh}_3)\text{Cl}$ (0.61g). {Yield: 89%; Found: C 60.94, H 5.53, N 0%; $\text{C}_{26}\text{H}_{27}\text{ClPRh}$ requires C 61.31, H 5.31 N 0%}

6.2.3 Preparation of Benzyltriethylammonium bis(trichlorostannato)-1,5-cyclooctadienetriphenylphosphinerhodium(I) -



This was prepared by a method similar to that of Pregosin et al⁽²⁴⁾. Tin(II) chloride (0.0397g, 0.21mmol) was added to a suspension of $\text{Rh}(\text{C}_8\text{H}_{12})\text{Cl}(\text{PPh}_3)$ (0.0524g, 0.10mmol) in 20ml of acetone, under a nitrogen atmosphere, and the mixture heated to 40°C. This was accompanied by a colour change from pale yellow to orange. A solution of benzyltriethylammonium chloride (0.0455g, 0.20mmol) in 5ml of dichloromethane was then added. The resulting orange solution was then treated with

15ml of 60-80 petroleum ether, giving deposition of an orange solid upon cooling to 0°C. The orange solid $[\text{Bz}(\text{Et})_3\text{N}][\text{Rh}(\text{C}_8\text{H}_{12})(\text{SnCl}_3)_2(\text{PPh}_3)]$ (0.06g) was separated by filtration, washed with 60-80 petroleum ether and dried under vacuum. It was then recrystallised from acetone/dichloromethane mixtures. {Yield: 55%; Found: C 39.64, H 4.64, N 1.21%; $[\text{Bz}(\text{Et})_3\text{N}][\text{Rh}(\text{C}_8\text{H}_{12})(\text{SnCl}_3)_2(\text{PPh}_3)]$ requires C 41.94, H 4.40, N 1.25%}.

Further recrystallisations of the product did not improve the above microanalytical data, with the %C not corresponding closely to that expected for $[\text{Bz}(\text{Et})_3\text{N}][\text{Rh}(\text{C}_8\text{H}_{12})(\text{SnCl}_3)_2(\text{PPh}_3)]$. A ^{31}P NMR spectrum of the product in CH_2Cl_2 at 25°C did not indicate contamination from other rhodium-phosphine complexes, indicating that only one rhodium-phosphine complex, the target material, was formed ($\delta(^{31}\text{P})/\text{ppm}$: 34.4d, $^1\text{J}(^{103}\text{Rh}, ^{31}\text{P})/\text{Hz}$: 137.2; lit. data for $[\text{PPN}][\text{Rh}(\text{C}_8\text{H}_{12})(\text{SnCl}_3)_2(\text{PPh}_3)]$ in acetone- d_6 /acetone at RT ⁽²⁴⁾, $\delta(^{31}\text{P})/\text{ppm}$: 40.6d, $^1\text{J}(^{103}\text{Rh}, ^{31}\text{P})/\text{Hz}$: 117). The product is considered to be the target material, with possible contamination from small amounts of $[\text{Bz}(\text{Et})_3\text{N}][\text{SnCl}_3]$ being an explanation for the discrepancies in the microanalytical data. It is also possible that the product isolated is $[\text{PPN}][\text{Rh}(\text{C}_8\text{H}_{12})(\text{SnCl}_3)_2(\text{PPh}_3)].\text{CH}_2\text{Cl}_2$ (c.f. a solvent molecule, CH_2Cl_2 , was present in a crystal of $[\text{PPN}]_2[\text{Rh}(\text{CO})_2(\text{SnCl}_3)_3]$, see Section 3.2.5). This formulation is in good agreement with the microanalytical data obtained. $\{[\text{Bz}(\text{Et})_3\text{N}][\text{Rh}(\text{C}_8\text{H}_{12})(\text{SnCl}_3)_2(\text{PPh}_3)].\text{CH}_2\text{Cl}_2$ requires C 39.94, H 4.24, N 1.16%}

6.2.4 Preparation of bis(triphenylphosphoranylidene)ammonium bis(trichlorostannato)-1,5-cyclooctadienetriphenylphosphine rhodium(I) - $[\text{PPN}][\text{Rh}(\text{C}_8\text{H}_{12})(\text{SnCl}_3)_2(\text{PPh}_3)]$

This was prepared by a method similar to that of Pregosin et al⁽²⁴⁾. Tin(II) chloride (0.1028g, 0.54mmol) was added to a solution of $\text{Rh}(\text{C}_8\text{H}_{12})\text{Cl}(\text{PPh}_3)$ (0.1332g, 0.26mmol) in 10ml of acetone, under a nitrogen atmosphere. The mixture was stirred at 20°C for 10 minutes to give a red solution. Bis(triphenylphosphoranylidene) ammonium chloride (0.1503g, 0.26mmol) in 5ml of CH_2Cl_2 was then added. The resulting deep red solution was reduced under vacuum by approximately a half, followed by addition of 30ml of 30-60 petroleum ether, to afford separation of a red oil. The solvent was removed and the oil was washed with 30-60 petroleum ether and then dried under vacuum to give the orange/red solid $[\text{PPN}][\text{Rh}(\text{C}_8\text{H}_{12})(\text{SnCl}_3)_2(\text{PPh}_3)]$ (0.23g). This solid was then recrystallised from acetone/dichloromethane mixtures. {Yield: 60%; Found: C 47.51, H 4.07, N 0.94%; $[\text{PPN}][\text{Rh}(\text{C}_8\text{H}_{12})(\text{SnCl}_3)_2(\text{PPh}_3)]$ requires C 50.88, H 3.90, N 0.96%;

$\delta(^{31}\text{P})/\text{ppm}$ in CH_2Cl_2 , 25°C : 38.3d, $^1\text{J}(^{103}\text{Rh}, ^{31}\text{P})/\text{Hz}$: 123.4; lit. data for $[\text{PPN}][\text{Rh}(\text{C}_8\text{H}_{12})(\text{SnCl}_3)_2(\text{PPh}_3)]$ in acetone- d_6 /acetone at RT ⁽²⁴⁾, $\delta(^{31}\text{P})/\text{ppm}$: 40.6d, $^1\text{J}(^{103}\text{Rh}, ^{31}\text{P})/\text{Hz}$: 117}.

The %C did not correspond closely to that expected for $[\text{PPN}][\text{Rh}(\text{C}_8\text{H}_{12})(\text{SnCl}_3)_2(\text{PPh}_3)]$, but the ^{31}P NMR data was in good agreement with the reported literature data for $[\text{PPN}][\text{Rh}(\text{C}_8\text{H}_{12})(\text{SnCl}_3)_2(\text{PPh}_3)]$. Only one ^{31}P doublet was observed, suggesting no contamination from other Rh-PPh₃ complexes. It is possible that the actual product was $[\text{PPN}][\text{Rh}(\text{C}_8\text{H}_{12})(\text{SnCl}_3)_2(\text{PPh}_3)].\text{CH}_2\text{Cl}_2$, containing a solvent molecule, CH_2Cl_2 . This would be in better agreement with the analytical data $\{[\text{PPN}][\text{Rh}(\text{C}_8\text{H}_{12})(\text{SnCl}_3)_2(\text{PPh}_3)].\text{CH}_2\text{Cl}_2$ requires C 48.87, H 3.81, N 0.90%}. Alternatively, the sample may be contaminated with small amounts of $[\text{PPN}][\text{SnCl}_3]$. The product appears to be composed mainly of the target material, and thus for reactions in which it is used, it is considered to be $[\text{PPN}][\text{Rh}(\text{C}_8\text{H}_{12})(\text{SnCl}_3)_2(\text{PPh}_3)]$.

6.2.5 Preparation of Trichlorostannate-1,5-cyclooctadiene

bis(triphenylphosphine) rhodium(I) - $\text{Rh}(\text{C}_8\text{H}_{12})(\text{SnCl}_3)(\text{PPh}_3)_2$

This complex was prepared by a method similar to that of Uson et al⁽²⁵⁾. Triphenylphosphine (0.24g, 0.92mmol) was added to a suspension of $\text{Rh}_2(\text{C}_8\text{H}_{12})_2\text{Cl}_2$ (0.11g, 0.22mmol) in 30ml of methanol, under a nitrogen atmosphere. The mixture was stirred for 15 minutes at 20°C to give an orange solution. Tin(II) chloride (0.0845g, 0.45mmol) was added to the stirred solution, giving immediate deposition of a bright red solid. The red solid $\text{Rh}(\text{C}_8\text{H}_{12})(\text{SnCl}_3)(\text{PPh}_3)_2$ (0.18g) was separated by filtration and dried under vacuum. The product was recrystallised from dichloromethane. (Yield: 20%; Found: C 53.36, H 4.38, N 0%; $\text{C}_{44}\text{H}_{42}\text{Cl}_3\text{P}_2\text{RhSn}$ requires C 54.94, H 4.37, N 0%; $\delta(^{31}\text{P})/\text{ppm}$ in CH_2Cl_2 at 25°C : 31.6d, $^1\text{J}(^{103}\text{Rh}, ^{31}\text{P})/\text{Hz}$: 156.3; lit. data for $\text{Rh}(\text{NBD})(\text{SnCl}_3)(\text{PPh}_3)_2$ at -20°C ⁽²⁵⁾, $\delta(^{31}\text{P})/\text{ppm}$: 35.5d, $^1\text{J}(^{103}\text{Rh}, ^{31}\text{P})/\text{Hz}$: 132}.

Although no ^{31}P NMR data is available in the literature for an authentic sample of $\text{Rh}(\text{C}_8\text{H}_{12})(\text{SnCl}_3)(\text{PPh}_3)_2$, the observed value may be compared with that for $\text{Rh}(\text{NBD})(\text{SnCl}_3)(\text{PPh}_3)_2$. An increase in frequency of this order of magnitude for the ^{31}P NMR signal, upon replacing the cyclooctadiene ligand by a norbornadiene ligand in complexes of this type is not uncommon e.g. $\delta(^{31}\text{P})/\text{ppm}$ in acetone- d_6 /acetone, at RT, for $[\text{PPN}][\text{Rh}(\text{COD})(\text{SnCl}_3)_2(\text{PPh}_3)]$ and $[\text{PPN}][\text{Rh}(\text{NBD})(\text{SnCl}_3)_2(\text{PPh}_3)]$ are 40.6d and 45.5d respectively⁽²⁴⁾. The product is considered to be the target complex, with the lower than expected %C possibly due

to small amounts of the starting material, $\text{Rh}_2(\text{C}_8\text{H}_{12})_2\text{Cl}_2$. Further recrystallisations did not improve the microanalytical data, and in general attempts were affected by the poor solubility of the product.

6.3 The Rhodium Catalysed Hydrocarbonylation of Ethene Promoted by Triphenylphosphine and Triphenylphosphine /Trichlorostannate Mixed Ligand Complexes

The catalytic reactions performed in this section and in Sections 6.4 and 6.5 were carried out in the Hastalloy C autoclave described in Appendix 2. The experimental procedures described in Chapter 4, Section 2, also apply to the reactions reported in Table 6.1. The calculation of rate and selectivity data, as outlined in Chapter 4, Section 2, also apply to reactions described in this chapter. Experimental constraints and the expected errors in the data reported in Chapter 4, also apply to the reactions and the data reported in Table 6.1. Degassed glacial acetic acid was used as solvent and a small volume of hydrochloric acid, found necessary for catalytic activity to occur (see Chapter 4 for details), was also added to each system.

The data obtained for the reactions described in this section are shown in Table 6.1.

The introduction of triphenylphosphine to a $\text{RhCl}_3 \cdot 3\text{H}_2\text{O}$ catalytic system (Reaction 6.3.2) in a Rh:PPh₃ molar ratio of 1:2 gave a rate of propanoic acid production which was much higher than when $\text{RhCl}_3 \cdot 3\text{H}_2\text{O}$ was used alone (Reactions 4.4 and 4.5, 1.88 and 1.89 Mol.Kg⁻¹.hr⁻¹ respectively, see Section 4.4), but only marginally higher than that for a $\text{RhCl}_3 \cdot 3\text{H}_2\text{O}/\text{SnCl}_2$ system employing a Sn:Rh molar ratio of 2:1 (Reaction 4.7, 2.71 Mol.Kg⁻¹.hr⁻¹, 85.1% selectivity, see Section 4.5). Thus, both PPh₃ and SnCl₂ promote the rate of the $\text{RhCl}_3 \cdot 3\text{H}_2\text{O}$ reaction to about the same degree, but the selectivity of the phosphine reaction (96.0%) exceeds that of the tin reaction (85.1%). The promotional effect of PPh₃ when used in a Rh:PPh₃ molar ratio of 1:2 may be due to the steric effect of the bulky triphenylphosphine ligands coordinated to the rhodium centre, which may promote steps occurring in the catalytic process, such as reductive elimination. The electronic properties of the PPh₃ ligand may also play an important part in the catalytic activity. Since PPh₃ is a strong σ -donor, rhodium complexes incorporating it as a ligand will be electron rich at the rhodium centre. An electron rich rhodium(I) centre will favour formation of 16-electron species usually associated with catalytic activity, rather than 18-electron species. Consequently, oxidative addition will become favourable.

Table 6.1 Data obtained for the hydrocarbonylation of ethene when using Rhodium-triphenylphosphine and Rhodium-triphenylphosphine/trichlorostannate mixed ligand complexes as catalytic precursors

Reactions 6.3.1-8 each contained 34ml of CH₃COOH and 2.4ml of 37% HCl_(aq), and were pressurised with 30 bar of CO and 30 bar of C₂H₄

Reaction Code	Reagents	Temperature/ °C	Rate (A) bar.hr ⁻¹	Rate (B) Mol.Kg ⁻¹ .hr ⁻¹	Moles of propanoic acid produced	% Selectivity for propanoic acid
6.3.1	Rh ₂ (COD) ₂ Cl ₂ 0.106 mmol	180	66	3.02	0.109	85.0
6.3.2	RhCl ₃ .3H ₂ O PPh ₃ 0.106 mmol 0.207 mmol	180	53	3.27	0.118	96.0
6.3.3	Rh(COD)Cl(PPh ₃) 0.109 mmol	180	43	2.27	0.082	81.1
6.3.4	Rh(COD)Cl(PPh ₃) SnCl ₂ 0.106 mmol 0.221 mmol	180	68	2.63	0.095	99.9
6.3.5	Rh(CO)Cl(PPh ₃) ₂ SnCl ₂ 0.108 mmol 0.230 mmol	180	52	2.47	0.089	89.5
6.3.6	◇ [Rh(COD)(SnCl ₃) ₂ (PPh ₃)] ⁻ 0.109 mmol	180	75	3.41	0.123	92.3
6.3.7	* [Rh(COD)(SnCl ₃) ₂ (PPh ₃)] ⁻ 0.070 mmol	180	53	2.97	0.107	96.1
6.3.8	Rh(COD)(SnCl ₃)(PPh ₃) ₂ 0.077 mmol	180	18	0.55	0.020	92.1

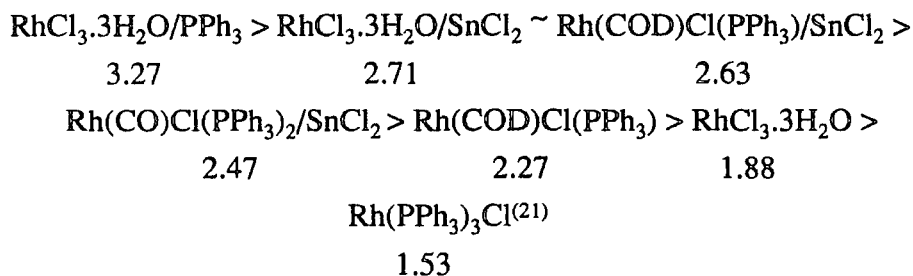
◇ Cation = [PPN]⁺ * Cation = [Bz(Et)₃N]⁺

Nevertheless, despite several HPIR spectroscopic studies it has not been possible to identify the active catalyst for this reaction.

The effect of having both PPh_3 and SnCl_3^- ligands in the same catalytic precursor complex is the purpose of Reactions 6.3.6 and 6.3.7. Data should be compared with that obtained for the $[\text{PPN}]^+$ and $[\text{Bz}(\text{Et})_3\text{N}]^+$ salts of $[\text{Rh}(\text{COD})(\text{SnCl}_3)_3]^{2-}$ (Reactions 4.29 and 4.28, Section 4.12), which gave rates of propanoic acid production of 2.43 and 2.99 $\text{Mol.Kg}^{-1}.\text{hr}^{-1}$ respectively. The replacement of one of the trichlorostannate ligands by a phosphine ligand leads to a significant increase in rate for the $[\text{PPN}]^+$ complex, but an almost identical rate for the $[\text{Bz}(\text{Et})_3\text{N}]^+$ complex. The initial rate of reaction, though, using $[\text{Rh}(\text{COD})(\text{SnCl}_3)_2(\text{PPh}_3)]^-$ was higher than that observed for salts of $[\text{Rh}(\text{COD})(\text{SnCl}_3)_3]^{2-}$, with catalysis in Reactions 6.3.6 and 6.3.7 starting in the temperature range 170-180°C. This observed activity at a lower temperature than for the non-phosphine containing rhodium-trichlorostannate complexes was a feature of several reactions reported in the above table, with Reactions 6.2.1, 6.2.2 and 6.2.4 being the exceptions, and may be due to the triphenylphosphine or trichlorostannate ligands of $[\text{Rh}(\text{L})_2(\text{SnCl}_3)_2(\text{PPh}_3)]^-$ being more susceptible to dissociation or displacement than a trichlorostannate ligand of $[\text{Rh}(\text{L})_2(\text{SnCl}_3)_3]^{2-}$, (where L_2 is initially COD, which is replaced under the reaction conditions by two carbonyl groups). Thus, enhancement of the ability of the 18-electron catalytic precursor to form a 16-electron active catalyst may be promoted by the presence of both a phosphine and SnCl_3^- , rather than by SnCl_3^- alone. Indeed, studies described later in Chapter 7 show that reaction of $[\text{Rh}(\text{COD})(\text{SnCl}_3)_2(\text{PPh}_3)]^-$ with CO at room temperature leads to the apparent formation of $\text{Rh}(\text{CO})_2(\text{SnCl}_3)(\text{PPh}_3)_2$ and the 16-electron complex $\text{Rh}(\text{CO})\text{Cl}(\text{PPh}_3)_2$, along with other unidentified Rh- PPh_3 species. This clearly indicates that dissociation of both SnCl_3^- and PPh_3 ligands occurs in solution, and therefore most surely occurs under catalytic conditions. Conversely, reaction of $[\text{Rh}(\text{COD})(\text{SnCl}_3)_3]^{2-}$ with CO at room temperature (see Section 3.2.5) formed $[\text{Rh}(\text{CO})_2(\text{SnCl}_3)_3]^{2-}$ as the single species in solution. The apparent dissociation of ligands in reactions of $[\text{Rh}(\text{COD})(\text{SnCl}_3)_2(\text{PPh}_3)]^-$ with CO may be due to the significant π -acceptor⁽²⁶⁻²⁹⁾ ability of the SnCl_3^- ligand, causing a weakening of other metal-ligand bonds. This is discussed in more detail in studies of the chemistry of Rh(I)-COD- SnCl_3 - PPh_3 complexes, reported in Chapter 7.

The rates of propanoic acid production for other systems reported in Table 6.1 may be compared with those for a $\text{RhCl}_3 \cdot 3\text{H}_2\text{O}$ catalytic system (Reaction 4.5), and a

RhCl₃.3H₂O/SnCl₂ catalytic system (Reaction 4.7). The observed rates, expressed in Mol.Kg⁻¹.hr⁻¹ are in the order:



An assessment of the data in the above scheme emphasises that both SnCl₂ and PPh₃ have promotional effects on the rate of propanoic acid production for a RhCl₃.3H₂O system. However, when both tin and phosphine species are present together in a rhodium catalytic system it is extremely difficult to determine whether the enhancement in activity is due to either or both of PPh₃ and SnCl₂. Indeed, the observed differences in activity for some of the systems remain unaccounted, and may also be due to additional factors not considered so far, such as, the solubility of the catalytic precursors and subsequent species formed.

GC analysis of the solutions for reactions 6.3.1-8 confirmed the by-products as being extremely small quantities of ethyl acetate, ethyl propanoate and chloroethane, the same by-products as those observed in other rhodium catalysed reactions (see Chapter 4).

Although addition of PPh₃ seems to have an effect on the catalytic activity of some Rh and Rh/Sn systems its role in other systems is unclear, and consequently further studies are required to fully understand the role of phosphine ligands in these systems.

A study of the reaction chemistry and properties of the rhodium(I)-trichlorostannate-triphenylphosphine complexes used in this chapter is reported in Chapter 7. The reaction chemistry is carried out under more ambient conditions, to investigate chemistry which may be occurring in the catalytic reactions.

6.4 The Rhodium Catalysed Hydrocarbonylation of Ethene Promoted by Zinc(II) Chloride

6.4.1 Catalytic Studies

Previous exploratory work indicated that ZnCl_2 promotes the rhodium-chloride catalysed hydrocarbonylation of ethene⁽²¹⁾, at a rate of propanoic acid production of $1.74 \text{ Mol.Kg}^{-1}.\text{hr}^{-1}$. The assessment of a promotional effect was, however, based upon data that a rhodium(I)-carbonyl-chloride system in the absence of a metal co-catalyst was not active in the hydrocarbonylation process. This has now been disproved and as a consequence new information is required on the effects of ZnCl_2 on this reaction.

Reaction 6.4.1 below employed a similar system to that used in Reaction 4.9 ($\text{RhCl}_3 \cdot 3\text{H}_2\text{O}/\text{SnCl}_2/\text{Bz}(\text{Et})_3\text{NCl}$), but with ZnCl_2 added as a possible promoter instead of SnCl_2 .

Reagents : $\text{RhCl}_3 \cdot 3\text{H}_2\text{O}$ 0.109 mmol, ZnCl_2 0.197 mmol,
 $\text{Bz}(\text{Et})_3\text{NCl}$ 0.306 mmol, 37% $\text{HCl}_{(\text{aq})}$ 2.4 ml,
 CH_3COOH 34 ml,
 CO - 30bar, C_2H_4 - 30bar
 Temperature : 180°C

Reaction Code	Rh : Zn : $\text{Bz}(\text{Et})_3\text{NCl}$ Molar Ratio	Moles of Propanoic Acid Produced	Rate/ $\text{bar}.\text{hr}^{-1}$	Rate/ $\text{Mol.Kg}^{-1}.\text{hr}^{-1}$	% Selectivity
6.4.1	1 : 2 : 3	0.046	20	1.28	90.0

The system in Chapter 4, Reaction 4.10 carried out in the absence of a metal co-catalyst, with just $\text{RhCl}_3 \cdot 3\text{H}_2\text{O}$ and $\text{Bz}(\text{Et})_3\text{NCl}$ as the catalytic precursors, gave an observed rate of propanoic acid production of $1.58 \text{ Mol.Kg}^{-1}.\text{hr}^{-1}$, with an increase in rate to $2.73 \text{ Mol.Kg}^{-1}.\text{hr}^{-1}$ upon addition of tin(II) chloride ($\text{Sn}:\text{Rh}$ molar ratio = 2:1, see Reaction 4.9). The observed rate for the zinc(II) chloride promoted system, (Reaction 6.4.1) was only $1.28 \text{ Mol.Kg}^{-1}.\text{hr}^{-1}$, whilst the observed rate for a previous system employing $\text{Zn}(\text{II})$ as a promoter was $1.74 \text{ Mol.Kg}^{-1}.\text{hr}^{-1}$ ⁽²¹⁾, the reaction being carried out in the same vessel in both cases, but not necessarily with the same rate of stirring. Allowing for the errors incurred in reading pressure gauges, pressurising

with the amount of required gas, and fluctuations in GC response (ca. +/-5-10%), it can be concluded that $ZnCl_2$ does not have a promotional effect on the rate of propanoic acid production for reactions described here, and may indeed inhibit this reaction (although the data obtained for Reactions 4.10 and 6.4.1 are not sufficiently different to confirm this). It seems, therefore, that formation of propanoic acid in Reaction 6.4.1 is merely due to the formation of $[Rh(CO)_2Cl_2]^-$ as the active catalyst in solution. Conclusions of previous studies,⁽²¹⁾ which claimed that Zn(II), and indeed other less active transition metal co-catalysts such as Fe(II), Ni(II) and Cu(II), have promotional ability, must therefore be treated with extreme caution. In each case catalytic activity is most likely due to $[Rh(CO)_2Cl_2]^-$ as the active catalyst, since rates of propanoic acid formation are similar to those obtained for Reaction 4.10 in these studies.

6.4.2 Exploration of the Reaction Chemistry of Rhodium(I) Carbonyl Chlorides and Zinc(II) Chlorides

To support the results in Reaction 6.4.1 several attempted reactions were carried out between rhodium(I) carbonyl chloride and zinc(II) chloride species of relevance to the catalytic process, under ambient conditions, using THF and acetic acid as solvents. The attempted reactions were carried out in glassware flushed with nitrogen and maintained under a nitrogen atmosphere throughout the experiment. The reactions were monitored as in Chapter 2 by following the changes in the positions of the carbonyl absorptions using Fourier Transform Infra-red spectroscopy, employing 16 scans at a resolution of $2cm^{-1}$. The solution state spectra were run using a CaF_2 liquid cell, and the solvents dried and degassed prior to use.

Reactions in THF

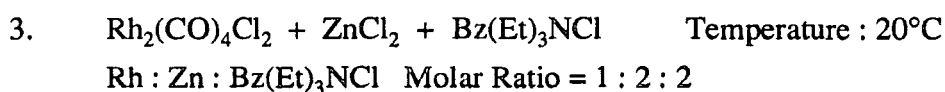


Rh : Zn Molar Ratio	$\nu(CO)/cm^{-1}$ Observed	Assignment
1 : 1	1984 _s 2063 _s 2004 _w 2081 _w	$[Rh(CO)_2Cl_2]^-$ Rh(CO) ₂ Cl(THF)
1 : 3	1984 _{ms} 2063 _{ms} 2004 _m 2081 _m	$[Rh(CO)_2Cl_2]^-$ Rh(CO) ₂ Cl(THF)
1 : 4	1984 _{ms} 2063 _{ms} 2004 _m 2081 _m	$[Rh(CO)_2Cl_2]^-$ Rh(CO) ₂ Cl(THF)
1 : 8	1984 _m 2063 _m 2004 _s 2081 _s	$[Rh(CO)_2Cl_2]^-$ Rh(CO) ₂ Cl(THF)

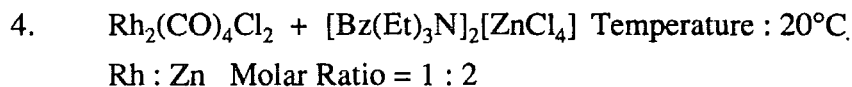
The carbonyl absorptions at 2004 and 2081 cm^{-1} increased in intensity, coupled with a decrease in the intensity of the absorptions at 1984 $_s$ and 2063 $_s\text{cm}^{-1}$ assigned to $[\text{Bz}(\text{Et})_3\text{N}][\text{Rh}(\text{CO})_2\text{Cl}_2]$, as the amount of ZnCl_2 in the system was increased. The yellow solutions became dark overnight, arising from decomposition, with loss of CO.



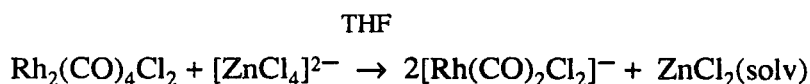
No changes in the $\nu(\text{CO})$ region were observed over a 2 hour period.



No reaction with ZnCl_2 was observed, with only carbonyl absorptions due to $[\text{Bz}(\text{Et})_3\text{N}][\text{Rh}(\text{CO})_2\text{Cl}_2]$ at 1984 and 2062 cm^{-1} being present.



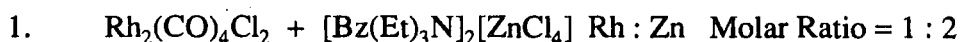
In the presence of a large amount of chloride ions $[\text{Bz}(\text{Et})_3\text{N}]_2[\text{ZnCl}_4]$ is a species likely to be formed during the heating process of the Rh-Zn catalytic system outlined in Reaction 6.4.1. The same complex has been isolated from a reaction of $\text{Bz}(\text{Et})_3\text{NCl}$ and ZnCl_2 in acetic acid (see Appendix 1). Its reaction with $\text{Rh}_2(\text{CO})_4\text{Cl}_2$ (Reaction 4 above) resulted only in the formation of $[\text{Bz}(\text{Et})_3\text{N}][\text{Rh}(\text{CO})_2\text{Cl}_2]$ according to the following equation :



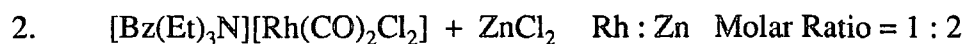
This reaction is probably made possible due to the presence in solution of the equilibrium



Reactions in Acetic Acid



The reaction gave carbonyl absorptions at 2002_s and 2076_s cm^{-1} corresponding to the formation of $[\text{Bz}(\text{Et})_3\text{N}][\text{Rh}(\text{CO})_2\text{Cl}_2]$, with reaction probably occurring similar to the corresponding reaction carried out in THF.



The reaction mixture was heated under reflux giving absorptions at 2037_s , 2093_s , and 2109_w cm^{-1} .

The absorptions observed at 2004 and 2081cm^{-1} in THF and at 2037 , 2093 and 2109cm^{-1} in acetic acid, following the reaction of $[\text{Bz}(\text{Et})_3\text{N}][\text{Rh}(\text{CO})_2\text{Cl}_2]$ with ZnCl_2 , are in the positions of the carbonyl absorptions observed when $\text{Rh}_2(\text{CO})_4\text{Cl}_2$ is added to the respective solvents. In THF, $\text{Rh}(\text{CO})_2\text{Cl}(\text{THF})$ forms, and in acetic acid $\text{Rh}_2(\text{CO})_4\text{Cl}_2$ forms. Thus, ZnCl_2 can be envisaged as abstracting chloride ions from $[\text{Bz}(\text{Et})_3\text{N}][\text{Rh}(\text{CO})_2\text{Cl}_2]$ causing formation of $\text{Rh}_2(\text{CO})_4\text{Cl}_2$ in acetic acid and $\text{Rh}(\text{CO})_2\text{Cl}(\text{THF})$ in THF, along with $[\text{Bz}(\text{Et})_3\text{N}]_2[\text{ZnCl}_4]$. This is similar to reactions described in Chapter 2 where SnCl_2 is also thought to abstract a chloride ion from $[\text{Rh}(\text{CO})_2\text{Cl}_2]^-$, giving $\text{Rh}(\text{CO})_2\text{Cl}(\text{THF})$ in THF. Unlike rhodium(I) carbonyl chloride/tin(II) chloride systems, where reaction of rhodium complexes with SnCl_3^- leads to rhodium-trichlorostannate complexes, in this case, however, there is no further reaction with zinc(II) chlorides to form a Rh-Zn complex,

The reactions carried out under ambient conditions at atmospheric pressure provide further evidence that a zinc-chloride species will not coordinate to a rhodium(I) carbonyl chloride species formed in the catalytic process, and therefore explain why ZnCl_2 is not a promoter in Reaction 6.4.1. Catalytic activity is probably due solely to formation of $[\text{Rh}(\text{CO})_2\text{Cl}_2]^-$ in solution, no evidence being found for the formation of Rh-Zn complexes.

6.5 Hydrocarbonylation of Other Alkenes

Successful hydrocarbonylation reactions for wide ranges of different alkenes, to form acids and esters, have been reported previously⁽³⁰⁾, and have been patented by the Monsanto company. Several reactions have been carried out in this work to investigate whether rhodium-chloride and rhodium-tin-chloride promoted systems will effect the hydrocarbonylation of alkenes in general.

High pressure reactions were attempted using the available alkenes, 1-hexene and 1,5-cyclooctadiene. The catalytic systems used were :

1. $\text{RhCl}_3 \cdot 3\text{H}_2\text{O}$, 37% $\text{HCl}_{(\text{aq})}$
2. $\text{RhCl}_3 \cdot 3\text{H}_2\text{O}$, SnCl_2 , 37% $\text{HCl}_{(\text{aq})}$
3. $\text{RhCl}_3 \cdot 3\text{H}_2\text{O}$, SnCl_2 , $\text{Bz}(\text{Et})_3\text{NCl}_{(\text{aq})}$, 37% $\text{HCl}_{(\text{aq})}$

In each case the autoclave was charged with the catalytic precursors, the solvent acetic acid, the liquid alkene, and the reactant gas carbon monoxide and then heated to a temperature of 180°C. The amount of catalyst, amount of alkene, amount of solvent, gas pressure and temperature were all varied throughout a series of reactions, but under no circumstances was any catalytic activity observed. This observation was confirmed by GC and GCMS analysis of the solutions, neither of which indicated that hydrocarbonylation to form organic acids had occurred. The reason for this lack of reactivity is unknown, but may relate to the solubility of the higher alkene in the solvent mixture used. Homogeneous catalytic reaction rates are known to depend on the efficiency of mixing of the reagents, and thus the apparent lack of catalytic activity may be solely a feature of inefficient stirring. Only a magnetic follower was used here, which may not provide thorough agitation. Further investigation of the hydrocarbonylation of longer chain alkenes and also alkynes (not studied as part of this thesis) is necessary if these rhodium-tin-chloride catalytic systems are to be able to compete with other highly versatile systems of which the iridium-iodide system is a prime example⁽³⁰⁾.

6.6 Conclusions

Triphenylphosphine appears to have a promotional effect on the catalytic activity of some rhodium-chloride and rhodium-tin-chloride systems. However, for several reactions the effect of PPh_3 and $\text{PPh}_3/\text{SnCl}_2$ systems is not totally clear, and consequently further studies need to be undertaken to fully understand the role of triphenylphosphine in catalytic systems.

Zinc(II) chloride had no promotional effect on the activity of rhodium-chloride catalytic systems, and solution state studies of reactions between rhodium(I) carbonyl chloride and tin(II) chloride species which form during catalysis indicated that formation of rhodium(I) zinc chloride complexes in solution does not occur.

Attempts to hydrocarbonylate alkenes other than ethene were unsuccessful, possibly due to insufficient mixing of the reagents. Consequently, further experiments are necessary to fully explore such systems.

6.7 References

1. H.C. Clark, A.B. Goel, C.S. Wong, *J. Organometal. Chem.*, 1980, 190, C101.
2. H.C. Clark, C.S. Wong, C. Billard, *J. Organometal. Chem.*, 1980, 190, C105.
3. H.C. Clark, J.A. Davies, *J. Organometal. Chem.*, 1981, 213, 503.
4. A.B. Goel, S. Goel, D. Van Der Veer, *Inorg. Chim. Acta.*, 1981, 54, L5; 1982, 64, L173.
5. H. Itatani, J.C. Bailar Jr., *Int. Eng. Chem. Prod. Res. Develop.*, 1972, 11, 146.
6. I. Schwager, J.F. Knifton, *J. Catal.*, 1976, 45, 256.
7. J.F. Knifton, *J. Org. Chem.*, 1976, 41, 793.
8. J.F. Knifton, *J. Organometal. Chem.*, 1980, 188, 223.
9. H.C. Clark, A.B. Goel, C. Billard, *J. Organometal. Chem.*, 1980, 182, 431.
10. G.K. Anderson, H.C. Clark, J.A. Davies, *Organometallics*, 1982, 1, 64.
11. G.C. Bond, M. Hellier, *J. Catal.*, 1967, 7, 217.
12. G. Consiglio, P. Pino, *Helv. Chim. Acta.*, 1976, 59, 642.
13. Y. Kawabata, T. Hayashi, I. Ogata, *J. Chem. Soc. Chem. Comm.*, 1979, 462.
14. J.F. Murray, J.R. Norton, *J. Am. Chem. Soc.*, 1979, 101, 4107.
15. J.F. Knifton, *J. Org. Chem.*, 1976, 41, 2885.
16. G.K. Anderson, C. Billard, H.C. Clark, J.A. Davies, C.S. Wong, *Inorg. Chem.*, 1983, 22, 439.
17. Y. Kawabata, T. Suzuki, I. Ogata, *Bull. Chem. Soc. Jpn.*, 1978, 361.
18. T. Hayashi, Y. Kawabata, T. Isoyama, *Bull. Chem. Soc. Jpn.*, 1981, 54, 3438.
19. C.U. Pittman Jr., Y. Kawabata, L.I. Flowers, *J. Chem. Soc. Chem. Commun.*, 1972, 9, 473.
20. G. Consiglio, P. Pino, L.I. Flowers, C.U. Pittman Jr., *J. Chem. Soc. Chem. Commun.*, 1973, 612.
21. N.J. Winter, Ph.D Thesis, University of Durham, 1991.
22. J.A. McCleverty, G. Wilkinson, *Inorg. Synth.*, 1966, 8, 214.
23. J. Chatt, L.M. Venanzi, *J. Chem. Soc.*, 1957, 4735.
24. M. Kretschmer, P.S. Pregosin, M. Garralda, *J. Organomet. Chem.*, 1983, 244, 175.
25. R. Uson, L. Oro, M.T. Pinillos, A. Arruebo, K.A.O. Starzewski, P.S. Pregosin, *J. Organomet. Chem.*, 1980, 192, 227.
26. W.A.G. Graham, *Inorg. Chem.*, 1968, 7, 315.
27. W. Jetz, P.B. Simons, J.A.J. Thompson, W.A.G. Graham, *Inorg. Chem.*, 1966, 5, 2217.

28. R.V. Lindsey, G.W. Parshall, U.G. Stolberg, *J. Am. Chem. Soc.*, 1965, 87, 658.
29. G.W. Parshall, *J. Am. Chem. Soc.*, 1966, 88, 704.
30. J.H. Craddock, A. Hershman, F.E. Paulik, J.F. Roth, U.S. Patent 3 579 551, 1971, *Chem. Abstr.*, 1970, 72, 110811j.

Chapter 7

The Reaction Chemistry of Several Rhodium(I) - Trichlorostannate Complexes

7.1 Introduction

This chapter, describing a study of the reaction chemistry of various rhodium(I)-tin(II) complexes, is divided into three sections, as follows:

1. Carbonylation of Rh-COD-PPh₃-SnCl₃ complexes, which were used for catalytic studies as described in Chapter 6 (Section 7.2.1-7.2.2).
2. The reaction chemistry of various Rh(I)-CO-SnCl₃ complexes with PPh₃, Cl⁻ and CO as described in Chapters 2, 3 and 4 (Section 7.2.3-7.2.6).
3. The reaction chemistry of other miscellaneous rhodium complexes of relevance to this thesis, with species such as CO, Cl⁻, SnCl₂, and PPh₃ (Section 7.2.7-7.2.8).

The aim of these experiments was to probe the reaction chemistry of various complexes which have been shown to be catalytically active or catalyst precursors in the hydrocarbonylation of ethene, in an attempt to understand the fundamental chemistry occurring in the high pressure, high temperature process. The reactions outlined in 1 and 3 above involve chemistry which may be occurring during the catalytic processes in which the various mixed ligand rhodium complexes have been shown to be active. The reaction chemistry of selected Rh-COD-PPh₃-SnCl₃ complexes has been previously studied using NMR and infra-red spectroscopic methods by Pregosin et al^(1,2) and Garcia et al⁽³⁾.

The reactions in 3 above are also discussed, with particular reference to the properties of the trichlorostannate ligand and its behaviour in competition with ligands such as PPh₃, CO and Cl⁻, the aim being to rationalise various ligand coordination abilities and the relative σ -donor and π -acceptor properties of the ligands involved.

7.2 Experimental

All solvents used were dried and degassed prior to use.

7.2.1 ^{31}P NMR Studies of the Reactions of Rh-COD- PPh_3 - SnCl_3 Complexes with CO

The complexes in general are sources of catalytically active species for the hydrocarbonylation of ethene (see Section 6.3), so their behaviour under a pressure of carbon monoxide is of interest. ^{31}P NMR data for the starting complexes used in Reactions 7.2.1.1 and 7.2.1.2 are shown in Table 7.1.

Complex	Solvent	$\delta(^{31}\text{P})/\text{ppm}$	$^1\text{J}(^{103}\text{Rh}, ^{31}\text{P})/\text{Hz}$
$\text{Rh}(\text{COD})(\text{SnCl}_3)(\text{PPh}_3)_2$	CH_2Cl_2	31.6 d	156.3
$*[\text{Rh}(\text{COD})(\text{SnCl}_3)_2(\text{PPh}_3)]^-$	CH_2Cl_2	34.4 d	137.2

* Cation = $[\text{Bz}(\text{Et})_3\text{N}]^+$

Table 7.1 Summary of the ^{31}P NMR data for the starting complexes used in Reactions 7.2.1.1 and 7.2.1.2.

7.2.1.1 Reaction of $\text{Rh}(\text{COD})(\text{SnCl}_3)(\text{PPh}_3)_2$ with CO

$\text{Rh}(\text{COD})(\text{SnCl}_3)(\text{PPh}_3)_2$ (0.05g, 0.052mmol), prepared as described in Chapter 6, was dissolved in 10ml of dichloromethane and the resultant solution bubbled with CO for 5 minutes, giving a colour change from orange to pale yellow. A ^{31}P NMR spectrum of the resultant solution was recorded (see Table 7.2). Upon standing, a yellow solid precipitated from the reaction solution. This was separated by filtration, and then dried under vacuum. Analytical data were consistent with $\text{Rh}(\text{CO})\text{Cl}(\text{PPh}_3)_2$ as the product, which was confirmed by infra-red spectroscopy. ($\nu(\text{CO})$ - 1971cm^{-1} in nujol, lit. 1977cm^{-1} in nujol⁽⁴⁾).

7.2.1.2 Reaction of $[\text{Bz}(\text{Et})_3\text{N}][\text{Rh}(\text{COD})(\text{SnCl}_3)_2(\text{PPh}_3)]$ with CO

$[\text{Bz}(\text{Et})_3\text{N}][\text{Rh}(\text{COD})(\text{SnCl}_3)_2(\text{PPh}_3)]$ (0.04g, 0.036mmol), prepared as described in Chapter 6, was dissolved in 10ml of dichloromethane and the resultant solution bubbled with CO for 5 minutes giving a colour change from pale orange to yellow. A ^{31}P NMR spectrum of the resultant solution was recorded (see Table 7.2).

Reaction Code	Reactants	$\delta(^{31}\text{P})/\text{ppm}$	$^1J(^{103}\text{Rh}, ^{31}\text{P})/\text{Hz}$	Assignment
7.2.1.1	$\text{Rh}(\text{COD})(\text{SnCl}_3)(\text{PPh}_3)_2$ + CO	32.8 d 29.2 d 26.4 d	87.0 128.1 126.8	$\text{Rh}(\text{CO})_2(\text{SnCl}_3)(\text{PPh}_3)_2$ $\text{Rh}(\text{CO})\text{Cl}(\text{PPh}_3)_2$ Unassigned
7.2.1.2	$*[\text{Rh}(\text{COD})(\text{SnCl}_3)_2(\text{PPh}_3)]^-$ + CO	34.7 d 32.8 d 29.3 d 26.6 d	132.2 83.0 126.9 147.8	$*[\text{Rh}(\text{COD})(\text{SnCl}_3)_2(\text{PPh}_3)]^-$ $\text{Rh}(\text{CO})_2(\text{SnCl}_3)(\text{PPh}_3)_2$ $\text{Rh}(\text{CO})\text{Cl}(\text{PPh}_3)_2$ $\text{Rh}(\text{COD})(\text{SnCl}_3)(\text{PPh}_3)?$

* Cation = $[\text{Bz}(\text{Et})_3\text{N}]^+$

Table 7.2 Summary of the ^{31}P NMR data for the reactions of $\text{Rh}(\text{COD})(\text{SnCl}_3)(\text{PPh}_3)_2$ and $[\text{Rh}(\text{COD})(\text{SnCl}_3)_2(\text{PPh}_3)]^-$ with CO in CH_2Cl_2

7.2.2 FT-IR Studies of the Reactions of Rh-COD-PPh₃-SnCl₃ Complexes with CO

Reactions 7.2.1.1 and 7.2.1.2 were repeated using the same stoichiometric amounts of reagents, and the positions of the carbonyl absorptions were monitored using FT-IR spectroscopy.

Reaction Code	Reactants	$\nu(\text{CO})/\text{cm}^{-1}$ Observed	Assignment
7.2.2.1	$\text{Rh}(\text{COD})(\text{SnCl}_3)(\text{PPh}_3)_2$ + CO	1980 _m 2016 _{ms} 2000 _s 2043 _w 2094 _{ms}	$\text{Rh}(\text{CO})\text{Cl}(\text{PPh}_3)_2$ Unassigned $\text{Rh}(\text{CO})_2(\text{SnCl}_3)(\text{PPh}_3)_2$ Unassigned
7.2.2.2	$*[\text{Rh}(\text{COD})(\text{SnCl}_3)_2(\text{PPh}_3)]^-$ + CO	2000 _m 2043 _w 2018 _s 2072 _{vw} 2095 _w 1979 _m 2017 _s (24 hours)	$\text{Rh}(\text{CO})_2(\text{SnCl}_3)(\text{PPh}_3)_2$ Unassigned Unassigned $\text{Rh}(\text{CO})\text{Cl}(\text{PPh}_3)_2$ Unassigned

* Cation = $[\text{Bz}(\text{Et})_3\text{N}]^+$

Table 7.3 Summary of the infra-red data for the reactions of $\text{Rh}(\text{COD})(\text{SnCl}_3)(\text{PPh}_3)_2$ and $[\text{Rh}(\text{COD})(\text{SnCl}_3)_2(\text{PPh}_3)]^-$ with CO in CH_2Cl_2

7.2.3 ^{31}P NMR Studies of the Reactions of Rh-CO-SnCl₃ Complexes with PPh₃

7.2.3.1 Reaction of the product of [Bz(Et)₃N][Rh(CO)₂Cl₂] + SnCl₂ with PPh₃
[Bz(Et)₃N][Rh(CO)₂Cl₂] (0.0604g, 0.143mmol) and SnCl₂ (0.0833g, 0.044mmol) were reacted in 5ml of THF at room temperature under a nitrogen atmosphere to give a red solution ($\nu(\text{CO}) - 2012\text{cm}^{-1}$, see Chapter 2 for details of this reaction). PPh₃ (0.0390g, 0.149mmol) was added to this mixture and gave an immediate orange colouration. A ^{31}P NMR spectrum was recorded (see Table 7.4). A further amount PPh₃ (0.0400g, 0.152mmol) was then added, causing the colour to become pale yellow. A ^{31}P NMR spectrum of this final solution was recorded (see Table 7.4). Both ^{31}P NMR spectra for this reaction are shown in Figure 7.1.

7.2.3.2 Reaction of [PPN]₂[Rh(CO)₂(SnCl₃)₃] with PPh₃
[PPN]₂[Rh(COD)(SnCl₃)₃] (0.1177g, 0.060mmol) was dissolved in 10ml of dichloromethane and bubbled with CO to yield [PPN]₂[Rh(CO)₂(SnCl₃)₃]. PPh₃ (0.0244g, 0.093mmol) was then added to this solution, giving a colour change from orange to pale orange. A ^{31}P NMR spectrum was recorded (see Table 7.4). Further PPh₃ (0.0276g, 0.105mmol) was then added, giving a yellow solution, and a further ^{31}P NMR spectrum was recorded (see Table 7.4). Both ^{31}P NMR spectra recorded for this reaction are shown in Figure 7.2. Separation of yellow crystals from this solution occurred overnight. These air stable crystals were removed by filtration and dried under vacuum. {Found : C 57.75, H 3.94, N 0, Cl 18.22%, Infra-red : $\nu(\text{CO})/\text{cm}^{-1} - 1970_{\text{s}}$ in nujol}.

The position of the carbonyl absorption suggested possible formation of Rh(CO)Cl(PPh₃)₂ {c.f. $\nu(\text{CO})-1977\text{cm}^{-1}$ in nujol⁽⁴⁾}. However the microanalytical data did not fit closely to that expected for Rh(CO)Cl(PPh₃)₂ {%Calc C 64.25, H 4.34, Cl 5.13}. Crystal structural data obtained for one of the crystals showed it to be the paramagnetic Rh(II) complex RhCl₂(PPh₃)₂ {%Calc C 61.85, H 4.29, Cl 10.15}, which has been isolated previously by Ogle et al⁽⁵⁾ from the reaction of Rh₂(COD)₂Cl₂ with PPh₃. Thus, the yellow crystals appear to contain both RhCl₂(PPh₃)₂ and Rh(CO)Cl(PPh₃)₂, and on the basis of microanalytical data, other unidentified materials.

7.2.3.3 Reaction of PPh_3 with the solid product obtained from $\text{Rh}_2(\text{CO})_4\text{Cl}_2 + \text{SnCl}_2 + \text{Bz}(\text{Et})_3\text{NCl}$ in Ethanol

This product was obtained from Reaction 3.2.2 described in Chapter 3, and is the solid generally obtained when rhodium(I) carbonyl chlorides and tin(II) chlorides are reacted together. Figure 3.3 (Chapter 3) shows the carbonyl absorptions observed at 2016, 2029, 2069 and 2079 cm^{-1} (nujol). Infra-red and ^{119}Sn NMR studies indicated that the product was mainly composed of $[\text{Bz}(\text{Et})_3\text{N}][\text{Rh}(\text{CO})_2(\text{SnCl}_3)_3]$, smaller quantities of $[\text{Bz}(\text{Et})_3\text{N}]_3[\text{Rh}(\text{CO})(\text{SnCl}_3)_4]$ and $[\text{Bz}(\text{Et})_3\text{N}]_2[\text{Rh}(\text{CO})(\text{SnCl}_3)_2\text{Cl}]$, and very small quantities of other rhodium carbonyl containing species. As a result all quoted and calculated values of quantities of reagents used in this reaction were based upon $[\text{Bz}(\text{Et})_3\text{N}]_2[\text{Rh}(\text{CO})_2(\text{SnCl}_3)_3]$ as the solid species. By reacting this mixture of Rh-CO-SnCl₃ complexes with PPh_3 it was hoped to gain further information about its composition.

0.1297g(0.103mmol) of the Rh-CO-SnCl₃ product was dissolved in 10ml of dichloromethane at room temperature under a nitrogen atmosphere to give a red solution. Addition of PPh_3 (0.0305g, 0.117mmol) gave an orange colouration. A ^{31}P NMR spectrum of the reaction mixture was immediately recorded (see Table 7.4). A further quantity of PPh_3 (0.0290g, 0.111mmol) was then added, giving a pale yellow colouration, and another ^{31}P NMR spectrum of the reaction mixture was recorded (see Table 7.4). Further addition of PPh_3 gave no change in the positions of the ^{31}P NMR signals. The ^{31}P NMR spectra recorded for this reaction are shown in Figure 7.3.

Reaction Code	Reactants	$\delta(^{31}\text{P})$ / ppm	$^1\text{J}(^{103}\text{Rh}, ^{31}\text{P})$ / /Hz	Assignment
7.2.3.1 ^a	* $[\text{Rh}(\text{CO})_2\text{Cl}_2]^- + \text{SnCl}_2$ + PPh_3 Rh:P molar ratio = 1:1	37.0 d 34.5 d 29.3 d	138.9 137.4 130.0	Unassigned Unassigned $\text{Rh}(\text{CO})\text{Cl}(\text{PPh}_3)_2$
	+ PPh_3 Rh:P molar ratio = 1:2	33.4 d	88.7	$\text{Rh}(\text{CO})_2(\text{SnCl}_3)(\text{PPh}_3)_2$
7.2.3.2 ^b	$\diamond [\text{Rh}(\text{CO})_2(\text{SnCl}_3)_3]^{2-}$ + PPh_3 Rh:P molar ratio = 1:2	32.8 d 29.3 d	86.4 126.8	$\text{Rh}(\text{CO})_2(\text{SnCl}_3)(\text{PPh}_3)_2$ $\text{Rh}(\text{CO})\text{Cl}(\text{PPh}_3)_2$
	+ PPh_3 Rh:P molar ratio = 1:4	32.8 d	87.3	$\text{Rh}(\text{CO})_2(\text{SnCl}_3)(\text{PPh}_3)_2$
7.2.3.3 ^b	Rh-CO-SnCl ₃ mix + PPh_3 Rh:P molar ratio = 1:1	34.6 d 32.7 d 29.2 d'	133.4 82.3 126.0	Unassigned $\text{Rh}(\text{CO})_2(\text{SnCl}_3)(\text{PPh}_3)_2$ $\text{Rh}(\text{CO})\text{Cl}(\text{PPh}_3)_2$
	+ PPh_3 Rh:P molar ratio = 1:2	32.7 d	88.8	$\text{Rh}(\text{CO})_2(\text{SnCl}_3)(\text{PPh}_3)_2$

* Cation = $[\text{Bz}(\text{Et})_3\text{N}]^+$ \diamond Cation = $[\text{PPN}]^+$ Solvent: a - THF, b - CH_2Cl_2

Table 7.4 Summary of ^{31}P NMR data for the reactions of Rh(I)-CO-SnCl₃ species with PPh_3

7.2.4 FT-IR Studies of the Reactions of Rh-CO-SnCl₃ Complexes with PPh_3

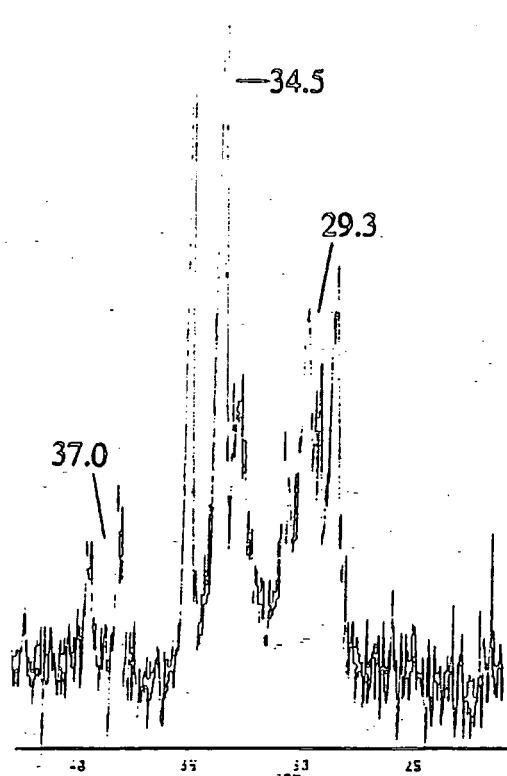
Reactions 7.2.3.1, 7.2.3.2 and 7.2.3.3 were repeated, and FT-IR spectroscopy used to monitor the reactions. The infra-red data for the starting complexes and for their reactions with PPh_3 are shown in Table 7.5 and Table 7.6 respectively.

Complex	Solvent	$\nu(\text{CO})/\text{cm}^{-1}$ Observed
$\diamond [\text{Rh}(\text{CO})_2(\text{SnCl}_3)_3]^{2-}$	CH_2Cl_2	2017 _s 2068 _w
* $[\text{Rh}(\text{CO})_2\text{Cl}_2]^-$ SnCl ₂	THF	2012 _s
Rh-CO-SnCl ₃ mixture (see Reaction 3.2.2)	CH_2Cl_2	2016 _s 2030 _{sh} 2069 _{vw} 2077 _w

* Cation = $[\text{Bz}(\text{Et})_3\text{N}]^+$ \diamond Cation = $[\text{PPN}]^+$

Table 7.5 Summary of infra-red data for Rh-CO-SnCl₃ starting materials prior to reaction with PPh_3

Figure 7.1 ^{31}P NMR Spectra for Reaction of $\text{Rh}(\text{CO})_2\text{Cl}_2$ with SnCl_2 and PPh_3
Rh: PPh_3 Molar Ratio = 1:1



Rh: PPh_3 Molar Ratio = 1:2

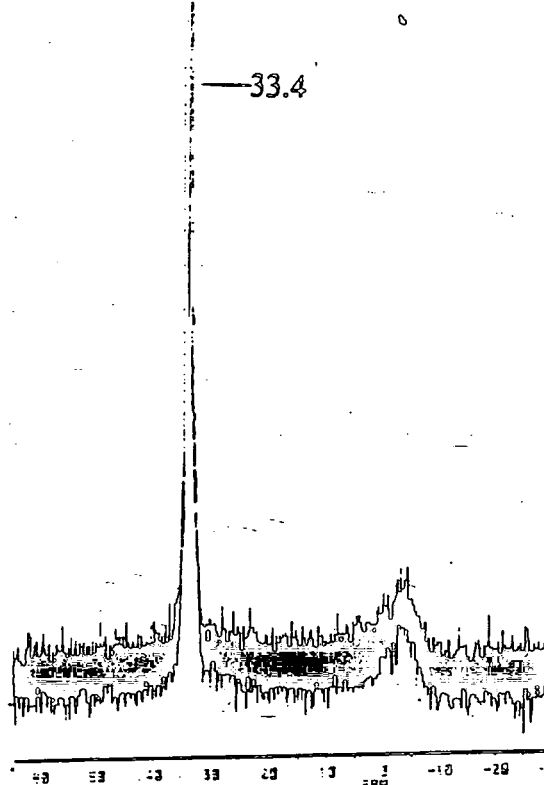
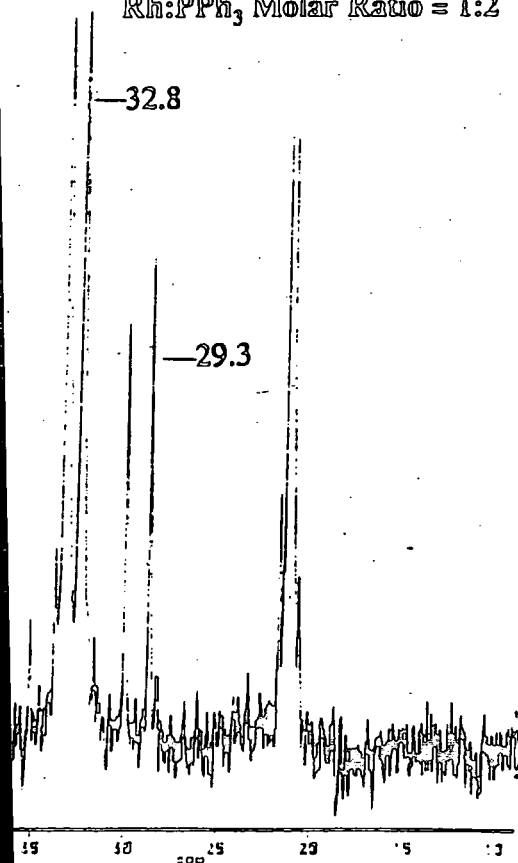


Figure 7.2 ^{31}P NMR Spectra for Reaction of $\text{Rh}(\text{CO})_2(\text{SnCl}_3)_2$ with PPh_3

Rh: PPh_3 Molar Ratio = 1:2



Rh: PPh_3 Molar Ratio = 1:4

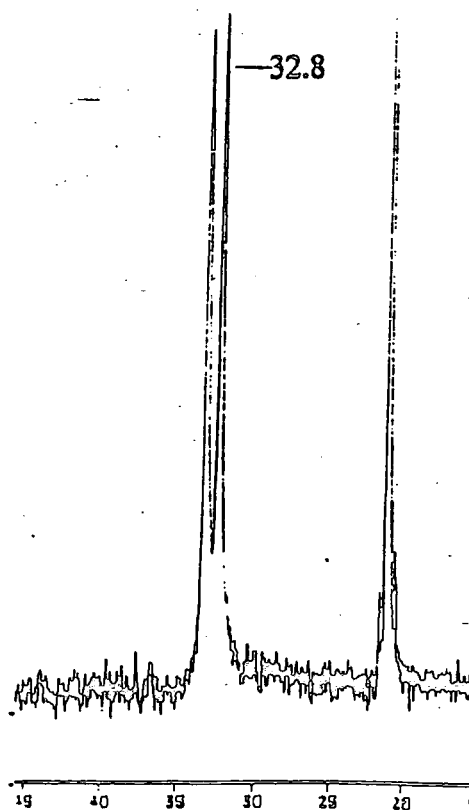
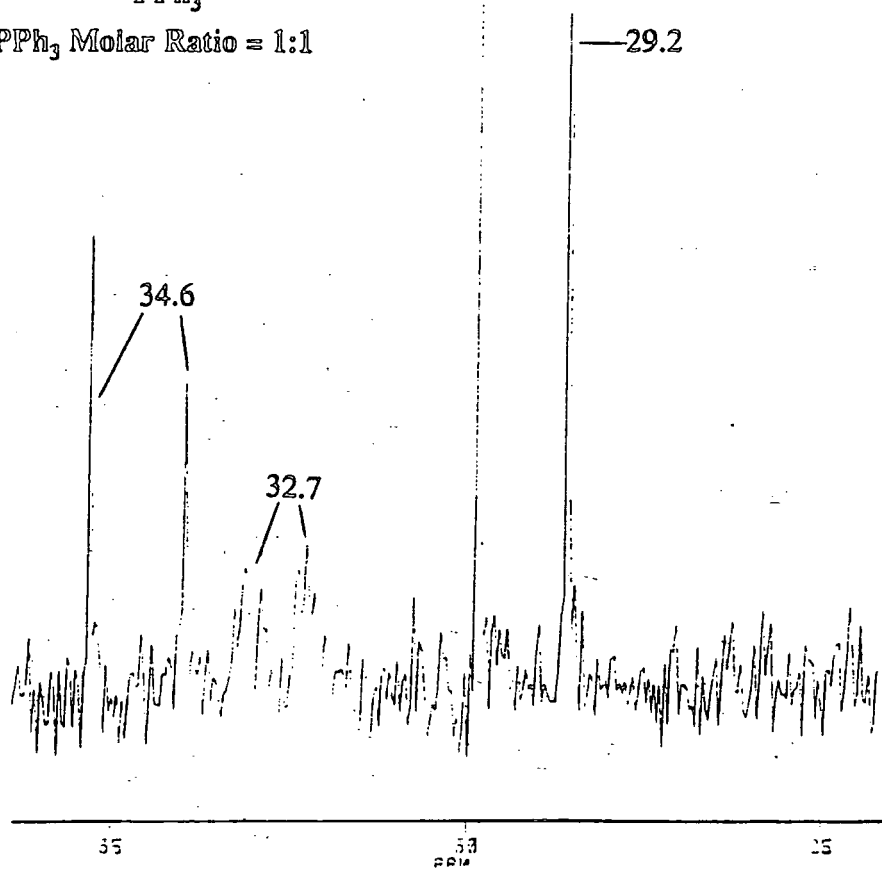
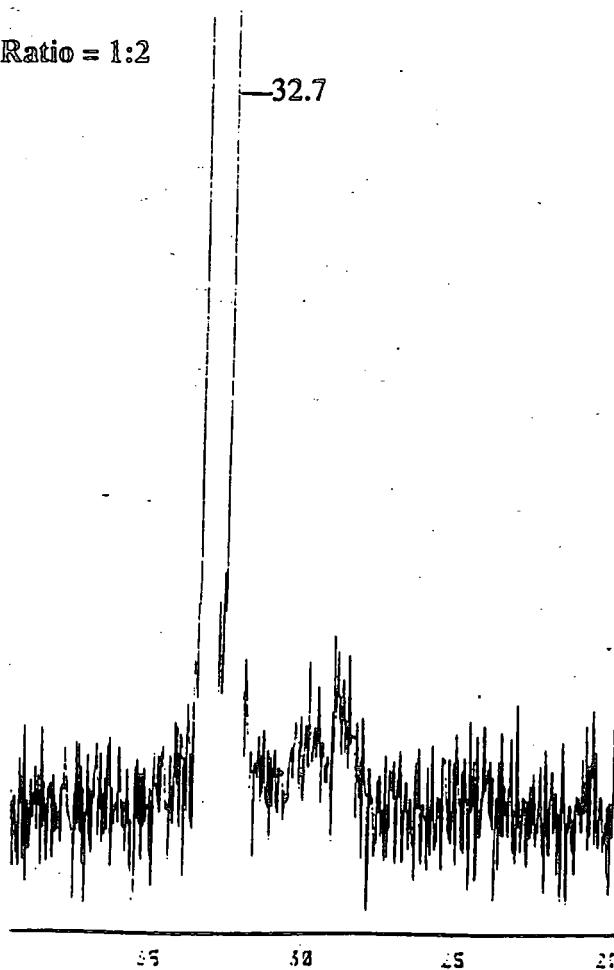


Figure 7.3 ^{31}P NMR Spectra for Reaction of Rh-CO-SnCl₃ Mixture with PPh₃

Rh:PPh₃ Molar Ratio = 1:1



Rh:PPh₃ Molar Ratio = 1:2



Reaction Code	Reactants	$\nu(\text{CO})/\text{cm}^{-1}$ Observed	Assignment
7.2.4.1 ^a	$\diamond [\text{Rh}(\text{CO})_2(\text{SnCl}_3)_3]^{2-}$ + PPh_3 Rh:P molar ratio = 1:2 + PPh_3 Rh:P molar ratio = 1:4	1978 _{sh} 2017 _m 1999 _s , 2045 _w 1999 _s , 2045 _w	$\text{Rh}(\text{CO})\text{Cl}(\text{PPh}_3)_2$ $[\text{Rh}(\text{CO})_2(\text{SnCl}_3)_3]^{2-}$? $\text{Rh}(\text{CO})_2(\text{SnCl}_3)(\text{PPh}_3)_2$ $\text{Rh}(\text{CO})_2(\text{SnCl}_3)(\text{PPh}_3)_2$
7.2.4.2 ^b	* $[\text{Rh}(\text{CO})_2\text{Cl}_2]^-$ + SnCl_2 + PPh_3 Rh:P molar ratio = 1:1 + PPh_3 Rh:P molar ratio = 1:3	1982 _s 1995 _s , 2041 _w 1980 _m 1994 _s , 2041 _w	$\text{Rh}(\text{CO})\text{Cl}(\text{PPh}_3)_2$? $\text{Rh}(\text{CO})_2(\text{SnCl}_3)(\text{PPh}_3)_2$ $\text{Rh}(\text{CO})\text{Cl}(\text{PPh}_3)_2$ $\text{Rh}(\text{CO})_2(\text{SnCl}_3)(\text{PPh}_3)_2$
7.2.4.3 ^a	Rh-CO-SnCl ₃ mixture (see Reaction 3.2.2) + PPh_3 Rh:P molar ratio = 1:1 + PPh_3 Rh:P molar ratio = 1:2	1978 _w 2018 _s 1979 _m 1999 _s , 2047 _w	$\text{Rh}(\text{CO})\text{Cl}(\text{PPh}_3)_2$ $[\text{Rh}(\text{CO})_2(\text{SnCl}_3)_3]^{2-}$? $\text{Rh}(\text{CO})\text{Cl}(\text{PPh}_3)_2$ $\text{Rh}(\text{CO})_2(\text{SnCl}_3)(\text{PPh}_3)_2$

* Cation = $[\text{Bz}(\text{Et})_3\text{N}]^+$ \diamond Cation = $[\text{PPN}]^+$ Solvent: a - CH_2Cl_2 , b - THF

Table 7.6 Summary of the infra-red data for the reactions of Rh(I)-CO-SnCl₃ species with PPh₃

7.2.5 The Reaction Chemistry of Rh-CO-SnCl₃ Complexes with Cl⁻

7.2.5.1 Reaction of $[\text{Bz}(\text{Et})_3\text{N}][\text{Rh}(\text{CO})_2\text{Cl}_2]$ with SnCl₂ in THF followed by addition of $\text{Bz}(\text{Et})_3\text{NCl}$

$[\text{Bz}(\text{Et})_3\text{N}][\text{Rh}(\text{CO})_2\text{Cl}_2]$ (0.0108g, 0.043mmol) was dissolved in 10ml of THF and reacted with SnCl₂ (0.0187g, 0.099mmol) under a nitrogen atmosphere. The reaction gave an instantaneous red colouration accompanied by a strong carbonyl absorption at 2012cm⁻¹, assigned to $[\text{Bz}(\text{Et})_3\text{N}]_2[\text{Rh}(\text{CO})_2(\text{SnCl}_3)_3]$ (This reaction is discussed in detail in Chapter 2). $\text{Bz}(\text{Et})_3\text{NCl}$ (0.0089g, 0.0039mmol) was then added to the solution. The reaction was monitored by FT-IR spectroscopy over a period of two hours. The strong absorption at 2012cm⁻¹ decreased in intensity over this period until it became weak. This was accompanied by the appearance and subsequent increase in intensity of absorptions at 1984 and 2062cm⁻¹ corresponding to $[\text{Bz}(\text{Et})_3\text{N}][\text{Rh}(\text{CO})_2\text{Cl}_2]$, at the expense of the absorption at 2012cm⁻¹. Repetition of this reaction with addition of a large excess of $\text{Bz}(\text{Et})_3\text{NCl}$ resulted in the immediate

loss of the absorption at 2012cm^{-1} to give those consistent with $[\text{Bz}(\text{Et})_3\text{N}][\text{Rh}(\text{CO})_2\text{Cl}_2]$.

7.2.5.2 Reaction of Rh(I)-CO-SnCl₃ complexes with chloride ions

Reactions of the isolated solid species $[\text{PPN}]_2[\text{Rh}(\text{CO})_2(\text{SnCl}_3)_3]$ and $[\text{Bz}(\text{Et})_3\text{N}]_2[\text{Rh}(\text{CO})(\text{SnCl}_3)_2\text{Cl}]$ with chloride ions sources such as $\text{Bz}(\text{Et})_3\text{NCl}$ and $37\%\text{HCl}_{(\text{aq})}$ also gave immediate formation of $[\text{Rh}(\text{CO})_2\text{Cl}_2]^-$ when the chloride ion source was added in large amounts.

7.2.6 Carbonylation of the product from the reaction of $[\text{Bz}(\text{Et})_3\text{N}][\text{Rh}(\text{CO})_2\text{Cl}_2] + \text{SnCl}_2$ in THF

Attempted reaction of the THF solution from the reaction of $[\text{Rh}(\text{CO})_2\text{Cl}_2]^-$ with SnCl_2 (see Reaction 7.2.5.1), by bubbling it with carbon monoxide at a pressure of 1 atm for 1 hour gave no change in the frequency or intensity of the carbonyl absorption at 2012cm^{-1} . Also, reactions of solutions of $[\text{PPN}]_2[\text{Rh}(\text{CO})_2(\text{SnCl}_3)_3]$ and $[\text{Bz}(\text{Et})_3\text{N}]_2[\text{Rh}(\text{CO})(\text{SnCl}_3)_2\text{Cl}]$ with CO indicated no changes in the frequencies or the intensities of the carbonyl absorptions for these complexes. Formation of new carbonyl absorptions was not observed for any reaction.

The lack of reactivity of these complexes with CO at 1 atm pressure is perhaps not surprising, in the light of other studies, e.g. the reaction of $[\text{Rh}(\text{diolefin})(\text{SnCl}_3)_3]^{2-}$ with CO in CH_2Cl_2 , which only ever results in the loss of the diolefin⁽⁶⁾ (see Chapter 3, Section 3.2.5) and not the SnCl_3^- ligands, reinforcing the suggestion of results reported here that CO will not displace trichlorostannate ligands.

7.2.7 The reaction chemistry of miscellaneous rhodium complexes followed by ³¹P NMR Spectroscopy

³¹P NMR data for the starting complexes used in Reactions 7.2.7.1 and 7.2.7.2 are given in Table 7.7.

Complex	Solvent	$\delta(^{31}\text{P})/\text{ppm}$	$^1J(^{103}\text{Rh}, ^{31}\text{P})/\text{Hz}$
$\text{Rh}(\text{CO})\text{Cl}(\text{PPh}_3)_2$	CH_2Cl_2	29.2 d	125.8
$^a\text{Rh}(\text{CO})\text{Cl}(\text{PPh}_3)_2^{(7)}$	CH_2Cl_2	29.1 d	124.0
$\text{Rh}(\text{COD})\text{Cl}(\text{PPh}_3)$	CH_2Cl_2	31.8 d	151.0

a - Data reported by Tolman et al⁽⁷⁾

Table 7.7 Summary of ^{31}P NMR data for the starting complexes used in Reactions 7.2.7.1 and 7.2.7.2

7.2.7.1 Reaction of $\text{Rh}(\text{CO})\text{Cl}(\text{PPh}_3)_2$ with SnCl_2

A mixture of $\text{Rh}(\text{CO})\text{Cl}(\text{PPh}_3)_2$ and SnCl_2 was found to be catalytically active in the hydrocarbonylation of ethene, outlined in Chapter 6. This reaction was carried out to probe the nature of the reaction chemistry between the two species.

$\text{Rh}(\text{CO})\text{Cl}(\text{PPh}_3)_2$ (0.0610g, 0.088mmol) was reacted with SnCl_2 (0.0345g, 0.182mmol) in 15ml of dichloromethane under a nitrogen atmosphere. Due to the insolubility of tin(II) chloride at room temperature, the reaction mixture was heated to a temperature of 40°C. The yellow solution became progressively darker and after a period of 1 hour became deep orange/brown in colour. A ^{31}P NMR spectrum of this solution was recorded (see Table 7.8). Attempts to obtain solid species from this solution resulted only in the isolation of the yellow solid $\text{Rh}(\text{CO})\text{Cl}(\text{PPh}_3)_2$.

7.2.7.2 Reaction of $\text{Rh}(\text{COD})\text{Cl}(\text{PPh}_3)$ with SnCl_2

This was another mixture found to be catalytically active in the hydrocarbonylation of ethene described in Chapter 6.

$\text{Rh}(\text{COD})\text{Cl}(\text{PPh}_3)$ (0.05g, 0.098mmol) was dissolved in 10ml of dichloromethane and reacted under a nitrogen atmosphere at 45°C with SnCl_2 (0.038g, 0.202mmol). There was a slight darkening of the orange solution after a period of approximately 20 minutes and a ^{31}P NMR spectrum was recorded (see Table 7.8). There was no further change with time in the positions of the ^{31}P NMR signals.

7.2.7.3 Reaction of $\text{Rh}(\text{COD})_2(\text{SnCl}_3)$ with PPh_3

$\text{Rh}(\text{COD})_2(\text{SnCl}_3)$ (0.020g, 0.037mmol) was dissolved in 10ml of dichloromethane at room temperature under a nitrogen atmosphere, giving an orange/red solution. PPh_3 (0.0193g, 0.075mmol) was added to this solution, resulting in a pale orange colouration. A ^{31}P NMR spectrum of this solution was recorded (see Table 7.8).

The attempted reaction of $\text{Rh}(\text{COD})\text{Cl}(\text{PPh}_3)$ with SnCl_2 indicated formation of a weak ^{31}P NMR doublet at 26.4 ppm, $^1J(^{103}\text{Rh}, ^{31}\text{P}) = 145.8$ Hz, which remains unassigned, with possible formation of a rhodium-trichlorostannate complex being unclear. The ^{31}P NMR signals of the starting complex were retained as the most prominent signals in the spectrum.

Reaction Code	Reactants	$\delta(^{31}\text{P})/\text{ppm}$	$^1J(^{103}\text{Rh}, ^{31}\text{P})/\text{Hz}$	Assignment
7.2.7.1	$\text{Rh}(\text{CO})\text{Cl}(\text{PPh}_3)_2$ SnCl_2	32.5 d 29.0 d 19.1 d	89.0 126.5 91.2	$\text{Rh}(\text{CO})_2(\text{SnCl}_3)(\text{PPh}_3)_2$ $\text{Rh}(\text{CO})\text{Cl}(\text{PPh}_3)_2$ Unassigned
7.2.7.2	$\text{Rh}(\text{COD})\text{Cl}(\text{PPh}_3)$ SnCl_2	26.4 d	145.8	$\text{Rh}(\text{COD})(\text{SnCl}_3)(\text{PPh}_3)?$
7.2.7.3	$\text{Rh}(\text{COD})_2(\text{SnCl}_3)$ PPh_3	31.2 d	149.9	$\text{Rh}(\text{COD})(\text{SnCl}_3)(\text{PPh}_3)_2?$

Table 7.8 Summary of the ^{31}P NMR data for Reactions 7.2.7.1-7.2.7.3 carried out in CH_2Cl_2

7.2.8 The reaction chemistry of miscellaneous rhodium complexes followed by FT-IR spectroscopy

7.2.8.1 Reaction of $\text{Rh}(\text{CO})\text{Cl}(\text{PPh}_3)_2$ with SnCl_2

The carbonyl absorptions of the reaction solution used in Reaction 7.2.5.1 were monitored using FT-IR spectroscopy. The data summarised for this reaction in Table 7.9 represents the infra-red spectrum after 1 hour. The solution became progressively darker over a 2 day period, after which a further infra-red spectrum was recorded (see Table 7.9).

7.2.8.2 Reaction of $\text{Rh}(\text{COD})_2(\text{SnCl}_3)$ with CO and PPh_3

$\text{Rh}(\text{COD})_2(\text{SnCl}_3)$ leads to a catalytically active species in the hydrocarbonylation of ethene, outlined in Chapter 4. Therefore, its reaction with carbon monoxide is of interest.

$\text{Rh}(\text{COD})_2(\text{SnCl}_3)$ (0.03g, 0.055mmol) was dissolved in 20ml of dichloromethane under a nitrogen atmosphere and was bubbled with carbon monoxide for 10 minutes, giving a colour change from pale red to orange. An infra-red spectrum of this solution was recorded (see Table 7.9). This solution was then reacted with PPh_3

(0.027g, 0.103mmol), to give a yellow solution, and another infra-red spectrum was recorded (see Table 7.9). Attempts to isolate solid species from this reaction were unsuccessful, resulting in decomposition to a brown/black oil.

Reaction Code	Reactants	$\nu(\text{CO})/\text{cm}^{-1}$ Observed	Assignment
7.2.8.1	$\text{Rh}(\text{CO})\text{Cl}(\text{PPh}_3)_2$ + SnCl_2	1978 _s 1 hour 1990 _s 2012 _w 2076 _w 2090 _m 2 days	$\text{Rh}(\text{CO})\text{Cl}(\text{PPh}_3)_2$ Unassigned
7.2.8.2	$\text{Rh}(\text{COD})_2(\text{SnCl}_3)$ + CO + PPh_3	2020 _{sh} 2035 _m 2056 _{mw} 2091 _s 2107 _{vw} 2000 _s 2045 _w	Unassigned $\text{Rh}(\text{CO})_4(\text{SnCl}_3)$ $\text{Rh}(\text{CO})_2(\text{SnCl}_3)(\text{PPh}_3)_2$

Table 7.9 Summary of the infra-red data for Reactions 7.2.8.1 and 7.2.8.2 carried out in CH_2Cl_2

7.3 Discussion

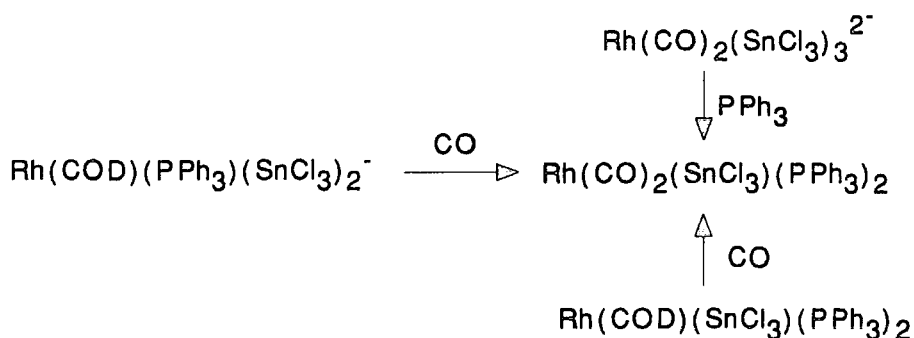
7.3.1 The Formation of Rh-SnCl₃-CO-PPh₃ Complexes

Examination of the ³¹P NMR and infra-red spectral data for the reactions reported in this chapter shows that most reactions have some common species as their products. The chemistry taking place in solution can be deduced from the spectral data obtained. However, attempts to isolate solid species were on the whole unsuccessful, with either decomposition of solution species during work-up, formation of oils, or formation of mixtures of species. It was not possible to separate the mixtures by solvent extraction, and their general insolubility meant that they were difficult to characterise by any means other than infra-red analysis. A common feature of the reactions designed to form rhodium(I) carbonyl trichlorostannate phosphine complexes, was the frequent separation from solution of the yellow solid $\text{Rh}(\text{CO})\text{Cl}(\text{PPh}_3)_2$, which was also detected in solution by infra-red and ³¹P NMR spectroscopy during several of the reactions.

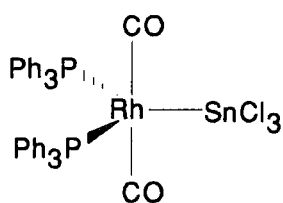
It is clear from the spectral data obtained for the reactions of the rhodium(I) diolefin complexes $\text{Rh}(\text{COD})(\text{SnCl}_3)(\text{PPh}_3)_2$ and $[\text{Bz}(\text{Et})_3\text{N}][\text{Rh}(\text{COD})(\text{SnCl}_3)_2(\text{PPh}_3)]$ with carbon monoxide, that the chemistry taking place is more complex than simply the displacement of the bidentate diolefin ligands by two carbon monoxide ligands. This

is illustrated by Figure 7.4 which shows the infra-red spectrum obtained for the reaction of $\text{Rh}(\text{COD})(\text{SnCl}_3)(\text{PPh}_3)_2$ with CO in CH_2Cl_2 (see Table 7.3). Several carbonyl absorptions are clearly observed, not just the two absorptions expected for $\text{Rh}(\text{CO})_2(\text{SnCl}_3)(\text{PPh}_3)_2$. The reactions of both $\text{Rh}(\text{COD})(\text{SnCl}_3)(\text{PPh}_3)_2$ and $[\text{Bz}(\text{Et})_3\text{N}][\text{Rh}(\text{COD})(\text{SnCl}_3)_2(\text{PPh}_3)]$ with CO gave common products in solution. Previous work indicated precipitation of $\text{Rh}(\text{CO})_2(\text{SnCl}_3)(\text{PPh}_3)_2$ upon reaction of $\text{Rh}(\text{COD})(\text{SnCl}_3)(\text{PPh}_3)_2$ with $\text{CO}^{(2)}$ and, contrary to work reported here, precipitation of $[\text{Rh}(\text{CO})_2(\text{SnCl}_3)_2(\text{PPh}_3)]^-$ upon reaction of $[\text{Rh}(\text{COD})(\text{SnCl}_3)_2(\text{PPh}_3)]^-$ with $\text{CO}^{(3)}$.

Examination of the ^{31}P NMR spectral data reported here, shows that in CH_2Cl_2 the ^{31}P NMR doublets at 32.8 ppm, $^1J(^{103}\text{Rh}, ^{31}\text{P}) = 86.4$ Hz, and at 29.3 ppm, $^1J(^{103}\text{Rh}, ^{31}\text{P}) = 126.8$ Hz (assigned to $\text{Rh}(\text{CO})(\text{PPh}_3)_2\text{Cl}$, see Table 7.7, $\delta(^{31}\text{P})/\text{ppm}$ 31.8d in CH_2Cl_2 , $^1J(^{103}\text{Rh}, ^{31}\text{P})/\text{Hz}$ 124.0⁽⁷⁾), for the reaction of $[\text{PPN}]_2[\text{Rh}(\text{CO})_2(\text{SnCl}_3)_3]$ with PPh_3 , ($\text{Rh}:\text{PPh}_3$ molar ratio = 1:2, see Table 7.4), are also common to the reactions of $\text{Rh}(\text{COD})(\text{SnCl}_3)(\text{PPh}_3)_2$ and $[\text{Bz}(\text{Et})_3\text{N}][\text{Rh}(\text{COD})(\text{SnCl}_3)_2(\text{PPh}_3)]$ with CO in CH_2Cl_2 (see Table 7.2). The carbonyl absorptions observed at 1999, 2017 and 2045cm^{-1} for the reaction of $[\text{PPN}]_2[\text{Rh}(\text{CO})_2(\text{SnCl}_3)_3]$ with PPh_3 in CH_2Cl_2 , ($\text{Rh}:\text{PPh}_3$ molar ratio = 1:2, see Table 7.6), are shown in Figure 7.5 and are also common to the reactions of $\text{Rh}(\text{COD})(\text{SnCl}_3)(\text{PPh}_3)_2$ and $[\text{Bz}(\text{Et})_3\text{N}][\text{Rh}(\text{COD})(\text{SnCl}_3)_2(\text{PPh}_3)]$ with CO in the same solvent (see Table 7.3). Addition of PPh_3 to $[\text{PPN}]_2[\text{Rh}(\text{CO})_2(\text{SnCl}_3)_3]$ in a $\text{PPh}_3:\text{Rh}$ molar ratio greater than 2:1 gave only the one remaining ^{31}P NMR doublet at 32.8 ppm (see Table 7.4), the same complex having carbonyl absorptions at 1999_s and 2045_wcm^{-1} (see Table 7.6). These spectral features are also observed in the reactions of $\text{Rh}(\text{COD})(\text{SnCl}_3)(\text{PPh}_3)_2$ and $[\text{Bz}(\text{Et})_3\text{N}][\text{Rh}(\text{COD})(\text{SnCl}_3)_2(\text{PPh}_3)]$ with CO (see Tables 7.2 and 7.3), and are consistent with the formation of a non-charged rhodium species containing neither $[\text{Bz}(\text{Et})_3\text{N}]^+$ or $[\text{PPN}]^+$ counter ions. This therefore indicates that PPh_3 replaces two trichlorostannate ligands upon reaction with $[\text{PPN}]_2[\text{Rh}(\text{CO})_2(\text{SnCl}_3)_3]$ and that SnCl_3^- is lost upon reaction of $[\text{Bz}(\text{Et})_3\text{N}][\text{Rh}(\text{COD})(\text{SnCl}_3)_2(\text{PPh}_3)]$ with CO. A ^{31}P NMR doublet at 32.8 ppm and accompanying carbonyl absorptions at 1999_s and 2045_wcm^{-1} (cf. $\nu(\text{CO})$ bands for complexes of the type $\text{Rh}(\text{CO})_2(\text{SnCl}_3)\text{L}_2$ ($\text{L}=\text{PPh}_3$, PEt_3) have been reported in the 1980-2040 cm^{-1} region⁽²⁾ are consistent with the formation of the 5-coordinate rhodium(I) complex $\text{Rh}(\text{CO})_2(\text{SnCl}_3)(\text{PPh}_3)_2$. The reactions can, therefore, be summarised as follows:



The ^{31}P chemical shift for $\text{Rh}(\text{CO})_2(\text{SnCl}_3)(\text{PPh}_3)_2$ is consistent with the SnCl_3^- ligand having strong π -acceptor properties⁽⁸⁻¹²⁾, and competing with the primarily σ -donating PPh_3 ligands for π -electron density from the same occupied rhodium d-orbitals. Thus, a weakening of the $\text{Rh}-\text{PPh}_3$ bond is produced, resulting in the relatively low frequency ^{31}P doublet. The $^1J(^{103}\text{Rh}, ^{31}\text{P})$ coupling constant of 88.4 Hz for the reaction of $[\text{PPN}]_2[\text{Rh}(\text{CO})_2(\text{SnCl}_3)_3]$ with PPh_3 to give $\text{Rh}(\text{CO})_2(\text{SnCl}_3)(\text{PPh}_3)_2$ (see Table 7.4) is lower than those for other 5-coordinate complexes $\{\text{Rh}(\text{COD})(\text{SnCl}_3)(\text{PPh}_3)_2: 156.3\text{Hz}, [\text{Bz}(\text{Et})_3\text{N}][\text{Rh}(\text{COD})-(\text{SnCl}_3)_2(\text{PPh}_3)]: 137.2\text{Hz}\}$, and is also consistent with the π -electron acceptor SnCl_3^- ligand competing with PPh_3 ligands for π -electron density from the same occupied rhodium d-orbitals. Longer $\text{Rh}-\text{P}$ distances are associated with lower values of $^1J(^{103}\text{Rh}, ^{31}\text{P})$ ⁽¹²⁾, and since SnCl_3^- is a stronger π -acceptor than PPh_3 , a resultant weakening of the $\text{Rh}-\text{SnCl}_3$ bond occurs. The ^{31}P NMR and infra-red data for $\text{Rh}(\text{CO})_2(\text{SnCl}_3)(\text{PPh}_3)_2$ are consistent with the trigonal bipyramidal rhodium(I) complex shown below. The two carbon monoxide ligands are shown trans to each other in axial positions with the bulkier triphenylphosphine and trichlorostannate ligands competing for π -electron density in equatorial positions.



Although no ^{119}Sn NMR data were obtained for the complex, the possibility that the 5-coordinate complex could contain a chloride ligand rather than a trichlorostannate ligand seems unlikely given that the ^{31}P NMR data is consistent with the presence of a significant π -acceptor ligand. $[\text{Rh}(\text{CO})_2\text{Cl}(\text{PPh}_3)_2]$ is also likely to be unstable,

Figure 7.4 Infra-red spectrum for reaction of $\text{Rh}(\text{COD})(\text{SnCl}_3)(\text{PPh}_3)_2$ with CO in CH_2Cl_2

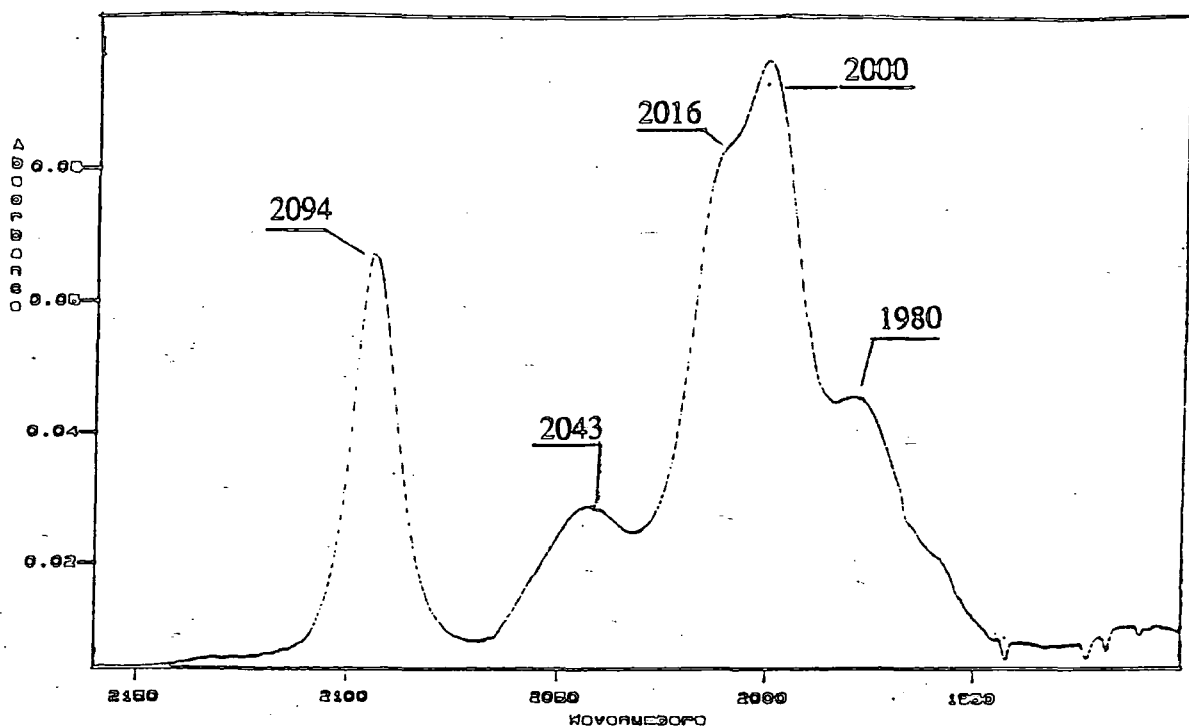
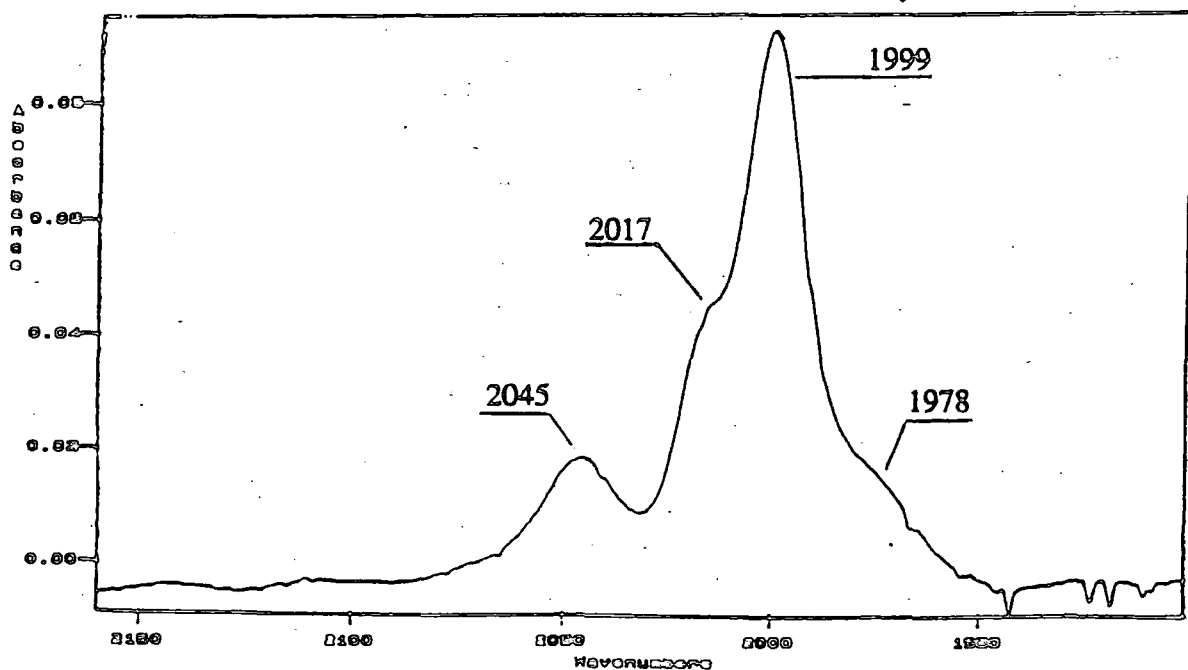


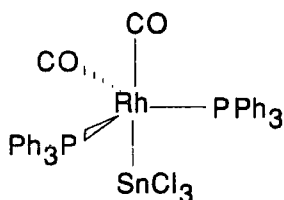
Figure 7.5 Infra-red spectrum for the reaction of $[\text{PPN}]_2[\text{Rh}(\text{CO})_2(\text{SnCl}_3)_3]$ with PPh_3 in CH_2Cl_2



with chloride ligands generally forming 4-coordinate but not 5-coordinate rhodium(I) complexes, since unlike SnCl_3^- groups they have no π -acceptor ability, and consequently are less capable of stabilising 5-coordinate 18-electron rhodium(I) complexes. The ability of PPh_3 to replace SnCl_3^- ligands during reaction with $[\text{Rh}(\text{CO})_2(\text{SnCl}_3)_3]^{2-}$ may be due to competition of SnCl_3^- ligands for π -electron density from the same rhodium d-orbitals, effectively weakening the Rh- SnCl_3 bonds, and thus making them more susceptible to dissociation or displacement by other groups.

Displacement of SnCl_3^- in $[\text{Rh}(\text{CO})_2(\text{SnCl}_3)_3]^{2-}$ by PPh_3 nucleophilic attack is envisaged, since it will reduce SnCl_3^- — SnCl_3^- , SnCl_3^- —CO and CO—CO competition for π -electron density, and also because the π -electron acceptor SnCl_3^- and CO ligands make the metal centre more electrophilic. Displacement of SnCl_3^- by PPh_3 strengthens the remaining Rh- SnCl bond, since SnCl_3^- is a stronger π -acceptor than PPh_3 , and is probably the reason why only two SnCl_3^- groups are replaced. Steric effects may also affect the extent of displacement of SnCl_3^- by PPh_3 groups in this reaction. The reason why the reaction of $[\text{PPN}]_2[\text{Rh}(\text{CO})_2(\text{SnCl}_3)_3]$ with PPh_3 does not seem to afford displacement of any CO ligands may relate to steric factors rather than electronic factors, since trichlorostannate groups and CO ligands compete with each other for π -electron density, yet the SnCl_3^- groups are displaced. The π -acceptor properties of SnCl_3^- allow it to form 5-coordinate complexes, but the additional π -acidic ligand also causes weakening of existing bonds from rhodium to SnCl_3^- groups and other π -acidic coordinated ligands, effectively increasing the possibility of ligand dissociation. Thus, the ability of the π -acceptor properties of SnCl_3^- to facilitate formation of 5-coordinate complexes, in agreement with previous reported work⁽¹³⁻¹⁷⁾, may also adversely affect the kinetic stability of these species, the labile groups depending on the arrangement of ligands with respect to the SnCl_3^- groups in a particular complex. The dissociation of PPh_3 and SnCl_3^- ligands occurring in the reactions reported in this chapter, is in agreement with studies reported in Chapters 2 and 3, where data was consistent with the dissociation of CO and SnCl_3^- ligands from Rh(I)-CO- SnCl_3 complexes, related by a series of equilibria. Dissociation appears to be favoured by complexes containing several strong π -acceptor SnCl_3^- ligands, since $\text{Rh}(\text{CO})_2(\text{SnCl}_3)(\text{PPh}_3)_2$ appears to be a robust 5-coordinate complex in solution.

Reaction of $\text{Rh}(\text{COD})(\text{SnCl}_3)(\text{PPh}_3)_2$ and $[\text{Rh}(\text{COD})(\text{SnCl}_3)_2(\text{PPh}_3)]^-$ with carbon monoxide is expected to yield initially a complex with CO ligands in adjacent positions to each other, via direct displacement of the dialkene. In the case of the reaction of $\text{Rh}(\text{COD})(\text{SnCl}_3)(\text{PPh}_3)_2$ with CO a possible structure for the initial product is shown below, and is preferred to a structure with the two CO groups in the equatorial plane, which would force bulky groups into less favoured axial positions.



Presumably isomerisation then occurs quickly to give the more stable conformation with the large SnCl_3^- and PPh_3 ligands in their preferred equatorial positions, and the CO ligands in axial positions, as indicated by infra-red and ^{31}P NMR data.

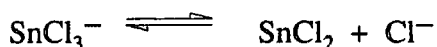
The ability of $[\text{Bz}(\text{Et})_3\text{N}][\text{Rh}(\text{COD})(\text{SnCl}_3)_2(\text{PPh}_3)]$ to form $\text{Rh}(\text{CO})_2(\text{SnCl}_3)(\text{PPh}_3)_2$ on reaction with carbon monoxide in CH_2Cl_2 is evidence of a disproportionation reaction occurring in solution, involving dissociation of SnCl_3^- and intermolecular group transfer of a triphenylphosphine ligand from another complex. The following are possible pathways:

- $$\text{Rh}(\text{CO})_2(\text{SnCl}_3)_2(\text{PPh}_3)^- \rightarrow \text{Rh}(\text{CO})_2(\text{SnCl}_3)(\text{PPh}_3) + \text{SnCl}_3^-$$

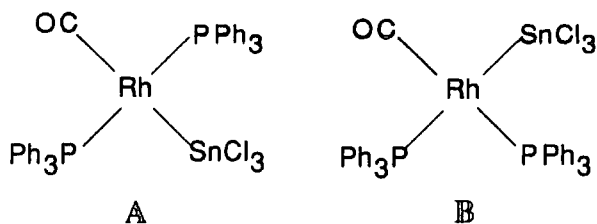
$$\text{Rh}(\text{CO})_2(\text{SnCl}_3)(\text{PPh}_3) + \text{PPh}_3 \rightarrow \text{Rh}(\text{CO})_2(\text{SnCl}_3)(\text{PPh}_3)_2$$
- $$\text{Rh}(\text{CO})_2(\text{SnCl}_3)_2(\text{PPh}_3)^- + \text{PPh}_3 \rightarrow \text{Rh}(\text{CO})_2(\text{SnCl}_3)(\text{PPh}_3)_2 + \text{SnCl}_3^-$$

Pathway (1) reflects the documented lability of the SnCl_3^- ligand⁽⁹⁾, effectively causing its dissociation. Two SnCl_3^- ligands strongly competing for π -electron density from the same occupied rhodium d-orbitals will effectively weaken each of the Rh- SnCl_3 bonds, therefore increasing the possibility of SnCl_3^- dissociation. Pathway (2) is also indicative of the weakening of Rh- SnCl_3 bonds caused by SnCl_3^- groups competing for π -electron density from the same occupied rhodium d-orbitals. The difference in this case is the direct replacement of SnCl_3^- by PPh_3 rather than the dissociative replacement mechanism occurring in (1). Other evidence for the lability of SnCl_3^- and PPh_3 ligands is provided by the formation of

$\text{Rh}(\text{CO})\text{Cl}(\text{PPh}_3)_2$, in both this reaction, and the reactions of $[\text{Rh}(\text{CO})_2(\text{SnCl}_3)_3]^{2-}$ and $[\text{Rh}(\text{COD})(\text{SnCl}_3)_2(\text{PPh}_3)]^-$ with PPh_3 and CO respectively. $\text{Rh}(\text{CO})\text{Cl}(\text{PPh}_3)_2$ has a ^{31}P NMR doublet at 29.2 ppm in CH_2Cl_2 , $^1J(^{103}\text{Rh}, ^{31}\text{P}) = 125.8$ Hz (see Table 7.7), which is consistent with the data reported by Tolman et al⁽⁷⁾ $\{\delta(^{31}\text{P}) 29.1$ ppm d, $^1J(^{103}\text{Rh}, ^{31}\text{P}) 124$ Hz, in CH_2Cl_2 at $28^\circ\text{C}\}$ ⁽⁷⁾. It also has a carbonyl infra-red absorption at 1978cm^{-1} in dichloromethane (see Tables 7.5 and 7.7), and was identified on the basis of both ^{31}P NMR and infra-red spectral data. For instance, formation of $\text{Rh}(\text{CO})\text{Cl}(\text{PPh}_3)_2$ from the reaction of $[\text{Rh}(\text{COD})(\text{SnCl}_3)_2(\text{PPh}_3)]^-$ with CO requires a disproportionation reaction involving intermolecular transfer of PPh_3 and dissociation of SnCl_3^- groups from rhodium. The dissociation of SnCl_3^- and subsequent formation of $\text{Rh}(\text{CO})\text{Cl}(\text{PPh}_3)_2$ in each of the reactions suggests that the following equilibrium exists in solution, in agreement with work reported in Chapter 2:



$\text{Rh}(\text{CO})\text{Cl}(\text{PPh}_3)_2$ was also identified in previous work reporting the reactions of $\text{Rh}(\text{I})$ -diolefin- $\text{SnCl}_3\text{-PR}_3$ complexes with CO ⁽³⁾. In work reported here a possible route for the formation of $\text{Rh}(\text{CO})\text{Cl}(\text{PPh}_3)_2$ may involve initial loss of CO from $\text{Rh}(\text{CO})_2(\text{SnCl}_3)(\text{PPh}_3)_2$ to form $\text{Rh}(\text{PPh}_3)_2(\text{CO})(\text{SnCl}_3)$. This would be more favourable than initial loss of the trichlorostannate ligand, since the two carbonyl groups trans to each other in $\text{Rh}(\text{CO})_2(\text{SnCl}_3)(\text{PPh}_3)_2$ are competing for π -electron density from the same occupied rhodium d-orbitals, effectively weakening each of the Rh-CO bonds, whereas the trichlorostannate ligand is competing for π -electron density from the same metal orbitals as two triphenylphosphine ligands, which are primarily σ -donors. Thus, the Rh-SnCl_3 bond is expected here to be much stronger than the Rh-CO bonds. Possible square planar arrangements of ligands around rhodium for $\text{Rh}(\text{PPh}_3)_2(\text{CO})(\text{SnCl}_3)$ are shown below:



However, steric and electronic factors are more likely to favour **B** than **A**. The three bulky ligands do not favour the stability of $\text{Rh}(\text{PPh}_3)_2(\text{CO})(\text{SnCl}_3)$, with loss of the most bulky trichlorostannate ligand probably thermodynamically preferred, being

replaced by a less bulky chloride ligand to give $\text{Rh}(\text{CO})\text{Cl}(\text{PPh}_3)_2$. This route to $\text{Rh}(\text{CO})\text{Cl}(\text{PPh}_3)_2$ will be especially favoured in the cases of the reactions of $[\text{PPN}]_2[\text{Rh}(\text{CO})_2(\text{SnCl}_3)_3]$ with PPh_3 and $[\text{Bz}(\text{Et})_3\text{N}][\text{Rh}(\text{COD})(\text{SnCl}_3)_2(\text{PPh}_3)]$ with CO , where loss of SnCl_3^- groups during formation of $\text{Rh}(\text{CO})_2(\text{SnCl}_3)(\text{PPh}_3)_2$ generates a source of chloride ions in solution.

Further evidence of the complex chemistry occurring in solution was the separation of the Rh(II) complex $\text{RhCl}_2(\text{PPh}_3)_2$ from the reaction of $[\text{PPN}]_2[\text{Rh}(\text{CO})_2(\text{SnCl}_3)_3]$ with PPh_3 . The formation of this complex is again consistent with a series of disproportionation reactions involving dissociation of SnCl_3^- and CO taking place in solution. A broad ^{31}P NMR signal is expected for $\text{RhCl}_2(\text{PPh}_3)_2$ since it is a paramagnetic complex. However, the complex was not detected in solution, suggesting that its precipitation is affected by a disturbance of the equilibria in solution, possibly upon removal of solvent, effecting a series of ligand dissociations.

The carbonyl absorptions observed at 2018 and 2095 cm^{-1} for the reactions of $\text{Rh}(\text{COD})(\text{SnCl}_3)(\text{PPh}_3)_2$ and $[\text{Bz}(\text{Et})_3\text{N}][\text{Rh}(\text{COD})(\text{SnCl}_3)_2(\text{PPh}_3)]$ with CO (see Table 7.3) remain unassigned. However, they may arise from the same species as that producing either of the two unidentified ^{31}P NMR signals at 34.7 ppm $^1J(^{103}\text{Rh}, ^{31}\text{P}) = 132.2$ Hz, or at 26.4 ppm $^1J(^{103}\text{Rh}, ^{31}\text{P}) = 126.8$ Hz (see Table 7.2). The absorption at 2017 cm^{-1} observed in the reaction of $[\text{PPN}]_2[\text{Rh}(\text{CO})_2(\text{SnCl}_3)_3]$ with PPh_3 may be due to residual starting material, although the expected absorption at 2068 cm^{-1} was not observed.

The reaction of $[\text{Bz}(\text{Et})_3\text{N}][\text{Rh}(\text{CO})_2\text{Cl}_2]$ with SnCl_2 in THF, followed by subsequent reaction with PPh_3 , also resulted in the formation of $\text{Rh}(\text{CO})_2(\text{SnCl}_3)(\text{PPh}_3)_2$, via initial production of $[\text{Bz}(\text{Et})_3\text{N}]_2[\text{Rh}(\text{CO})_2(\text{SnCl}_3)_3]$ in solution (see Tables 7.4 and 7.6). The infra-red spectrum for the reaction of $[\text{Bz}(\text{Et})_3\text{N}][\text{Rh}(\text{CO})_2\text{Cl}_2]$ with SnCl_2 and PPh_3 (see Figure 7.6), clearly shows the absorptions at 1995_s and 2041 cm^{-1} , assigned to $\text{Rh}(\text{CO})_2(\text{SnCl}_3)(\text{PPh}_3)_2$.

Spectroscopic studies of the reaction of PPh_3 with the mixture of species obtained from the reaction of $\text{Rh}_2(\text{CO})_4\text{Cl}_2$, SnCl_2 and $\text{Bz}(\text{Et})_3\text{NCl}$ in ethanol (Reactions 7.2.3.3 and 7.2.4.3), indicates that the product consists mainly of $[\text{Bz}(\text{Et})_3\text{N}]_2[\text{Rh}(\text{CO})_2(\text{SnCl}_3)_3]$, since $\text{Rh}(\text{CO})_2(\text{SnCl}_3)(\text{PPh}_3)_2$ was the main species formed in CH_2Cl_2 solution, and is in agreement with infra-red and ^{119}Sn NMR data for this mixture of solids reported in Chapter 3. No explanation, however, was given

for the carbonyl absorptions observed at 2028 and 2079 cm^{-1} (nujol) for this mixture of species.

Reaction of $\text{Rh}(\text{CO})\text{Cl}(\text{PPh}_3)_2$ with SnCl_2 in CH_2Cl_2 solution at 40°C gave a ^{31}P NMR doublet at 32.5 ppm $^1J(^{103}\text{Rh}, ^{31}\text{P}) = 89.0$ Hz (see Table 7.8), ascribed to the formation of $\text{Rh}(\text{CO})_2(\text{SnCl}_3)(\text{PPh}_3)_2$, which would again require a disproportionation reaction to occur, involving intermolecular group transfer of CO. A ^{31}P NMR doublet at 19.1 ppm $^1J(^{103}\text{Rh}, ^{31}\text{P}) = 91.2$ Hz (see Table 7.8) was also observed. The chemical shift, at relatively high field (low frequency), and the coupling constant value, are consistent with a 5-coordinate rhodium(I) complex containing SnCl_3^- competing with PPh_3 for π -electron density⁽¹²⁾, but the doublet cannot be assigned from the available data. The starting material $\text{Rh}(\text{CO})\text{Cl}(\text{PPh}_3)_2$ remained in solution throughout the reaction and was detected as the major species by ^{31}P NMR spectroscopy. Not surprisingly $\text{Rh}(\text{CO})\text{Cl}(\text{PPh}_3)_2$ was also recovered from the reaction mixture upon cooling to room temperature. Studies by Young⁽¹⁸⁾ reported the reversibility of the reaction of $\text{Rh}(\text{CO})\text{Cl}(\text{PPh}_3)_2$ with SnCl_2 according to the following equilibrium. However, data reported in this chapter indicates that under the reaction conditions any such equilibrium in solution will be highly in favour of $\text{Rh}(\text{CO})\text{Cl}(\text{PPh}_3)_2$:



The formation of $\text{Rh}(\text{CO})_2(\text{SnCl}_3)(\text{PPh}_3)_2$ was not observed during the monitoring of the same reaction by infra-red spectroscopy. This is also consistent with the position of the above equilibrium being highly in favour of $\text{Rh}(\text{CO})\text{Cl}(\text{PPh}_3)_2$. The only infra-red absorption observed upon heating the reaction mixture was due to the starting material $\text{Rh}(\text{CO})\text{Cl}(\text{PPh}_3)_2$. Other very weak absorptions at 1990, 2012, 2076 and 2090 cm^{-1} were observed after a two day period following cooling of the reaction mixture, but remain unassigned.

The reaction of $\text{Rh}(\text{COD})_2(\text{SnCl}_3)$ with CO in CH_2Cl_2 , followed by reaction with PPh_3 (see Table 7.9) also provides evidence for the formation of $\text{Rh}(\text{CO})_2(\text{SnCl}_3)(\text{PPh}_3)_2$ in solution. Reaction with CO at atmospheric pressure appears to form $\text{Rh}(\text{CO})_4(\text{SnCl}_3)$ in solution as indicated by the four carbonyl absorptions shown in Figure 7.7.

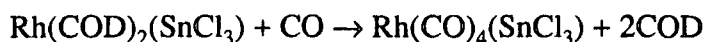


Figure 7.6 Infra-red spectrum for the reaction of $[\text{Bz}(\text{Et})_3\text{N}][\text{Rh}(\text{CO})_2\text{Cl}_2]$ with SnCl_2 and PPh_3 in THF

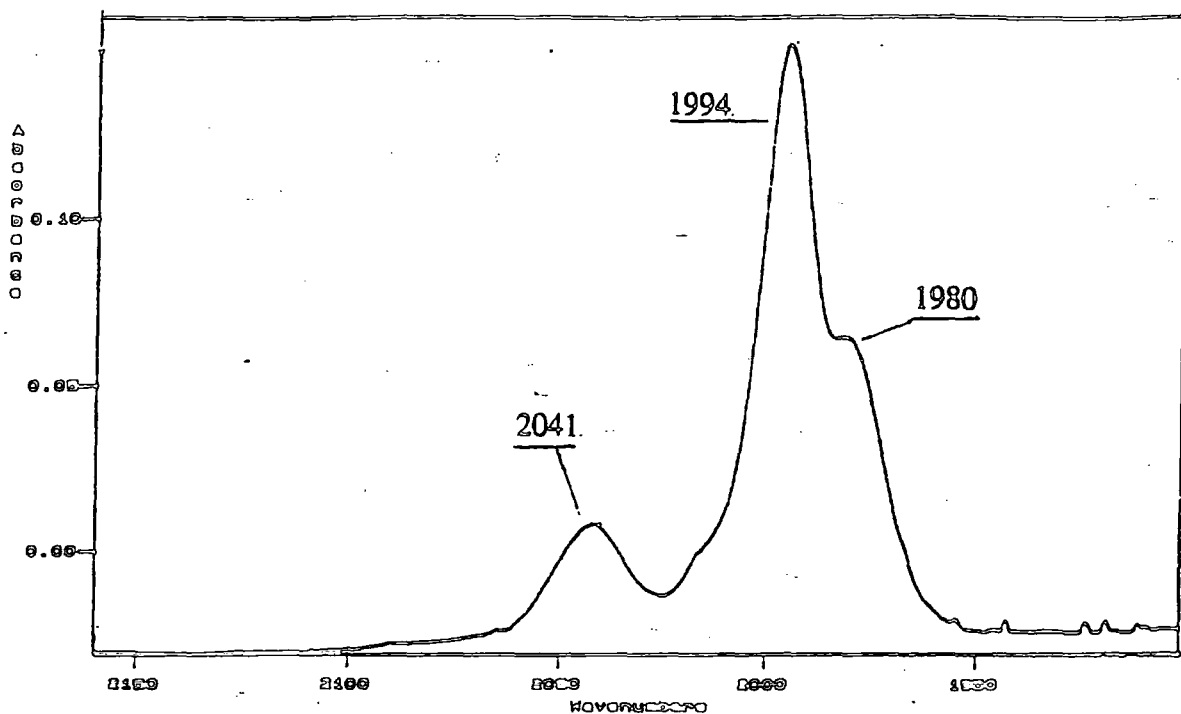
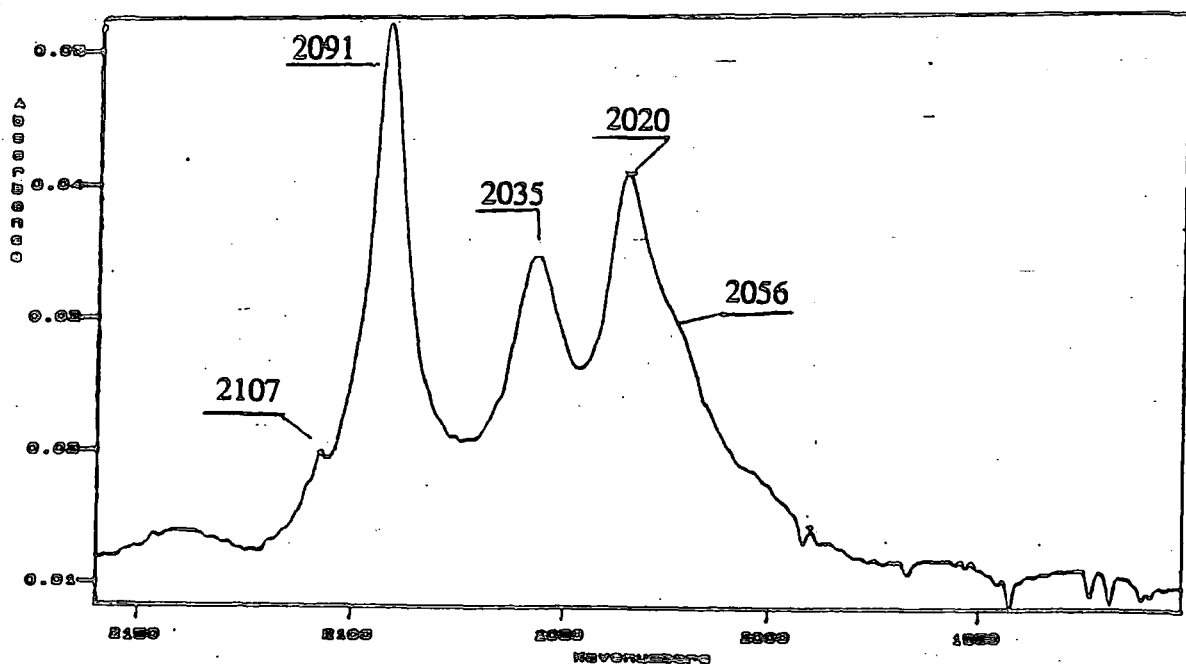
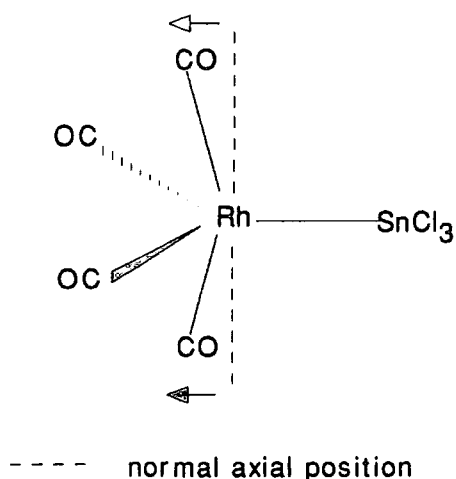


Figure 7.7 Infra-red spectrum for the reaction of $\text{Rh}(\text{COD})_2(\text{SnCl}_3)$ with CO in CH_2Cl_2



This pattern of carbonyl absorptions {a very weak absorption at the highest frequency (2107cm^{-1}), along with three stronger absorptions at lower frequencies ($2035, 2056, 2091\text{cm}^{-1}$)} is most consistent with the ligands in the distorted trigonal bipyramidal arrangement shown below. The bulky SnCl_3^- ligand is shown in its preferred equatorial position. Two of the CO ligands are shown in equatorial positions, with the other two possibly slightly bent out of the axial positions expected for a trigonal bipyramidal arrangement.



Reaction of this species with PPh_3 gave a complex with carbonyl infra-red absorptions at 2000_s and 2045_w cm^{-1} , indicating displacement of two carbonyl ligands by two triphenylphosphine ligands to give $\text{Rh}(\text{CO})_2(\text{SnCl}_3)(\text{PPh}_3)_2$ in a trigonal bipyramidal conformation, as proposed earlier.



The fact that CO ligands compete a SnCl_3^- ligand and with one another for π -electron density from occupied rhodium d-orbitals leads to their susceptibility towards displacement by the primarily σ -donating PPh_3 ligand. The reaction probably stops after displacement of two CO ligands, since the Rh-CO bonds will become progressively stronger upon loss of each CO group, and will thus become less susceptible to displacement by other ligands.

The reaction of $\text{Rh}(\text{COD})_2(\text{SnCl}_3)$ with PPh_3 indicated displacement of a single 1,5-cyclooctadiene ligand by two PPh_3 ligands to give $\text{Rh}(\text{COD})(\text{SnCl}_3)(\text{PPh}_3)_2$ based on the position and $^1J(^{103}\text{Rh}, ^{31}\text{P})$ coupling constant of the single ^{31}P NMR doublet observed.

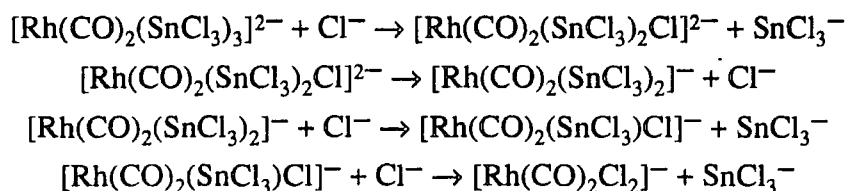


7.3.2 The Reaction of Cl⁻ with Rh-CO-SnCl₃ Complexes

The reaction of [Bz(Et)₃N]₂[Rh(CO)₂(SnCl₃)₃] with Bz(Et)₃NCl in THF proceeds quickly at room temperature when the Sn:Rh molar ratio is 2:1 or greater, and is complete in less than 30 seconds.

Infra-red spectral data show that the chloride ions displace the strong π-electron acceptor SnCl₃⁻ ligands of [Rh(CO)₂(SnCl₃)₃]²⁻ to form [Rh(CO)₂Cl₂]⁻. Interestingly, of the two strong π-acceptor ligands CO and SnCl₃⁻, in the complex, the weaker π-acceptor CO ligands are not displaced by chloride ions. In attempting to explain the surprising result, both the π-electron acceptor properties of the SnCl₃⁻ and CO ligands, and the nucleophilicity of the Cl⁻ and SnCl₃⁻ ions need to be taken into account.

A possible systematic pathway for this reaction is illustrated below:



Initial displacement of a SnCl₃⁻ ligand of [Rh(CO)₂(SnCl₃)₃]²⁻ by Cl⁻ nucleophilic attack at the metal centre to form [Rh(CO)₂(SnCl₃)₂Cl]²⁻, is envisaged. This reaction is favourable since it reduces the SnCl₃⁻—SnCl₃⁻, SnCl₃⁻—CO, and CO—CO competition for π-electron density, and also because the π-electron acceptor SnCl₃⁻ and CO ligands increase the electrophilic properties of the rhodium centre. It appears unlikely from the results of experiments described in Chapter 3, which led to the isolation of tri- and tetra-trichlorostannate complexes that two SnCl₃⁻ ligands will have the ability to stabilise the 5-coordinate 18-electron rhodium(I) complex [Rh(CO)₂(SnCl₃)₂Cl]²⁻, containing the σ-electron donating Cl⁻ ligand. Further, in solution (see Chapters 2 and 3), [Rh(CO)₂(SnCl₃)₃]²⁻ has been established as the favoured 5-coordinate complex. As a consequence of the anticipated instability of [Rh(CO)₂(SnCl₃)₂Cl]²⁻, the more stable 4-coordinate 16-electron complex [Rh(CO)₂(SnCl₃)₂]⁻ may be formed upon loss of the Cl⁻ ligand. The preferred conformation of [Rh(CO)₂(SnCl₃)₂]⁻ will have the bulky SnCl₃⁻ ligands trans to each other, and therefore competing with each other for π-electron density.

Consequently, since SnCl_3^- is a stronger π -acceptor than CO, and thought to be a stronger trans directing ligand, nucleophilic attack by Cl^- is expected to displace one of the more labile SnCl_3^- ligands, rather than CO, to form $[\text{Rh}(\text{CO})_2(\text{SnCl}_3)\text{Cl}]^-$. Unfortunately, however, these arguments cannot be extended further to explain the final step of this fast reaction, i.e. displacement of the remaining SnCl_3^- ligand of $[\text{Rh}(\text{CO})_2(\text{SnCl}_3)\text{Cl}]^-$ by Cl^- . The trans effect properties of SnCl_3^- would suggest that of the four ligands it is the least likely to be displaced. One possible explanation is that the various equilibria are driven towards formation of $[\text{Rh}(\text{CO})_2\text{Cl}_2]^-$ by removal of tin from solution, possibly as $[\text{Bz}(\text{Et})_3\text{N}][\text{SnCl}_3]$, but there was no evidence for the formation of an insoluble product. The solution remained clear over the study period of 2 hours.

7.4 Conclusions

It is clear from the data reported that because of its significant π -electron acceptor properties, the SnCl_3^- ligand has the ability to form 5-coordinate 18-electron rhodium(I) complexes. However, it is also clear that 5-coordinate $\text{Rh}(\text{I})\text{-CO-SnCl}_3\text{-PPh}_3$ complexes are not entirely stable in solution, and disproportionate to form other complexes. Several Rh-PPh_3 and Rh-CO complexes are formed in reactions of $\text{Rh}(\text{COD})(\text{SnCl}_3)(\text{PPh}_3)_2$ and $[\text{Rh}(\text{COD})(\text{SnCl}_3)_2(\text{PPh}_3)]^-$ with CO, and in the reaction of $[\text{Rh}(\text{CO})_2(\text{SnCl}_3)_3]^{2-}$ with PPh_3 , and include $\text{Rh}(\text{CO})_2(\text{SnCl}_3)(\text{PPh}_3)_2$ and $\text{Rh}(\text{CO})\text{Cl}(\text{PPh}_3)_2$. In addition there are several uncharacterised Rh-PPh_3 species formed, related by a series of disproportionation reactions in solution, which involve dissociation of SnCl_3^- and PPh_3 . The dissociation of ligands from the 18-electron $\text{Rh}(\text{I})\text{-COD-SnCl}_3\text{-PPh}_3$ complexes upon reaction with CO has implications for their use as catalysts, reported in Chapter 6. Work reported here with phosphine complexes indicates that 18-electron complexes readily form 16-electron catalytically active species under catalytic conditions, with $\text{Rh}(\text{CO})\text{Cl}(\text{PPh}_3)_2$, detected by infra-red and ^{31}P NMR spectral studies, a possible active catalyst or precursor.

7.5 References

1. M. Kretschmer, P.S. Pregosin, M. Garralda, *J. Organometal. Chem.*, 1983, 244, 175.
2. R. Uson, L.A. Oro, M.T. Pinillos, A. Arruebo, K.H.A.O. Starzewski, P.S. Pregosin, *J. Organometal. Chem.*, 1980, 192, 227.
3. V. Garcia, M.A. Garralda, E. Zugasti, *J. Organometal. Chem.*, 1987, 322, 249.
4. J.A. McCleverty, G. Wilkinson, *Inorg. Synth.*, 1966, 8, 214.
5. C.A. Ogle, C. Masterman, J.L. Hubbard, *J. Chem. Soc. Chem. Comm.*, 1990, 1733.
6. M. Kretschmer, P.S. Pregosin, H. Rügger, *J. Organometal. Chem.*, 1983, 241, 87.
7. C.A. Tolman, P.R. Meakin, D.L. Lindner, P.J. Jesson, *J. Am. Chem. Soc.*, 1974, 96, 2762.
8. W. Jetz, P.B. Simons, J.A.J. Thompson, W.A.G. Graham, *Inorg. Chem.*, 1966, 5, 2217.
9. W.A.G. Graham, *Inorg. chem.*, 1968, 7, 315.
10. R.V. Lindsey Jr., G.W. Parshall, U.G. Stolberg, *J. Am. Chem. Soc.*, 1965, 87, 658.
11. G.W. Parshall, *J. Am. Chem. Soc.*, 1966, 88, 704.
12. P.S. Pregosin, R.W. Kunz, *NMR 16, ³¹P and ¹³C NMR of Transition Metal Phosphine Complexes*, Springer-Verlag, Berlin-Heidelberg, 1979, 25.
13. P. Porta, H.M. Powell, R.J. Mawby, L.M. Venanzi, *J. Chem. Soc. (A)*, 1967, 455.
14. M.R. Churchill, K.K.G. Lin, *J. Am. Chem. Soc.*, 1974, 96, 76.
15. R.D. Cramer, R.V. Lindsey Jr., C.T. Prewitt, U.G. Stolberg, *J. Am. Chem. Soc.*, 1965, 87, 658.
16. C.Y. Hsu, M. Orchin, *J. Am. Chem. Soc.*, 1965, 97, 3553.
17. R.Uson, L.A. Oro, M.T. Pinillos, A. Arruebo, K.H.A.O. Starzewski, P.S. Pregosin, *J. Organometal. Chem.*, 1980, 192, 227.
18. J.F. Young, *Adv. Inorg. Chem. Radiochem.*, 1968, 11, 91.

Chapter 8

Conclusions

8.1 Conclusions

High pressure batch catalytic studies and high pressure infra-red studies of catalytic systems have provided detailed information about the homogeneous rhodium-chloride catalysed hydrocarbonylation of ethene to form propanoic acid. The studies have also clarified the role of tin(II) chloride as a promoter for this process. NMR and infra-red spectroscopic studies carried out at room temperature and atmospheric pressure along with infra-red spectroscopic studies carried out under catalytic conditions have provided information about the chemistry of species in the catalytic process and the role of tin. Rh(I)-CO-SnCl₃ complexes have been isolated and characterised, and their subsequent addition as precursors in the catalytic process has indicated the type of species likely to be present in solution for the rhodium-tin-chloride hydrocarbonylation of ethene. The properties of the SnCl₃⁻ ligand and its effect on the formation of Rh(I)-CO-SnCl₃ complexes and their chemistry has also been studied.

[Rh(CO)₂Cl₂]⁻ was shown to be an active catalyst for the rhodium-chloride catalysed hydrocarbonylation of ethene to form propanoic acid. High pressure infra-red studies have shown that it is also likely to be an active component in the catalytic systems containing tin(II) chloride species. Tin(II) chloride as a co-catalyst was shown to have an effect on the rate of propanoic acid production for a rhodium-chloride catalytic process, but a clear promotional effect was only observed for systems employing a Sn:Rh molar ratio of 2:1. High pressure infra-red studies for a system with a Sn:Rh molar ratio of 2:1 indicated carbonyl absorptions which would be consistent with either [Rh(CO)₂(SnCl₃)₃]²⁻, [Rh(CO)(SnCl₃)₄]³⁻ or [Rh(CO)(SnCl₃)₂Cl]²⁻ in solution, along with equally strong absorptions assigned to [Rh(CO)₂Cl₂]⁻. On the basis of infra-red data it was not possible to differentiate between the Rh(I)-CO-SnCl₃ complexes. High pressure studies indicated that the full potential of SnCl₂ to promote rhodium-chloride catalysis has not been reached, because of the tendency of the rhodium-tin complexes formed to revert to [Rh(CO)₂Cl₂]⁻ in large quantities, in the presence of the high concentration of chloride ions in the catalytic system. However, HCl_(aq), which is the source of chloride ions in the systems, is necessary for catalytic activity, with decreasing concentrations of it giving a decrease in propanoic acid production. A Sn:Rh molar ratio of 1:1 gave activity similar to that of a rhodium-chloride system where [Rh(CO)₂Cl₂]⁻ is the active catalyst, while catalytic systems with Sn:Rh molar ratios higher than 2:1 give a decrease in the selectivity for propanoic acid, possibly due to the tin(II) chloride forming 18-electron 5-coordinate rhodium(I) complexes,

containing several SnCl_3^- ligands. Such complexes are not normally associated with catalytic activity. Introduction of the alkylammonium salt, benzyltriethylammonium chloride, to rhodium-chloride and rhodium-tin-chloride systems gave no enhancement in the catalytic activity, clearly indicating that the ability of $[\text{Bz}(\text{Et})_3\text{N}]^+$ to form ion-pairs with active species has little effect on the reaction.

HCl was found necessary for hydrocarbonylation to occur and lower concentrations of it were accompanied by a decrease in propanoic acid production. The role of HCl is attributed to the generation of an intermediate rhodium hydride by oxidative addition. The data for a series of experiments involving the use of deuterated liquid reagents indicate that during catalysis the carbonylation step occurring at an active rhodium centre will be fast. The rate of reaction was also dependant on the ethene pressure in the system, with a first order relationship possibly applying.

Catalyst injection studies showed no improvement in the selectivity for propanoic acid when the active rhodium species was added at 180°C as opposed to room temperature. Thus, while formation of by-products can occur during the heating process of the reaction, it can also occur during hydrocarbonylation, and is accentuated by low concentrations of $\text{HCl}_{(\text{aq})}$ and increasing amounts of tin(II) chloride beyond a Sn:Rh ratio of 2:1. The by-products detected in significant quantities throughout the series of catalytic studies were chloroethane, ethyl propanoate and ethyl acetate, resulting from reductive elimination of chloroethane prior to the carbonylation stage in the catalytic cycle.

The reaction chemistry of rhodium(I) carbonyl chlorides and tin(II) chlorides was carried out at atmospheric pressure to investigate the reaction chemistry occurring between species present in the catalytic process. $[\text{Rh}(\text{CO})_2\text{Cl}_2]^-$ and $\text{Rh}_2(\text{CO})_4\text{Cl}_2$ react with SnCl_2 and SnCl_3^- in both THF and CH_2Cl_2 to form Rh(I)-CO- SnCl_3 complexes. Infra-red and ^{119}Sn NMR data identified the 5-coordinate 18-electron rhodium(I) complex $[\text{Rh}(\text{CO})_2(\text{SnCl}_3)_3]^{2-}$ as the favoured species formed in solution. Irrespective of the Rh:Sn molar ratio of the starting materials, when SnCl_2 is added to $[\text{Rh}(\text{CO})_2\text{Cl}_2]^-$, the reaction does not involve sequential formation of Rh- SnCl_3 complexes,



but direct formation of the last complex $[\text{Rh}(\text{CO})_2(\text{SnCl}_3)_3]^{2-}$. However, reactions of $\text{Rh}_2(\text{CO})_4\text{Cl}_2$ with $\text{SnCl}_2/\text{Cl}^-$ and SnCl_3^- in THF indicated that a 4-coordinate

The effect of tin(II) chloride on the rhodium-chloride catalysed hydrocarbonylation of ethene to form propanoic acid may relate to the changes in π -electron acceptor and trans effect properties when SnCl_3^- replaces chloride ligand(s). These properties will affect the processes occurring at an active rhodium(I) centre during the catalytic cycle, and the SnCl_3^- ligand, having a high trans effect is a likely cause of the increase in the rate of propanoic acid production.

Although it has not been possible to identify one particular rhodium-tin complex as a catalytic species several likely possibilities have been explored. Batch catalytic studies have indicated that the precursors $[\text{Rh}(\text{CO})_2(\text{SnCl}_3)_3]^{2-}$, $[\text{Rh}(\text{COD})(\text{SnCl}_3)_3]^{2-}$ and $[\text{Rh}(\text{CO})(\text{SnCl}_3)_2\text{Cl}]^{2-}$ lead to catalytically active species. Also, carbonyl absorptions observed in high pressure infra-red studies are consistent with $[\text{Rh}(\text{CO})_2(\text{SnCl}_3)_3]^{2-}$, $[\text{Rh}(\text{CO})(\text{SnCl}_3)_4]^{3-}$ and $[\text{Rh}(\text{CO})(\text{SnCl}_3)_2\text{Cl}]^{2-}$ being precursors, although $\nu(\text{CO})$ data did not allow differentiation between these possibilities, all of which have a strong absorption in the region 2005-2018 cm^{-1} . Although reaction conditions used to probe the chemistry of rhodium(I) carbonyl chlorides and tin(II) chlorides were different to those used for catalytic work, the general predominance of the 5-coordinate 18-electron rhodium(I) complex $[\text{Rh}(\text{CO})_2(\text{SnCl}_3)_3]^{2-}$ at atmospheric pressure and room temperature, suggests that it may be the favoured rhodium-tin catalytic precursor, undergoing conversion to a catalytically active 4-coordinate 16-electron complex such as $[\text{Rh}(\text{CO})_2(\text{SnCl}_3)\text{X}]^-$ ($\text{X} = \text{Cl}^-$ or SnCl_3^-) under the catalytic conditions, via SnCl_3^- dissociation, and possible further displacement of SnCl_3^- by Cl^- . Dissociation of CO and SnCl_3^- from $[\text{Rh}(\text{CO})_2(\text{SnCl}_3)_3]^{2-}$ to form other 4- and 5-coordinate complexes occurs at room temperature (see Figure 8.1), and therefore can most certainly occur under catalytic conditions.

APPENDICES

Appendix 1 Preliminary Synthesis

This section includes details of the syntheses complexes which have been used as starting materials for experimental work described throughout this thesis.

1. Preparation of μ,μ' -dichlorotetracarbonyldirhodium(I) - $\text{Rh}_2(\text{CO})_4\text{Cl}_2$

This complex was prepared by a method similar to that used by Wilkinson and McCleverty⁽¹⁾. Rhodium(III) chloride trihydrate (3g) was placed on a sintered frit enclosed in a glass tube. A stream of carbon monoxide was passed through the tube, which was maintained at a temperature of 90°C around the region of the frit. The carbon monoxide was bubbled through methanol at the start of the reaction, as a means of initiation. As the first traces of product were formed the bubbler was removed. Bright red needle shaped crystals condensed on the cooler part of the tube over a period of 24 hours. The air stable material (1.92g) was collected and stored in a dessicator.

Yield: 86%

Infra-red: $\nu(\text{CO})/\text{cm}^{-1}$ in nujol: 2034_s, 2088_s, 2104_w

2. Preparation of Benzyltriethylammonium dichlorodicarbonylrhodium(I) - $[\text{Bz}(\text{Et})_3\text{N}][\text{Rh}(\text{CO})_2\text{Cl}_2]$

This complex was prepared by the method of Cleare and Griffith⁽²⁾. Rhodium(III) chloride trihydrate (0.98g, 3.72mmol) was heated under reflux in a nitrogen atmosphere, with 7.5ml of 37% $\text{HCl}_{(\text{aq})}$, 6ml of formic acid and 1.5ml of water, until the solution became pale yellow after a period of two hours. The solution was allowed to cool and filtered to remove impurities. Benzyltriethylammonium chloride (1.25g, 5.49mmol) was added to the solution to precipitate the pale yellow solid $[\text{Bz}(\text{Et})_3\text{N}][\text{Rh}(\text{CO})_2\text{Cl}_2]$ (1.25g). The air and moisture sensitive crystals were separated by filtration, dried under vacuum and collected under a nitrogen atmosphere. The $[\text{PPN}]^+$ salt of the dichlorodicarbonylrhodium(I) anion was prepared in the same way.

Yield: 81%

Infra-red: $\nu(\text{CO})/\text{cm}^{-1}$: 1991_s, 2081_s

3. Preparation of μ,μ' -dichlorodi-1,5-cyclooctadienedirrhodium(I)-
 $\text{Rh}_2(\text{C}_8\text{H}_{12})_2\text{Cl}_2$

This was prepared by the method of Crabtree et al⁽³⁾. Rhodium(III) chloride trihydrate (0.50g, 1.90mmol) and 12ml of 1,5-cyclooctadiene in 60ml of absolute ethanol were heated under reflux, under a nitrogen atmosphere, for approximately 12 hours to give deposition of a yellow solid. Upon cooling the solid was separated by filtration, washed with ethanol and dried under vacuum. The air stable solid collected, $\text{Rh}_2(\text{C}_8\text{H}_{12})_2\text{Cl}_2$ (0.36g) was stored in a dessicator.

Yield: 77%

Found: C 38.21, H 4.98, N 0%; $\text{C}_{16}\text{H}_{24}\text{Cl}_2\text{Rh}_2$ requires C 38.57, H 4.82, N 0%

4. Preparation of μ,μ' -dichlorotetraethenedirrhodium(I) - $\text{Rh}_2(\text{C}_2\text{H}_4)_4\text{Cl}_2$

This was prepared by a method similar to that of Cramer⁽⁴⁾. Rhodium(III) chloride trihydrate (0.50g, 1.90mmol) was dissolved in 0.75ml of water upon warming. 12ml of methanol was then added, giving a deep red solution. The solution was stirred and bubbled vigorously with ethene, giving precipitation of a red/orange solid which accumulated over a period of 6 hours. The product, $\text{Rh}_2(\text{C}_2\text{H}_4)_4\text{Cl}_2$ (0.15g) was filtered, washed with 3ml of methanol and dried under vacuum.

Yield: 41%

Found: C 24.07, H 4.18, N 0%; $\text{C}_8\text{H}_{16}\text{Cl}_2\text{Rh}_2$ requires C 24.69, H 4.12, N 0%

5. Preparation of Benzyltriethylammonium trichlorostannate -
 $[\text{Bz}(\text{Et})_3\text{N}][\text{SnCl}_3]$

Anhydrous tin(II) chloride (0.20g, 1.05mmol) and benzyltriethylammonium chloride (0.25g, 1.10mmol) were heated to 85°C in 60ml of glacial acetic acid, under a nitrogen atmosphere, until they became soluble. The pale yellow solution was stirred at this temperature for 30 minutes and then allowed to cool. The volume was reduced under vacuum by approximately 10ml until crystals were precipitated. The off-white needle shaped crystals of $[\text{Bz}(\text{Et})_3\text{N}][\text{SnCl}_3]$ (0.26g) were separated by filtration, dried under vacuum and stored in a nitrogen atmosphere.

Yield: 59%

Found: Sn 27.2, Cl 23.8, C 37.4, H 5.3, N 3.3%; $\text{C}_{13}\text{H}_{22}\text{Cl}_3\text{NSn}$ requires Sn 28.5, Cl 25.5, C 37.3, H 5.5, N 3.2%

6. Preparation dibenzyltriethylammonium zinc(II) tetrachloride -
[Bz(Et)₃N]₂[ZnCl₄]

Zinc(II) chloride (0.30g, 2.20mmol) and Bz(Et)₃NCl (1.00g, 4.39mmol) were heated under reflux, under a nitrogen atmosphere in a mixture of 60ml of THF and 40ml of acetic acid for approximately 15 minutes until a clear solution was obtained. Approximately 1/3 of the solvent was removed under vacuum, to give deposition of white crystals. The crystals of [Bz(Et)₃N]₂[ZnCl₄] (0.80g) were separated by filtration and dried under vacuum.

Yield: 61%

Found: Cl 23.4, C 52.5, H 7.6, N 4.5%; C₂₆H₄₄Cl₄N₂Zn requires Cl 24.0, C 52.8, H 7.4, N 4.7%

References

1. J.A. McCleverty, G. Wilkinson, *Inorg. Synth*, 1966, 8, 211.
2. M.J. Cleare, W.P. Griffith, *J. Chem. Soc.(A)*, 1970, 2788.
3. G. Giordani, P.H. Crabtree, *Inorg. Synth.*, 1979, 19, 218.
4. R. Cramer, *Inorg. Chem.*, 1962, 1, 722.

Appendix 2 High Pressure Autoclaves

For the work carried out in Chapters 4, 5 and 6, two different types of autoclave were used. One was an Infra-Red cell used in Chapter 5 and the other was a standard autoclave used in Chapters 4 and 6.

1. Infra-Red Autoclave

The autoclave design was essentially the same as that of Whyman⁽¹⁾. The construction of the autoclave is shown in Figure 1. The main body is constructed of Hastalloy C. The body of the autoclave (A) is surrounded by a heating jacket (B). Gases are introduced via the inlet (C), with gases and solution mixed by the 'flip-flop' stirrer (D). Temperature control was achieved by means of a thermocouple inserted in to the well (E). The head of the autoclave (F) contains the 'flip-flop' stirrer which oscillates in the area (G), by employment of a copper solenoid (H). The head of the autoclave seals in to the body by means of a viton 'O' ring (I) backed by one made of P.T.F.E. (J). The bolt closure at the head of the autoclave (K) is also sealed in this way (L). The window holders (M) are screwed in to the main body where they seal by means of a viton 'O' ring (N). The Infra-Red beam passes through the CaF₂ windows (P) which are held in place by the retaining caps (Q), and sealed with a viton 'O' ring (R). The viton 'O' rings are resistant to acetic acid and dichloromethane but expand in THF.

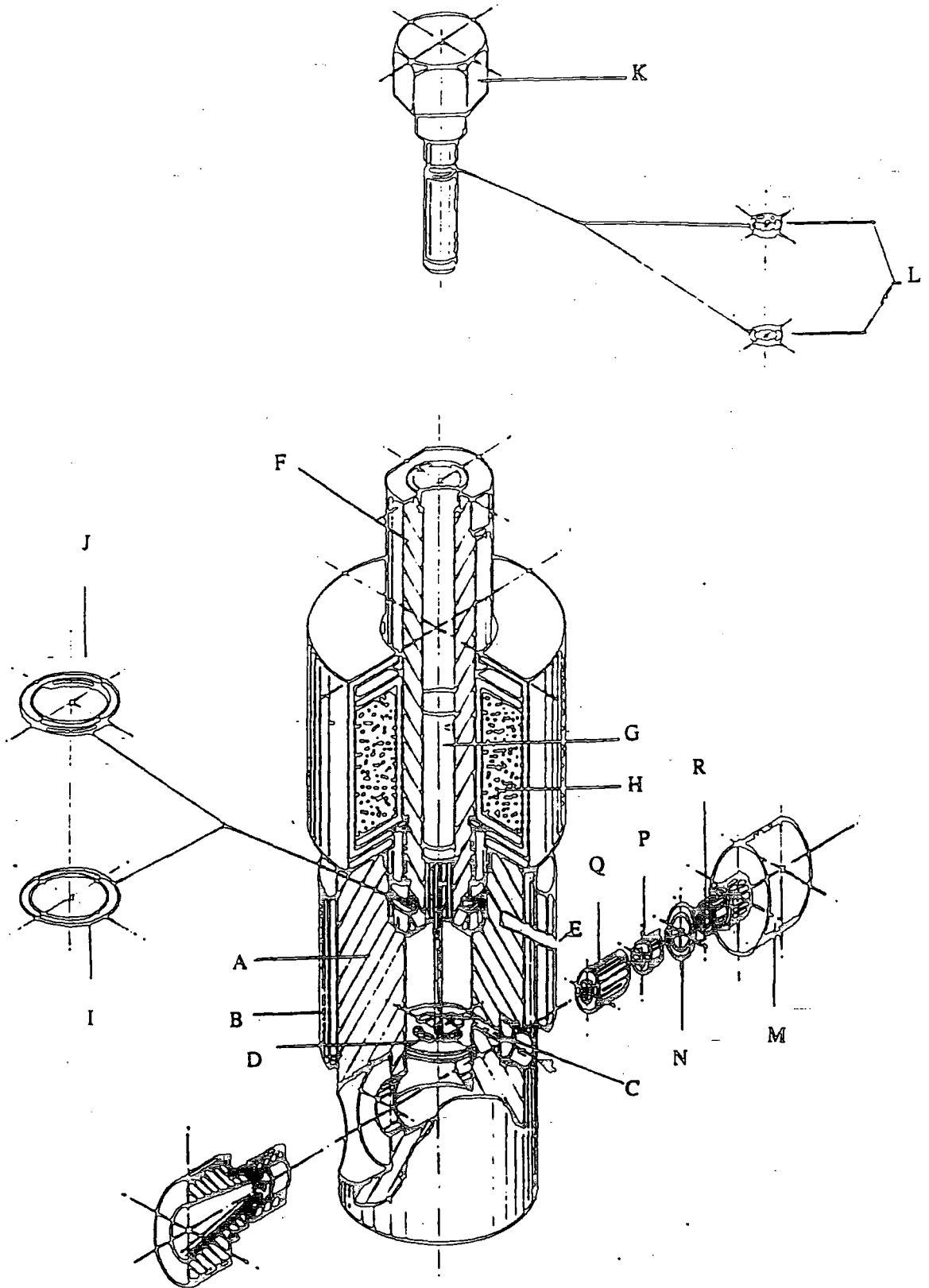
Method of use

A background spectrum of the appropriate solvent was acquired at room temperature, under the appropriate pressure of the reaction gas. Liquid and solid reactants were then added to the solvent in the autoclave, and the head screwed in to place. The autoclave was first flushed with nitrogen gas and then the reaction gas. The required pressure of the reaction gas was then introduced. The required temperature was set using a 'eurotherm' heater and the stirrer switched on. Gas pressure was monitored by reading a dialled pressure gauge via a television camera. Absorbance spectra were recorded using a Mattson Instruments Alpha Centauri FT-IR Spectrometer. The background spectrum was automatically subtracted from the sample spectrum.

References

1. W. Rigby, R. Whyman, K. Wilding, J. Phys. E. Scientific Instruments, **1970**, 3, 372.

Figure 1 High Pressure Infra-Red Autoclave



2. Standard Hastalloy Autoclave used for batch catalytic studies

The 37H autoclave used for studies in Chapters 4 and 6 is represented by Figure 2. The autoclave is made of a Hastalloy C276 alloy and has a total volume of 120ml. Solvents and solids were introduced by the solids inlet which was then screwed down. All solvents were degassed prior to use. The autoclave was first of all flushed with nitrogen gas twice, before pressurising to the required value with the reaction gases, usually carbon monoxide and ethene. The pressure was monitored by a dialled pressure gauge using a television camera. The temperature was controlled using a 'eurotherm' heater and the reagents mixed by means of a magnetic follower type stirrer bar.

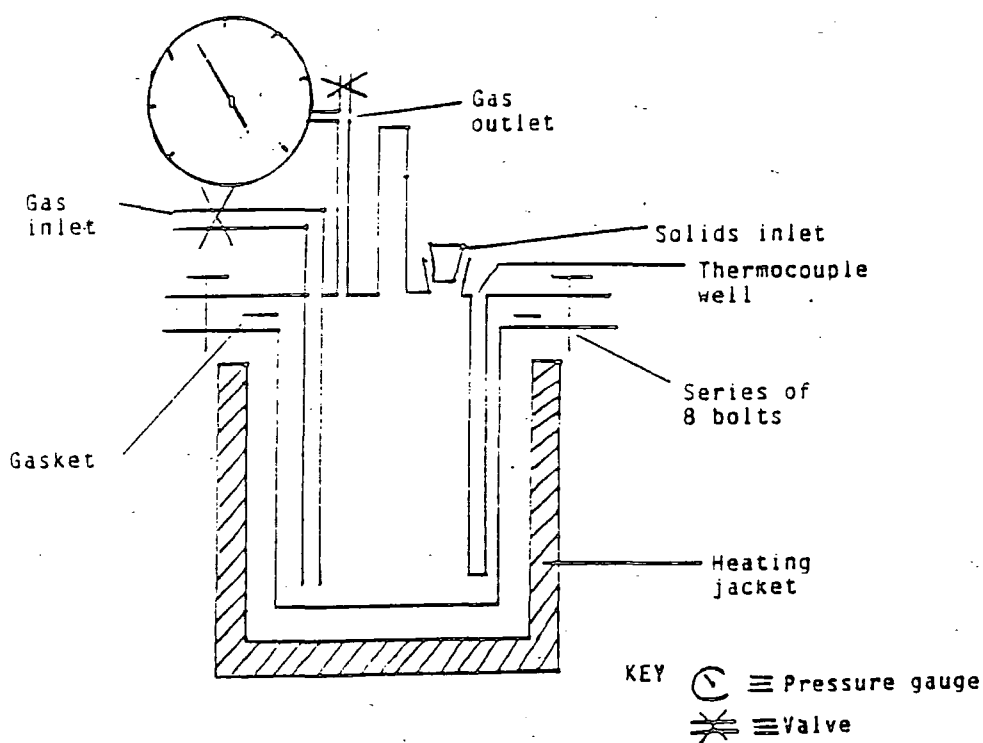


Figure 2 Standard 37H Autoclave

Appendix 3 Instrumental Parameters

1. NMR Spectroscopy

All spectra were recorded using a Bruker AC250 Spectrometer, incorporating a 5.9 Tesla Oxford Instruments Magnet.

1.1 ^{31}P NMR

Reference	1% H_3PO_4
Scan Frequency	101.256 MHz
Sweep Width	62500.000 MHz
Pulse Width	3.5
Line Broadening	4.000 Hz

1.2 ^{119}Sn NMR

Reference	Me_4Sn
Scan Frequency	93.275 MHz
Sweep Width	55555.556 MHz
Pulse Width	3
Line Broadening	4.000 Hz

1.3 ^1H NMR

Reference	Me_4Si
Scan Frequency	250.133 MHz
Sweep Width	3048.780 MHz
Line Broadening	0 Hz

1.4 Solid State ^{119}Sn NMR

Scan Frequency	11.862 MHz
Acquisition Time	4.9 msec
Relaxation Delay	30 sec
Pulse Width	45°
Spin Rate	9780 Hz

2. Mattson Alpha Centauri FT-IR Spectrometer

Data Type	Absorbance
Detector	DTGS
Apodisation	Triangular
Phase Correction	Phaseapod
Iris Size	25%
Amplifier Gain	1

Interpretation carried out using PC-FIRST package

2.1 Rhodium(I) Carbonyl Chloride/Tin(II) Chloride Spectra in Chapter 2

Range	2200-1900 cm^{-1}
Resolution	2 cm^{-1}
No. of Sample Scans	16
No. of Background Scans	16

2.2 Spectra in Chapters 3, 5, 6 and 7

Range	2200-1900 cm^{-1}
Resolution	2 cm^{-1}
No. of Sample Scans	16
No. of Background Scans	16

3. Gas Chromatograph Mass Spectroscopy

Gas Chromatograph Mass Spectroscopy was carried out using a Fisons Trio 1000 Mass Spectrometer and a Hewlett Packard 5890 Series 2 Gas Chromatograph, containing a Hewlett Packard cross-linked methyl silicone column. The column was 25 m long, had an inner diameter of 0.2 mm and a film thickness of 0.33 μm . Helium was used as the carrier gas.

4. Gas Chromatography

Gas chromatography was carried out using a Varian model 3700 Gas Chromatograph containing a DB-FFAP column, which was 15 m long, had an inner diameter of 0.53 mm and a film thickness of 1.0 μm . A temperature programme of 10°C rise per minute from 40°C to 240°C was used with a final time of 10 minutes. Nitrogen was used as the carrier gas. Integration was carried out using a Spectra Physics Chrom Jet integrator.

5. Elemental Analysis

5.1 CHN Analysis

This was carried out using a Carlo Erba Elemental Analyser 1106.

5.2 Chlorine Analysis

The sample was combusted in oxygen, followed by potentiometric titration of the product with silver nitrate.

5.3 Tin Analysis

The sample was dissolved by acid digestion, and the tin component determined by Atomic Absorption using a Perkin Elmer 5000 spectrometer. Anhydrous tin(II) chloride was used as a standard.

5.4 Rhodium Analysis

The sample was dissolved by acid digestion, and the rhodium component determined by atomic absorption using a Perkin Elmer 5000 spectrometer. Dichlorotetracarbonyldirrhodium(I) was used as a standard.

Appendix 4 Scientific Meetings and Colloquia Attended

The following is a list of scientific meetings attended outside Durham:

1. Presentation of poster at XVth International Conference on Organometallic Chemistry in Warsaw, Poland, 8-14th August 1992.
2. Talk at BP Chemicals (CASE) Conference in Hull, 6th January 1993.
3. Talk at North East Graduate Symposium at Newcastle University, April 1993.

UNIVERSITY OF DURHAM

Board of Studies in Chemistry

COLLOQUIA, LECTURES AND SEMINARS GIVEN BY INVITED SPEAKERS

1ST AUGUST 1990 TO 31ST JULY 1991

- ALDER, Dr. B.J. (Lawrence Livermore Labs., California) 15th January, 1991
Hydrogen in all its Glory
- BELL[†], Prof. T. (SUNY, Stony Brook, U.S.A.) 14th November, 1990
Functional Molecular Architecture and Molecular Recognition
- ✓ BOCHMANN[†], Dr. M. (University of East Anglia) 24th October, 1990
Synthesis, Reactions and Catalytic Activity of Cationic Titanium Alkyls
- BRIMBLE, Dr. M.A. (Massey University, New Zealand) 29th July, 1991
Synthetic Studies Towards the Antibiotic Griseusin-A
- BROOKHART, Prof. M.S. (University of N. Carolina) 20th June, 1991
Olefin Polymerizations, Oligomerizations and Dimerizations Using Electrophilic Late Transition Metal Catalysts
- BROWN, Dr. J. (Oxford University) 28th February, 1991
Can Chemistry Provide Catalysts Superior to Enzymes?
- BUSHBY[†], Dr. R. (Leeds University) 6th February, 1991
Biradicals and Organic Magnets
- COWLEY, Prof. A.H. (University of Texas) 13th December, 1990
New Organometallic Routes to Electronic Materials
- CROUT, Prof. D. (Warwick University) 29th November, 1990
Enzymes in Organic Synthesis
- ✓ DOBSON[†], Dr. C.M. (Oxford University) 6th March, 1991
NMR Studies of Dynamics in Molecular Crystals
- ✓ GERRARD[†], Dr. D. (British Petroleum) 7th November, 1990
Raman Spectroscopy for Industrial Analysis
- HUDLICKY, Prof. T. (Virginia Polytechnic Institute) 25th April, 1991
Biocatalysis and Symmetry Based Approaches to the Efficient Synthesis of Complex Natural Products
- ✓ JACKSON[†], Dr. R. (Newcastle University) 31st October, 1990
New Synthetic Methods: α -Amino Acids and Small Rings
- ✓ KOCOVSKY[†], Dr. P. (Uppsala University) 6th November, 1990
Stereo-Controlled Reactions Mediated by Transition and Non-Transition Metals

<u>LACEY</u> , Dr. D. (Hull University) Liquid Crystals	31st January, 1991
✓ <u>LOGAN</u> , Dr. N. (Nottingham University) Rocket Propellants	1st November, 1990
<u>MACDONALD</u> , Dr. W.A. (ICI Wilton) Materials for the Space Age	11th October, 1990
<u>MARKAM</u> , Dr. J. (ICI Pharmaceuticals) DNA Fingerprinting	7th March, 1991
✓ <u>PETTY</u> , Dr. M.C. (Durham University) Molecular Electronics	14th February, 1991
✓ <u>PRINGLE</u> ⁺ , Dr. P.G. (Bristol University) Metal Complexes with Functionalised Phosphines	5th December, 1990
✓ <u>PRITCHARD</u> , Prof. J. (Queen Mary & Westfield College, London University) Copper Surfaces and Catalysts	21st November, 1990
<u>SADLER</u> , Dr. P.J. (Birkbeck College London) Design of Inorganic Drugs: Precious Metals, Hypertension + HIV	24th January, 1991
<u>SARRE</u> , Dr. P. (Nottingham University) Comet Chemistry	17th January, 1991
<u>SCHROCK</u> , Prof. R.R. (Massachusetts Institute of Technology) Metal-ligand Multiple Bonds and Metathesis Initiators	24th April, 1991
<u>SCOTT</u> , Dr. S.K. (Leeds University) Clocks, Oscillations and Chaos	8th November, 1990
✓ <u>SHAW</u> ⁺ , Prof. B.L. (Leeds University) Syntheses with Coordinated, Unsaturated Phosphine Ligands	20th February, 1991
<u>SINN</u> ⁺ , Prof. E. (Hull University) Coupling of Little Electrons in Big Molecules. Implications for the Active Sites of (Metalloproteins and other) Macromolecules	30th January, 1991
<u>SOULEN</u> ⁺ , Prof. R. (South Western University, Texas) Preparation and Reactions of Bicycloalkenes	26th October, 1990
<u>WHITAKER</u> ⁺ , Dr. B.J. (Leeds University) Two-Dimensional Velocity Imaging of State-Selected Reaction Products	28th November, 1990

⁺ Invited specifically for the postgraduate training programme.

✓ Lectures attended

UNIVERSITY OF DURHAM

Board of Studies in Chemistry

COLLOQUIA, LECTURES AND SEMINARS FROM INVITED SPEAKERS

1991 – 1992 (August 1 – July 31)

1991

- October 17 Dr. J.A. Salthouse, University of Manchester
Son et Lumiere – a demonstration lecture
- October 31 Dr. R. Keeley, Metropolitan Police Forensic Science
Modern forensic science
- ✓ November 6 Prof. B.F.G. Johnson[†], Edinburgh University
Cluster–surface analogies
- November 7 Dr. A.R. Butler, St. Andrews University
Traditional Chinese herbal drugs: a different way of treating disease
- ✓ November 13 Prof. D. Gani[†], St. Andrews University
The chemistry of PLP–dependent enzymes
- November 20 Dr. R. More O'Ferrall[†], University College, Dublin
Some acid–catalysed rearrangements in organic chemistry
- ✓ November 28 Prof. I.M. Ward, IRC in Polymer Science, University of Leeds
The SCI lecture: the science and technology of orientated polymers
- ✓ December 4 Prof. R. Grigg[†], Leeds University
Palladium–catalysed cyclisation and ion–capture processes
- December 5 Prof. A.L. Smith, ex Unilever
Soap, detergents and black puddings
- ✓ December 11 Dr. W.D. Cooper[†], Shell Research
Colloid science: theory and practice

1992

- January 22 Dr. K.D.M. Harris[†], St. Andrews University
Understanding the properties of solid inclusion compounds
- January 29 Dr. A. Holmes[†], Cambridge University
Cycloaddition reactions in the service of the synthesis of piperidine and indolizidine natural products

January	30	Dr. M. Anderson, Sittingbourne Research Centre, Shell Research Recent Advances in the Safe and Selective Chemical Control of Insect Pests
/ February	12	Prof. D.E. Fenton [†] , Sheffield University Polynuclear complexes of molecular clefts as models for copper biosites
February	13	Dr. J. Saunders, Glaxo Group Research Limited Molecular Modelling in Drug Discovery
/ February	19	Prof. E.J. Thomas [†] , Manchester University Applications of organostannanes to organic synthesis
February	20	Prof. E. Vogel, University of Cologne <i>The Musgrave Lecture</i> Porphyrins: Molecules of Interdisciplinary Interest
February	25	Prof. J.F. Nixon, University of Sussex <i>The Tilden Lecture</i> Phosphaalkynes: new building blocks in inorganic and organometallic chemistry
February	26	Prof. M.L. Hitchman [†] , Strathclyde University Chemical vapour deposition
March	5	Dr. N.C. Billingham, University of Sussex Degradable Plastics – Myth or Magic?
/ March	11	Dr. S.E. Thomas [†] , Imperial College Recent advances in organoiron chemistry
March	12	Dr. R.A. Hann, ICI Imagedata Electronic Photography – An Image of the Future
March	18	Dr. H. Maskill [†] , Newcastle University Concerted or stepwise fragmentation in a deamination-type reaction
April	7	Prof. D.M. Knight, Philosophy Department, University of Durham Interpreting experiments: the beginning of electrochemistry
May	13	Dr. J-C Gehret, Ciba Geigy, Basel Some aspects of industrial agrochemical research

[†] Invited specially for the postgraduate training programme.

/ Lectures attended

UNIVERSITY OF DURHAM

Board of Studies in Chemistry

COLLOQUIA, LECTURES AND SEMINARS FROM INVITED SPEAKERS

1992 - 1993 (August 1 - July 31)

1992

- October 15 Dr M. Glazer & Dr. S. Tarling, Oxford University & Birbeck College, London
It Pays to be British! - The Chemist's Role as an Expert Witness in Patent Litigation
- ✓ October 20 Dr. H. E. Bryndza, Du Pont Central Research
Synthesis, Reactions and Thermochemistry of Metal (Alkyl) Cyanide Complexes and Their Impact on Olefin Hydrocyanation Catalysis
- ✓ October 22 Prof. A. Davies, University College London
The Ingold-Albert Lecture The Behaviour of Hydrogen as a Pseudometal
- October 28 Dr. J. K. Cockcroft, University of Durham
Recent Developments in Powder Diffraction
- October 29 Dr. J. Emsley, Imperial College, London
The Shocking History of Phosphorus
- ✓ November 4 Dr. T. P. Kee, University of Leeds
Synthesis and Co-ordination Chemistry of Silylated Phosphites
- November 5 Dr. C. J. Ludman, University of Durham
Explosions, A Demonstration Lecture
- November 11 Prof. D. Robins, Glasgow University
Pyrrolizidine Alkaloids : Biological Activity, Biosynthesis and Benefits
- November 12 Prof. M. R. Truter, University College, London
Luck and Logic in Host - Guest Chemistry
- ✓ November 18 Dr. R. Nix, Queen Mary College, London
Characterisation of Heterogeneous Catalysts
- November 25 Prof. Y. Vallee, University of Caen
Reactive Thiocarbonyl Compounds
- ✓ November 25 Prof. L. D. Quin, University of Massachusetts, Amherst
Fragmentation of Phosphorous Heterocycles as a Route to Phosphoryl Species with Uncommon Bonding
- November 26 Dr. D. Humber, Glaxo, Greenford
AIDS - The Development of a Novel Series of Inhibitors of HIV
- December 2 Prof. A. F. Hegarty, University College, Dublin
Highly Reactive Enols Stabilised by Steric Protection
- December 2 Dr. R. A. Aitken, University of St. Andrews
The Versatile Cycloaddition Chemistry of $\text{Bu}_3\text{P} \cdot \text{CS}_2$
- December 3 Prof. P. Edwards, Birmingham University
The SCI Lecture - What is Metal?
- December 9 Dr. A. N. Burgess, ICI Runcorn
The Structure of Perfluorinated Ionomer Membranes

1993

- January 20 Dr. D. C. Clary, University of Cambridge
Energy Flow in Chemical Reactions
- January 21 Prof. L. Hall, Cambridge
NMR - Window to the Human Body
- ✓ January 27 Dr. W. Kerr, University of Strathclyde
Development of the Pauson-Khand Annulation Reaction : Organocobalt Mediated
Synthesis of Natural and Unnatural Products
- January 28 Prof. J. Mann, University of Reading
Murder, Magic and Medicine
- February 3 Prof. S. M. Roberts, University of Exeter
Enzymes in Organic Synthesis
- February 10 Dr. D. Gillies, University of Surrey
NMR and Molecular Motion in Solution
- ✓ February 11 Prof. S. Knox, Bristol University
The Tilden Lecture Organic Chemistry at Polynuclear Metal Centres
- ✓ February 17 Dr. R. W. Kemmitt, University of Leicester
Oxatrimethylenemethane Metal Complexes
- February 18 Dr. I. Fraser, ICI Wilton
Reactive Processing of Composite Materials
- February 22 Prof. D. M. Grant, University of Utah
Single Crystals, Molecular Structure, and Chemical-Shift Anisotropy
- February 24 Prof. C. J. M. Stirling, University of Sheffield
Chemistry on the Flat-Reactivity of Ordered Systems
- ✓ March 10 Dr. P. K. Baker, University College of North Wales, Bangor
'Chemistry of Highly Versatile 7-Coordinate Complexes'
- March 11 Dr. R. A. Y. Jones, University of East Anglia
The Chemistry of Wine Making
- March 17 Dr. R. J. K. Taylor, University of East Anglia
Adventures in Natural Product Synthesis
- March 24 Prof. I. O. Sutherland, University of Liverpool
Chromogenic Reagents for Cations
- May 13 Prof. J. A. Pople, Carnegie-Mellon University, Pittsburgh, USA
The Boys-Rahman Lecture Applications of Molecular Orbital Theory
- May 21 Prof. L. Weber, University of Bielefeld
Metallo-phospha Alkenes as Synthons in Organometallic Chemistry
- June 1 Prof. J. P. Konopelski, University of California, Santa Cruz
Synthetic Adventures with Enantiomerically Pure Acetals
- June 2 Prof. F. Ciardelli, University of Pisa
Chiral Discrimination in the Stereospecific Polymerisation of Alpha Olefins
- June 7 Prof. R. S. Stein, University of Massachusetts
Scattering Studies of Crystalline and Liquid Crystalline Polymers

- June 16 Prof. A. K. Covington, University of Newcastle
Use of Ion Selective Electrodes as Detectors in Ion Chromatography
- June 17 Prof. O. F. Nielsen, H. C. Ørsted Institute, University of Copenhagen
Low-Frequency IR - and Raman Studies of Hydrogen Bonded Liquids

✓ lectures attended.

File Ref. CG137/E(CH)

